Photocopy and Use Authorization

In presenting this thesis in partial fulfillment of the requirements for an advanced degree at Idaho State University, I agree that the Library shall make it freely available for inspection. I further state that permission for extensive copying of my thesis for scholarly purposes may be granted by the Dean of the Graduate School, Dean of my academic division, or by the University Librarian. It is understood that any copying or publication of this thesis for financial gain shall not be allowed without my written permission.

Signature ___________________________________

Date ______________________________________

The Structural Design, Simulation, and Analysis of a Wave Impact Simulation Device for the Component Flooding Evaluation Laboratory

by

Larinda Nichols

A thesis

submitted in partial fulfillment

of the requirements for the degree of

Master of Science in the Department of Nuclear Science and Engineering

Idaho State University

Spring 2018

COMMITTEE APPROVAL

To the Graduate Faculty:

The members of the committee appointed to examine the thesis of Larinda Nichols find it satisfactory and recommend that it be accepted.

Dr. Bruce Savage,

Major Advisor

Dr. Chad Pope,

Committee Member

Dr. Brian Williams,

Graduate Faculty Representative

To my children, Dennis and Ayla…

May you never forget how we got here. There are no words that can describe my love for you.

Thank you for helping mommy achieve her goals.

To my own mother…

What a long strange trip this has been. I couldn't have done it without you.

To my Sammy…

You are truly my Atlas.

ACKNOWLEDGEMENTS

Dr. George Imel for his countless hours of patience with me. I am in constant awe of his humble brilliance. I want to be Dr. Imel when I grow up.

Dr. Chad Pope. You make every student feel uniquely important even though you are the busiest man I know. Thank you for teaching me the importance of balance. Your leadership and encouragement has helped me to accomplish more than I ever thought possible.

VITA

Larinda is the youngest of her four siblings, all born and raised in Southeast Idaho. On the day Larinda was born, her older brother Myron crawled under the kitchen table and cried. He was devastated that his mother had given birth to yet another girl and not the little brother he had wanted so badly. So like all good brothers, he decided instead to teach Larinda everything a boy should know. How to ride a bike. How to ride horses. How to snow machine and 4-wheel. He even taught Larinda how to wrestle. The elementary wrestling coaches were sure it was only a joke when she showed up to practice in her black spandex shorts with the pink ruffle. But Larinda made her brother very proud when she took 2nd place in the wrestling tournament that year. When she entered high school, Larinda decided it was time to support her wrestling buddies in a “less awkward way,” so she turned in her wrestling outfit for a pair of pom-poms.

After high school, Larinda went on to receive a degree in Graphic Communications from Idaho State University. She worked in Pocatello for three years at a local magazine company until the birth of her first child Dennis, followed by his little sister Ayla two years later. Larinda stayed at home and raised the two children until the youngest started kindergarten. But rather than going back to work, Larinda realized that nothing could be as challenging as raising two toddlers. So, she came back to ISU to embark on what would become a seven-year adventure in Nuclear and Mechanical Engineering.

TABLE OF CONTENTS

LIST OF FIGURES

LIST OF TABLES

LIST OF ABBREVIATIONS

BWR	Boiling Water Reactor
CFD	Computational Fluid Dynamics
CFEL	Component Flooding Evaluation Laboratory
FEA	Finite Element Analysis
INL	Idaho National Laboratory
LWRS	Light Water Reactor Sustainability
NRC	Nuclear Regulatory Commission
PET	Pressurized Evaluation Tank
PWR	Pressurized Water Reactor
WISD	Wave Impact Simulation Device

ABSTRACT

Structural Design, Simulation, and Analysis of a Wave Impact Simulation Device

for the Component Flooding Evaluation Laboratory

Thesis Abstract--Idaho State University (2018)

A Wave Impact Simulation Device (WISD) has been designed for the Idaho State University Component Flooding Evaluation Laboratory (CFEL). The WISD will be used to test the resilience of components and component sub-assemblies when subjected to a 10 ft. by 10 ft. jet of water using a pneumatically driven, ten level water system. The ten channels shall be constructed of 10 ft. x 10 ft. x 3/8 in. thick, A36 steel plates supported by interspersed 1/4 in. steel rod supports. The gates of the prototype shall be 1-3/4 in. keyed shafts with 3/8 in thick steel, rectangular plates spanning the width of each channel. Electromagnets will be used for the gate mechanism to achieve a 90.8 rad/s angular velocity and 90-degree travel time of 0.02 seconds.

Key Words: wave impact simulation, component flooding evaluation, tsunami research

1. INTRODUCTION

"To stay the course, sometimes you have to make waves."

(Author Unknown)

In 2017, the United States obtained approximately 20% of the nation's electrical energy from nuclear power. Of the 99 licensed to operate nuclear power plants, 65 are Pressurized Water Reactors and the remaining 34 are Boiling Water Reactors (World Nuclear Association 2018). Both require large quantities of water. Not only is water used to transfer the heat energy from the reactor to the steam turbines, but it is also essential for cooling and moderating the reactor core. Thus, it is reasonable that these nuclear plants were built near large bodies of water, where a continuous and plentiful supply of coolant is readily obtainable.

The drawback to this strategy was never more apparent than on March 11, 2011 when tsunami waves of approximately 50 feet eventually led to the meltdown of three reactor cores at the Fukushima Daiichi Nuclear Power Plant. An estimated 940 PBq (25,405,405 Ci) of radioactivity was released in just six days (World Nuclear Association 2017). It was one of the most massive nuclear accidents occurring to date, and it dealt yet another sharp blow to an already struggling nuclear industry.

Within four months, the United States Nuclear Regulatory Commission (NRC) had established a "Near-Term Task Force" to review its current processes and regulations. A classified report, also dated four months after Fukushima, identified 34 nuclear plants considered to be "at heightened risk of flood damage due to upstream dam failures" (Perkins, Bensi, Philips, and Sancaktar 2011). The true potential of flood damage was now realized. Complex testing on individual components and component subassemblies under various flooding conditions was essential in circumventing future nuclear disasters.

In 2015, a partnership between the U.S. Department of Energy's Light Water Reactor Sustainability Program (LWRS) and Idaho State University's Component Flooding Evaluation Laboratory (CFEL) was formed to improve flood risk analysis at nuclear power plants. The experimental program would develop fragility curves and reliability models based on water rise, spray, and wave impact testing. Risks associated with both internal and external flooding to nuclear power plants would then be identified and used to better quantify safety margin.

Currently, the CFEL team is collecting valuable experimental data using a portal evaluation tank, referred to as the PET. Commercial doors, both hollow and steel, are tested for failure using the PET's unique structural capabilities. Data on flowrate, pressure, mode of failure, and fracture patterns all contribute to the development of the fragility curves and reliability models necessary for a more accurate risk assessment. Additionally, the relationship between water height and door strength observed by the CFEL team has already provided previously unknown information to the LWRS Program.

A second structure, known as the Wave Impact Simulation Device (WISD), is also proposed for component testing at CFEL. The device will simulate impact forces equivalent to those of a full-scale tsunami wave by way of rapid water acceleration. Component resilience, response, and/or failure when subjected to these forces will be observed, and the data extracted from each experiment will be used to further advance the analysis models being developed by the team. The following thesis shall focus on the development of a physical prototype for the WISD.

2. BACKGROUND

The work performed in this thesis is a continuation of research begun in 2015 by Gregory David Roberts. In his thesis “Research and Development of a Wave Impact Simulation Device for the Idaho State University Component Flooding Evaluation Laboratory,” Roberts successfully identified the concept for a high velocity jet to satisfy the requirements of the project. Namely, the velocity and momentum of a 20 ft. wave must be replicated in a near vertical 10 ft. by 10 ft. section of water for impact testing (Roberts 2016).

Roberts’ approach to tsunami wave celerity was to use shallow water wave equations. He justified his approach by stating the governing characteristics of tsunami waves during impact include an inundation and turbulence that cannot be described by generalized wave theory. Under this assumption, Roberts found that a 20 ft. wave would have a maximum horizontal fluid velocity of 25.4 ft/s. Obtaining the constant 25.4 ft/s velocity was made a key requirement for the WISD.

Using the computational fluid dynamics (CFD) software Flow-3D, Roberts was able to simulate resultant wave profiles for various device geometries, configurations, and driving mechanisms. Ten design approaches were documented in his work. His conclusion was that the most promising design for delivering a near vertical, 10-ft. by 10-ft. wave, at 25.4 feet per second was to use a system of plates coupled with rapid response gates. Roberts WISD concept is illustrated in Figure 1 and Figure 2.

Roberts concluded his research by recommending the most viable displacement mechanism for accelerating the static reservoir section of water to its required velocity before exiting the plate section would be a pneumatic air system. Adjustments to the angle of entry and length of exit conduit were also recommended as they were found to have a substantial impact on the velocity and flow profile.

The following thesis includes research, calculations, simulations, and analyses on the many iterations undertaken by the WISD team to design a device meeting all project requirements as established by Roberts.

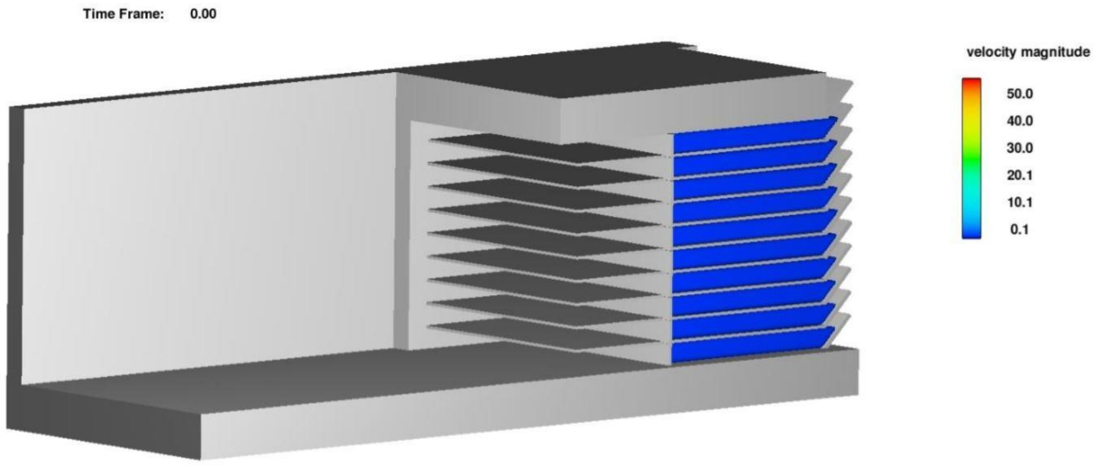

Figure 1. WISD concept developed by Gregory Roberts at t = 0 seconds (Roberts 2016).

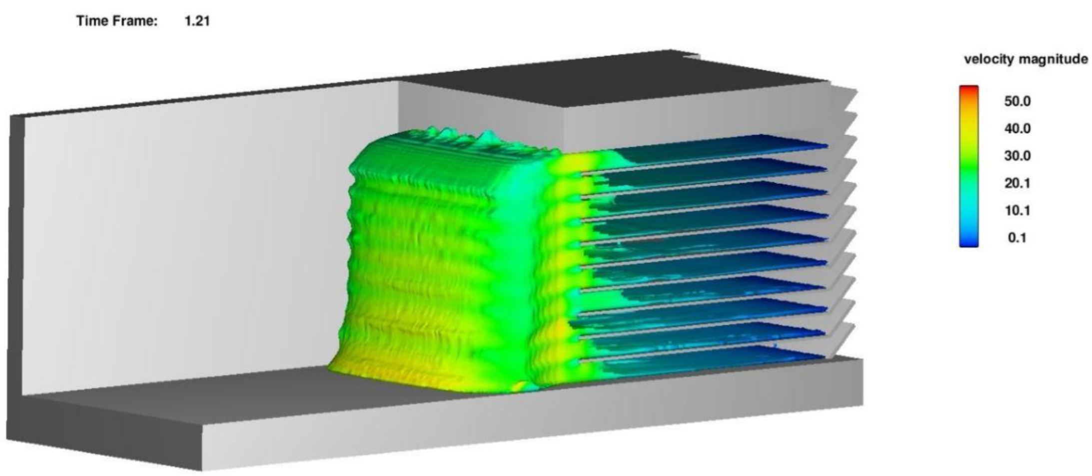

Figure 2. WISD concept developed by Gregory Roberts at t = 1.21 seconds (Roberts 2016).

3. LITERATURE REVIEW

The purpose of the WISD is to subject various components and component subassemblies to worse-case, wave impact scenarios, then observe their response. The device must be of sufficient strength to withstand the forces generated by a substantial volume of water in both stationary and turbulent flow conditions, but also sleek enough to minimize interference with the desired wave formation. A successful solution to these requirements would first require preliminary research. A literature review was performed to glean information from other current laboratory wave generation methods.

3.1 PAST AND CURRENT TSUNAMI SIMULATION MODELS

Historically, analytical approaches to tsunami research date back to as far as 1896 after the Meiji Great Sanriku Tsunami claimed 22,000 Japanese lives (Shuto and Fujima 2009). Wave heights up to 30 ft. were recorded as far as the Hawaiian Islands (Yuichiro 2001). Rudimentary countermeasures for evacuation where introduced in 1933 when the largest recorded normal-faulting earthquake in history produced the Showa Great Sanriku Tsunami (Okal, Kirby and Kalligeris 2016). By 1941, tsunami forecasting and admonitions to relocate dwelling houses to higher ground were based on severe weather patterns. Then, proactive measures in tsunami engineering for elaborating coastal structures for tsunami defense were sought after the 80-ft. waves of the 1960 Chilean Tsunami left two million homeless (Pallardy 2017). But in 1983, the unanticipated Japan Sea Earthquake Tsunami wreaked havoc during an otherwise beautiful, fair-weather day. The need for more comprehensive tsunami disaster prevention had become imperative (Shuto and Fujima 2009).

Today, tsunami disaster prevention continues through event forecasting, defense structures, and evacuation. However, tsunami research has evolved into a far more complex subject, and a deeper investigation into tsunami-resistance has begun to develop (Shuto and Fujima 2009). Discussing all the many facets of tsunami research is well beyond the scope of this paper. Instead, the following sections will focus primarily on the methods used for laboratory wave generation. The intent of approaching the literature review in this manner was to determine which methods, if any, could be applicable to the design of the WISD prototype.

HR Wallingford and University College London, United Kingdom

The collaborative efforts of Hydraulics Research (HR) Wallingford and the University College of London has resulted in the design and construction of three generations of tsunami simulators. The First Generation Tsunami Simulator, developed in 2008, was a 5.9 ft. tall, 3.9 ft. wide, and 15.7 ft. long tank with a variable height outlet placed in a 147.6 ft. long, 3.9 ft. wide, 2-dimensional flume, (see Figure 3). The flume replicated long duration tsunami waves on a 1:50 scale using a pneumatic system and almost 20,000 gallons of water. To generate waves, the First Generation Tsunami Simulator pulled water from the test flume into a sealed tank using a high capacity vacuum pump. Once the tank was full, the vacuum was released using an air control valve. The water rushing back into the test flume took on the desired waveform. The shape of the waveform generated was controlled by adjusting the position of the air control valve. Vacuum pressure in the tank was controlled using a computer automated 45-degree butterfly valve, (Allsop, Chandler, and Zaccaria 2014).

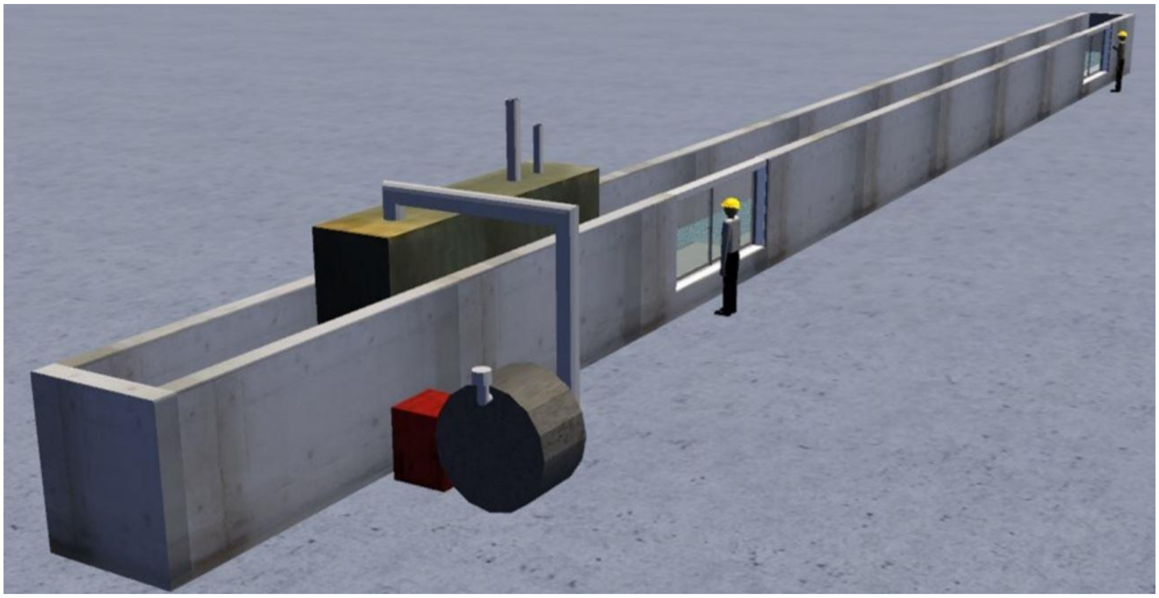

Figure 3. Simulated model of the First Generation Tsunami Simulator.

In 2011, a CFD model of the First Generation Tsunami Simulator was developed to identify structural modifications that would be necessary to improve upon the initial design. Construction of a Second Generation Tsunami Simulator was undertaken in 2014. The height and width of the tank were increased to 11.5 ft. and 5.9 ft., respectively. The tank length was decreased to 13.1 ft. and the variable height of the outlet in the First Generation was replaced with a permanent 1.3 ft. outlet. A flow shaper was also added to the outlet to reduce the amount of turbulence generated by the wave, (Allsop, Chandler, and Zaccaria 2014).

The Second Generation Tsunami Simulator flume length and width was likewise increased to 328.1 ft. and 5.9 ft., respectively. This allowed for more uniform wave development, as well as increased the range of processes and structures to be tested. A second vacuum pump, two ultrasonic level sensors, and updated computer software were also included in the modifications for the new design, (Allsop, Chandler, and Zaccaria 2014).

The Third Generation Tsunami Simulator was developed in 2016 to improve generation of crest-led and trough-led tsunamis. Installed in the HR Wallingford 13.1 ft. wide by 229.7 ft. long Fast Flow Facility, the tank is 13.1 ft. tall, 13.1 ft. wide, and 14.4 ft. long, with an outlet height of 1.31 ft., (see Figure 4). This latest iteration of tsunami simulator uses a proportional-integral-derivative (PID) feedback system for closed-loop wave generation. Current testing includes the investigation of tsunami run-up, forces and pressures on seawalls, and forces acting on single buildings. (Chandler, Allsop, Granged, and McGovern 2016).

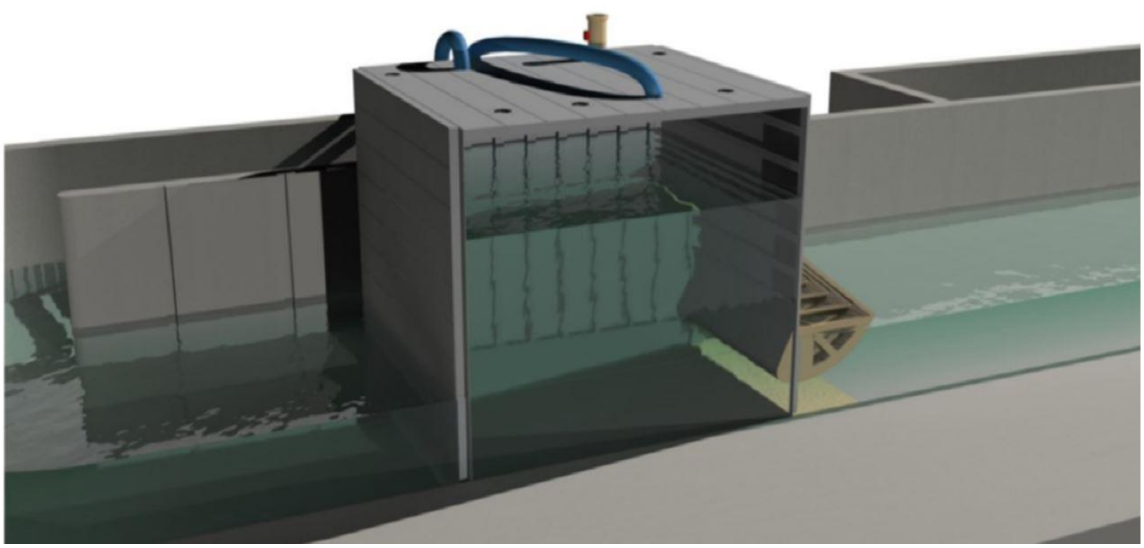

Figure 4. Simulated model of the Third Generation Tsunami Simulator.

All three HR Wallingford Tsunami Simulators use pneumatics in lieu of the traditional piston approach for creating waves. This design allows for longer wave periods to be generated, up to 2 minutes (Lloyd and Rossetto 2012).

Civil Engineering Department of Clemson University, United States

The rectangular wave tank located at the Flow Physics Laboratory of Clemson University is 40 ft. long, 2 ft wide and 2 ft deep, (see Figure 5). The five modular sections of the wave tank are constructed using clear plexiglass panels, supported by grated steel framing. Waves are generated in the tank using a vertical plate driven by a linear actuator system. The linear actuator system consists of a horizontal actuator, servo-electrical motor, and logic controller. The 5 ft. stroke of the actuator moves the vertical plate in linear proportion to the input voltage signal of the logic controller. The maximum velocity and acceleration achieved by the piston-type system is 5 ft/s and 32.8 ft/s^2, respectively. A sand beach of 1:20 was installed at the opposite end of the tank from the actuator to mimic the environmental conditions of a tsunami-based event (Mohammadi and Testik, 2010).

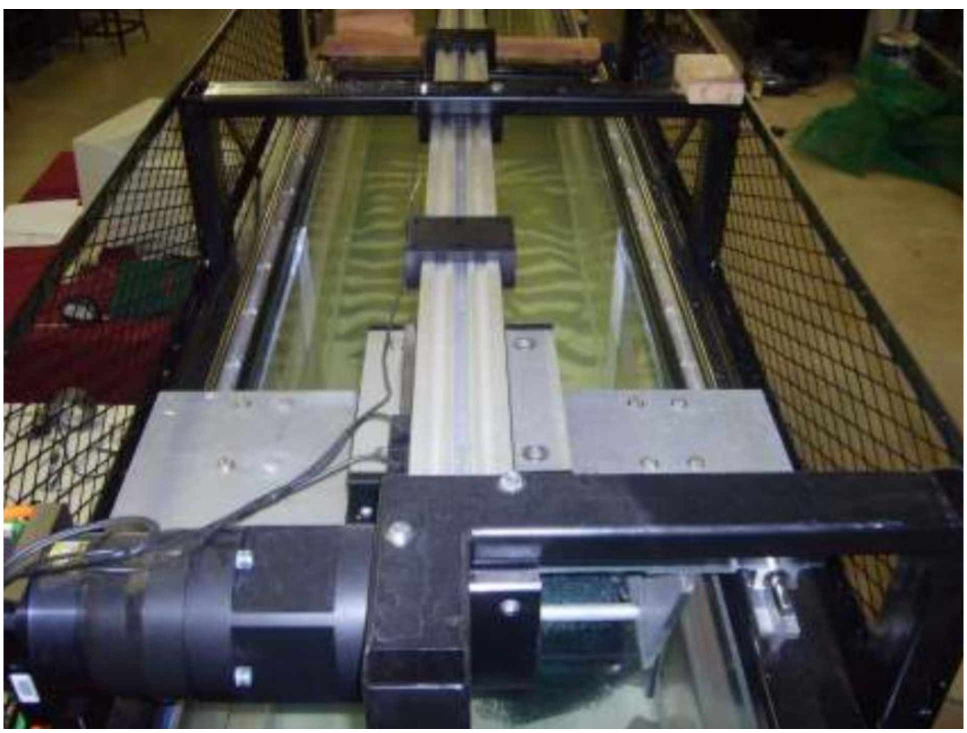

Figure 5. Piston-type wave generation in the Flow Physics Laboratory wave tank.

Plymouth University Marine Institute, United Kingdom

The Ocean Basin wave tank at the Coastal Ocean and Sediment Transport (COAST) laboratory of Plymouth University is primarily used for marine renewable energy testing in the UK. Waves up to 3 ft. high are generated by 24, hydraulically drive, paddle-type wave boards. The basin is approximately 115 ft. long, 50 ft. wide, and 10 ft. deep basin, (see Figure 6). A 6-degree, sloping, moveable floor and recirculating hydraulic system allows the Ocean basin to produce specialty waveforms for both short and long-crest waves (Kirke, Freeman, and Miranda 2015).

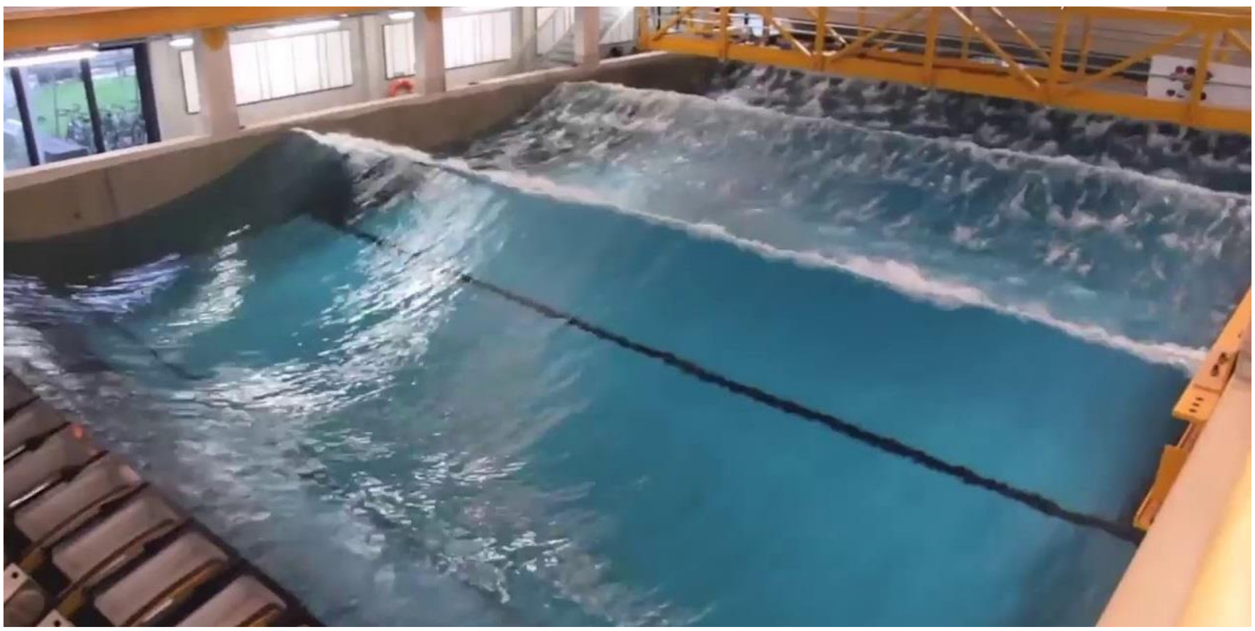

Figure 6. Ocean Basin wave tank at Plymouth University, UK.

LWI Institute for Hydromechanics, The Netherlands

The Deltares Delta Flume is considered one of the largest wave flume facilities in the world at 755 ft long, 16.5 ft wide, and 31 ft high, (see Figure 7). The reservoir for the flume contains 2.4 million gallons of water, approximately the capacity of four Olympic size swimming pools. Three pumping stations are needed to move the water to and from the flume at 264 gallons per second. The Delta Flume uses hydraulic cylinders to move 23 ft. piston-type wave boards. The waves produced by this motion can be up to 15 ft. high with wave periods from 1 to 20 seconds (Streicher, Hofland, and Lindenbergh 2013).

Figure 7. Top view of Delta Deltares wave flume.

National Institute of Maritime Port and Airport Research, Japan

The Large Hydro-Geo Flume (LHGF) was completed in 2000 under an initiative from the National Institute of Maritime Port and Airport Research Institute (PARI) to promote the redesign of naval and oceanic facilities for tsunami resistance. Large-scale experiments from 1:5 to 1:1 are conducted in the 604 ft. long, 11.5 ft. wide, 40 ft. deep flume to edify the potential failure of coastal structures and foundations, (see Figure 8). The flume also includes a 13 ft. deep bed of sand to simulate sea-seabed interactions (Shimosako, Takahashi, Suzuki, and Kang. 2002).

Regular and irregular waves up to 11.5 ft. are generated with piston-type wavemakers driven by the rack and pinion system of four AC electric servomotors. A current generator is also installed in the flume to produce a 6.5 ft/s current using two propeller pumps with a rotational speed of 240 RPM (Shimosako, Takahashi, Suzuki, and Kang. 2002).

Figure 8. Large Hydro-Geo Flume at PARI, Japan.

O.H. Hinsdale Wave Research Laboratory of Oregon State University, United States

The Large Wave Flume at Oregon State University is used for international research on wave-structure interactions, nearshore hydrodynamics and sediment transport, marine renewable energy, tsunami and coastal hazards, and fixed and floating structures. The flume is 342 ft. long, 12 ft. wide, and 15 ft. deep with a maximum water depth of 6.5 ft. for tsunami waves and 9 ft. for wind waves, (see Figure 9). A piston-type, hydraulic actuator moves a horizontal wave board at 13.1 ft/s using an oil hydraulic pump driven by a 140 hp servo-hydraulic electric motor. The 1:12 sloping beach at the end of the flume is used to measure wave runup and tsunami inundation (Rhinefrank, Sschacher, Prudell, and Hammagren 2010).

Figure 9. Large Wave Flume at Oregon State University.

W. M. Keck Hydraulics Laboratory of California Institute of Technology, United States

The W.H. Keck Hydraulics Laboratory West Tank is 123.8 ft. long, 2 ft. deep, and 15.5 in. wide, (see Figure 10). There are thirteen separate modules that make up the tank. Twelve of the modules are identical, while the thirteenth module includes a movable block section installed by J. L. Hammack in 1972 during his early attempts at tsunami wave generation. The walls of each module were constructed with glass panels, mounted to steel rails (Goring 1979).

The hydraulic system consists of a 40-gallon oil reservoir, a 7.5 hp piston-type pump, wire cloth filters, a 3000 psi unloading valve, two 10-gallon bladder accumulators, a servo-valve, and two 8 ft. hydraulic cylinders (Goring 1979).

Figure 10. West Tank at W.M. Keck Hydraulics Laboratory

3.2 CONCLUSIONS FROM LITERATURE REVIEW

The research conducted for the literature review revealed that the primary mechanism currently in use for wave generation is a hydraulically driven, piston-type wavemaker. The exception was the pneumatic approach used by HR Wallingford and the University College of London. However, the wave characteristics encountered for each of the aforementioned devices were not found to be consistent with the needs of the WISD for a near-vertical wave striking a previously un-inundated area. Furthermore, the space and budgetary requirements of integrating a piston-type or pneumatic method was not practical for the WISD project. The WISD design shall require a new approach to wave generation that has not yet been explored by other organizations.

4. DESIGN METHODOLOGY

The design conditions for the WISD were as follows:

1. Prototype shall have a discharge area of approximately 10 ft. x 10 ft.
2. Scale model shall be 1:5 of the prototype (2 ft. x 2 ft.).
3. Wave exiting discharge area shall have a near vertical flow profile.
4. Plates shall be designed for minimal thickness and minimal deflection.
5. Gates shall open near instantaneously.
6. Leakage through closed gates shall be minimal.

The framework for a WISD structural design meeting these design conditions included hand calculations, computational modeling, and finite element analysis. First, hand calculations were performed to determine appropriate plate thicknesses, shaft diameters, and gate requirements for the WISD prototype. These results were then used to create various models in SOLIDWORKS Simulation for finite element analysis (FEA). Once an acceptable design was found to meet all requirements of the project, a 1:5 scaled physical model was built for additional testing and refinement for a full-size prototype.

The WISD structural design team was comprised of three CFEL members. Rojin Tuladhar continued the computational FLOW-3D analyses begun by Gregory Roberts in 2015 to identify resultant pressure and configuration requirements for several team concepts. The electrical research and component integration performed by Jash Soumadipta enabled the team to retrieve actual velocity and flow data from the physical model. Larinda Nichols led the design and analysis for all mechanical and structural components to determine feasibility and compliance with the given design conditions.

The work identified in the following thesis is the result of all three members sharing information as they worked concurrently during each stage of the design process. As such, minor design parameters were often adjusted as the investigation into various concepts revealed previously unknown issues or advantages. For each adjustment made, an explanation has been included in this work.

5. SOFTWARE VALIDATION

5.1 HAND CALCULATIONS

Performing the initial calculations by hand served two purposes. First, the hand calculations provided a general estimate for the thickness requirements of each plate, depending on its support configuration. Second, the results from the hand calculations were then used to validate the SOLIDWORKS computational modeling software.

Due to the large width to thickness ratio anticipated for this application, equations from Roark's Formulas for Stress and Strain (6th Edition) were chosen as they specifically address thin metal plates with uniform cross-sections. Case No. 6 of Roark's Table 26, "Formulas for flat plates with straight boundaries and constant thickness" for a "rectangular plate, two long edges fixed, two short edges simply supported" was used under the assumption that each plate will be simply supported length-wise by the WISD housing using clamps or bolts. This case is illustrated below in Figure 11.

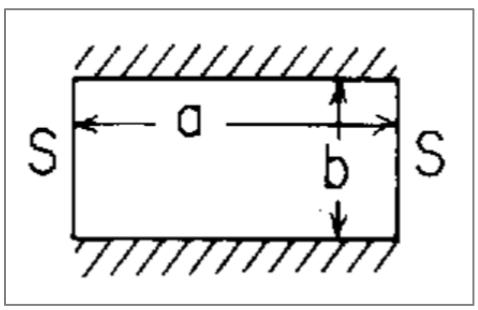

Figure 11. Case No. 6 for flat plates with straight boundaries and constant thickness (Young 1989).

Based on Case No. 6, the maximum stress at the center of the long edge of each plate can be found using Equation 1 below, where *q* represents a uniform pressure to the plate (in psi), *b* represents the width (in inches), *a* represents length (in inches) and *t* is the plate thickness (in inches). Specific variables for β are tabulated for each length to width ratio, (see Table 1).

$$Max\ \sigma = \frac{-\beta q b^2}{t^2} \quad [1]$$

Table 1. Tabulated Specific Values for β (Young 1989)

a/b	**1**	**1.2**	**1.4**	**1.6**	**1.8**	**2**	**∞**
β	0.4182	0.4626	0.4860	0.4968	0.4971	0.4973	0.500

The maximum deflection at the center of the plate can be found using Equation 2, where q, b, and t are the same values used in Equation 1, and E represents the Modulus of Elasticity of the material. Tabulated specific values for α are shown in Table 2.

$$Max\ y = \frac{-\alpha q b^4}{E t^3} \quad [2]$$

Table 2. Tabulated Values for α (Young1989)

a/b	**1**	**1.2**	**1.4**	**1.6**	**1.8**	**2**	**∞**
α	0.0210	0.0243	0.0262	0.0273	0.0280	0.0283	0.0285

The preliminary design conditions specified that each plate must support approximately 1 ft. of water. The hydrostatic pressure at this depth was found using the equation for hydrostatic pressure.

$$P = \gamma h \quad [3]$$

Assuming general atmospheric conditions at sea level, the specific weight of water (γ) is 63.4 lb/ft^3, or approximately 0.0361 lb/in^3. Multiplying the specific weight by the 12-inch depth, the pressure of the water was found to be 0.4333 psi. In Roark's formula's, pressure is represented by the variable q in the equations above. Also, the material properties used for the A36 carbon steel plates are shown in Table 3.

Table 3. Material Properties of A36 Plain Carbon Steel (Hibbeler 2005)

Elastic Modulus (psi)	Poisson's Ratio	Yield Strength (psi)	Mass Density (lb/in^3)
30,457,925	0.3	31,995	0.282

Equations 1 and 2 were used along with values obtained from Table 1, Table 2, and Table 3 to determine the maximum stress and deflection of 10 ft. x 10 ft., 5 ft. x 10 ft., and 2-1/2 ft. x 10 ft. plates of various thickness when supporting 1 ft. of water. Details of these calculations can be found in Appendix A, p 78.

Table 4. Maximum Yield and Deflection for a 10 ft. x 10 ft. Plate Using Roark's Formulas

	Ratio (w/l)	Tabulated Value	Tabulated Value	Pressure (psi)	Weight (lb)	Max Yield (psi)	Max Deflect (in)
	a/b	**β**	**α**	**q**	**w**	**σ**	**y**
3/8 in.	1	0.4182	0.021	0.433	1522	18557	1.175
1/4 in.	1	0.4182	0.021	0.433	1015	41753	3.965
3/16 in.	1	0.4182	0.021	0.433	761	74228	9.399
1/8 in.	1	0.4182	0.021	0.433	507	167012	31.72

Table 5. Maximum Yield and Deflection for a 5 ft. x 10 ft. Plate Using Roark's Formulas

	Ratio (w/l)	Tabulated Value	Tabulated Value	Pressure (psi)	Weight (lb)	Max Yield (psi)	Max Deflect (in)
	a/b	**β**	**α**	**q**	**w**	**σ**	**y**
3/8 in.	2	0.4973	0.0283	0.433	761	5517	0.099
1/4 in.	2	0.4973	0.0283	0.433	507	12413	0.334
3/16 in.	2	0.4973	0.0283	0.433	380	22067	0.792
1/8 in.	2	0.4973	0.0283	0.433	254	49650	2.672

Table 6. Maximum Yield and Deflection for a 2-1/2 ft. x 10 ft. Plate Using Roark's Formulas

	Ratio (w/l)	Tabulated Value	Tabulated Value	Pressure (psi)	Weight (lb)	Max Yield (psi)	Max Deflect (in)
	a/b	**β**	**α**	**q**	**w**	**σ**	**y**
3/8 in.	4	0.5000	0.0285	0.433	380	1387	0.006
1/4 in.	4	0.5000	0.0285	0.433	254	3120	0.021
3/16 in.	4	0.5000	0.0285	0.433	190	5547	0.050
1/8 in.	4	0.5000	0.0285	0.433	127	12480	0.168

Here it should be noted that for these formulas to remain applicable to the WISD plates, the following assumptions from Roark's Formulas for Stress and Strain must hold true: "(1) the plate is flat, of uniform thickness, and of homogeneous isotropic material; (2) the thickness is not more than about one-quarter of the least transverse dimension, and the maximum deflection is not more than about one-half the thickness; (3) all forces – loads and reactions – are normal to the plane of the plate; (4) the plate is nowhere stressed beyond the elastic limit" (Young1989).

All results from Table 4, Table 5, and Table 6 were in agreement with assumptions (1) and (3). However, assumption (4) requires that the maximum stress does not exceed the yield stress of the material. In comparing each result to the maximum yield strength of the A36 steel shown in Table 3, only the eight plates shown in Table 7 met assumption (4).

Table 7. Plate Geometries Meeting Roark's Requirement (4)

Plate Size	Weight (lb) w	Max Yield (psi) σ
10 ft. x 10 ft. x 3/8 in.	1522	18557
5 ft. x 10 ft. x 3/8 in.	761	5517
5 ft. x 10 ft. x 1/4 in.	507	12413
5 ft. x 10 ft. x 3/16 in.	380	22067
2-1/2 ft. x 10 ft. x 3/8 in.	380	1387
2-1/2 ft. x 10 ft. x 1/4 in.	254	3120
2-1/2 ft. x 10 ft. x 3/16 in.	190	5547
2-1/2 ft. x 10 ft. x 1/8 in.	127	12480

The final assumption, (3), requires a plate deflection less than half of the original thickness. Therefore, the deflection of each plate in Table 7 was then compared to its respective thickness. The four plates listed below in Table 8 were the only configurations shown to meet all four requirements.

Table 8. Plate Geometries Meeting All Four Roark's Requirements

Plate Size	**Weight (lb)**	**Max Yield (psi)**	**Factor of Safety**	**Max Deflect (in)**	**Max Deflect per Plate Thickness**
	w	**σ**	**N**	**y**	
5 ft. x 10 ft. x 3/8 in.	761	5517	5.8	0.099	0.26
2-1/2 ft. x 10 ft. x 3/8 in.	380	1387	23	0.006	0.02
2-1/2 ft. x 10 ft. x 1/4 in.	254	3120	10	0.021	0.08
2-1/2 ft. x 10 ft. x 3/16 in.	190	5547	5.8	0.050	0.27

After establishing reasonable solutions for plate thickness using the hand calculations above, each of the four configurations of Table 8 were modeled and using SOLIDWORKS computational software. All material properties, fixtures, and external load (pressure) were simulated to replicate the parameters and conditions assumed in the hand calculations. The FEA analysis for each study took approximately twenty minutes using SOLIDWORKS 2016 x84 Student Edition on an Intel(R)Core(M) i7-7700HQ CPU @ 2.80 GHz and 16.0 GB RAM. Mesh settings were set to solid, fine, and curvature-based. The results for each case are discussed below. Additional details of SOLIDWORKS Simulation settings can be found in Appendix B, p 89.

5.2 COMPARISON OF SOLIDWORKS RESULTS TO HAND CALCULATIONS

Validation 1: 5 ft. x 10 ft. x 3/8 in. A36 Steel Plate

The FEA analysis of the 5 ft. x 10 ft. x 3/8 in. plate showed a maximum yield stress of 5109 psi, approximately 400 psi less than the maximum yield stress calculated using Roark's formulas, (see Figure 12). The FEA maximum deflection was 0.111 in., a slight increase from the hand calculated value of 0.099 in, (see Figure 13).

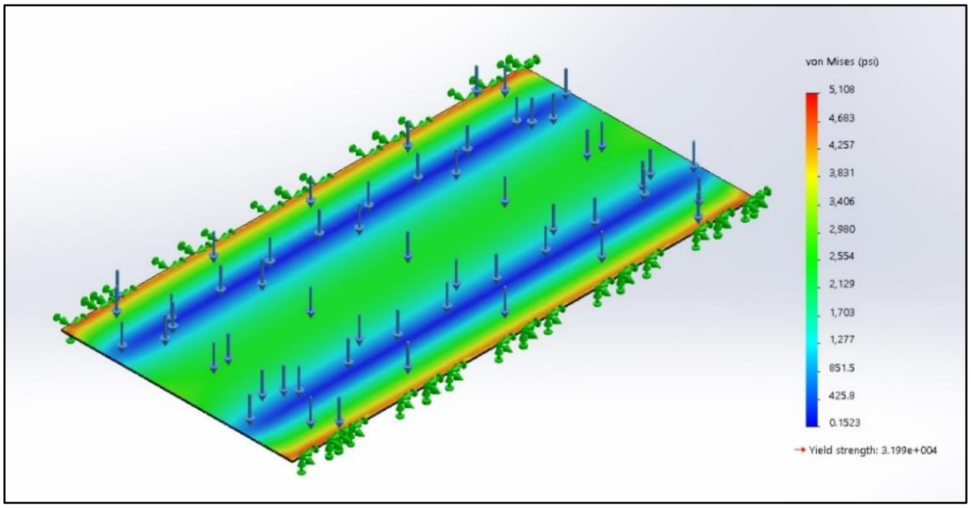

Figure 12. Von-Mises stress of the 5 ft. x 10 ft. x 3/8 in. plate with long edges fixed under 0.433 psi.

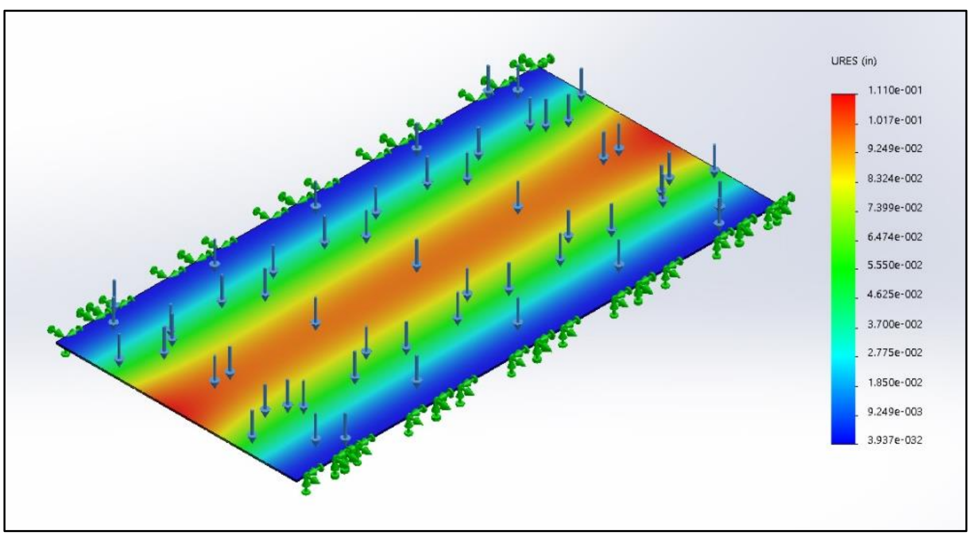

Figure 13. Deflection of the 5 ft. x 10 ft. x 3/8 in. plate with long edges fixed under 0.433 psi.

Validation 2: 2-1/2 ft. x 10 ft. x 3/8 in. A36 Steel Plate

The FEA analysis of the 2-1/2 ft. x 10 ft. x 3/8 in. plate showed a maximum yield stress of 1191 psi, approximately 200 psi less than the maximum yield stress calculated using Roark's formulas, (see Figure 14). The FEA maximum deflection was 0.007 in., in close agreement with the hand calculated value of 0.006 in., (see Figure 15).

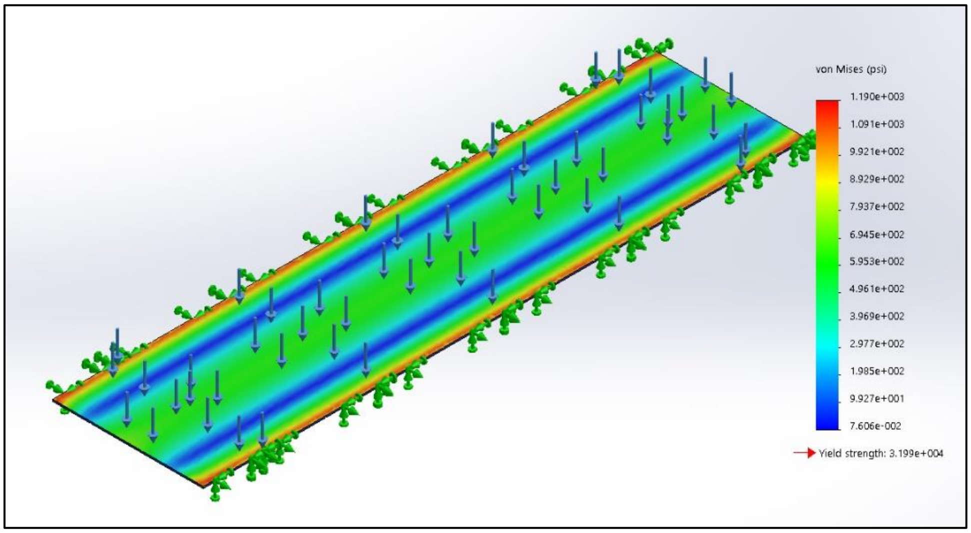

Figure 14. Von-Mises stress of 2-1/2 ft. x 10 ft. x 3/8 in. plate with long edges fixed under 0.433 psi.

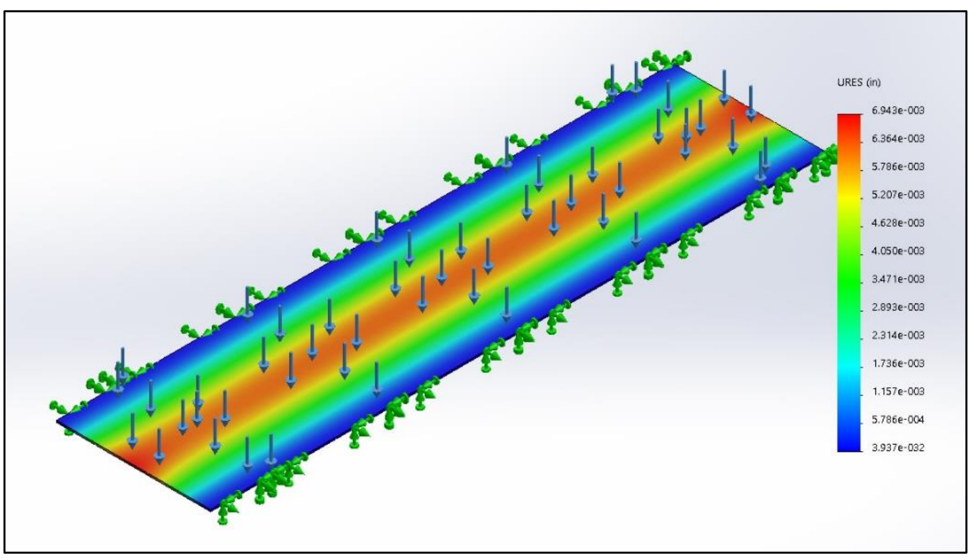

Figure 15. Deflection of 2-1/2 ft. x 10 ft. x 3/8 in. plate with long edges fixed under 0.433 psi.

Validation 3: 2-1/2 ft. x 10 ft. x 1/4 in. A36 Steel Plate

The FEA analysis of the 2-1/2 ft. x 10 ft. x 1/4 in. plate showed a maximum yield stress of 2689 psi, approximately 400 psi less than the maximum yield stress calculated using Roark's formulas, (see Figure 16). The FEA maximum deflection was 0.020 in., a slight increase from the hand calculated value of 0.021 in., (see Figure 17).

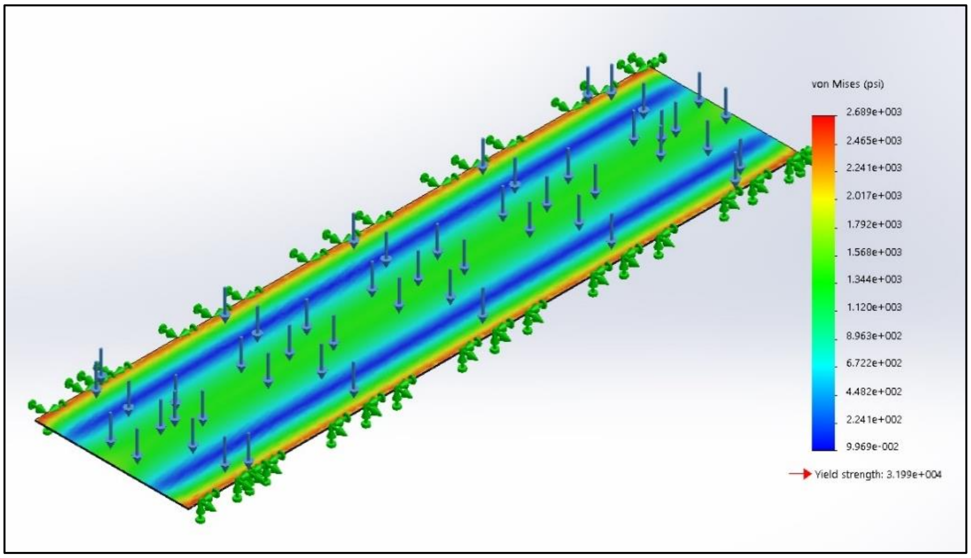

Figure 16. Von-Mises stress of 2-1/2 ft. x 10 ft. x 1/4 in. plate with long edges fixed under 0.433 psi.

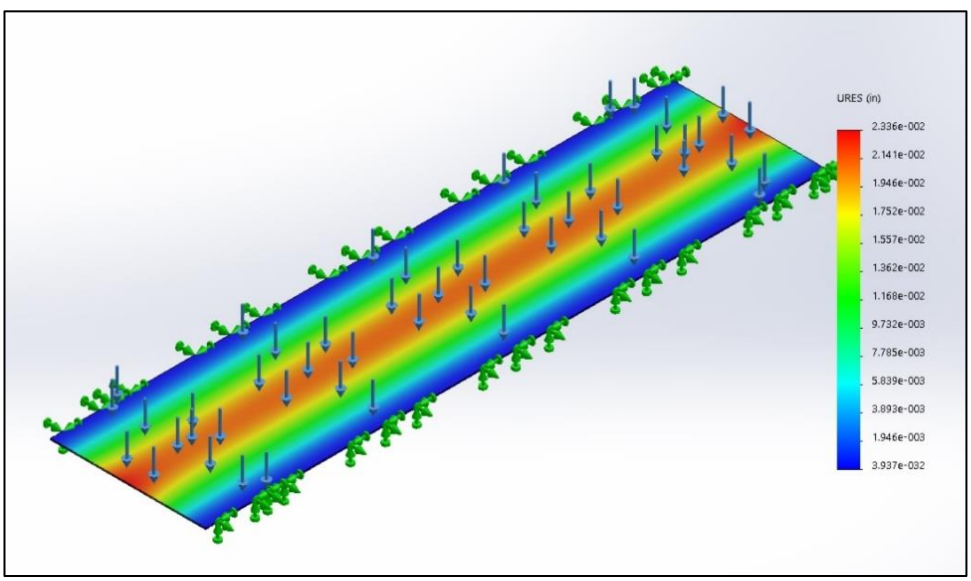

Figure 17. Deflection of 2-1/2 ft. x 10 ft. x 1/4 in. plate with long edges fixed under 0.433 psi.

Validation 4: 2-1/2 ft. x 10 ft. x 3/16 in. A36 Steel Plate

The FEA analysis of the 2-1/2 ft. x 10 ft. x 3/16 in. plate showed a maximum yield stress of 4703 psi, approximately 850 psi less than the maximum yield stress calculated using Roark's formulas, (see Figure 18). The FEA maximum deflection was 0.055 in., a slight increase from the hand calculated value of 0.050 in., (see Figure 19).

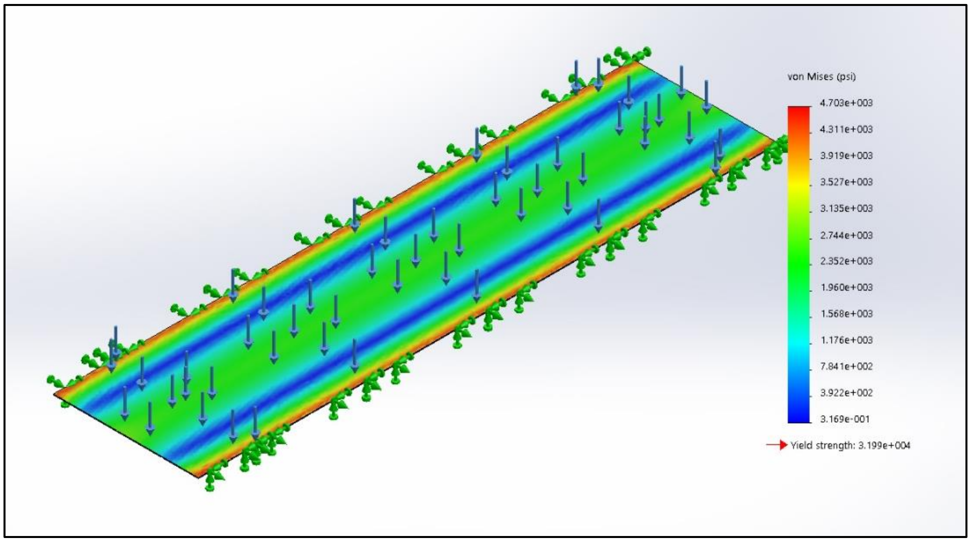

Figure 18. Von-Mises stress of 2-1/2 ft. x 10 ft. x 3/16 in. plate with long edges fixed under 0.433 psi.

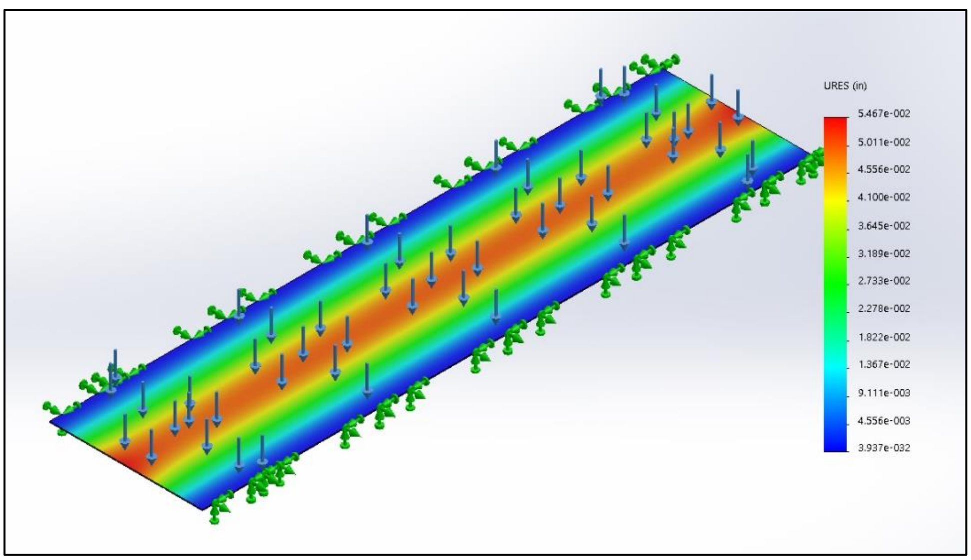

Figure 19. Deflection of 2-1/2 ft. x 10 ft. x 3/16 in. plate with long edges fixed under 0.433 psi.

Table 9 compares the results obtained using the SOLIDWORKS FEA versus those found using Roark's Formulas. Overall percent difference was within 16.5% for yield stress and 11.5% for deflection.

Table 9. Comparison of Hand Calculation and SOLIDWORKS FEA Results

PLATE SIZE	MAXIMUM YIELD STRESS (psi)			MAXIMUM DEFLECTION (in)		
	ROARK'S	SOLIDWORKS	% DIFF	ROARK'S	SOLIDWORKS	% DIFF
5 ft. x 10 ft. x 3/8 in.	5517	5109	7.70	0.099	0.111	11.5
2-1/2 ft. x 10 ft. x 3/8 in.	1387	1191	15.2	0.006	0.007	10.9
2-1/2 ft. x 10 ft. x 1/4 in.	3120	2689	14.9	0.021	0.023	10.5
2-1/2 ft. x 10 ft. x 3/16 in.	5547	4703	16.5	0.050	0.055	9.30

The uncertainty associated with Roark's Formulas is given by Young as approximately 7% due to the experimentally derived values for α and β used in each equation. SOLIDWORKS does not explicitly state uncertainty values for FEA results since each result is heavily dependent on the mesh settings used. Finer mesh settings require more complex calculations to be performed by the program; thereby, increasing the reliability of each outcome.

Both methods were deemed in satisfactory agreement, and the software was considered reliable for all further design. Validation was important since the model would become more complex as additional elements were added such as shafts, rods, gates, multiple plate configurations, etc., and hand calculations would be difficult and highly susceptible to more errors.

6. WISD PROTOTYPE DESIGN

Establishing an acceptable structural design for WISD was an iterative process based on preliminary hand calculations and computational modelling. First, adequate plate thickness had to be identified before an accompanying gate system could be developed. Then, the configuration of the gate system would dictate the mechanical aspects of WISD operation. Finally, a comprehensive review of the final design was necessary to ensure all components would operate as designed and not interfere with the processes of one another.

6.1 DESIGN AND ANALYSIS OF WISD PLATES

Establishing a plate thickness, geometry, and configuration best suited for the WISD prototype was the first step in the design process. The results of the software validation indicated that thinner plates could be used if the spanning width was decreased. Plates spanning the entire 10-ft. width would require additional thickness, but they would be less invasive on the developing wave than multiple sections per channel. Design iterations were used to identify the advantages and disadvantages of each option.

Plate Design Iteration 1: Four 2-1/2 ft. Plates per 10 ft. Wide Channel

Model Details: Four 2.5 ft. x 10 ft. x 3/32 in. A36 steel plates were designed to span the 10-ft. wide channel. A single plate was modeled with the long edges fixed from translation and rotation. A total of 36 plates would be required for the entire prototype, (see Figure 20). A uniform pressure of 0.433 psi was applied over the face of the plate.

FEA Results: The maximum von-Mises stress was observed to be 17,446 psi, (see Figure 21), with a maximum deflection of 0.044 in., (see Figure 22).

Remarks: The maximum stress did not exceed the 36,000 psi yield stress of A36 steel, and the 0.044 in. deflection was considered minimal. However, it was unclear how dividing the 10 ft. channel into four separate 2-1/2 ft. sections might affect the target flow profile. FLOW-3D models of the multiple channel configuration were created by WISD member, Rojin Tuladhar. The vertical flow profile appeared unchanged from a single channel of 10-ft width but installing supports for each section was considered a disadvantage. The team agreed more options should be explored.

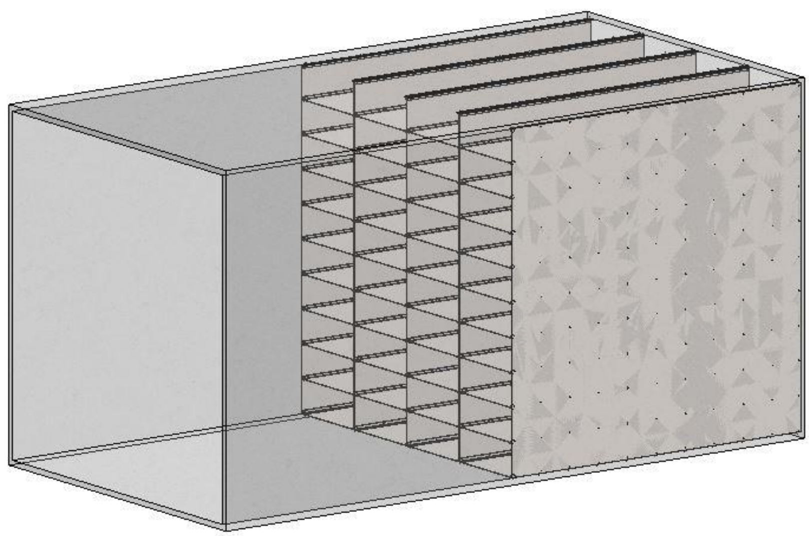

Figure 20. Overview of the 2-1/2 ft. x 10 ft. x 3/32 in. plate system.

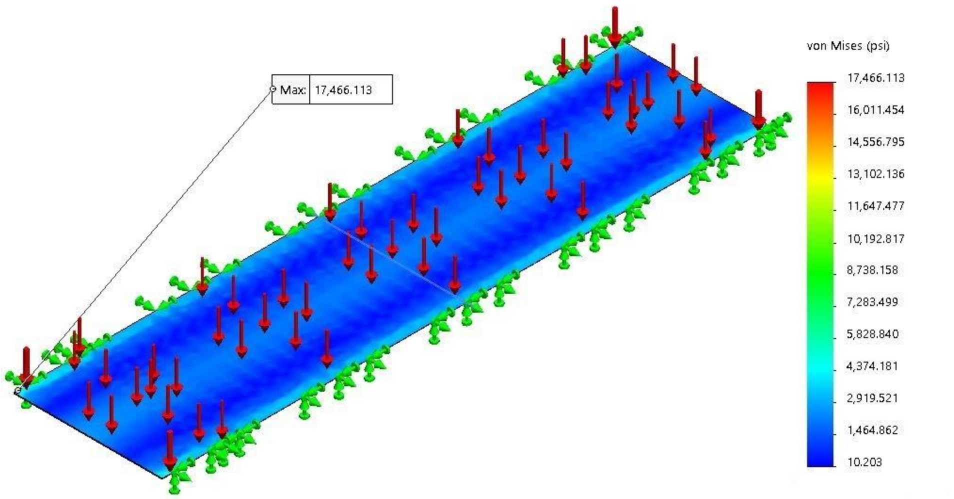

Figure 21. Von-Mises stress of a 2-1/2 ft. x 10 ft. x 3/32 in. plate with long edges fixed under 0.433 psi.

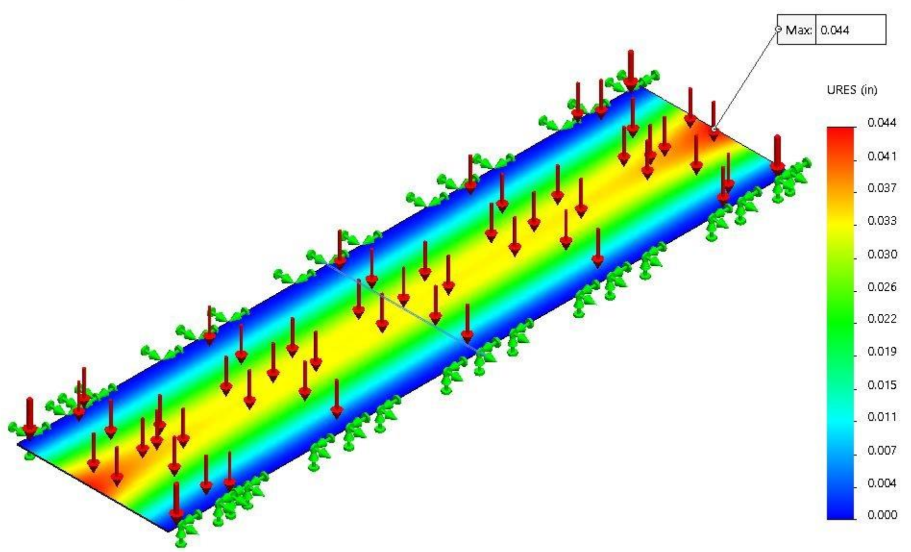

Figure 22. Deflection of a 2-1/2 ft. x 10 ft. x 3/32 in. plate with long edges fixed under 0.433 psi.

Plate Design Iteration 2: A Single 10 ft. Wide Plate per 10 ft. Channel

Model Details: A 10 ft. x 10 ft. x 1 in. thick plate was modeled with long edges fixed. A total of 9 plates would be required for the reservoir section of the prototype, (see Figure 23). A uniform pressure of 0.433 psi was applied over the face of the plate.

FEA Results: Maximum von-Mises stress was 2,743 psi, (see Figure 24). Maximum deflection was 0.099 in., (see Figure 25).

Remarks: Each 10 ft. x 10 ft. x 1 in. plate would weigh approximately 4,084 lbs., a significant issue for installation and safety issues. A 1 in. thick plate was also scrutinized as being highly disruptive to a developing flow profile. The solution was to use a thinner plate and investigate different options for supporting it.

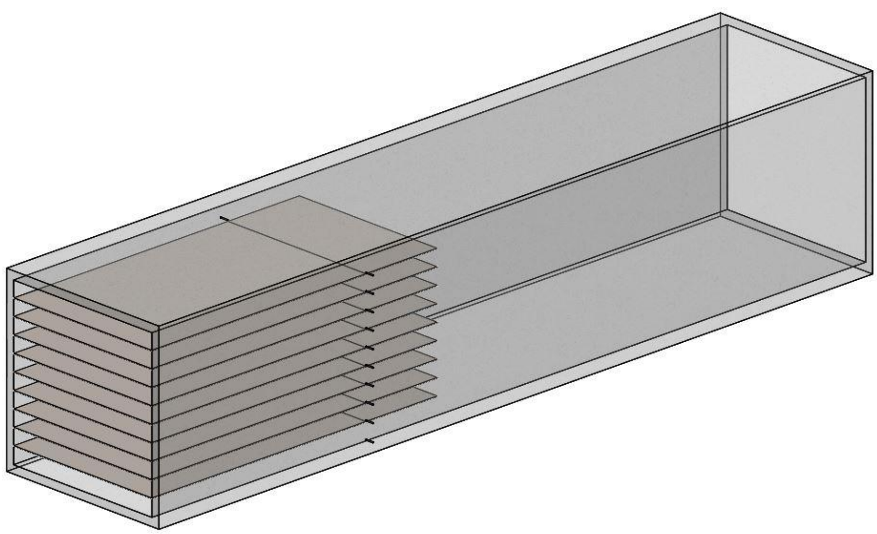

Figure 23. Overview of the 10 ft. x 10 ft. x 1 in. plate system.

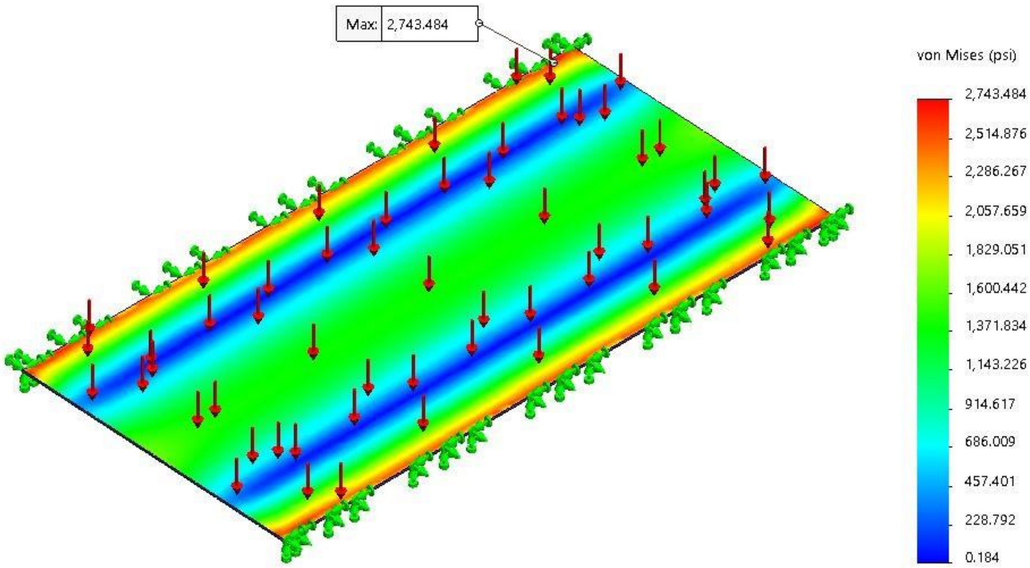

Figure 24. Von-Mises stress of a 10 ft. x 10 ft. x 1 in. plate with long edges fixed under 0.433 psi.

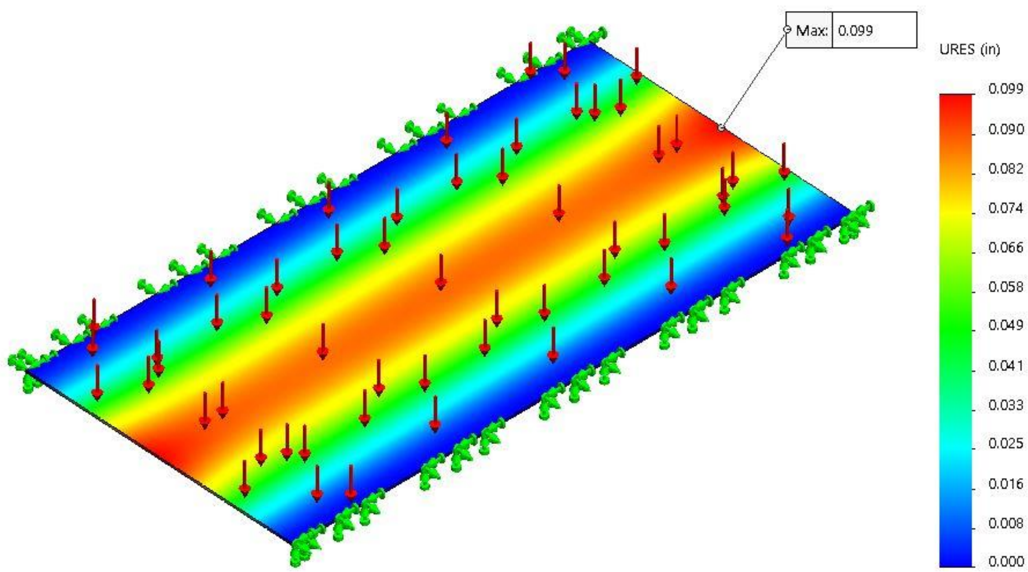

Figure 25. Deflection stress of a 10 ft. x 10 ft. x 1 in. plate with long edges fixed under 0.433 psi.

Plate Design Iteration 3: Plate Thickness Decreased and Number of Fixed Edges Increased

Model Details: A 10 ft. x 10 ft. x 3/8 in. plate was modeled with three sides fixed in place. A uniform pressure of 0.433 psi was applied over the face of the plate.

FEA Results: Maximum von-Mises stress was 19,327 psi, (see Figure 26). Maximum deflection was 1.852 in., (see Figure 27).

Remarks: The 19,327 psi maximum stress did not exceed the 36,000 psi yield stress of A36 steel, but the deflection was substantial at 1.852 in.. Additional support was deemed necessary.

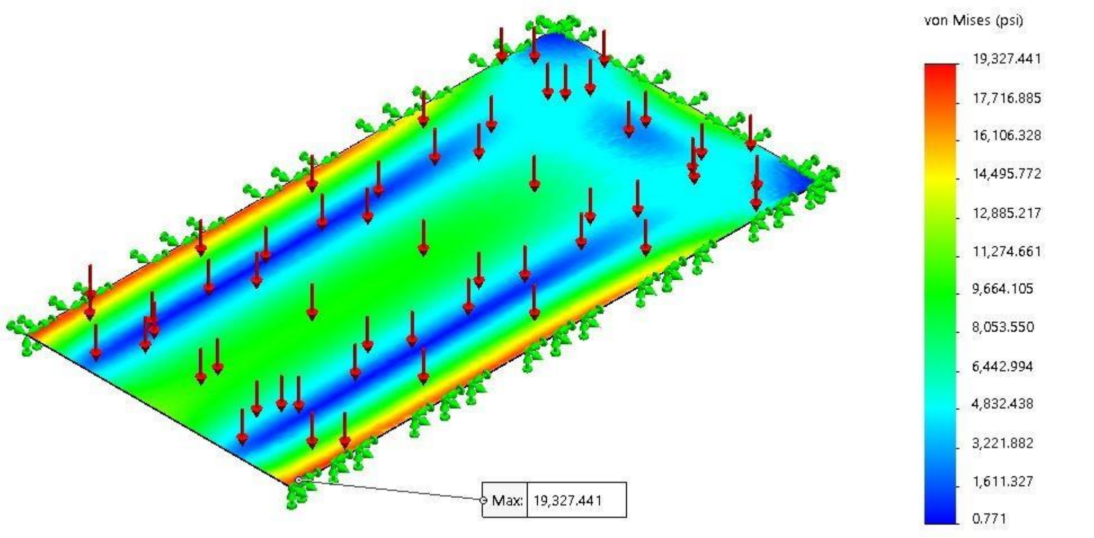

Figure 26. Von-Mises stress of a 10 ft. x 10 ft. x 3/8 in. plate with three fixed edges under 0.433 psi.

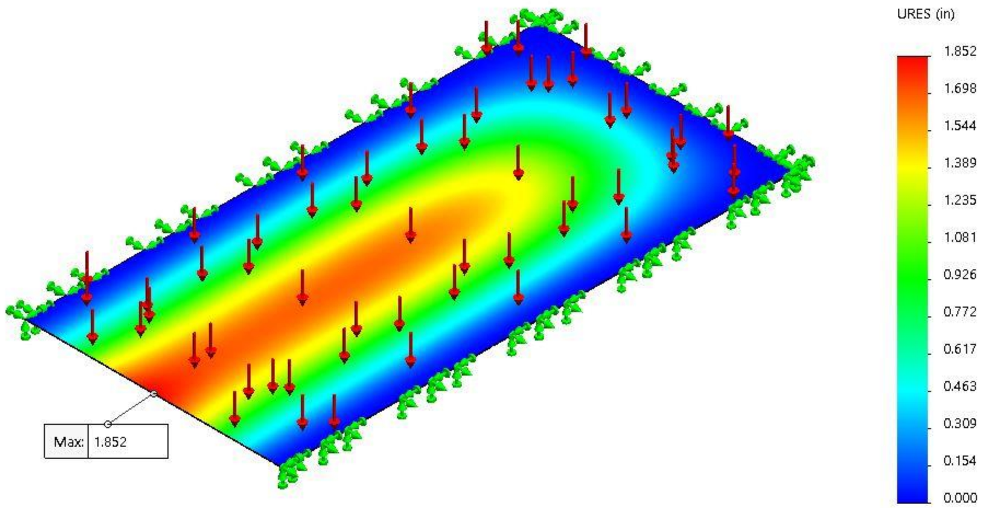

Figure 27. Deflection of a 10 ft. x 10 ft. x 3/8 in. plate with three fixed edges under 0.433 psi.

Plate Design Iteration 4: Fixed Edges Increased to all Four Sides of Plate

Model Details: A 10 ft. x 10 ft. x 3/8 in. thick plate was modeled with all four sides fixed. A uniform pressure of 0.433 psi was applied over the face of the plate.

FEA Results: Maximum von-Mises stress was 18,098 psi, (see Figure 28). Maximum deflection was 1.630 in., (see Figure 29).

Remarks: The maximum stress was reduced from 19,327 to 18,098 psi, and the deflection was reduced from 1.852 in. to 1.630 in. The deflection was still considered excessive. The team began research on thin supports to decrease deflection at the center of the plate.

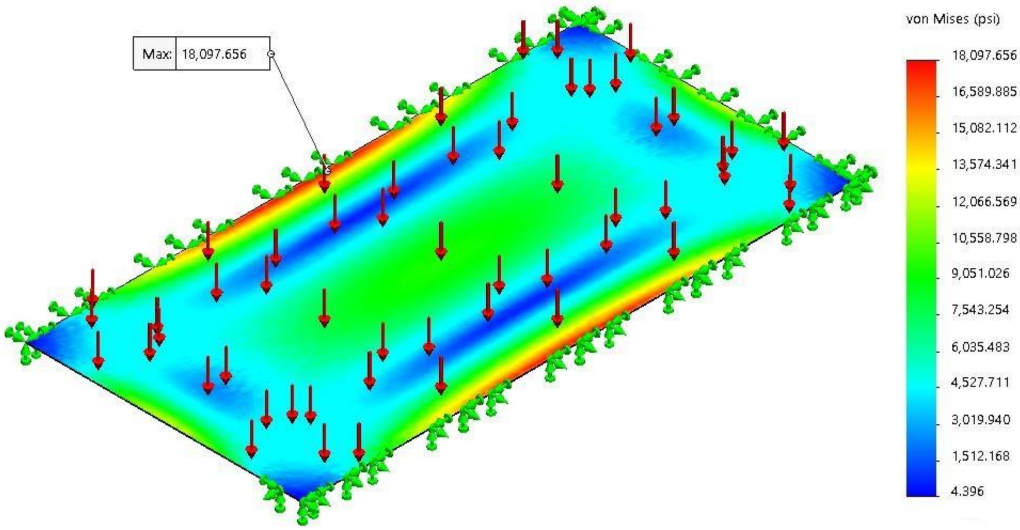

Figure 28. Von-Mises stress of a 10 ft. x 10 ft. x 3/8 in. plate with three fixed edges under 0.433 psi.

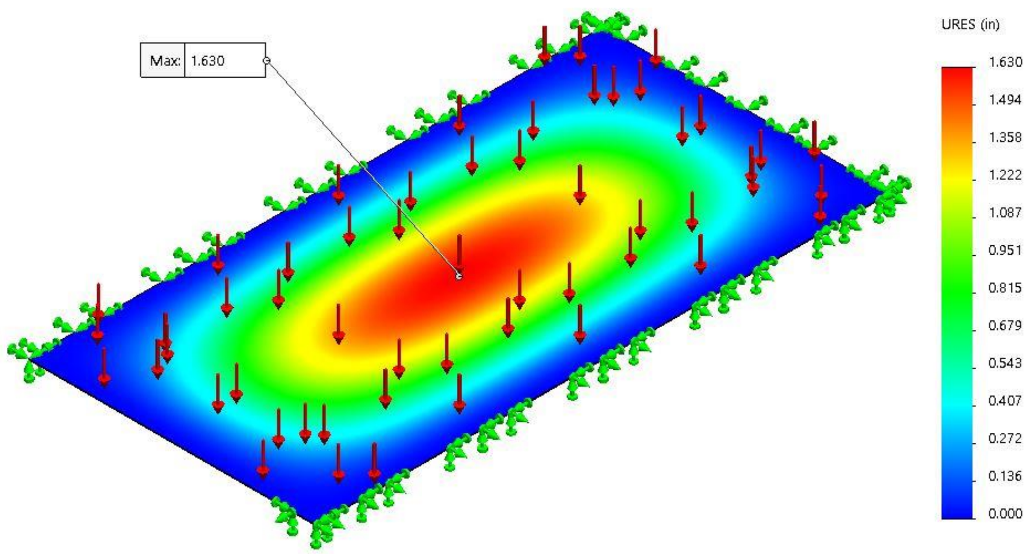

Figure 29. Deflection of a 10 ft. x 10 ft. x 1 in. plate with three fixed edges under 0.433 psi.

It was at this time in the design process that the concurrent FLOW-3D research being performed by WISD member Rojin Tuladhar showed that increasing the hydrostatic head from 1ft to 3 ft. would aid in the development of a near vertical flow profile. The FLOW-3D simulation also indicated as much as 20 psi of air pressure would be required to accelerate the water from stagnation to a constant 25.4 ft/s velocity before it exists the conduit.

The change in design parameters from 0.433 psi to approximately 21.3 psi substantially increased the difficulty in developing an adequately thin, yet adequately strong prototype plate. The need for additional plate supports became imperative. It was assumed that adding supports to the reservoir section would have less of an impact on the target velocity profile than adding supports to the plates located downstream of the gate system. Furthermore, the water contained in the post-gate section would not be static. It would be in constant motion when acting upon by the 20 psi horizontal, pneumatic force. As such, the design focus was shifted from the reservoir plates to the post-gate plates to determine the stress and deflection behavior under these new parameters.

Plate Design Iteration 5: Investigation of Static vs. Dynamic Effects on Post Gate Plates

Model Details: Nine 10 ft. x 5 ft. x 1/2 in. plates were modeled with three edges fixed in place (exit edge remained simply supported). All nine plates were included in the simulation to observe the overall behavior of the plate system, (see Figure 30). Two FEA studies were performed to compare the behavior of all nine plates when subjected to a static, then dynamic load. For the static study, a uniform 1.3 psi pressure was applied vertically to the top plane of each plate. The dynamic study included a non-linear, time-dependent study based on the 20 psi horizontal force also acting on the water column.

FEA Results: The static analysis showed a maximum von-Mises stress of 8,864 psi would develop in all nine plates when a 1.3 psi pressure is applied, (see Figure 31). The maximum deflection was 0.413 in., (see Figure 32). In the time-dependent analysis, the maximum von-Mises stress was 8,372 psi, (see Figure 33), and the maximum deflection was 0.442 in. for the 20 psi horizontal and 1.3 psi vertical loads, (see Figure 34 and Figure 35).

Remarks: The time-dependent simulation used 67 time steps from the onset of deflection to cessation. Figure 34 and Figure 35 each contain six time step images showing the deflection at each respective time step. The stress to each plate at maximum deflection is shown in Figure 33. A comparison between the two studies confirmed flowing water through all nine plates would yield maximum stress and deflection values similar to those of the static study. The minor variance between the two stress and deflection values were instead attributed to using two different FEA methods (static linear vs. dynamic non-linear) to solve the system. Regardless, the nearly 1/2 in. deflection was not considered acceptable. The plate thickness could not be increased any further, and the investigation into an alternative support system continued.

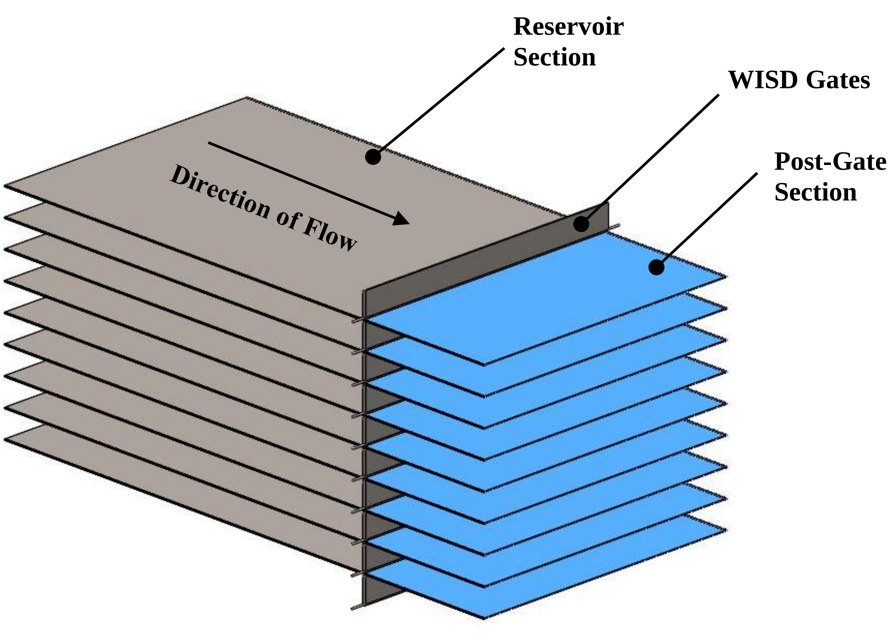

Figure 30. Overview of the 10 ft. x 5 ft. x 1/2 in. post-gate system.

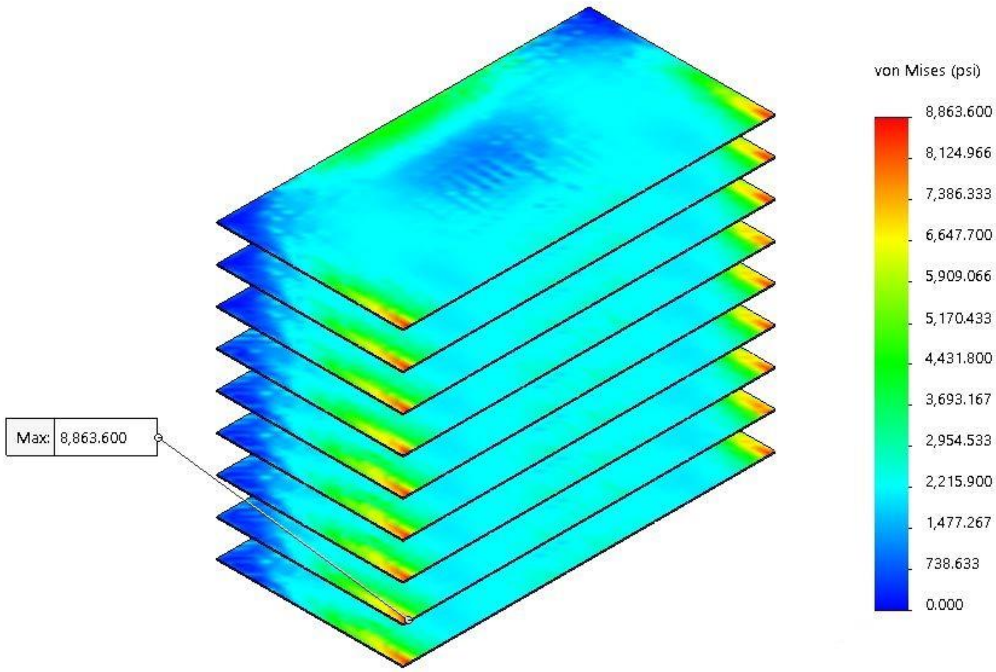

Figure 31. Von-Mises stress for nine 10 ft. x 5 ft. x 1/2 in. plates under a 1.3 psi static load.

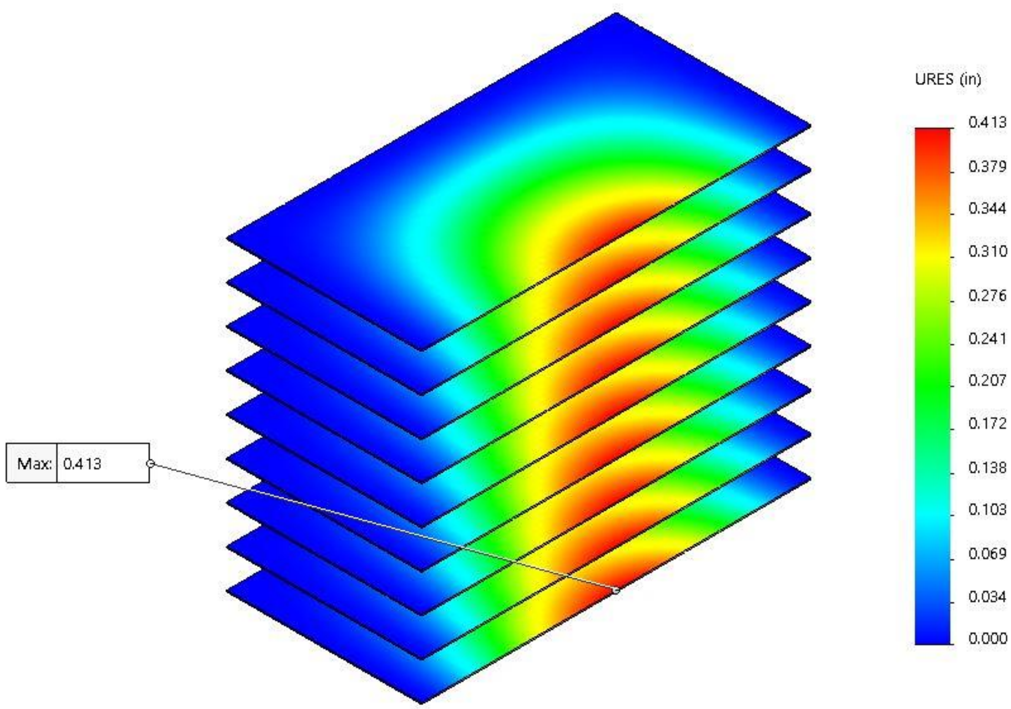

Figure 32. Deflection for the nine 10 ft. x 5 ft. x 1/2 in. plates under a 1.3 psi static load.

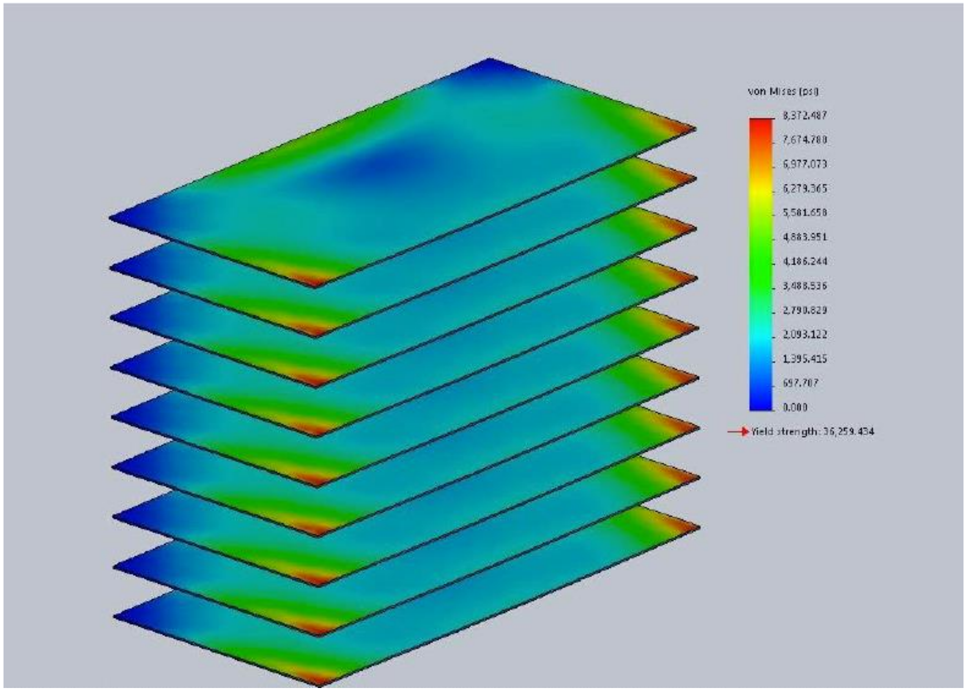

Figure 33. Von-Mises stress for the nine 10 ft. x 5 ft. x 1/2 in. plates under static and dynamic loading.

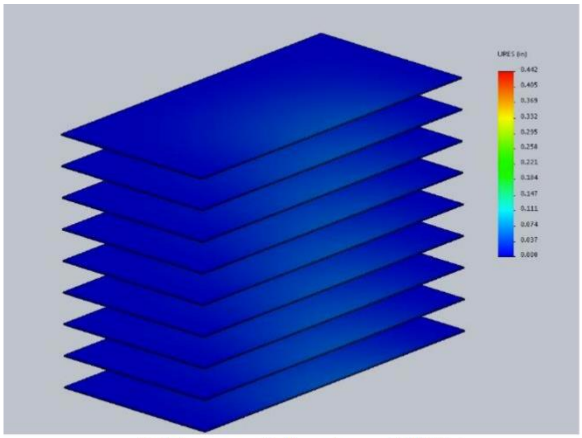

$t \approx 0.01s$, *max deflection* ≈ 0.053 *in.*

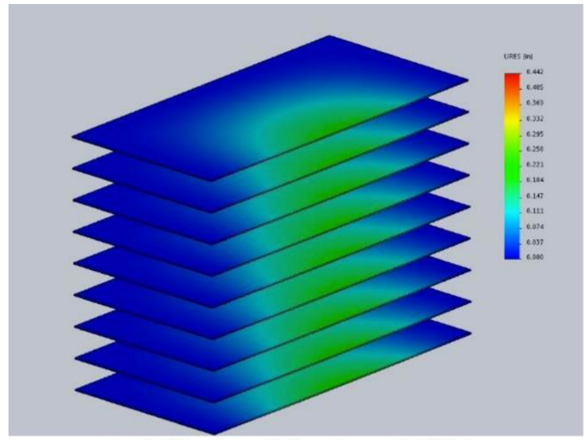

$t \approx 0.05s$, *max deflection* ≈ 0.201 *in.*

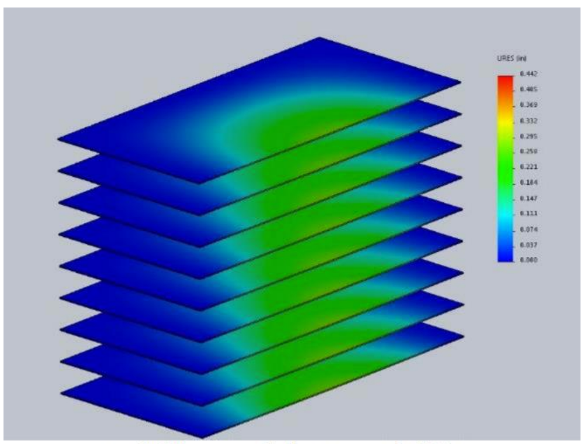

$t \approx 0.10s$, *max deflection* ≈ 0.278 *in.*

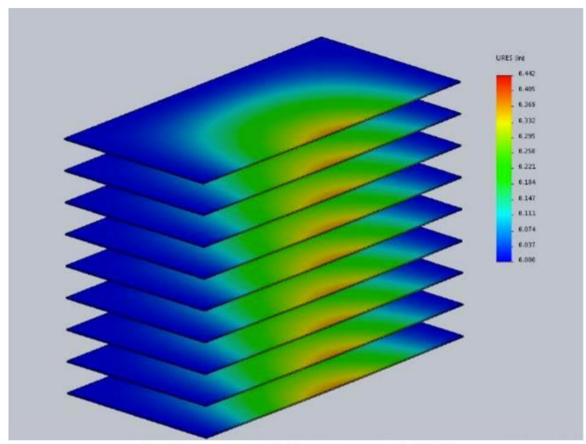

$t \approx 0.15s$, *max deflection* ≈ 0.370 *in.*

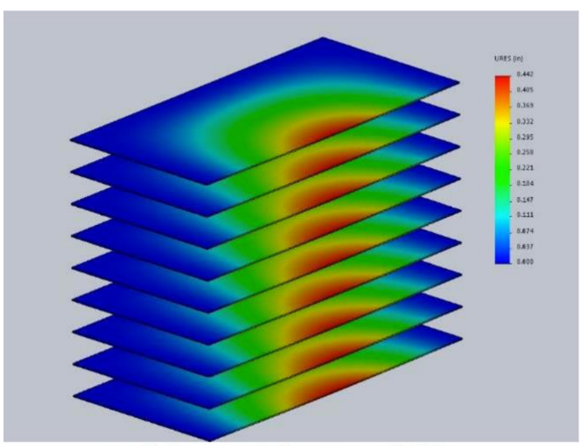

$t \approx 0.2s$, *max deflection* $= 0.442$ *in.*

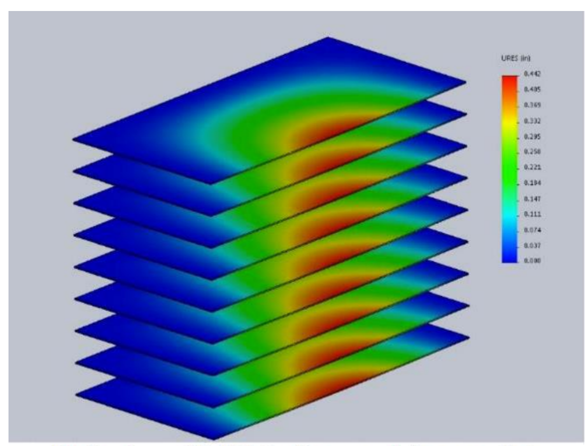

Deflection of 0.442 in. from $t \approx 0.2s$ *to* $t \approx 0.6s$

Figure 34. Onset of deflection of the 10 ft. x 5 ft. x 1/2 in. plates under static and dynamic loading.

(t =0.01 to t = 0.2 seconds)

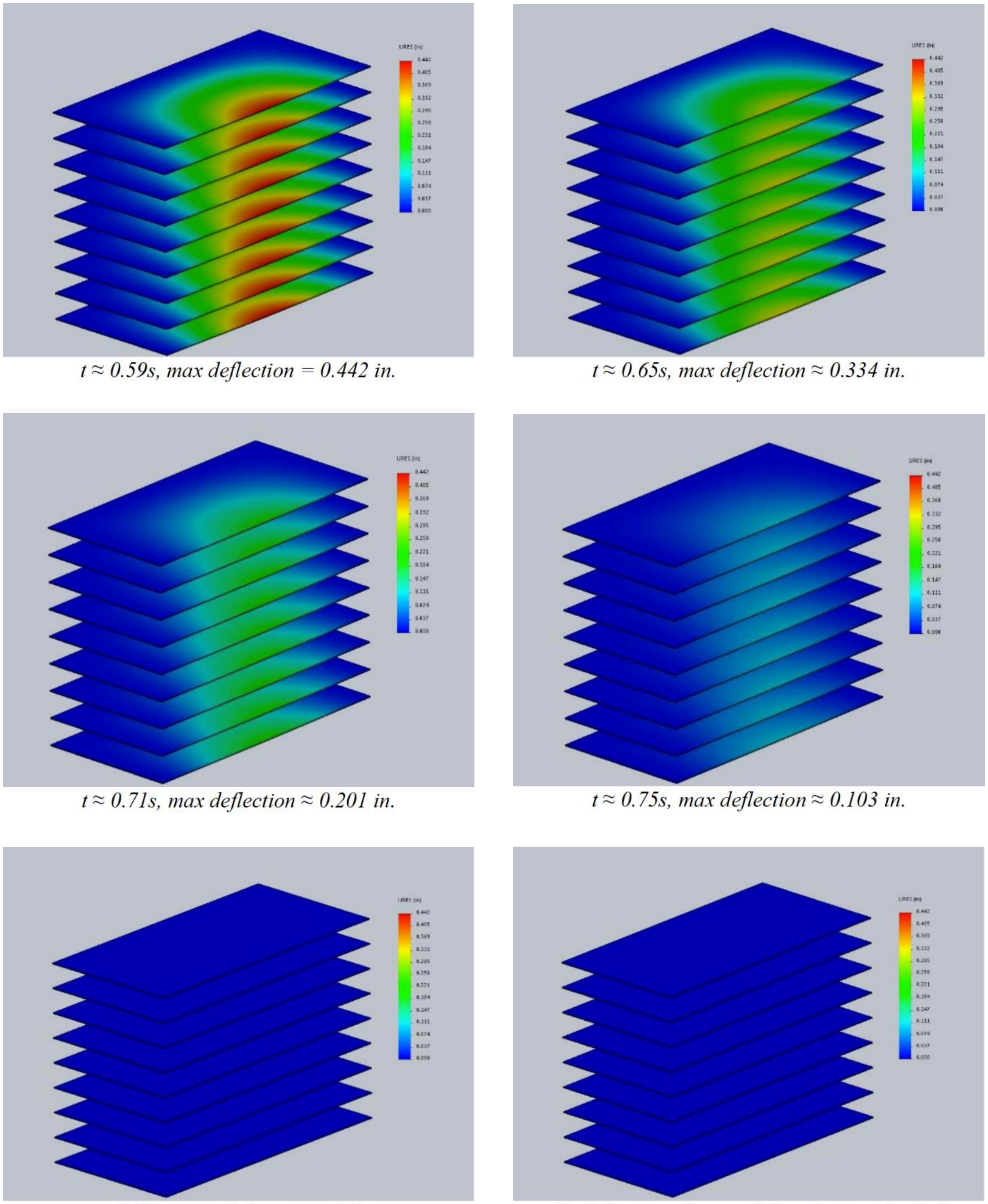

$t \approx 0.59s$, max deflection = 0.442 in.

$t \approx 0.65s$, max deflection ≈ 0.334 in.

$t \approx 0.71s$, max deflection ≈ 0.201 in.

$t \approx 0.75s$, max deflection ≈ 0.103 in.

$t \approx 0.80$ s, max deflection = 0.0 in.

No deflection after $t = 0.8$ s, plates unloaded.

Figure 35. Cessation of deflection of the 10 ft. x 5 ft. x 1/2 in. plates under static and dynamic loading.

(t = 0.6 to t = 0.9 seconds)

Plate Design Iteration 6: Cross Beams Added to Plate for Additional Support

Model Details: A 10 ft. x 5 ft. x 3/8 in. plate was modeled with long edges fixed. Cross beams measuring 1 in. x 1/4 in. x 10 ft. were attached to the underside of the plate at 4 ft. intervals, (see Figure 36). A uniform pressure of 1.3 psi was applied over the face of the plate, accounting only for hydrostatic pressure.

FEA Results: Maximum von-Mises stress was observed to be 4,873 psi, (see Figure 37), with a maximum deflection of 0.101 in., (see Figure 38).

Remarks: Both maximum stress and deflection were considered acceptable; however, the interference of a horizontal support system with the target flow profile was unknown. Thin vertical supports would be a less invasive option.

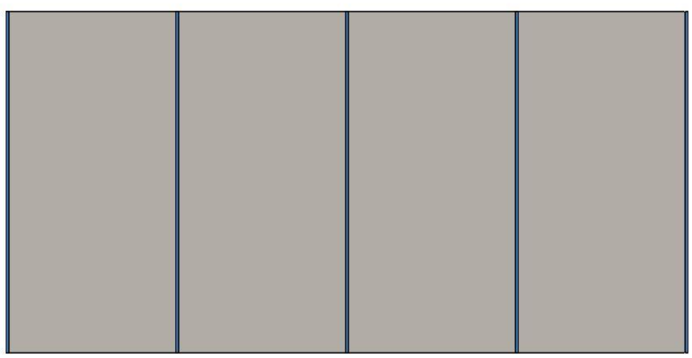

Figure 36. Bottom view of crossbeams attached to a 10 ft. x 5 ft. x 3/8 in. plate.

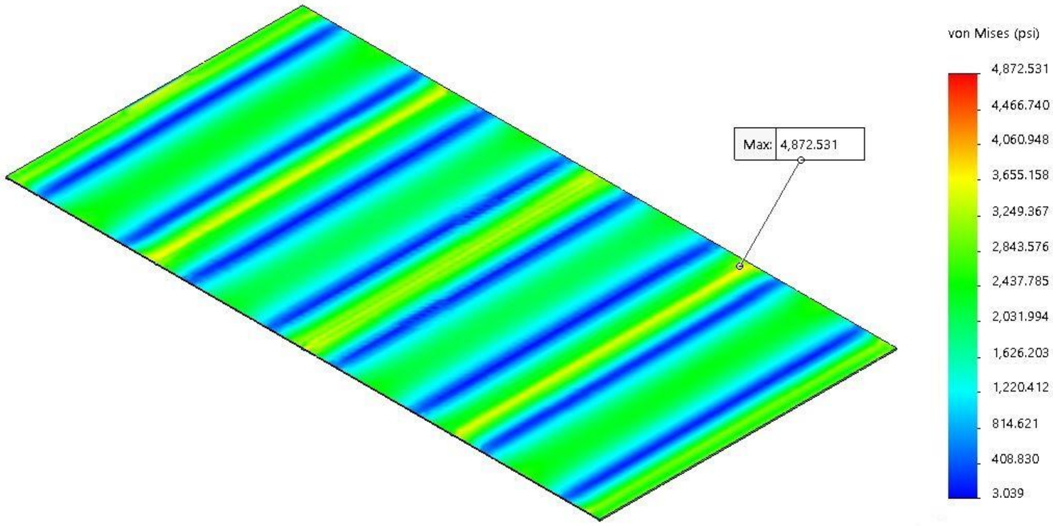

Figure 37. Von-Mises stress of a 10 ft. x 5 ft. x 3/8 in. plate with crossbeams under 1.3 psi.

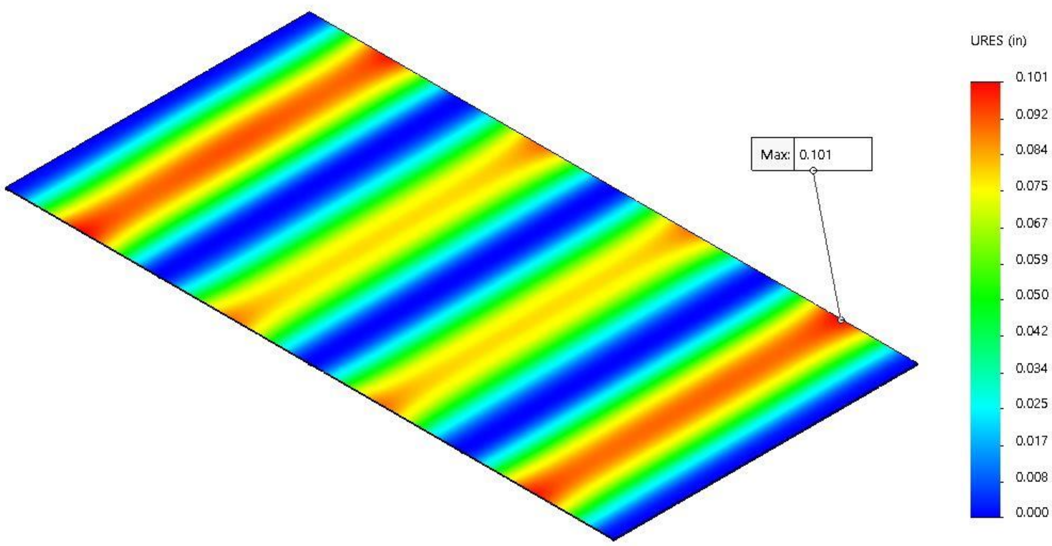

Figure 38. Deflection of a 10 ft. x 5 ft. x 3/8 in. plate with crossbeams under 1.3 psi.

Plate Design Iteration 7: A Thin Steel Support Installed at Exit Edge of Post-Gate Plates

Model Details: A 10 ft. x 5 ft. x 3/8 in. plate was modeled with long edges fixed in place. A 1/4 in. thick, steel vertical support was fixed to the plate using 3/8 in. notches at 12 in. intervals, (see Figure 39). A uniform pressure of 1.3 psi was applied over the face of the plate.

FEA Results: Maximum von-Mises stress was 17,074 psi, (see Figure 40), and maximum deflection was 0.383 in., (see Figure 41).

Remarks: The appearance of the stress concentration surrounding the vertical support was a concern for future cracking and/or failure in the support. But the overall improvement of placing a vertical support in the center of each plate was considered progress.

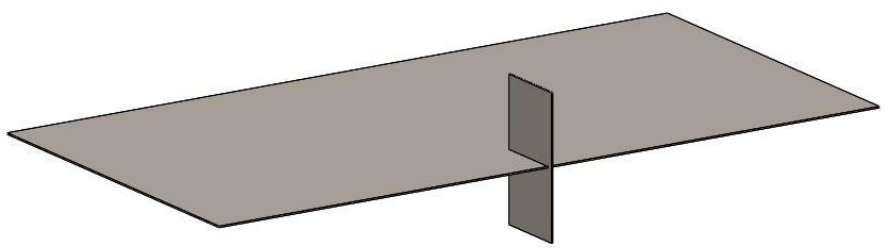

Figure 39. A 10 ft. x 5 ft. x 3/8 in. plate supported using 1/4 in. thick, notched steel.

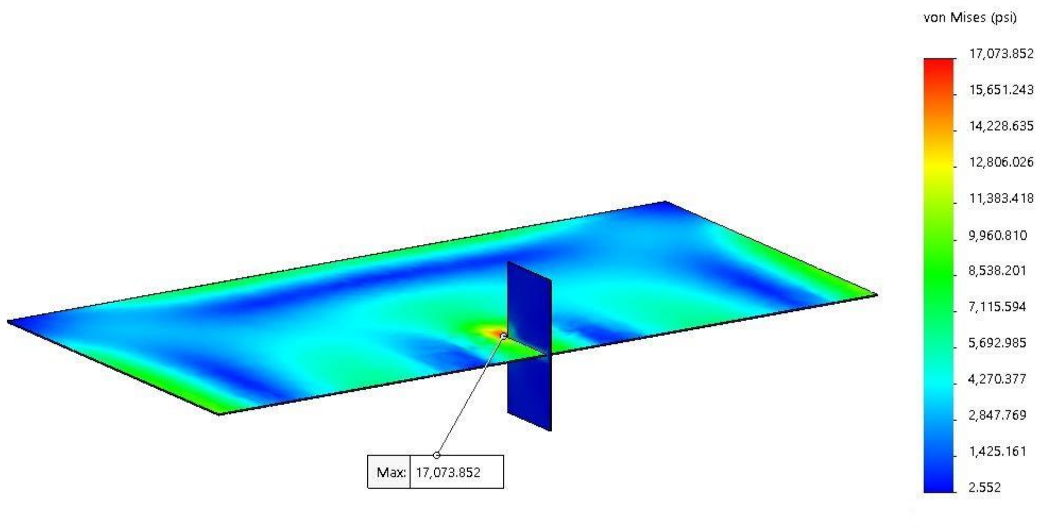

Figure 40. Von-Mises stress of a 10 ft. x 5 ft. x 3/8 in. plate under 1.3 psi with thin vertical support.

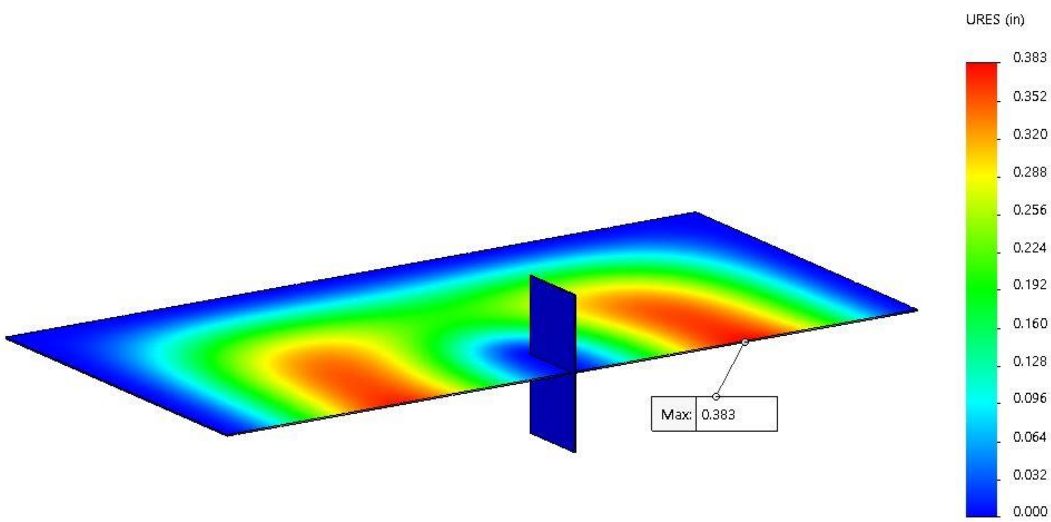

Figure 41. Deflection of a 10 ft. x 5 ft. x 3/8 in. plate under 1.3 psi with thin vertical support.

Plate Design Iteration 8: Thin Vertical Support Replaced by Two Rods

Model Details: A 10 ft. x 5 ft. x 3/8 in. plate was modeled with long edges fixed in place. The vertical support of Plate Design Iteration 8 was replaced by two 1/4 in. steel rods, fixed in tension to the top and bottom of the device housing, (see Figure 42). Washers were attached to at each opening in the plate to provide reinforcement, (see Figure 43). The rod was modeled as fixed to each washer and rod under the assumption that the components would be welded in the physical system. The distance from the edge of the plate to the first and second rod was 6 in. and 18 in., respectively. A uniform pressure of 1.3 psi was applied over the face of the plate.

FEA Results: The maximum von-Mises stress was 16,254 psi, (see Figure 44), and the maximum deflection was 0.049 in., (see Figure 45).

Remarks: High stress concentration were observed at the location of each fixture, even with the addition of the reinforcing washers. The deflection, however, was significantly decreased by 0.334 in.. It was hypothesized that additional rods would mitigate the stress concentrations but welding several threaded rods to each limited access plate was not feasible.

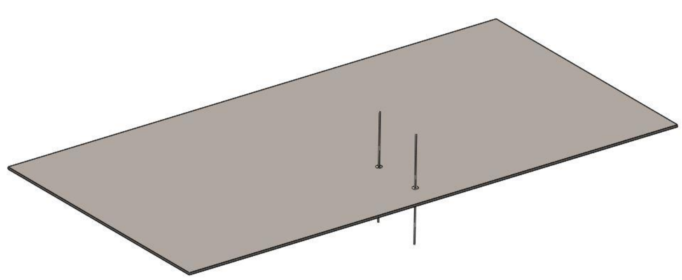

Figure 42. Overview of vertical rod plate support.

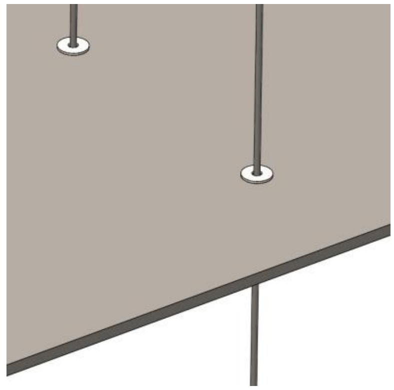

Figure 43. Close-up of vertical rod and washer attachments.

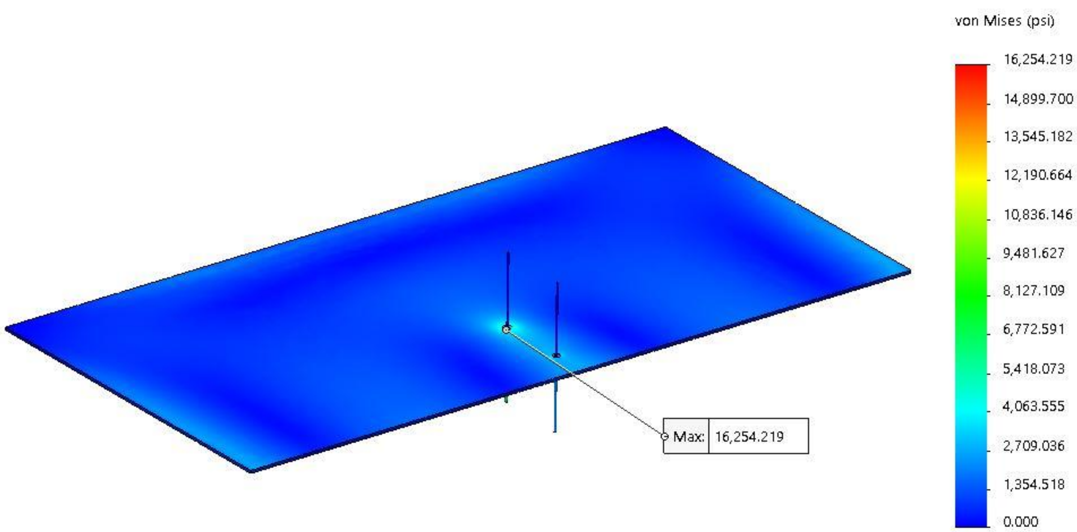

Figure 44. Von-Mises stress of a 10 ft. x 5 ft. x 3/8 in. plate under 1.3 psi with two support rods.

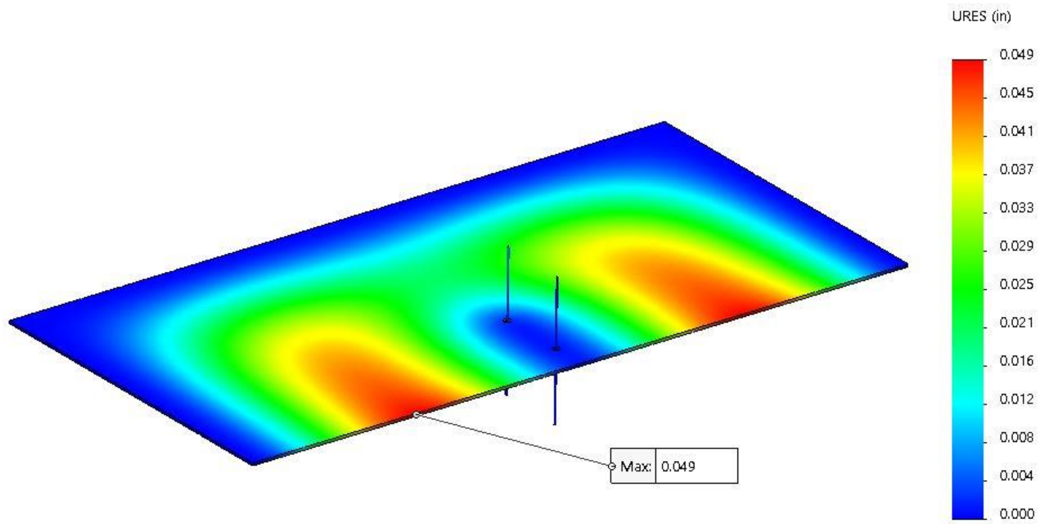

Figure 45. Deflection of a 10 ft. x 5 ft. x 3/8 in. plate under 1.3 psi with two support rods.

Plate Design Iteration 9: Threaded Rods and Rivet Nuts for Additional Plate Support

Model Details: One 10 ft. x 5 ft. x 3/8 in. was modeled with long edges fixed in place. Threaded rivet nuts were installed in intervals across each plate, (see Figure 46). Six 1/4 in. steel threaded rods are threaded through each rivet nut, then fixed in tension to the top and bottom of the device housing, (see Figure 47). The distance from the edge to the first and second rod in the center of the plate was 12 in. and 24 in., respectively. The distance from the edge to the first and second rod on each side of the center supports was 6 in. and 18 in., respectively. A uniform pressure of 1.3 psi was applied over the face of the plate.

FEA Results: The maximum von-Mises stress was 15,801 psi, (see Figure 48), and maximum deflection was 0.043 in., (see Figure 49).

Remarks: The 15,801 psi maximum von-Mises stress in the plate was reduced to almost half the 36,000 psi yield stress of A36 steel. The 0.043 in. maximum deflection was small enough to be considered reasonably negligible. The concept of using thin, threaded rods coupled with low-profile rivet nuts had succeeded in distributing the stress and deflection of each plate more uniformly than had previous design iteration. Thin vertical rods also meant less disruption to the wave development. The system was designed for each rod to be threaded continuously through each rivet nut in the plates below from above the WISD housing. This provided flexibility for future modifications since adding or removing supports could be done with ease as necessary. More information about the large flange rivet nuts used for this design can be found in Appendix C, p 90.

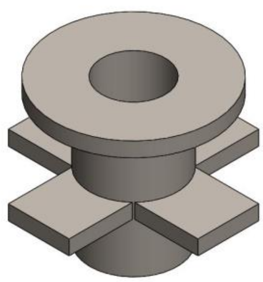

Figure 46. Close-up of expanded rivet nut after installation.

(Plate, rod, and threads removed for clarity.)

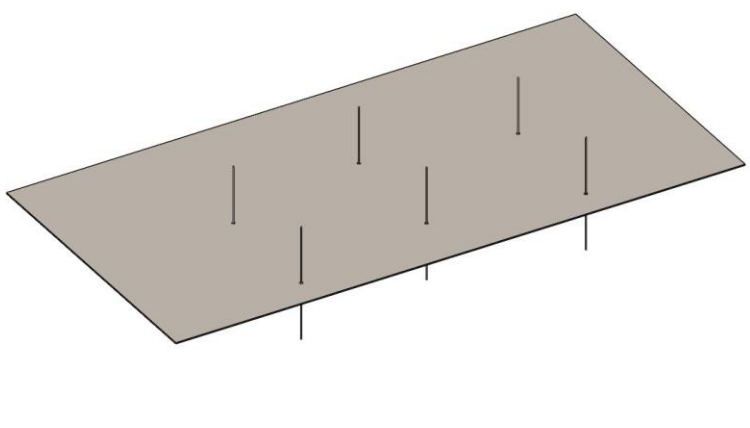

Figure 47. Overview of threaded rivet nut and rod plate supporting system.

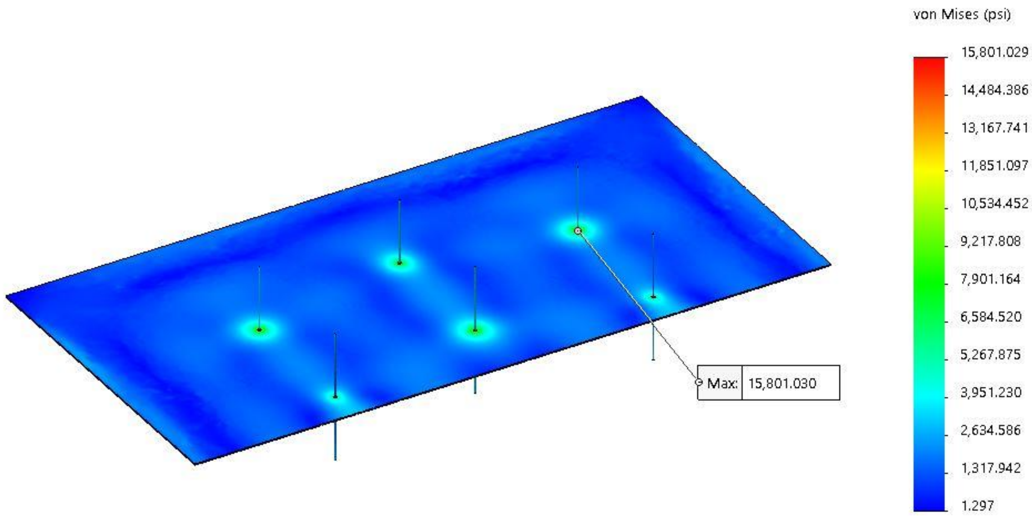

Figure 48. Von-Mises stress of a 10 ft. x 5 ft. x 3/8 in. plate under 1.3 psi with rivet nut/rod supports.

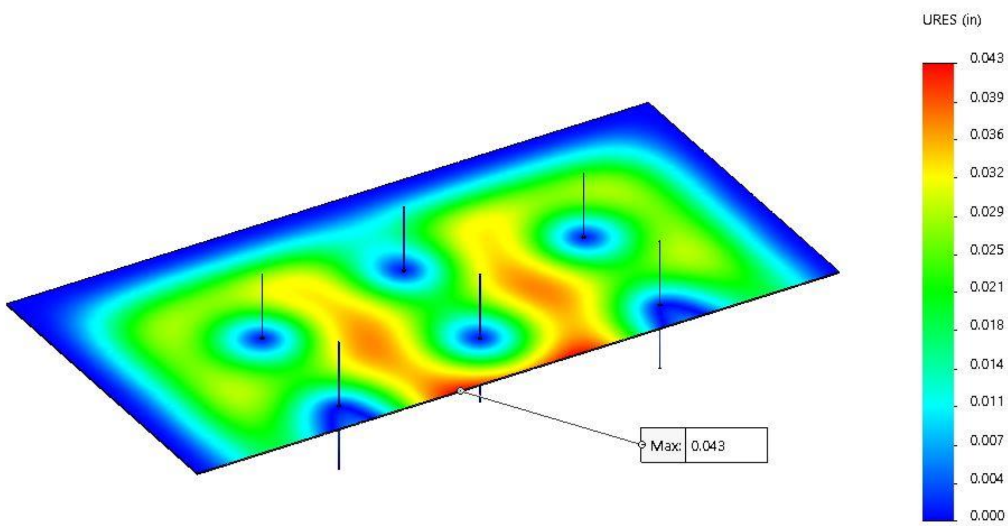

Figure 49. Deflection of a 10 ft. x 5 ft. x 3/8 in. plate under 1.3 psi with rivet nut/rod supports.

Summary of Plate Design Iterations

The results of the nine plate design iterations are shown below in Table 10.

Table 10. Summary of plate design iteration results

ITER.	WIDTH	LENGTH	THICK.	SUPPORT	PRESSURE	STRESS	DEFLECT.
1	2-1/2 ft.	10 ft.	3/32 in.	Long sides fixed	0.433 psi	17,446 psi	0.044 in.
2	10 ft.	10 ft.	1 in.	Long sides fixed	0.433 psi	2,743 psi	0.099 in.
3	10 ft.	10 ft.	3/8 in.	Three sides fixed	0.433 psi	19,327 psi	1.852 in.
4	10 ft.	10 ft.	3/8 in.	All sides fixed	0.433 psi	18,098 psi	1.630 in.
5	5 ft.	10 ft.	1/2 in.	Three sides fixed	1.3 psi	8,864 psi	0.413 in.
6	5 ft.	10 ft.	3/8 in.	Crossbeams	1.3 psi	4,873 psi	0.101 in.
7	5 ft.	10 ft.	3/8 in.	Thin vertical sheet	1.3 psi	17,074 psi	0.383 in.
8	5 ft.	10 ft.	3/8 in.	Two welded rods	1.3 psi	16,254 psi	0.049 in.
9	5 ft.	10 ft.	3/8 in.	Six threaded rods	1.3 psi	15,801 psi	0.043 in.

6.2 DESIGN AND ANALYSIS OF WISD GATES

The success of the WISD is largely dependent on the functionality of the gate system. As part of the project requirements, the gate system must have the following capabilities:

1. Gates must be designed to withstand high water pressures before water is released.
2. Gate design should not interfere with the target flow profile.
3. All gates must open near instantaneously.
4. Leakage from reservoir prior to gates opening should be kept at a bare minimum.

The FLOW-3D simulations performed by Greg Roberts, used the concept of ten bottom hinged-gates, opening each channel simultaneously as the water reservoir behind them became pressurized (Roberts 2016). As such, each gate would be a rectangular valve driven by a single, rotating shaft. A gate thickness and shaft size capable of withstanding both hydrostatic and pneumatic pressures from the reservoir section would need to be determined.

The amount of torque on the gate shaft was calculated under two main assumptions. First, the shaft was assumed fixed on each end (although the mechanism for holding the shaft in place had not yet been determined). And second, the gate would be permanently fixed to the shaft, and both components would be potentially subjected to 21.3 psi of hydrostatic and pneumatic pressure. Each gate must span the entire 10 ft. width of the channel; therefore, the resultant deflection and stress from the applied pressure would ultimately determine the configuration best suited for the task.

The method for attaching the gate to the shaft also presented the team with an obstacle. Since the shaft would need to drive the movement of the gate, the two required a strong, permanent bond. A keyed shaft is a standard rod designed with a machined groove running the length of the shaft to accommodate the placement of a key. The key is a small piece of metal fabricated to fit snugly into the groove of the shaft and accommodate other keyed components, such as gears and pulleys. The attached components can then be driven by the rotation of the shaft. Using the same concept, a thin plate of metal with a thickness equivalent to the respective key was assumed fixed into the keyway of the shaft using an all-around filet weld at the interface between shaft and plate. The shaft was designed to extend past the plate for 3 in. in each direction to allow space for the driving mechanism to be later installed. An overview of the simple gate created by the keyed shaft and plate is shown below in Figure 50.

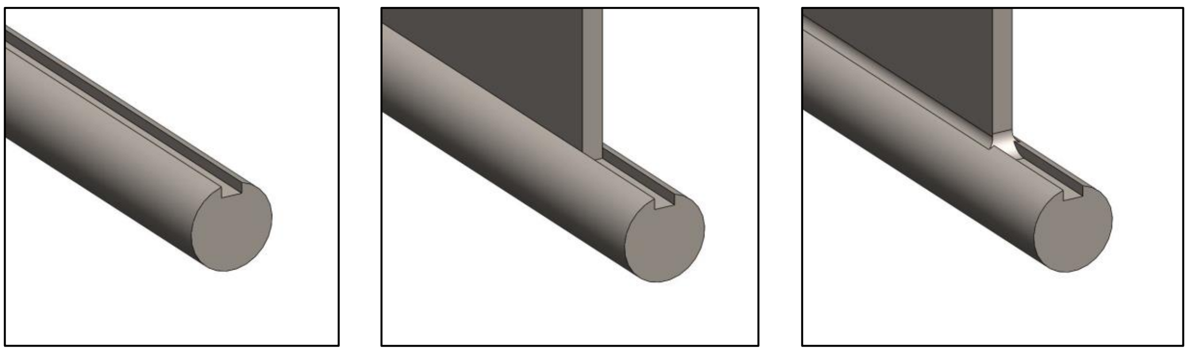

Figure 50. Isometric view of gate plate attached to keyed shaft.

(Left: keyed shaft, Center: plate inserted into keyway, Right: all around fillet weld)

The 10 ft. channel span of the shaft, coupled with the 21.3 psi pressure acting on the gate from the water and compressed air would cause a large bending moment to occur on both pieces. To determine the extent of the bending moment, hand calculations from *Shigleys Mechanical Engineering Design* were used, (see Appendix D, p 92). The first calculation was performed to determine the minimum diameter required to withstand the 20 psi pneumatic pressure and 1.3 psi hydrostatic pressure using the full 36,000 psi yield strength of A36 steel. The resulting diameter was 3.88 in. The next calculation removed the 20 psi pneumatic pressure to observe a minimum diameter requirement for only the 1.3 psi hydrostatic pressure, assuming the gates and compressed air could be released simultaneously. The reduction of pressure decreased the required rod diameter to 2.12 in. Further reduction of the hydrostatic pressure to 0.433 psi to account for only 1 ft. head of head reduced the required shaft diameter to 0.71 in.

The stress and deflection of the plate for all three pressure conditions was also determined. Using the same calculation approach as before, a 0.04 in. rod was found to be sufficient for the 36,000 psi yield strength. However, the calculated deflection was 17.22 in., a value not possible for a 12 in. gate. Unlike the shaft, the required gate thickness would be driven by the resultant deflection. This was address by decreasing the allowable deflection to 0.01 in. (for minimal deflection), then calculating the required thickness to achieve it. The plate thickness required for the 0.01 in. deflection was approximately 0.50 in., (see Appendix D, p 92 for calculations).

After observing the stress and strain behavior of the shaft and gate as isolated components, it was then necessary to observe them as a single system since the hand calculations had assumed the attaching component was fixed. Five configurations using standard shaft sizes and corresponding plate thicknesses based on key width were modeled in SOLIDWORKS for FEA analysis. Standard keyed shaft dimensions from 1 in. to 2-1/2 in. are shown below in Table 11.

Table 11. Standard Keyed Shaft Sizes (Grainger 2018)

SHAFT DIAMETER (in.)		KEY WIDTH/PLATE THICKNESS (in.)	
Fraction	**Decimal**	**Fraction**	**Decimal**
1	1	1/4	0.25
1 1/4	1.25	1/4	0.25
1 1/2	1.5	3/8	0.375
1 3/4	1.75	3/8	0.375
2	2	1/2	0.5
2 1/4	2.25	1/2	0.5
2 1/2	2.5	5/8	0.625

Gate Design Iteration 1: 1 in. Keyed Shaft with a 1/4 in. Thick Rectangular Plate

Model Details: A 12 in. x 10 ft. x 1/4 in. thick steel plate was fixed into the keyway of a 1 in. x 10-1/2 ft. A36 steel keyed shaft. The shaft was fixed from rotation at each end, and a uniform pressure of 0.433 psi was applied perpendicular to the plate.

FEA Results: Deflection at the center of the gate was approximately 1.76 in., (see Figure 51).

Remarks: The 1.76 in. deflection was considered too large.

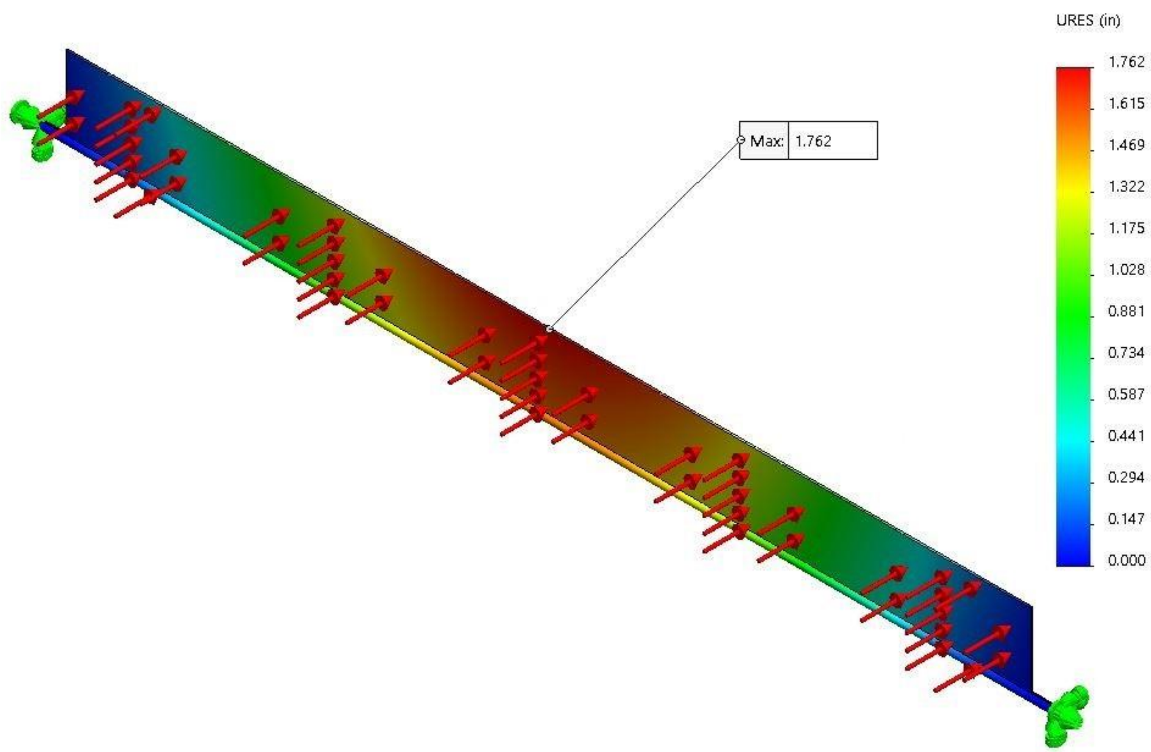

Figure 51. Deflection of a 1 in. keyed shaft with a 1/4 in. rectangular gate under 0.433 psi.

Gate Design Iteration 2: 1-1/4 in. Keyed Shaft with a 1/4 in. Thick Rectangular Plate

Model Details: A 12 in. x 10 ft. x 1/4 in. thick steel plate was fixed into the keyway of a 1-1/4 in. x 10-1/2 ft. keyed A36 steel shaft. The shaft was fixed from rotation at each end, and a uniform pressure of 0.433 psi was applied perpendicular to the plate.

FEA Results: Deflection at the center of the gate was approximately 0.82 in., (see Figure 52).

Remarks: Deflection decreased from 1.76 in. to 0.82 in., but less deflection was desired.

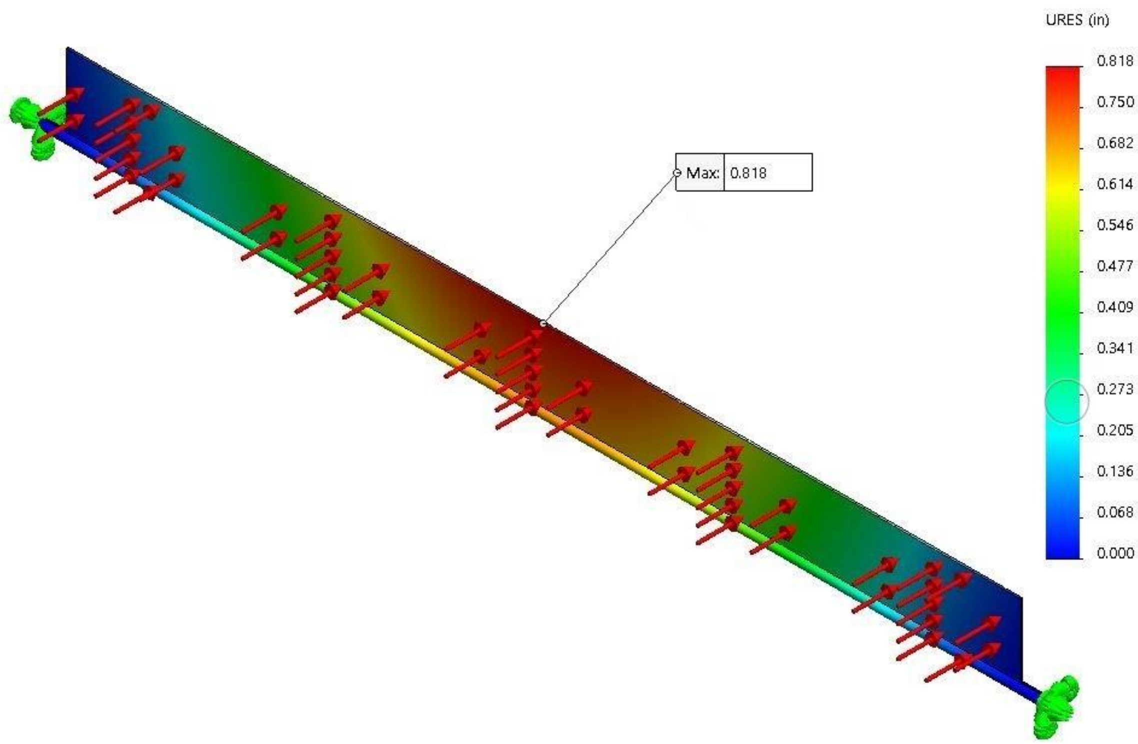

Figure 52. Deflection of a 1-1/4 in. keyed shaft with a 1/4 in. rectangular gate under 0.433 psi

Gate Design Iteration 3: 1-1/2 in. Keyed Shaft with a 3/8 in. Thick Rectangular Plate

Model Details: A 12 in. x 10 ft. x 3/8 in. thick steel plate was fixed into the keyway of a 1-1/2 in. x 10-1/2 ft. A36 steel keyed shaft. The shaft was fixed from rotation at each end, and a uniform pressure of 0.433 psi was applied perpendicular to the plate.

FEA Results: Deflection at the center of the gate was 0.38 in., (see Figure 56).

Remarks: Deflection was decreased from 0.82 in. to 0.38 in., but team decided a deflection less than 1/4 in. would be optimal.

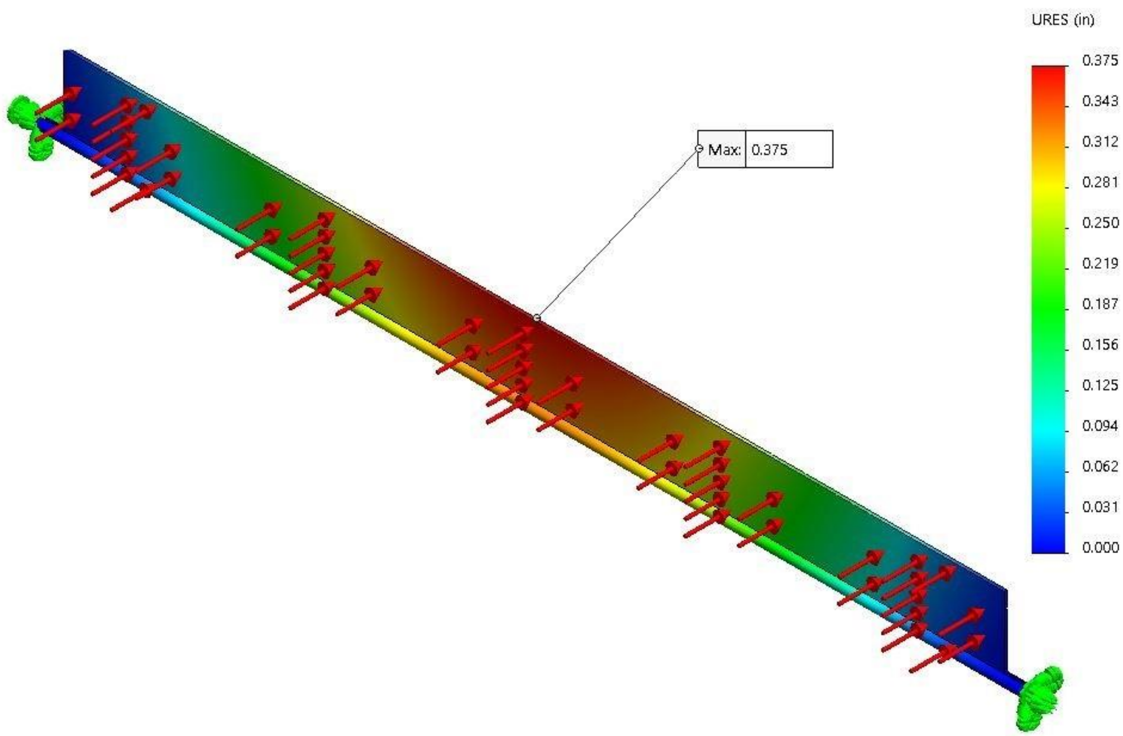

Figure 53. Deflection of a 1-1/2 in. keyed shaft with a 3/8 in. rectangular gate under 0.433 psi

Gate Design Iteration 4: 1-3/4 in. Keyed Shaft with a 3/8 in. Rectangular Plate

Model Details: A 12 in. x 10 ft. x 3/8 in. thick steel plate was fixed to the keyway of a 1-3/4 in. x 10-1/2 ft. A36 steel keyed shaft. The shaft was fixed from rotation at each end, and a uniform pressure of 0.433 psi was applied perpendicular to the plate.

FEA Results: Deflection at the center of the gate was 0.22 in., (see Figure 54).

Remarks: The results of the analysis showed the 1-3/4 in. shaft coupled with a 3/8 in. thick plate was an optimal configuration. The 0.22 in. deflection of the gate was less than 1/4 in. and the 3/8 in. gate plate thickness would remain consistent with the surrounding WISD plates. Also, the 9,600 psi maximum von-Mises stress using the 1-3/4 in. keyed shaft and 3/8 in. thick rectangular plate yields a factor of safety of 3.8, (see Figure 55).

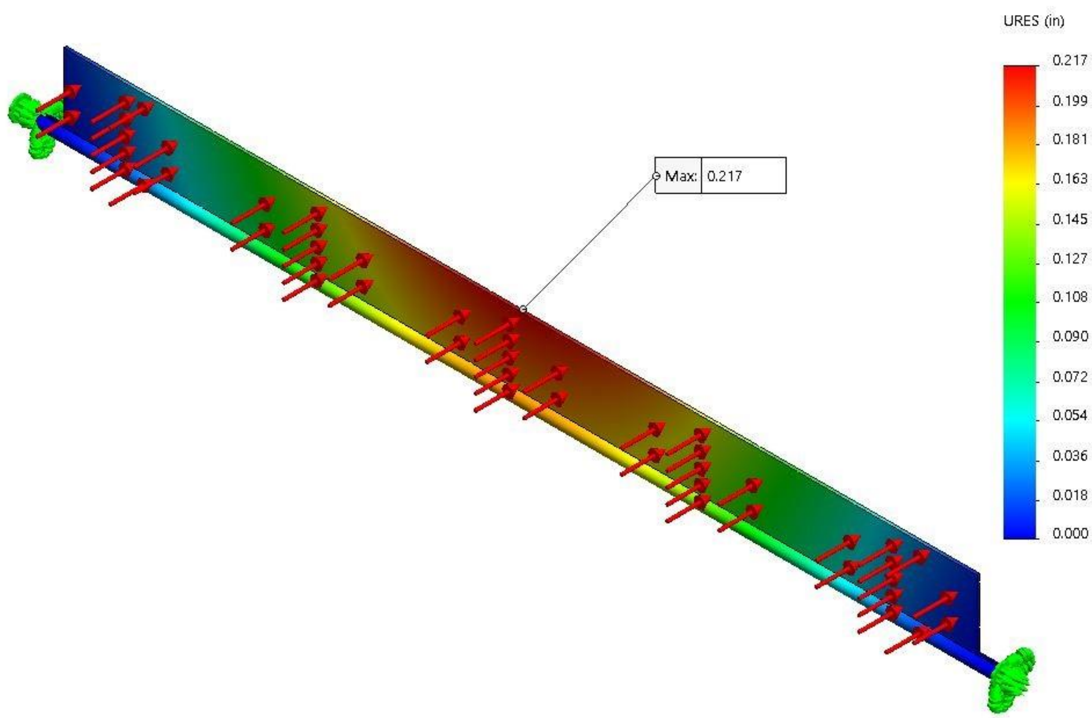

Figure 54. Deflection of a 1-3/4 in. keyed shaft with a 3/8 in. rectangular gate under 0.433 psi

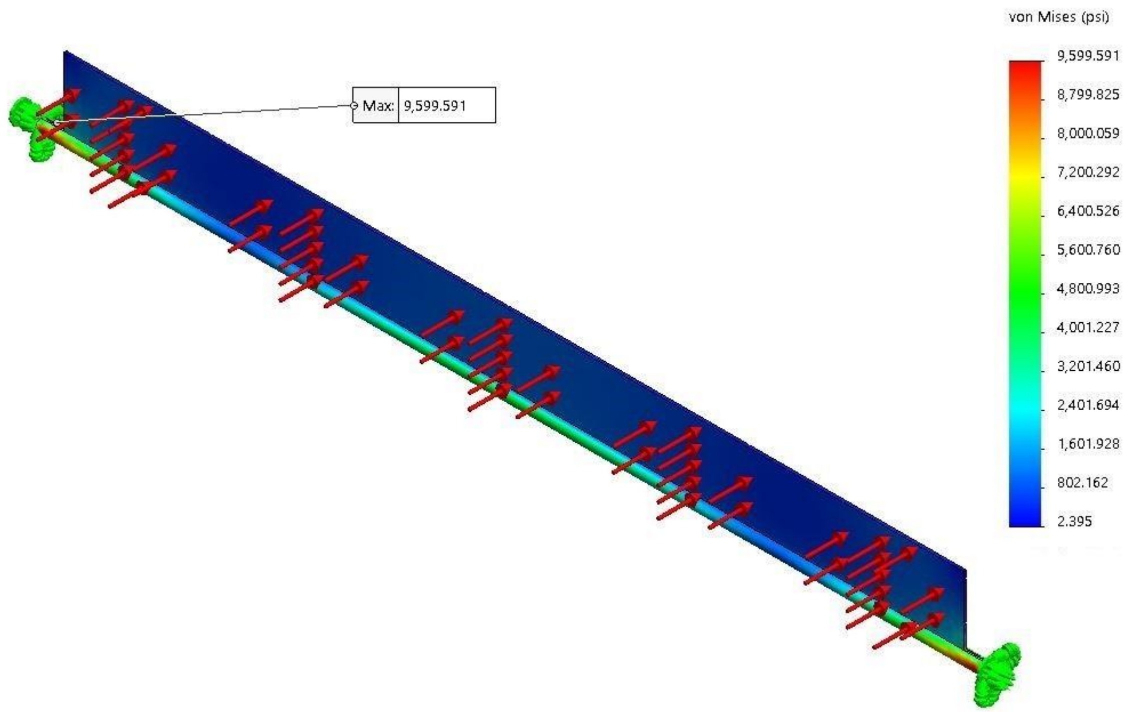

Figure 55. Von-Mises stress of a 1-3/4 in. keyed shaft with a 3/8 in. rectangular gate under 0.433 psi

After establishing a 1-3/4 in. keyed shaft and a 3/8 in. thick gate plate would be adequate for the WISD prototype, one more design iteration was performed to determine if adding more support to each end of the shaft would further decrease the deflection by reducing the bending moment on the shaft. Custom shaft supports were designed to hinge each end of the shaft to the adjoining WISD plate. The addition of the two hinges did decrease the deflection approximately 10%, from 0.22 in. to 0.20 in., but the maximum von-Mises stress increased from 9,600 psi to 9,691 psi (about 1%). The sole advantage of acquiring custom machined supports would be the minimal 0.02 in. decrease in deflection. The team agreed pursuing the custom supports was not practical. However, an overview of the custom support design has been included below for future reference.

Gate Design Iteration 5: 1-3/4 in. Keyed Shaft, 3/8 in. Thick Rectangular Plate, Custom Hinges

Model Details: A 12 in. x 10 ft. x 3/8 in. thick steel plate was fixed into the keyway of a 1-3/4 in. x 10-1/2 ft. A36 steel keyed shaft. Two custom machined hinges were fixed at each end of the gate plate to the adjoining plate of the WISD, (see Figure 56, Figure 57, and Figure 58). The shaft was fixed from rotation at each end, and a uniform pressure of 0.433 psi was applied perpendicular to the plate.

FEA Results: Deflection at the center of the gate was reduced to 0.20 in., (see Figure 59). Maximum von-Mises stress increased from to 9,691 psi, (see Figure 60)

Remarks: The cost associated with acquiring custom machined parts was not practical for the minimal 0.02 in. decrease in deflection. The concept was not pursued further.

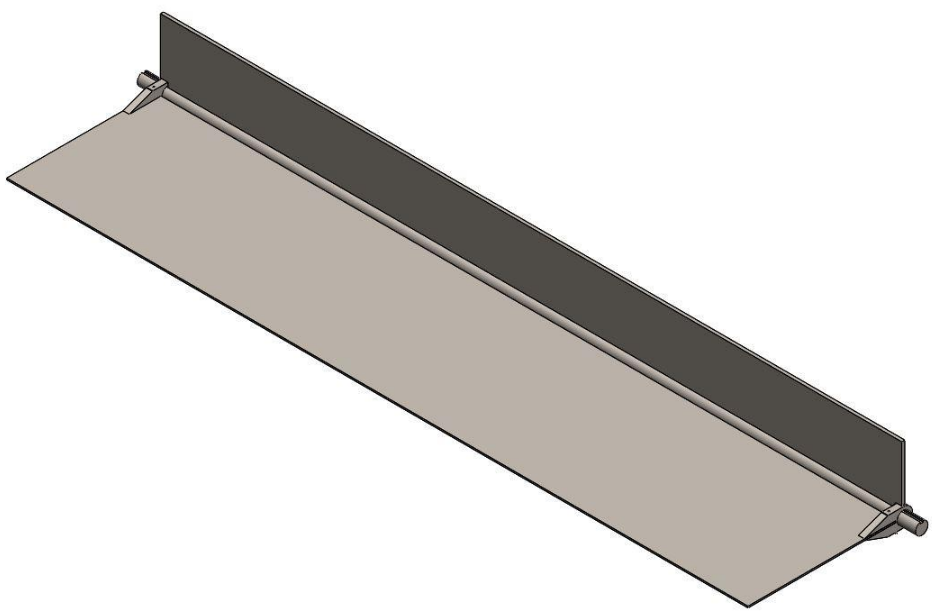

Figure 56. Isometric view of custom hinges supporting closed gate.

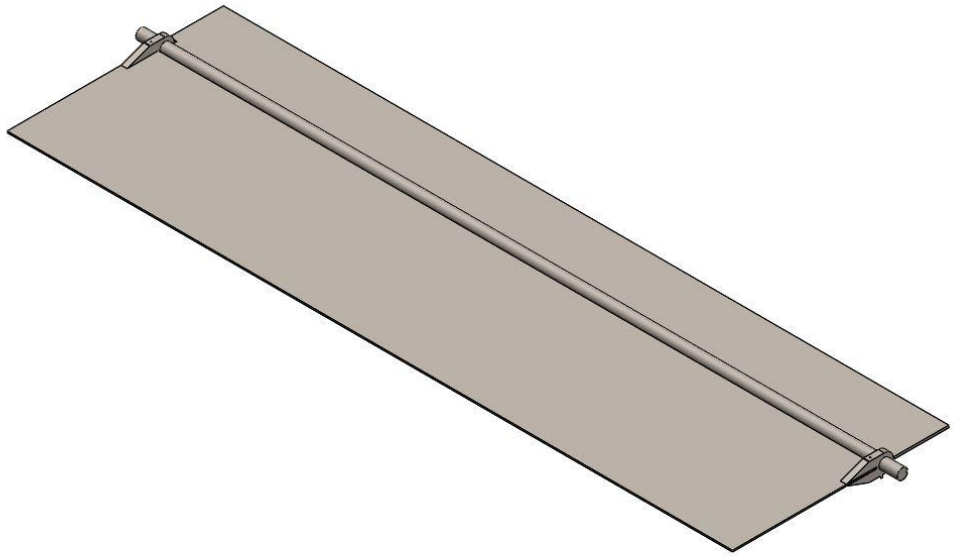

Figure 57. Isometric view of custom hinges supporting open gate

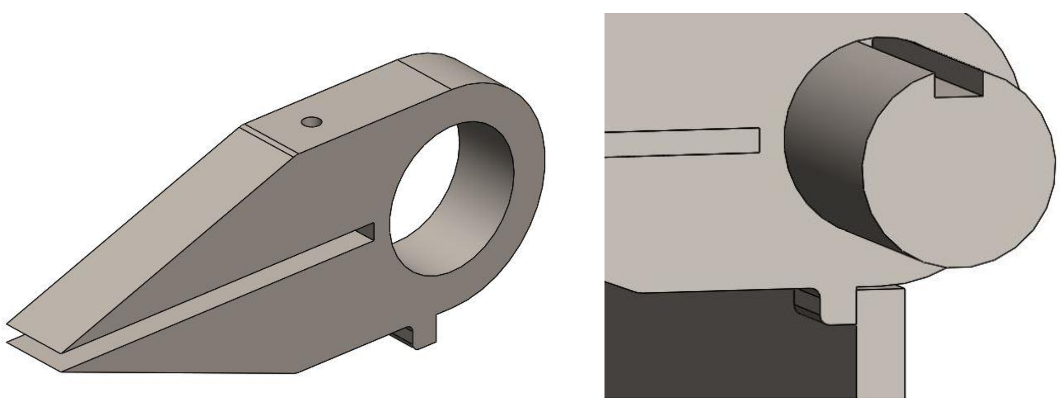

Figure 58. Close-up of custom machined hinge (left) and installation (right).

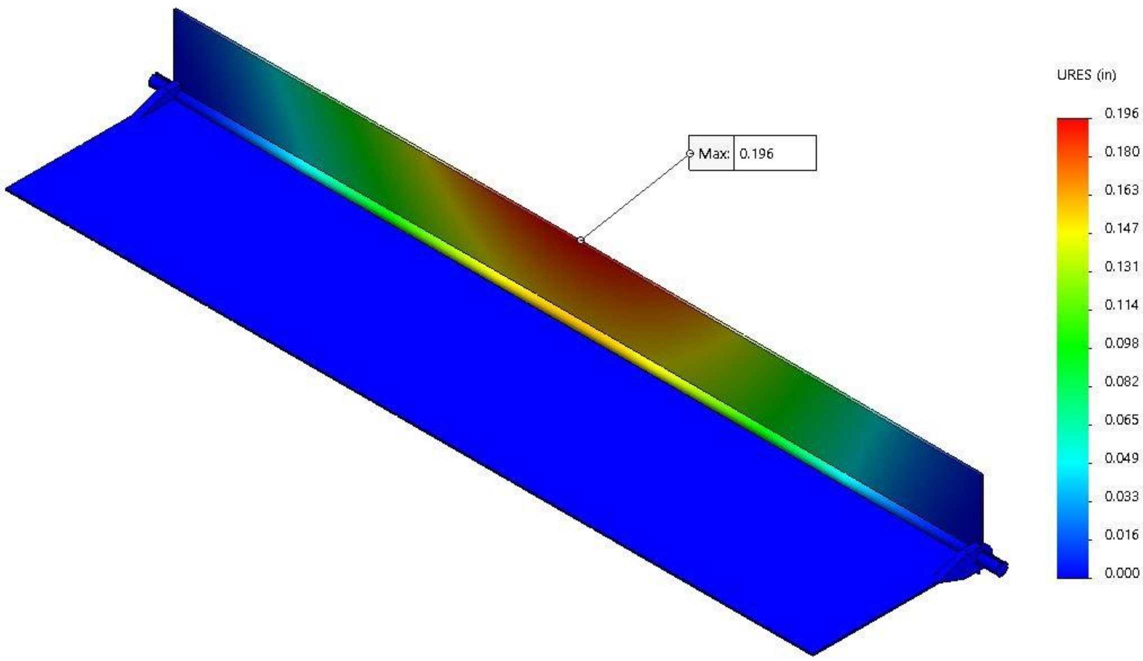

Figure 59. Deflection of 1-3/4 in. shaft, 3/8 in. rectangular gate, and custom hinges under 0.433 psi.

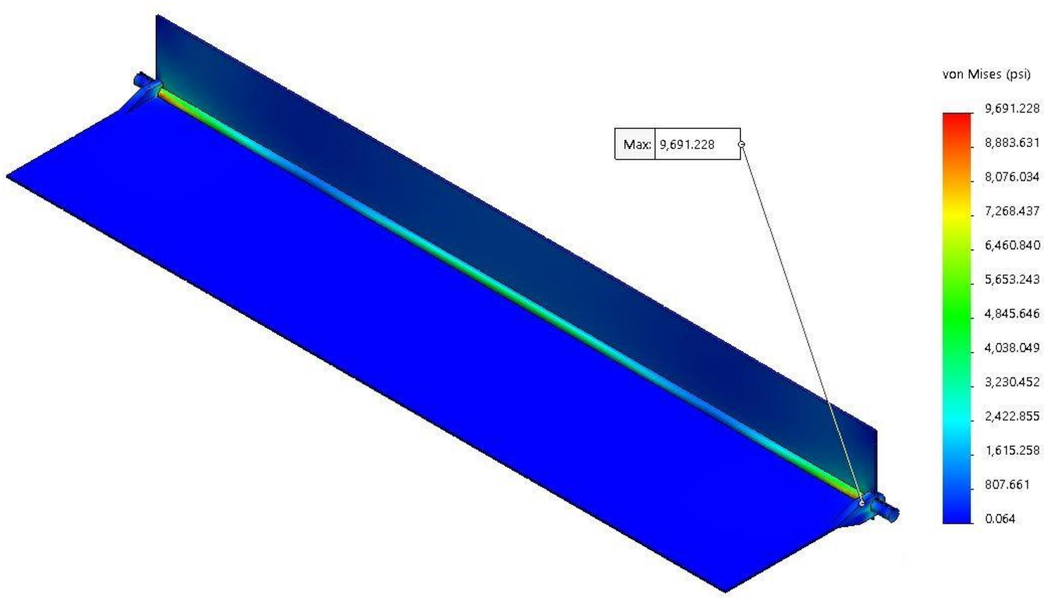

Figure 60. Von-Mises stress of 1-3/4 in. shaft, 3/8 in. thick gate, and custom hinges under 0.433 psi..

Summary of Gate Design Iterations

The results of the four gate design iterations are shown below in Table 12.

Table 12. Summary of gate design iteration results

ITERATION	SHAFT DIAMETER	GATE THICKNESS	MAX STRESS	MAX DEFLECTION
1	1 in.	1/4 in.	54,890 psi	1.76 in.
2	1-1/4 in.	1/4 in.	27,722 psi	0.818 in.
3	1-1/2 in.	3/8 in.	15,762 psi	0.375 in.
4	1-3/4 in.	3/8 in.	9,599 psi	0.217 in.

Overview of Structural Components Chosen for WISD Prototype

Based on the results of the previous sections, the structural basis of the WISD prototype will consist of the following A36 plain carbon steel components:

QTY = 10	1-3/4 in. x 10-1/2 ft. long keyed shaft (gate system)
QTY = 10	10 ft. x 10-7/16 in. x 3/8 in. plate (gate system)
QTY = 9	10 ft. x 5 ft. x 3/8 in. plate (plates after gate system)
QTY = 9	10 ft. x 10 ft. x 3/8 in. plate (plates before gate system)
QTY = 21	1/4 in. x 126 in. threaded rod (plate support)
QTY = 21	1/4 in. large flange, threaded rivet nut (plate support)

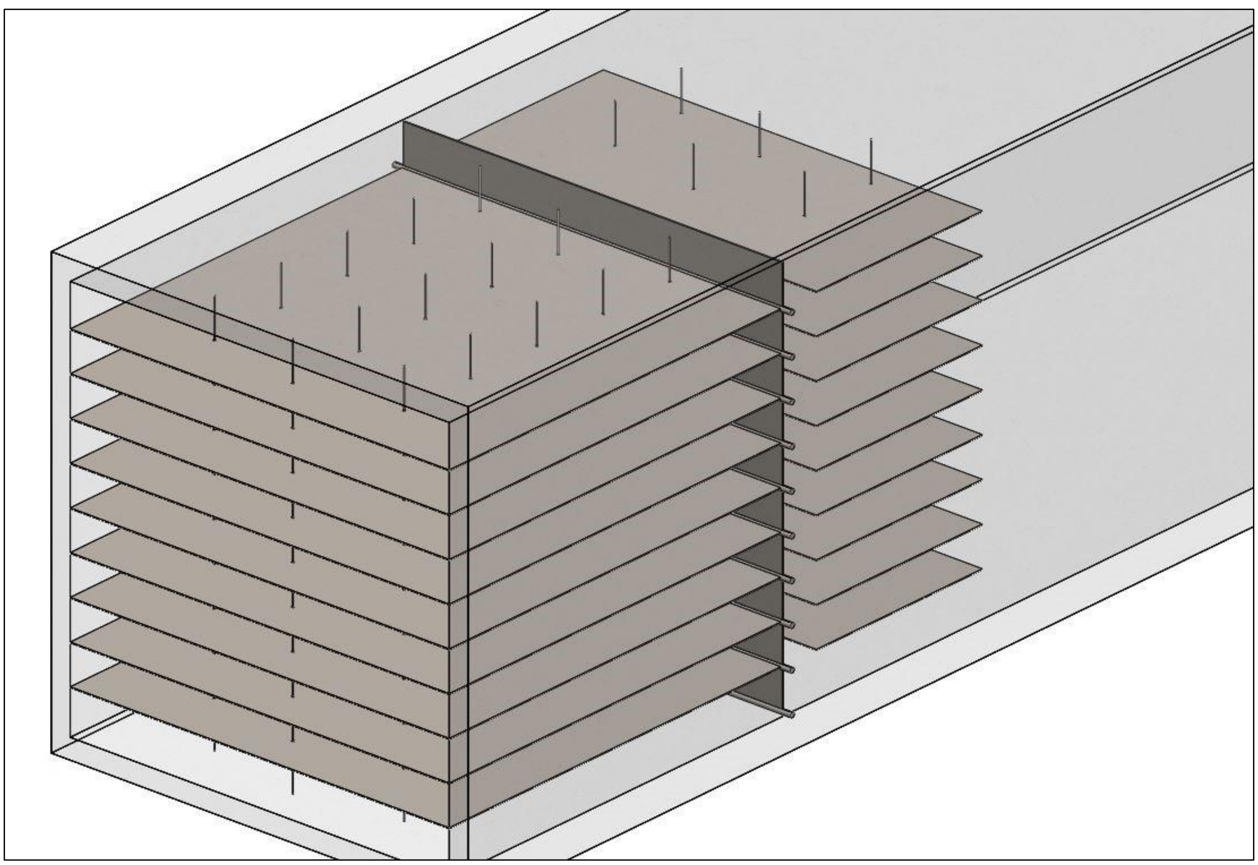

Figure 61. Simulation of chosen prototype components assembled within the WISD housing.

6.3 GATE MECHANISM

A key specification for the gate system was to ensure that all ten gates to open as quickly as possible. In similar applications, fast response requirements are typically met using clutches or brakes. The issue with using these devices for the WISD gate mechanism is they operate principally on friction and can momentarily inhibit movement until the device is completely disengaged. The rotating gate shafts require a more immediate release from their static position to develop the angular velocity necessary to satisfy the rapid response requirement.

A more suitable option was to use electromagnets. Electromagnets, primarily electromagnetic locks, are commercially available with various holding force capacities. These devices are low profile, easy to operate, and quick to respond. While connected to a power source, an electromagnet is held fixed to its respective strike plate with a predesignated amount of holding force. The fail-open mechanism allows the magnet to immediately disengage from the strike plate the moment power is removed from the magnet. Thus, a set of electromagnets affixed to each side of the gate shaft will hold all ten gates tightly closed while energized, then allow uninhibited, instantaneous rotation by simply interrupting the power source to the magnets.

To determine the total holding force required by each magnet, the 0.433 psi hydrostatic pressure of 1 ft. head of water was multiplied by the 12 in. height of the channel and 120 in. width of the gate. The result was a 624 lbf required holding force per channel, or 312 lbf holding force per magnet. However, to ensure a factor of safety of at least 2.0, two standard electromagnet locks with 650 lbf holding force were specified for the final design, (see Appendix E, p 78).

The angular velocity of the shaft after the magnet disengages from the strike plate was also calculated using the 1 ft. head hydrostatic moment of 1248 lbf-in acting on the area of each plate and a shaft diameter of 1-3/4 in. The angular velocity was found to be 90.8 radians/second with a total travel time of 0.02 s for the entire 90-degree rotation, (see Appendix F, p 102 for calculation details). Initially, it was thought a helical spring should also be incorporated into the gate mechanism to supplement the angular velocity of the shaft; however, hand calculations showed the moment created by 1 ft. of hydrostatic head will provide more than sufficient torque to quickly rotate the shaft.

The electromagnets were integrated with the final WISD design using the 3 in. extension already designed into each end of the gate shaft. A 3/8 in. thick rectangular mounting plate was fixed to each 3 in. peripheral section assuming a welded connection, and the strike plates were attached to each mount using a single bolt. The electromagnet was secured to a secondary support system located on the outside of the WISD using machine screws. A 1 in. thick rubber damper was also installed on the secondary support system to help absorb the impact of the fast-moving gate as it reaches its final destination. Figure 62 and Figure 63 below provide a simulated overview of the electromagnet operation. The WISD housing, plates, and supports have been removed for clarity.

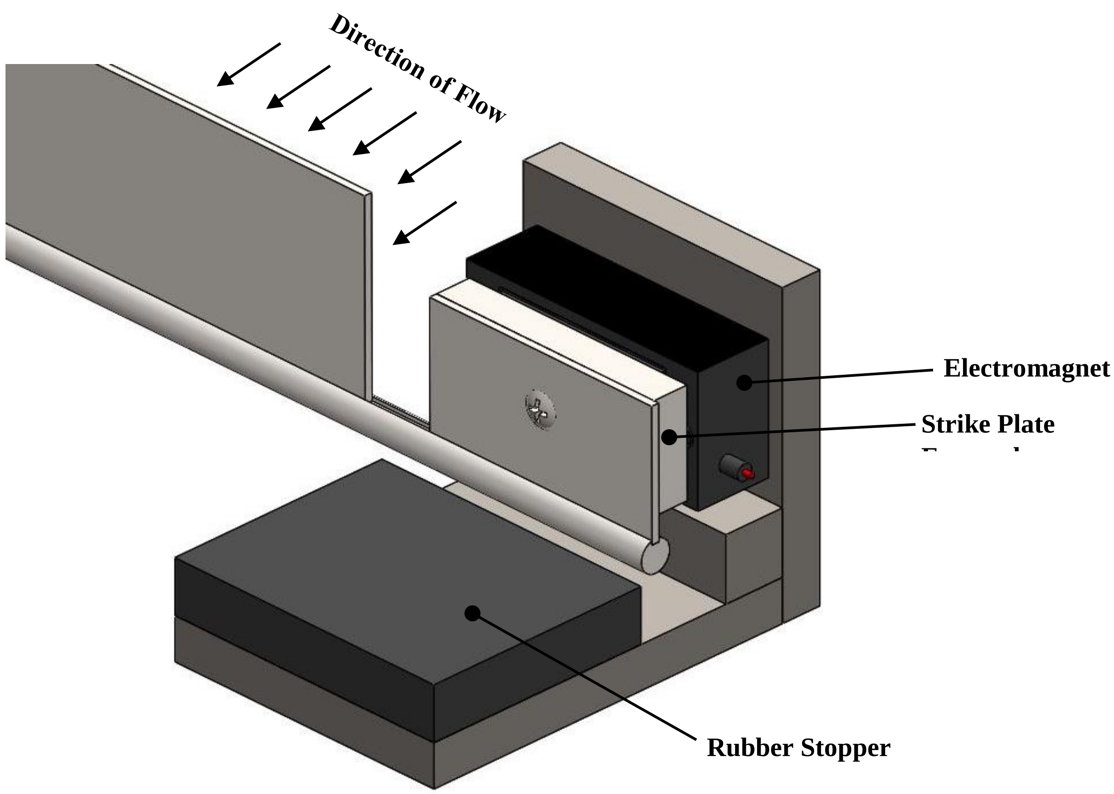

Figure 62. Simulation of the energized electromagnet holding gate in closed position.

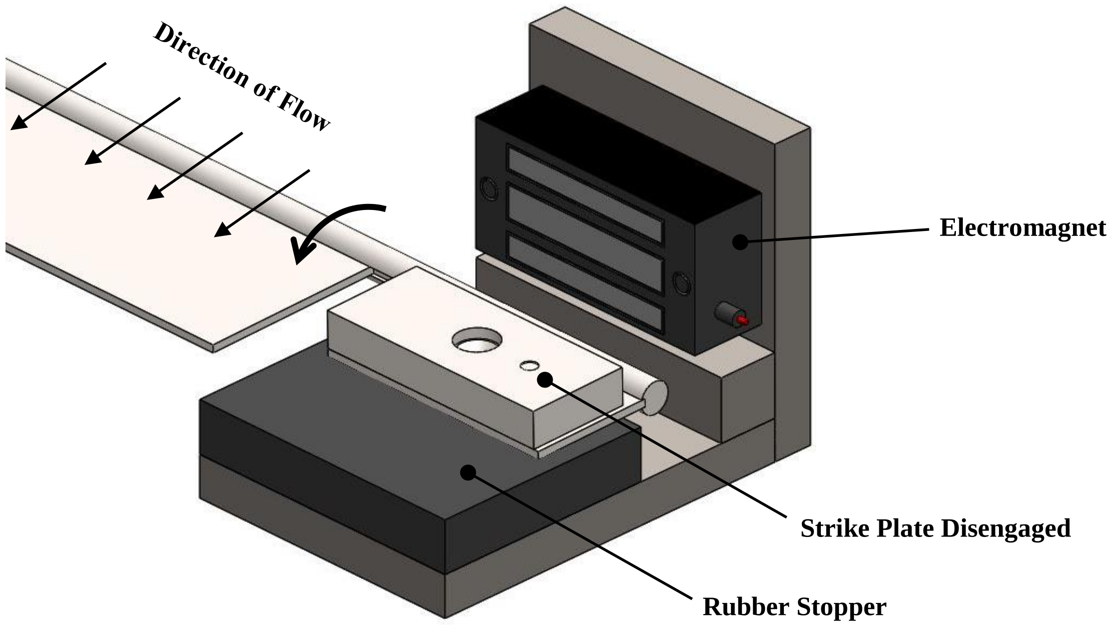

Figure 63. Simulation of the de-energized electromagnet releasing gate to opening position.

It should also be noted that the recoil of the strike plate as it impacts the rubber stopper was assumed to be negligible since the 1 ft. deep column of water rushing over the open gate is not expected to allow the gate to lift once the shaft has rotated into its final position. Should this become an issue in the physical model, the rubber stopper on each end could be easily replaced with a second set of electromagnets.

7. DESIGN OF A 1:5 SCALE PHYSICAL MODEL

Testing and experimentation of the overall design of the full-size prototype began with the design of a 1:5 scale physical model of a single channel. All parameters of the WSID established in the preceding sections (including plate thickness, gate thickness, shaft size, and electromagnet holding force) were scaled proportionally to one-fifth of their original dimensions as follows, (see Table 13).

Table 13. WISD Structural Parameters for 1:5 Scale Model

COMPONENT	ORIGINAL PARAMETER	1:5 SCALED EQUIVALENT
Plate Width	120 in.	24 in.
Plate Length	120 in.	24 in.
Plate Thickness	0.375 in.	0.075 in.
Gate Width	12 in.	2.4 in.
Gate Length	120 in.	24 in.
Gate Thickness	3/8 in.	0.075 in.
Shaft Length	126 in.	25.2 in.
Shaft Diameter	1-3/4 in.	0.15 in.
Holding Force	600 lbf.	120 lbf.

The concurrent team research on the time, velocity, and pressure required to accelerate the stagnate water in the reservoir section of the full-size prototype to the exit conduit would also be tested using the 1:5, single channel model. The prototype-model similarities for time, velocity, and pressure were found using the 1:5 model scale ratio with a Froude Model, (see Table 14).

Table 14. WISD Time, Velocity, and Pressure for 1:5 Scale Model

PARAMETER	SIMILARITY MODEL TO PROTOTYPE	1:5 SCALED EQUIVALENT
Time	1s = 2.24 s	0.38 s
Velocity	1ft/s = 2.24 ft/s	11.36 ft/s
Pressure	1 psi = 5 psi	0.868 psi

The body of the scaled physical model was made of clear plexiglass, allowing the team to observe the behavior of the water as it moved through the designed system. Plexiglass also enabled the installation of sensors on the outside of the model to record the velocity data of each test without visual obstruction.

7.1 THE 1:5 SCALE SECTIONAL MODEL

The 1:5 scale model was designed using a series of interchangeable sections to allow for flexibility in determining an optimal plate length for the target wave development. Each section includes square flanges attached to each end to bond the model together during testing. A basic layout of the sectional approach to the 1:5 scale model is shown in Figure 64.

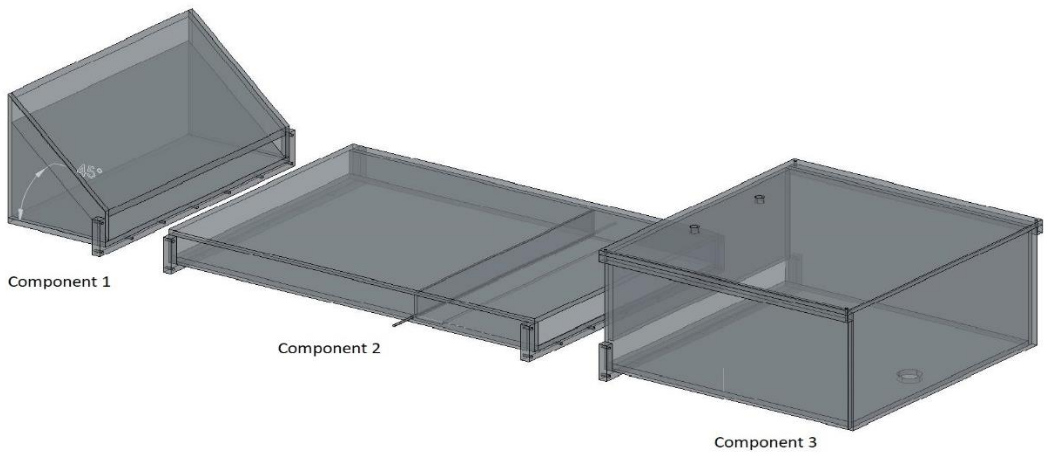

Figure 64. Basic layout of 1:5 sectional model.

The three components shown in Figure 64 represent the inlet section, gate section, and outlet section. During testing, water would be added through an inlet located at the end of Component 1 until the capacity of Component 1 and Component 2 (up to the gate) is reached. Air pressure would then be applied to the body of water through another inlet, also located at the end of Component 1.

The experiment begins once power is cut to the electromagnets holding the gate in place. As the gate opens, water rushes forward to Component 3 under the force from the applied air pressure. The 45-degree angle inlet at Component 1 was one of three inlet angles shown to increase the vertical flow profile in the FLOW-3D simulation. Two more versions of Component 1 were designed to accommodate the two remaining angles of 25-degrees and 35-degrees for testing. Not shown in Figure 64 are the additional sections designed to increase or decrease the lengths between Components for wave development. The sections range from 2.4 in. long to 24 in. long to simulate between 1 ft. and 10 ft. in the prototype, respectively. Complete drawings for this system can be found in Appendix H, p 113.

7.2 THE PIPE MODEL

FLOW-3D simulations of the 1:5 scaled model showed that the scale model could produce a near-vertical flow profile similar to the prototype if adequate pressure between 3 and 5 psi was quickly applied to the stagnant body of water. However, the mechanics of rapid air application had not yet been established by the team. An inlet port had been added to the sectional model for the air to enter, but the expansion of compressed air, the pressure loss across the pipe leading from air compressor to inlet, and other minor losses needed to be resolved prior to constructing the sectional model for testing.

A simple device for measuring pressure and velocity was devised. A pipe model would be constructed in the form of a u-tube using 4 in. NPS Schedule 40 clear PVC pipe, (see Figure 65). The u-tube shape allowed water to rest in the bottom of the device without the need for gates using a 45-degree angled inlet and outlet. The water would be filled to a depth of 1 ft. to simulate the head of a prototype channel, and the pressure to accelerate this water to a steady 11.36 ft/s velocity using compressed air could be investigated.

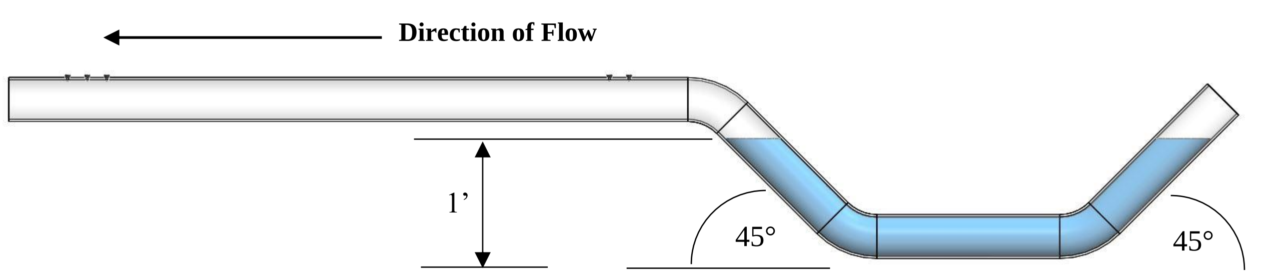

Figure 65. Pipe model for pneumatic testing.

8. PNEUMATICS

The decision to use a pneumatic system to accelerate the column of water in the reservoir section of the WISD to the required velocity of 25.4 ft/s before exiting the conduit was based on the research and recommendations of 2016 WISD member, Gregory Roberts. For a 1:5 scale model of the full-size prototype, the required velocity would be decreased to 11.36 ft/s, as previously shown in Table 14. The pressure given by FLOW-3D to achieve a constant 11.36 ft/s velocity be the exit of the scale model was 3 psi to 5 psi, depending on the inlet angle.

The initial length of the pipe model was designed to be 10 ft. overall, approximately 5 ft. for the u-tube section and 5 ft. for the horizontal outlet. The team agreed that this length could be adjusted as required. The air compressor specified for testing was a 60-gallon tank rated for 9.0 scfm at 100 psi with a standard 1/4 in. outlet. The pipe model was designed for a 4 in. NPS Schedule 40 clear PVC pipe with an inner diameter of 4.026 in. To minimize abrupt changes in pipe diameter from the 1/4 in. outlet of the compressor to the 4 in. PVC, the team chose a 2 in. NPS Schedule 40 PVC pipe to couple the two lines.

The FLOW-3D model also showed that the air pressure would need to be applied, then removed in approximately 0.38 seconds for a steady 11.36 ft/s velocity wave to develop. The valves controlling the pressure would therefore need to be fast-acting, actuated valves as manually opening and closing the valves could not be accomplished in the necessary timeframe. Solenoid valves with response times less than 50 milliseconds were chosen for the task. The following diagram illustrates the concept chosen by the team for applying the air pressure to the pipe model, (see Figure 66). Valves 1 and 3 are normally open (NO) solenoid valves that close when energized. Valve 2 is a normally closed (NC) solenoid valve that opens when energized. Power to all three valves is controlled by a multifunction timer relay.

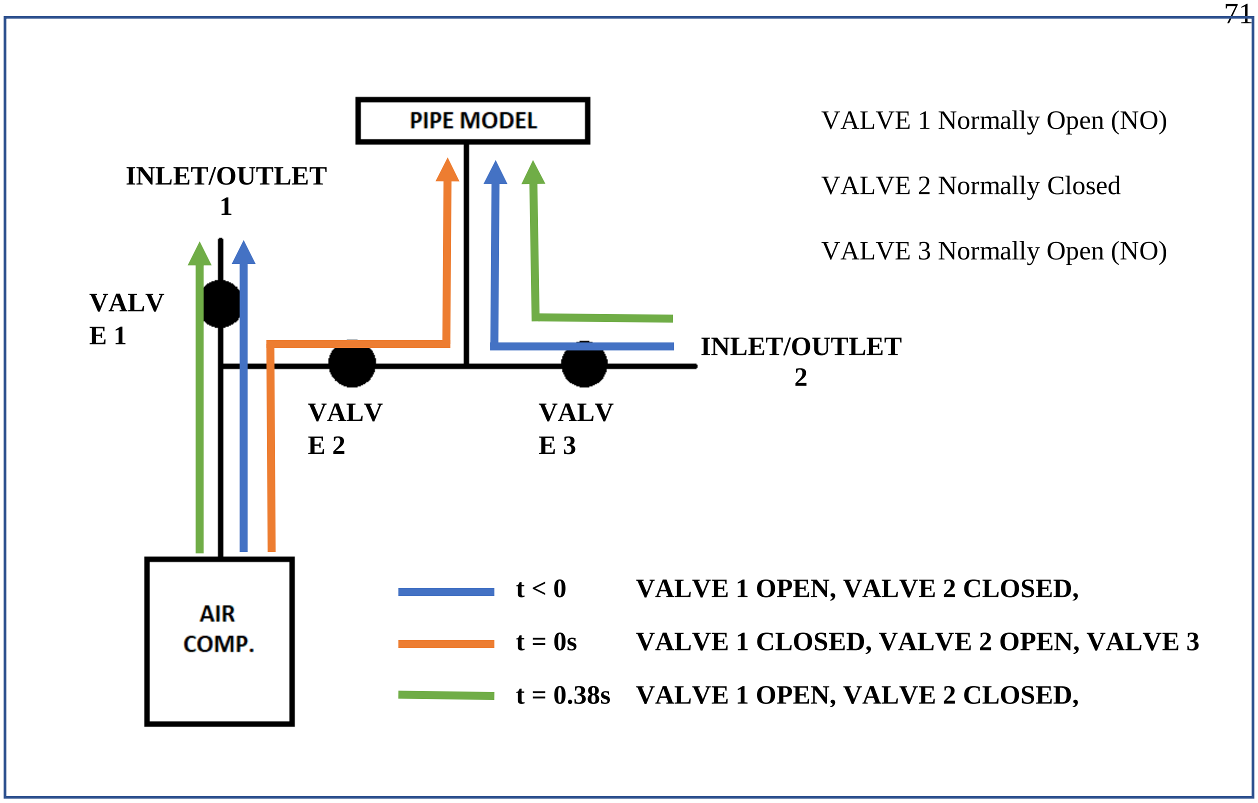

Figure 66. Diagram of pneumatic system for pipe model.

At t < 0 seconds, all three valves are in their normal state (unenergized). The compressor is turned on to allow steady state air flow to develop through the unenergized NO Valve 1. The section of pipe from Inlet/Outlet 2 to the pipe model is open to atmosphere since NO Valve 3 is also unenergized. At t = 0 seconds, all three valves become energized using the timer relay. NO Valve 1 closes, NC Valve 2 opens, and NO Valve 3 closes. Flow is directed from the air compressor through Valve 2 to the pipe model. At t = 0.38 seconds, the timer relay opens the circuit to all three valves and they return to their normal unenergized state. Air flow is directed back to the open Valve 1 since Valve 2 is now closed. Valve 3 allows atmospheric pressure to enter the pipe model so that a vacuum does not develop behind the moving column of water as the air pressure is removed. A simulated model using SOLIDWORKS is shown for the entire system below, (see Figure 67).

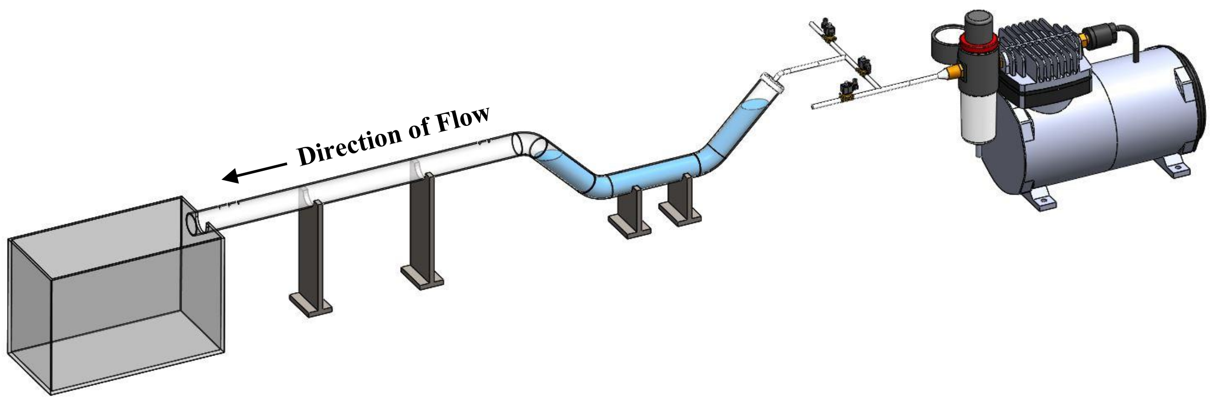

Figure 67. SOLIDWORKS simulation of complete pipe model assembly.

The team was able to locate three 2 in. 120V/60Hz rated for 5-100 psig that would meet the requirement of a less than 50 millisecond response time; however, the valves were not cost effective for the WISD budget. The 5 psig minimum inlet pressure was also a concern as it limited the team's testing range. Valve 1 would always receive the required minimum 5 psig when in use, but the other two valves would receive less than required 5 psig when Valve 1 was open. If Valve 3 does not re-open after t = 0.38 seconds, a vacuum could develop behind the water column in the tube, slowing or even stopping water flow.

The pipe size connecting the compressor to the model was then reduced to a 1 in. NPS Schedule 40 PVC to enable 1 in. valve connections. The 1 in. valves had the same reaction time as the 2 in. valves but were less expensive and rated for 0-125 psi. Then after reviewing the design, it was noted that the only valve requiring a larger orifice for flow control was Valve 2. Valve 1 and 3 were only in place to direct the flow to Valve 2 or atmosphere. Therefore, Valves 1 and 3 were further reduced to 1/2 in. 120V/50Hz solenoid valves with a 0-150 psi pressure rating. The team agreed to leave the pipe size unchanged from 1 in. and use reducers to connect the 1/2 in. valves.

9. RECOMMENDATIONS FOR FUTURE WORK

The construction of the pipe model is currently underway at CFEL. Experimentation with the pipe model will allow the WISD team to gather data for various configurations of input pressure and solenoid opening time, then determine the optimal combination required to produce the velocity, wave profile, and wave development length anticipated in the 1:5 scale model. If the team can recreate the same output conditions in the 1:5 scale model using the relationship established in the pipe model, the pneumatic approach discussed in this work should be similarly applicable for a full-size prototype design.

One of the largest obstacles facing the team throughout this investigation was the difficulty in creating a near-vertical flow profile. In each FLOW 3-D simulation, the flow was observed to move more rapidly in the bottom portion of the wave than it did near the top. The team understood this to be a logical behavior due to gravity that would eventually need to be revisited. As such, a second recommendation for future work would be the refinement of the outlet conduit. Several roughening materials, such as sandpaper, were discussed as potential candidates; however, the team was unable to study these effects further due to the time constraints of the project. Experimentation with various materials may provide the friction necessary for slowing the progression of the lower portion of the wave, thereby achieving a more accurate vertical wave profile.

Finally, the results discussed throughout the course of this thesis are based solely on computational modeling. The physical 1:5 scale model and full-size prototype will undoubtedly require modifications. In general, the WISD team recommends approaching the construction of a physical model in a manner similar to the methodology used here. First, establish the strength of materials to safely achieve a working system. Second, ensure that modifications to any component will not adversely impact the function of another. And third, experiment on a smaller scale prior to making any adjustments to the larger physical system.

10. CONCLUSION

A prototype for the Wave Impact Simulation Device (WISD) has been designed to meet the requirements of a near vertical wave profile, a uniform velocity of 25.4 ft/s, and a rapid-response release system. The prototype will incorporate a pneumatically driven, ten level water system. The ten channels of the prototype will be constructed of 10 ft. x 10 ft. x 3/8 in. thick, A36 steel plates supported by interspersed 1/4 in. steel rod and rivet nut supports. The maximum deflection under a uniform 1.3 psi pressure (equivalent to 3 ft. of hydrostatic head) was found to be 0.04 in. using the SOLIDWORKS Simulation FEA. The gates of the prototype consist of 1-3/4 in. keyed shafts with 3/8 in. thick steel, rectangular plates spanning the width of each channel. Electromagnets were chosen as the preferred gate mechanism to achieve a 90.8 rad/s angular velocity and 90-degree travel time of 0.02 seconds.

All design requirements and resultant parameters from the WISD prototype simulation study were reduced to 1:5 of their respective value to accommodate scale-model testing. The scale model will allow experimentation on the proposed prototype design to verify and/or modify parameters as necessary, prior to the construction of a full-size system. A complete set of drawings for one level of the 1:5 scale model was included in this work. To establish the pneumatic requirements for achieving a near vertical, constant velocity wave profile, a third model was designed to study the effects of compressed air and response time of fast-acting solenoid valves. This model, referred to as the pipe model, is currently under construction at CFEL. Once the relationship between input pressure, valve opening time, velocity, wave profile, and wave development length is established, the same pneumatic approach will be applied to the 1:5 scale model, and eventually, the full-size WISD prototype.

REFERENCES

Akin, J. E. 2010. “Finite Element Analysis Concepts: via SolidWorks”. Singapore: World Scientific, 2010.

Allsop, W., I. Chandler, and M. Zaccaria. 2014. “Improvements in the Physical Modelling of Tsunamis and Their Effects.” 5th International Conference on the Application of Physical Modelling in Coastal and Port Engineering and Science. Varna, Bulgaria: Coastlab 14.

Araki, S., Kunimatsu, W., Nishiyami, S., Furuse, T., Aoki, S., and Kotake, Y. 2016. “Experimental Study on Tsunami Wave Load Acting on Storage Tank in Coastal Area.” Journal of Loss Prevention in the Process Industries. No. 50, 347-354.

Basco, A., and Salzano, E. 2016. “The Vulnerability of Industrial Equipment to Tsunami.” Journal of Loss Prevention in the Process Industries. No. 50, 301-307.

Bhandari, B. 2016. “Flooding Fragility Experiments.” Master’s Thesis, Idaho State University.

Budynas, Richard G., and J. Keith Nisbett. Shigleys Mechanical Engineering Design. New York, NY: McGraw-Hill Education, 2015.

Chandler, I. D., Allsop, W. H., Granged, I. B., and McGovern, D. J. 2016. “Understanding Wave Generation in Pneumatic Tsunami Simulators.” Proceedings of the 6th International Conference on the Application of Physical Modelling in Coastal and Port Engineering and Science. Ottawa, Canada: Coastlab16.

Cooper, A., Cuomo, G., Bourban, S., Turnbull, M., and Roscoe, D. 2012. “Testing TELEMAC-2D Suitability for Tsunami Propogation from Source to Near Shore.” XIXth TELEMAC-MASCARET User Conference. Oxford, UK, October 18-19, 2012.

Dimakopoulos, A. S., Guercio, A., and Cuomo, G. 2014. “Advanced Numerical Modelling of Tsunami Wave Propagation, Transformation, and Run-up.” Proceedings of the Institution of Civil Engineering and Computational Mechanics 167, 3. September 2014.

“Fukushima Accident.” World Nuclear Association. October 2017. Accessed February 23, 2018. http://www.world-nuclear.org/information-library/safety-and-security/safety-of-plants/fukushima-accident.aspx.

Hibbeler, R. C. Mechanics of materials. Upper Saddle River, NJ: Pearson Prentice Hall, 2005.

Hiraishi, T., Shimomisu, Y., and Kyoto, F. 2015. “Development of New Tsunami Generator.” Applied Mechanics and Materials. Vol. 802, 45-50.

“How to Create the Perfect Wave.” INGENIA 2016, No. 69 24-29.

Kirke, A., Freeman, S., and Miranda, E. R. 2015. “Wireless Interactive Sonification of Large Waves to Demonstrate the Facilities of a Large-Scale Research Wave Tank.” Massachusetts Institute of Technology. Computer Music Journal 39:3, 59-70.

Liszewski, A. 2007. “World’s First Tsunami Simulator Tank.” OhGizmo!

Lloyd, T. O. and Rossetto, T. 2012. “A Comparison Between Existing Tsunami Load Guidance and Large-Scale Experiments with Long-Waves.” Proceedings of the World Conference on Earthquake Engineering. Libson, Portugal. 2012.

Malek-Mohammadi, S. and Testik, F. Y. 2010. “New Methodology for Laboratory Generation of Solitary Waves.” Journal of Waterway, Port, Coastal, and Ocean Engineering. ASCE. September/October 2010 286-294.

Mello, P. C., Perez, N., Adamowski, J. C., and Nichimoto, K. 2014. “Wave Focalization in a Wave Tank by Using Time Reversal Technique. Ocean Engineering. No. 123 2016, 314-326.

Munson, Bruce Roy, Donald F. Young, and Theodore H. Okiishi. Fundamentals of Fluid Mechanics. New York: Wiley, 2002.

“Nuclear Power in the “USA.” World Nuclear Association. February 2018. Accessed February 23, 2018. http//www.world-nuclear.org/information-library/country-profiles/countries-t-z/usa-nuclear-power.aspx.

Okal, E. A., S. H. Kirby, and N. Kalligeris. 2016. “The Showa Sanriku Earthquake of 1933, March 2: A Global Seismological Reassessment.” Geophysical Journal International, (206)(3) 1492-1514.

Pallardy, Richard. 2017. Chile Earthquake of 1960. Encyclopedia Britannica, Inc.

Perkins, R. H., Bensi, M. T., Philips, Sancaktar, S. 2011. “Screening Analysis Report for the Proposed Generic Issue on Flooding of Nuclear Power Plant Sites Following Upstream Dam Failures.” U.S. Nuclear Regulatory Commission Office of Nuclear Regulatory Research Division of Risk Analysis. Document No. GI-204.

Pope, C. L., Wells, A., Kamerman, D. A., Bhandari, B., Roberts, G., Tahhan, A., Muchmore, C., Ryan, E., and Suresh, S. 2016. “Nuclear Power Plant Component Reliability Under Flooding Conditions.” U.S. Department of Energy, Light Water Reactor Sustainability.

Rhinefrank, K., Schacher, A., Prudell, J., Hammagren, E., Stillinger, C., Naviaux, D., Brekken, T., and Jouanne, A. V. 2010. “Scaled Wave Energy Device Performance Evaluation Through High Resolution Wave Tank Testing.” Oceans 2010. IEEE.

Roberts, G. 2016. “Research and Development of a Wave Impact Simulation Device for the Idaho State University Component Flooding Evaluation Laboratory.” Master’s Thesis, Idaho State University.

Rossetto, T., Allsop, W., Robinson, D., Chavet, I., and Bazin, P. H. 2008. “Analysis of Tsunami Hazards by Modelling Tsunami Wave Effects.” Proceedings of FLOODrisk 2008. Flood Risk Management: Research and Practice. Oxford, UK, September 30-October 2, 2008. 515-521.

Shimosako, K., Takahashi, S., Suzuki, K. and Kang, Y. 2002. “Large Hydro-Geo Flume and its Use for Coastal Engineering Research.” Technical Note of National Institute for Land and Infrastructure Management 41, 81-89.

Shuto, N., and K. Fujima. 2009. “A Short History of Tsunami Research and Countermeasures in Japan.” Proceedings of the Japan Academy. Series B, Physical and Biological Sciences, 85(8). 267-275.

Soumadipta, J. 2018. “High-Speed Velocity Measurement Instrumentation of Air-Driven Water Jet for a Wave Impact Simulation Device.” Master’s Thesis, Idaho State University.

Streicher, M., Hofland, B., and Lindenbergh, R. C. 2013. “Laser Ranging for Monitoring Water Waves in the New Deltares Delta Flume.” ISPRS Annals of the Photogrammetry, Remote Sensing and Spatial Information Sciences. Volume II-5/W2, 271-276.

Tahhan, A., Muchmore, C., Nichols, L., Wells, A., Roberts, G., Ryan, E., Suresh, S., Bhandari, B., and Pope, C. 2017. “Development of Experimental and Computational Procedures for Nuclear Power Plant Component Testing Under Flooding Conditions.” V009T15A068. 10.1115/ICONE25-67985.

Tar, T., Kato, N., Suzuki, H., Nagai, Y., Ohnishi, K., and Okubayashi, T. 2016. “Experimental and Numerical Study on the Reduction of Tsunami Flow Using Multiple Flexible Pipes.” Journal of Loss Prevention in the Process Industries. No. 50, 364-385.

Tuladhar, R. 2018. “Physical Experiment Study and Numerical Modeling of a Wave Impact Simulation Device (WISD).” Master’s Thesis, Idaho State University.

Young, WC, and RJ Roark. Roarks Formulas for Stress and Strain, 6th ed. New York: McGraw Hill, 1989.

Yuichiro, Tanioka. 2001. “Sediment Effect on Tsunami Generation of the 1896 Sanriku Tsunami Earthquake.” In Geophysical Research Letters, Vol. 28, No. 17, by Tetsuzo Seno Earthquake Institute, 3389-3392. Tokyo: Seismology and Volcanology Research Department, Meteorological Research Institute. 267-275.

APPENDIX A: Hand Calculations for Required Plate Thickness

CFEL-W 5/15/17 Hand Calculations Larinda Nichols 1/9

Wave Machine

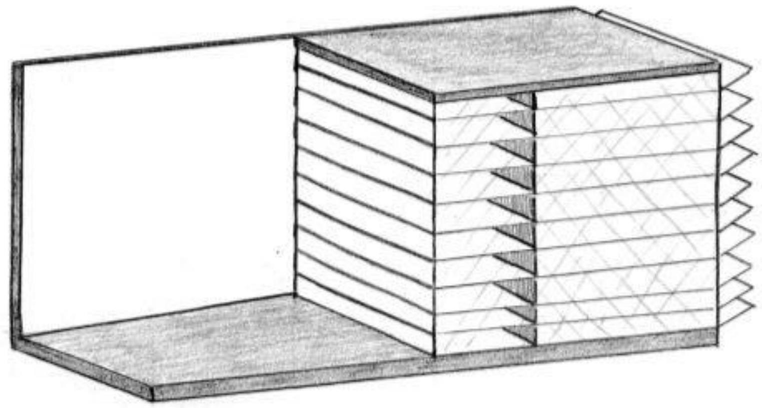

Current Assumptions

Overall Dimensions:

Plate length behind gates = 10 ft

End angle for each plate = 45°

Plate length after gates = 5 ft

Overall exit area = 10 ft × 10 ft

Number of plates = 9

Surrounding concrete = 1 ft thick

Volume of entire water column:

Without plates = 10 ft × 10 ft × 10 ft $\approx$ 1000 ft^3

Pressure at bottom of column behind gates:

$P = \gamma h$

$\gamma_{H_2O}(60°F) = 62.4\ lbf/ft^3$

$h_{H_2O} = 10\ ft$

$P_{Bottom} = 624\ \frac{lbf}{ft^2}\left(\frac{1\ ft^2}{144\ in^2}\right) = 4.33\ psi$

L. Nichols 2/9

From Greg Robert's Simulation:

- 10 Gate Components
- 1.5 in. thick
- Horizontal Rotation (90° about y-axis)
- $\omega = \pm 15.708$ ft/s
- 0.1 sec.

Target wave speed = 25.4 ft/s

Current design Maximum Velocity = 24.8259 to 25.4243 ft/s
(4 cell/ft to 14 cell/ft mesh)

* Simulation time of Maximum Velocity ≈ 0.621 to 0.642s

[see Table 2 for more information (Roberts, Thesis)

Project Considerations

1. Gate mechanism
2. Leakage
3. Plate Weight*
4. Maintenance access
5. Air pressure to displace fluid
6. Ease of plate insertion/removal
7. Fluid reservoir
8. Power required to operate
9. Flow channel
10. Material* & Cost
11. Observation area

[* Material assumptions
- Concrete housing
- Steel plates
- Steel gates]

L. Nichols 3/9

GATE CONCEPTS

1. Bottom hinged
2. Butterfly valve

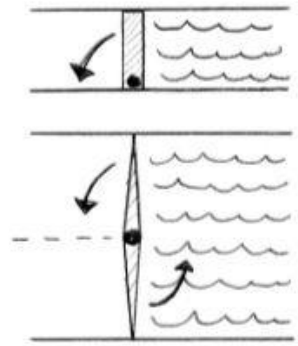

Gate Considerations

- Rotational inertia
- Time to rotate open
- Force to rotate open
- Force to resist water column
- Mechanism for action
- Stress/strain/fatigue on gate and mechanism
- Leakage
- Water profile disruption

Forces on Gates (Hydrostatic Magnitude)

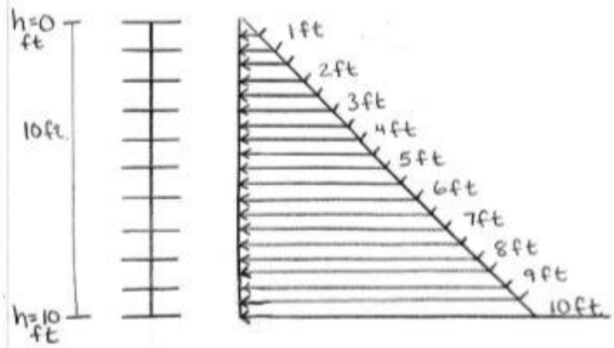

- Gate is 10 ft. Wide and ~1 ft. Tall
- $\gamma = 62.4\ lb/ft^3$
- Possible Gate of 5 ft. Wide and ~1 ft Tall
- Linear Distribution

Individual Gates: (Linear distribution)

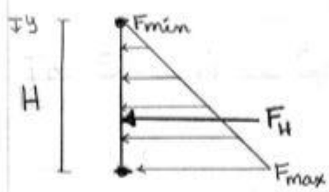

F_H acts at $2/3\,H$ ($y_R = 2/3\,H$)

$F_H = P_{ave} \cdot A$

$H_c = 1/2\,H$ (Rectangular Gate)

$P_{ave} = \gamma_{H_2O} H_c$

L. Nichols 4/9

Bottom Hinged Gate

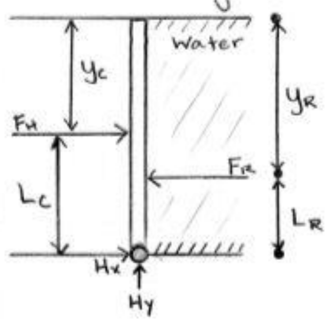

Assume bottom gate, 5ft wide

$A = (5ft)(1ft) = 5ft^2$

$y_c = h_c = 9.5\ ft$

$F_R = \gamma h_c A = (62.4\ lb/ft^3)(9.5ft)(5ft^2)$

$$\underline{\underline{F_R = 2964\ lb.}}$$

$$y_R = y_c + \frac{I_{xc}}{y_c A} = 9.5ft + \frac{(5ft)(1ft)^3}{(9.5ft)(5ft^2)} \Rightarrow y_R = \underline{\underline{9.605\ ft}}$$

$$\Sigma M_H = 0 = F_R L_R - F_H L_c = F_R(10-9.605)ft - F_H(10-9.5)ft$$

$$F_H = \frac{F_R(0.395ft)}{0.5ft} = \frac{(2964lb)(0.395ft)}{0.5ft}$$

$$\underline{\underline{F_H = 2341.56\ lb}}$$

Torque Required at hinge for $\Sigma M_H = 0$ is $\underline{\underline{1170.78\ lb\text{-}ft}}$

Center Hinged Gate

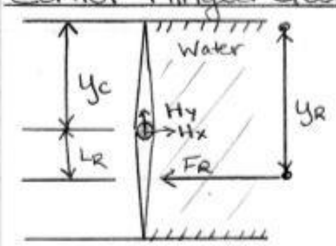

Again, assume bottom gate, 5ft wide

$A = 5ft^2$, $y_c = 9.5\ ft$

$\underline{\underline{F_R = 2964\ lb}}$ (same as above)

$\underline{\underline{y_R = 9.605\ ft}}$ (same as above)

But now the torque required for $\Sigma M_H = 0$,

$$T_H = F_R L_R = (2964lb)(y_R - y_c)$$

$$T_H = (2964\ lb)(9.605\ ft - 9.5\ ft)$$

$$T_H = (2964\ lb)(0.105)$$

$$\underline{\underline{T_H = 311.22\ lb\text{-}ft}}$$

L. Nichols 5/9

Plate Analysis

Assumption: Plates will be 5 ft wide

For plates 15 feet in length

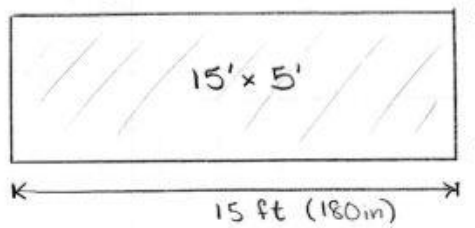

Carbon Steel (Shig)

$w = 0.282\ lbf/in^3$
$E = 30.0\ Mpsi$
$G = 11.5\ Mpsi$
$\nu = 0.292$

Sheet thickness		Weight/sheet (lb)
3/16 in.	(0.1875 in)	$0.282\ lb/in^3\ (180in)(60in)(0.1875in) \cong 571$
1/4 in.	(0.25 in)	$0.282\ lb/in^3\ (180in)(60in)(0.25in) \cong 762$
3/8 in.	(0.375 in)	$0.282\ lb/in^3\ (180in)(60in)(0.375in) \cong 1142$
1/2 in.	(0.5 in)	$0.282\ lb/in^3\ (180in)(60in)(0.5in) \cong 1523$

* Least amt of weight ≅ 571 lb/sheet (for 15' × 5' × 3/16")

* Total number of sheets needed = 2/level × 9 levels = 18

For plates 10' × 5'

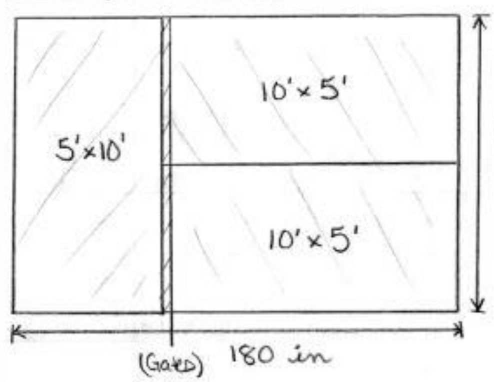

Area of each plate
→ $A = 120" \times 60" = 7200\ in^2$

Total number of plates
3/level × 9 levels = 27

Weight per Plate

3/16 in.	≅ 381 lb.
1/4 in.	≅ 508 lb
3/8 in.	≅ 762 lb.
1/2 in.	≅ 1015 lb.

★ Need to analyze: Force, Deflection, Stress, and slope to determine thickness required for application.

Assume simply supported:

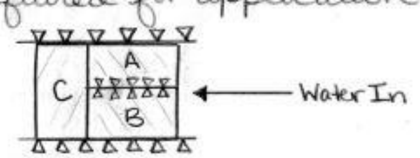

L. Nichols 6/9

Forces, Deflection and Stress on Plates

Analyzing bottom plate (plate #9) since the force will be greatest here.

$$P = \gamma h = (62.4\ \text{lb/ft}^3)(9\ \text{ft}) = 561.6\ \text{lb/ft}^2 \left(\frac{1\ \text{ft}^2}{144\ \text{in}^2}\right) = 3.9\ \text{psi}$$

$$A = (10' \times 5') = (120\ \text{in} \times 60\ \text{in}) = 7200\ \text{in}^2$$

Calculations Using "Roark's Formulas for Stress & Strain"
- CH11, TABLE 11.4, Formulas for Flat Plates with Straight Boundaries & Const. Thickness

Case No. 2. Rectangular Plate; three edges simply supported, one edge free

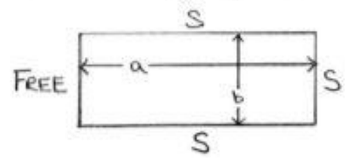

2a. Loading uniform over entire plate

2b. Loading uniformly increasing along a

(These calculations assume $\nu = 0.3$, steel) ✓

For plates A and B (10' × 5') $a = 10\ \text{ft} = 120\ \text{in}$
$b = 5\ \text{ft} = 60\ \text{in}$
Case 2a. (Uniform)

For plate C (5' × 10') $a = 5\ \text{ft} = 60\ \text{in}$
$b = 10\ \text{ft} = 120\ \text{in}$
Case 2b. (Increasing)

2a. $\sigma_{max} = \dfrac{\beta q b^2}{t^2}$ $\quad y_{max} = \dfrac{-\alpha q b^4}{E t^3}$ $\quad$ from table, $\dfrac{a}{b} = 2 \left\{ \begin{array}{l} \beta = 0.79 \\ \alpha = 0.165 \end{array} \right.$

$q = 3.9\ \text{psi}$ (plate #9)

For 3/16" thick: $\sigma_{max} = \dfrac{(0.79)(3.9\ \text{lb/in}^2)(60\ \text{in})^2}{(0.1875)^2} = 315{,}495\ \text{psi}$

$$n = \frac{S_{yt}}{\sigma_{max}} = \frac{57{,}990\ \text{psi}}{315{,}495\ \text{psi}} = 0.565$$

Factor of safety is <1, no need to proceed further with 3/16" thick plate (unless we use something other than plain carbon steel.

L. Nichols 7/9

(Roark's Formulas Continued)

For 3/8" thick : $\sigma_{max} = \frac{(0.79)(3.9\ lb/in^2)(60in)^2}{(0.375in)^2} = 78{,}873.6\ psi$

$n = \frac{S_{yt}}{\sigma_{max}} = \frac{57{,}990\ psi}{78{,}873.6\ psi} = 0.735$! (less < 1)

For 1/2" thick : $\sigma_{max} = \frac{(0.79)(3.9\ lb/in^2)(60in)^2}{(0.5in)^2} = 44366.4\ psi$

$n = \frac{S_{yt}}{\sigma_{max}} = \frac{57{,}990\ psi}{44{,}366.4\ psi} = 1.31$ (factor of safety)

Deflection using 1/2" thick carbon steel:

$y_{max} = -\frac{\alpha q b^4}{E t^3} = \frac{(-0.165)(3.9\ lb/in^2)(60in)^4}{(30.46E6\ lb/in^2)(0.5in)^3} = -2.2\ in.$

Max deflection ≈ −2.2 inches

For plate C, 1/2" thick carbon steel (plain)

2b. $\sigma_{max} = \frac{\beta q b^2}{t^2}$, $y_{max} = \frac{-\alpha q b^4}{E t^3}$ from table, $\frac{a}{b} = 0.5 \left\{ \begin{array}{l} \beta = 0.11 \\ \alpha = 0.026 \end{array} \right.$

$\sigma_{max} = \frac{(0.11)(3.9\ lb/in^2)(120in)^2}{(0.5in)^2} = 24{,}710.4\ psi$ (n = 2.34)

$y_{max} = \frac{(-0.026)(3.9\ lb/in^2)(120in)^4}{(30.46E6\ lb/in^2)(0.5in)^3} = -5.52\ in$!

- Deflection is almost 1/2 the height of the 1 ft opening.
- Need to look into stronger/stiffer steel, or maybe "fix" plates to the sides of the channel.

Option 1: "Fix" plates on sides of flume, other 2 sides "simply" supported

Plates A + B → Case 4

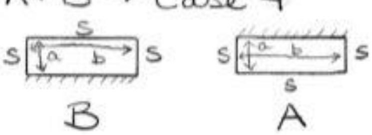

B A

Plate C → Case 5

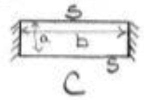

C

L. Nichols 8/9

Option 2: Stronger/Stiffer Steel

		S_{yt}	Price
Currently:	A-36 Carbon Steel	58 Kpsi	\$1-1.50/lb
	T304 Stainless	85 Kpsi	\$3/lb
	Astralloy	140-240 Kpsi	?

Cold Rolled?
Galvanized?

Option 3: Decrease width/span of plates.
Maybe 2.5' x 10' plates?

First, looking at option 1: Additional Support

Fixed along sides of channel:

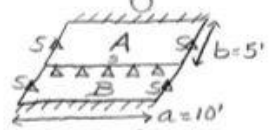

- "Fix" using bolts inside flume housing?

Case 4: $\sigma_{max} = \frac{\beta q b^2}{t^2}$, $y_{max} = -\frac{\alpha q b^4}{E t^3}$ $\quad \frac{a}{b} = 2 \Big\} \begin{matrix} \beta = 0.73 \\ \alpha = 0.054 \end{matrix}$

For 3/16" thick: $\sigma_{max} = \frac{(0.73)(3.9\ lb/in^2)(60in)^2}{(0.1875in)^2} = 291{,}532.8$ psi

• Doesn't decrease σ_{max} by much. (originally 315,495psi)

Next, try decreasing width/span of plates (option 3)

For plates before gates open:

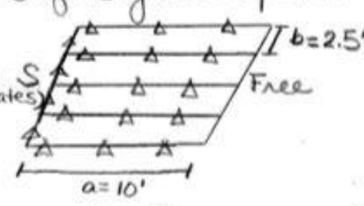

$a = 10' = 120 in$
$b = 2.5' = 30 in$

Case 2a: $\sigma_{max} = \frac{\beta q b^2}{t^2}$, $y_{max} = \frac{-\alpha q b^4}{E t^3}$ $\quad \frac{a}{b} = 4 \Big\} \begin{matrix} \beta = 0.80 \\ \alpha = 0.167 \end{matrix}$

[3/16" thick] $\sigma_{max} = \frac{(0.8)(3.9\ lb/in^2)(30in)^2}{(0.1875in)^2} = 79{,}872\ psi$

$n = \frac{S_{yt}}{\sigma_{max}} = \frac{57{,}990\ psi}{79{,}872\ psi} = 0.726$! (less < 1)

L. Nichols 9/9

For 3/8" → $\sigma_{max} = \frac{(0.8)(39\ lb/in^2)(30\ in)^2}{(0.375\ in)^2} = 19{,}968\ psi$

$$n = \frac{S_{yt}}{\sigma_{max}} = \frac{57{,}990\ psi}{19{,}968\ psi} = 2.9\ \checkmark$$

$$y_{max} = -\frac{\alpha q b^4}{E t^3} = \frac{(-0.167)(39\ \frac{lb}{in^2})(30\ in)^4}{(30.46E6\ lb/in^2)(0.375\ in)^3} = -0.33\ in$$

This configuration would work best if possible.

Factor of Safety = 2.9
Max Deflection = 0.33 in
Weight of 2.5' × 10' × 3/8" plates = 380.7 lb

★ Issue for plates after gate section?

To discuss: Plate options before gate section
Plate option after gate section
Options for steel
Additional Support for plates

CFEL-W 6/28/17 Hand Calculations Larinda Nichols 1/1

New Geometry: 4-30 in. Plates per Level (10 ft. Plates)
Plate thickness = 3/16 in.

Individual Plate Weight = (0.282 lb/in³)(120 in)(30 in)(0.1875 in)

W_{each} = 190.35 lb.

Roark's Maximum Formulas (6)

$$\sigma_{max} = -\frac{(0.5)(3.9\ psi)(30\ in)^2}{(0.1875\ in)^2} = 49{,}920\ psi$$

$$n = \frac{S_{yt}}{\sigma_{max}} = \frac{57{,}990\ psi}{49{,}920\ psi} = 1.16$$

$$y_{max} = -\frac{(0.0285)(3.9\ lb/in^2)(30\ in)^4}{(30.46E6\ lb/in^2)(0.1875)in^3} = 0.44839\ in$$

WISD - ROARKS FORMULAS FOR PLATE STRESS AND DEFLECTION

Channel Height (ft)	1
Channel Width (ft)	10
Specific Density Water (lb/ft^3)	62.4
Pressure on Plate (psi)	0.433

	Width (ft) b	Width (in) b	Length (ft) a	Length (in) a
Geometry 1	10	120	10	120
Geometry 2	5	60	10	120
Geometry 3	2.5	30	10	120

	(in)	(in)
Thickness 1	3/8	0.3750
Thickness 2	1/4	0.2500
Thickness 3	3/16	0.1875
Thickness 4	1/8	0.1250

ROARK'S TABULATED VALUES	a/b	1	1.2	1.4	1.6	1.8	2	∞
	β	0.4182	0.4626	0.486	0.4968	0.4971	0.4973	0.5000
	α	0.021	0.0243	0.0262	0.0273	0.028	0.0283	0.0285

Elastic Modulus (psi)	30,457,924.91
Poisson's Ratio	0.3
Yield Strength (psi)	31,994.45
Mass Density (lb/in^3)	0.281793

CASE NO. 6 - MAX YIELD

$$Max\ \sigma = \frac{-\beta q b^2}{t^2}$$

CASE NO. 6 - MAX DEFLECTION

$$Max\ y = \frac{-\alpha q b^4}{E t^3}$$

10'x10' GEOMETRY	Width (in) b	Length (in) a	Ratio (w/l) a/b	Tabulated Value β	Tabulated Value α	Pressure (psi) q	Thickness (inches) t	Volume (in^3) V	Weight (lb) w	Max Yield (psi) σ	Factor of Safety N	Max Deflect (in) y	Max Deflect vs. Thickness
3/8"	120	120	1	0.4182	0.021	0.433	0.3750	5400	1521.68	18556.93	1.7	1.1748	3.1
1/4"	120	120	1	0.4182	0.021	0.433	0.2500	3600	1014.45	41753.09	0.8	3.9650	16
3/16"	120	120	1	0.4182	0.021	0.433	0.1875	2700	760.84	74227.71	0.4	9.3986	50
1/8"	120	120	1	0.4182	0.021	0.433	0.1250	1800	507.23	167012.4	0.2	31.7202	254

5'x10' GEOMETRY	Width (in) b	Length (in) a	Ratio (w/l) a/b	Tabulated Value β	Tabulated Value α	Pressure (psi) q	Thickness (inches) t	Volume (in^3) V	Weight (lb) w	Max Yield (psi) σ	Factor of Safety N	Max Deflect (in) y	Max Deflect vs. Thickness
3/8"	60	120	2	0.4973	0.0283	0.433	0.3750	2700	760.84	5516.715	5.8	0.0990	0.3
1/4"	60	120	2	0.4973	0.0283	0.433	0.2500	1800	507.23	12412.61	2.6	0.3340	1.3
3/16"	60	120	2	0.4973	0.0283	0.433	0.1875	1350	380.42	22066.86	1.4	0.7916	4.2
1/8"	60	120	2	0.4973	0.0283	0.433	0.1250	900	253.61	49650.43	0.6	2.6717	21

2.5'x10' GEOMETRY	Width (in) b	Length (in) a	Ratio (w/l) a/b	Tabulated Value β	Tabulated Value α	Pressure (psi) q	Thickness (inches) t	Volume (in^3) V	Weight (lb) w	Max Yield (psi) σ	Factor of Safety N	Max Deflect (in) y	Max Deflect vs. Thickness
3/8"	30	120	4	0.5000	0.0285	0.433	0.3750	1350	380.42	1386.667	23.1	0.0062	0.02
1/4"	30	120	4	0.5000	0.0285	0.433	0.2500	900	253.61	3120	10.3	0.0210	0.08
3/16"	30	120	4	0.5000	0.0285	0.433	0.1875	675	190.21	5546.667	5.8	0.0498	0.27
1/8"	30	120	4	0.5000	0.0285	0.433	0.1250	450	126.81	12480	2.6	0.1682	1.35

GEOMETRIES MEETING ROARK'S RESTRICTIONS	Width (in) b	Length (in) a	Ratio (w/l) a/b	Tabulated Value β	Tabulated Value α	Pressure (psi) q	Thickness (inches) t	Volume (in^3) V	Weight (lb) w	Max Yield (psi) σ	Factor of Safety N	Max Deflect (in) y	Max Deflect vs. Thickness
3/8" - 5'x10' Plate	60	120	2	0.4973	0.0283	0.433	0.3750	2700	760.84	5516.715	5.8	0.0990	0.26
3/8" - 2.5'x10' Plate	30	120	4	0.5000	0.0285	0.433	0.3750	1350	380.42	1386.667	23.1	0.0062	0.02
1/4" - 2.5'x10' Plate	30	120	4	0.5000	0.0285	0.433	0.2500	900	253.61	3120	10.3	0.0210	0.08
3/16" - 2.5'x10' Plate	30	120	4	0.5000	0.0285	0.433	0.1875	675	190.21	5546.667	5.8	0.0498	0.27

COMPARISON OF ROARK RESULTS WITH SOLIDWORKS

	MAXIMUM YIELD STRESS (psi)			MAXIMUM DEFLECTION (in)		
	ROARK'S	SOLIDWORKS	% DIFF	ROARK'S	SOLIDWORKS	% DIFF
3/8" - 5'x10' Plate	5516.7	5108.5	7.7	0.0990	0.1110	11.5
3/8" - 2.5'x10' Plate	1386.7	1190.5	15.2	0.0062	0.0069	10.9
1/4" - 2.5'x10' Plate	3120.0	2688.7	14.9	0.0210	0.0234	10.5
3/16" - 2.5'x10' Plate	5546.7	4703.0	16.5	0.0498	0.0547	9.3

APPENDIX B: SOLIDWORKS Simulation Settings

Study Properties

Analysis type	Static
Mesh type	Solid Mesh
Thermal Effect:	On
Thermal option	Include temperature loads
Zero strain temperature	298 Kelvin
Include fluid pressure effects from	Off
Solver type	FFEPlus
Inplane Effect:	Off
Soft Spring:	Off
Inertial Relief:	Off
Incompatible bonding options	Automatic
Large displacement	Off
Compute free body forces	On
Friction	Off
Use Adaptive Method:	Off

Mesh information

Mesh type	Solid Mesh
Mesher Used:	Curvature-based mesh
Jacobian points	29 Points
Maximum element size	1.20561 in
Minimum element size	0.0602806 in
Mesh Quality	High

Mesh information - Details

Total Nodes	99486
Total Elements	49183
Maximum Aspect Ratio	6.2275
% of elements with Aspect Ratio < 3	98.1
% of elements with Aspect Ratio > 10	0
% of distorted elements(Jacobian)	0

SOLIDWORKS Analyzed with SOLIDWORKS Simulation

APPENDIX C: Rivet Nuts for Plate Supports

Rivetnut - Plusnut

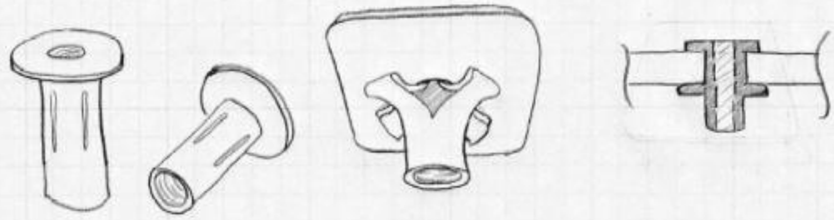

Optimal Configuration

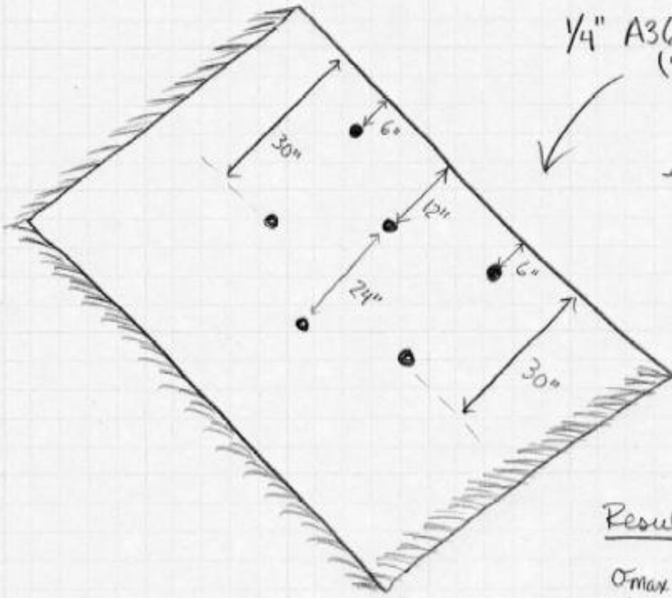

1/4" A36 Steel
(5'x10')

~0.4335 psi
Pressure
(uniform)

Results

σ_{max} = 15,801 psi
y_{max} = 0.043 psi

Plusnut

1/4-20 - Thread Size (S25P500)

Grip = 1/4"
Hole Size = 0.347"
Body diameter = 0.346"
Head/Flange height = 0.058"
Head Diameter = 0.625"
Overall length = 1.292"
Final length = 0.505"

RIVNUT® PN - PLUSNUT®

The Rivnut® PN – Plusnut® has been designed to provide the ultimate pull out strength in thin sheet metals and plastic. Its slotted body splits into four legs providing a wide load-bearing surface on the backside of the parent material. The Rivnut® PN – Plusnut® also features the widest grip range of any blind threaded nut. A grip ID mark is included on the head of the fastener for grip range identification.

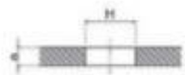

Class 2B or Metric Class 6H threads
Steel C1010-1008
Cadmium plating per QQ-P-416

All Dimensions Shown In Inches

d	e	H		D	E	B	L	L2	
Thread Size	Grip Range	Hole Size		Body Diameter Max.	Head Height Ref.	Head Diameter Ref.	Overall Length Ref.	Installed Length Ref.	Product Code
		Min.	Max.						
6-32	0.020-0.150	0.209	0.214	0.208	0.032	0.438	0.688	0.335	RN632150PN
6-32	0.150-0.270	0.209	0.214	0.208	0.032	0.438	0.797	0.335	RN632270PN
8-32	0.020-0.150	0.242	0.247	0.241	0.038	0.438	0.694	0.340	RN832150PN
8-32	0.150-0.270	0.242	0.247	0.241	0.038	0.438	0.819	0.340	RN832270PN
10-32	0.020-0.175	0.273	0.278	0.272	0.038	0.500	0.819	0.425	RN1032175PN
10-32	0.175-0.320	0.273	0.278	0.272	0.038	0.500	0.959	0.425	RN1032320PN
1/4-20	0.020-0.280	0.347	0.352	0.346	0.058	0.625	1.058	0.505	RN2520280PN
1/4-20	0.280-0.500	0.347	0.352	0.346	0.058	0.625	1.292	0.505	RN2520500PN
5/16-18	0.020-0.280	0.438	0.443	0.437	0.062	0.750	1.203	0.570	RN5161828PN
5/16-18	0.280-0.500	0.438	0.443	0.437	0.062	0.750	1.437	0.570	RN5161850PN
3/8-16	0.020-0.280	0.515	0.522	0.514	0.088	0.875	1.306	0.605	RN3816280PN
3/8-16	0.280-0.500	0.515	0.522	0.514	0.088	0.875	1.525	0.605	RN3816500PN

All Dimensions Shown In Millimeters

d	e	H		D	E	B	L	L2	
Thread Size	Grip Range	Hole Size		Body Diameter Max.	Head Height Ref.	Head Diameter Ref.	Overall Length Ref.	Installed Length Ref.	Product Code
		Min.	Max.						
M4x0.7	0.50-3.80	6.13	6.25	6.12	0.96	11.1	17.6	8.6	RN47038PN
M4x0.7	3.80-6.85	6.13	6.25	6.12	0.96	11.1	20.8	8.6	RN47068PN
M5x0.8	0.50-4.45	7.48	7.62	7.47	0.96	12.7	22.0	9.9	RN58045PN
M5x0.8	4.45-8.10	7.48	7.62	7.47	0.96	12.7	24.8	9.9	RN58081PN
M6x1.0	0.50-7.10	8.80	8.93	8.79	1.50	15.9	26.9	12.8	RN61071PN
M6x1.0	7.10-12.70	8.80	8.93	8.79	1.50	15.9	32.8	12.8	RN610127PN
M8x1.25	0.50-7.10	11.11	11.50	11.10	1.57	19.0	30.5	14.5	RN812571PN
M8x1.25	7.10-12.70	11.11	11.50	11.10	1.57	19.0	36.5	14.5	RN8125127PN
M10x1.50	0.50-7.10	13.07	13.26	13.06	2.24	22.2	33.2	15.8	RN101571PN
M10x1.50	7.10-12.70	13.07	13.26	13.06	2.24	22.2	38.7	15.8	RN1015127PN

APPENDIX D: Hand Calculations for Shaft and Gate Design

Given: 20 psi (air pressure, prototype)
4 psi (air pressure, 1:5 Sectional model)
1.3005 psi (hydrostatic pressure, prototype)
0.2601 psi (hydrostatic pressure, 1:5 sect. model)

Dimensions of Prototype:

10' × 10' Opening
9 Levels / Channels
Each plate = 1/4" thick (9 gates × 1/4" = 2.25")
Remaining Space (Gates) = 117.75"
Each gate = 11.775" high

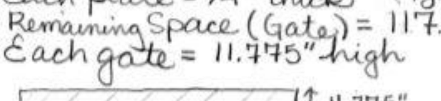

Dimensions of 1:5 Sectional Model:

1:5 for each gate height = 2.355"

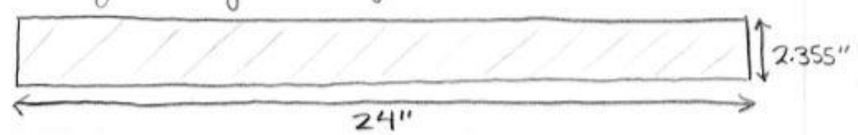

*Gates should open in ~0.1 sec

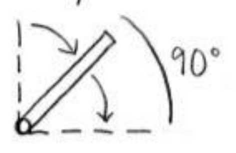

$$\left(\frac{90^\circ}{\text{tenth sec}}\right)\left(\frac{10\text{ tenth secs}}{1\text{ sec}}\right) = \frac{900^\circ}{\text{sec}}$$

$$\frac{900^\circ}{\text{sec}}\left(\frac{2\pi}{360^\circ}\right) = 15.708\text{ rad/sec } (\omega)$$

Assume standard A36 (ASTM) Steel:

Revolutions: $\frac{1/4\text{ revolution}}{0.1\text{ sec}} = \frac{1\text{ revolution}}{0.4\text{ secs}}(2.5) = \frac{2.5\text{ rev}}{\text{sec}}$

$$\frac{2.5\text{ rev}}{\text{sec}}\left(\frac{60\text{ sec}}{\text{min}}\right) = 150\text{ rev/min } (\omega) \text{ (rotation)}$$

Torque:

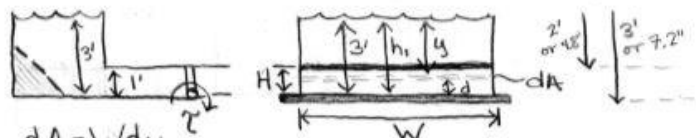

$dA = W\,dy$

And Force ⇒ $dF = P\,dA = \gamma y W\,dy$
(for hydrostatic pressure)

S.A. L. Nichols 2/4

Need to incorporate pressure from pressurized air.

Magnitude and Location of Total Force F_{R_H} = Hydrostatic, F_{R_A} = Air Pressure

$F_{R_H} = \gamma h_c A \quad , \quad F_{R_A} = PA$

For Prototype, (assuming 3' of total Head)

$F_{R_H\text{-}P} = (62.4\ \text{lb/ft}^3)(2.5\text{ft})(1\text{ft})(10\text{ft}) = 1560\ \text{lbf}$

$F_{R_A\text{-}P} = (20\ \text{psi})(12\text{in})(120\text{in}) = 28{,}800\ \text{lbf}$

Total $F_R = 30{,}360\ \text{lbf}$

For 1:5 Scaled Sectional Model, (assuming 7.2" Head)

$F_{R_H\text{-}M} = (62.4\ \text{lb/ft}^3)(0.5\text{ft})(0.2\text{ft})(2\text{ft}) = 12.48\ \text{lbf}$

$F_{R_A\text{-}M} = (4\ \text{psi})(2.4\text{in})(24\text{in}) = 230.4\ \text{lbf} \Rightarrow F_R = 242.88\ \text{lbf}$

Center of Pressure for Prototype,

$x_R = \dfrac{I_{xyc}}{y_c A} + x_c \quad , \quad y_R = \dfrac{I_{xc}}{y_c A} + y_c$

$x_R = 0$ (area is symmetric)

$y_R = \dfrac{\frac{1}{12}(120\text{in})(12\text{in})^3}{(30\text{in})(120\text{in})(12\text{in})} + (30\text{in}) = 30.4\ \text{in.}$

~ 5.6 in. above shaft

Center of Pressure for 1:5 sectional model,

$x_R = 0$

$y_R = \dfrac{\frac{1}{12}(24\text{in})(2.4\text{in})^3}{(6\text{in})(24\text{in})(2.4\text{in})} + (6\text{in}) = 6.08\ \text{in.}$

~ 1.12 in above shaft

✓ (1/5 dist as Prototype)

So, torque on Shaft is:

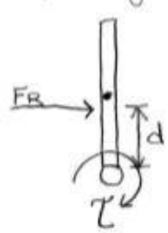

Prototype $\Rightarrow \tau_P = (30{,}360\ \text{lbf})(5.6\text{in}) = 170{,}016\ \text{lbf-in}$

1:5 Sectional Model $\Rightarrow \tau_m = (242.88\ \text{lbf})(1.12\text{in}) = 272.0256\ \text{lbf-in}$

S.A L.Nichols 3/4

With 2.0 Factor of Safety,

Prototype $F_R = 60,720$ lbf $\tau = 340,032$ lbf-in.

Model $F_R = 485.76$ lbf $\tau = 544.0512$ lbf-in.

Determine required thickness of Gate,

Treating gate as cantilever beam

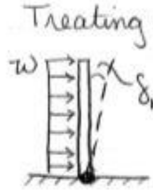

$$P_p = \frac{60,720 \text{ lbf}}{(12 \text{ in})(120 \text{ in})} = 42.167 \text{ psi}$$

$$P_m = \frac{485.76 \text{ lbf}}{(2.4 \text{ in})(24 \text{ in})} = 8.4333 \text{ psi}$$

$$w_p = (42.167 \text{ psi})(120 \text{ in}) = 5060.04 \text{ lbf/in}$$
$$w_m = (8.4333 \text{ psi})(24 \text{ in}) = 202.399 \text{ lbf/in}$$

For 1/16" maximum deflection,

$$\delta_{max} = -\frac{wL^4}{8EI} \rightarrow \delta_{max} = \frac{-wL^4}{8E(\frac{1}{12}bh^3)} \rightarrow h^3 = \frac{-wL^4}{(\frac{1}{16}\text{in})8E(\frac{1}{12}b)}$$

$$h_p^3 = \frac{-(5060.04 \text{ lbf/in})(12 \text{ in})^4}{(\frac{1}{16}\text{in})8(29\times10^6 \text{psi})(\frac{1}{12})120 \text{ in}} = 0.7236 \text{ in}^3$$

minimum thickness, $h_p = 0.8978$ in

$$h_m^3 = \frac{-(202.399 \text{ lbf/in})(2.4 \text{ in})^4}{(\frac{1}{16}\text{in})8(29\times10^6 \text{psi})(\frac{1}{12})24 \text{ in}} = 0.000232 \text{ in}^3$$

minimum thickness, $h_m = 0.0614$ in

Confirming results with Solidworks FEA using h_p + h_m,

$\delta_p = 0.059$ in ✓

$\delta_m = 0.059$ in ✓

Standard Plate thicknesses will be chosen

$h_p = 1$ in.

$h_m = 3/16$ in.
(0.0125 in less than 1/5, but closest found)

S.A. L. Nichols 4/4

So with 2.0 FOS, gate thickness results in Solidworks FEA,

Prototype, $h_p = 1.0\,in$, $\delta_p = 0.043\,in$, $\sigma_p = 16{,}489\,psi$ ✓

Model, $h_m = 3/16\,in$, $\delta_m = 0.002\,in$, $\sigma_m = 3{,}767\,psi$ ✓

Next, determining Shaft diameter. Treating gate as "Key",

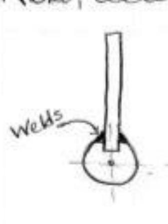

Torsion: $\tau_{max} = \frac{Tr}{J}$, where $J = \frac{\pi d^4}{32}$

Then, $\tau_{max} = \frac{16T}{\pi d^3}$

Maximum Bending Stress: $\sigma_{max} = \frac{32M}{\pi d^3}$

For Prototype, assume 1.25" diameter rod

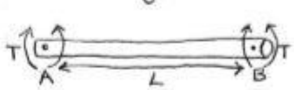

$\tau_{max} = \frac{16(340{,}032\ lb\text{-}in)}{\pi(1.25in)^3} = 886{,}666\ psi$

Overview:

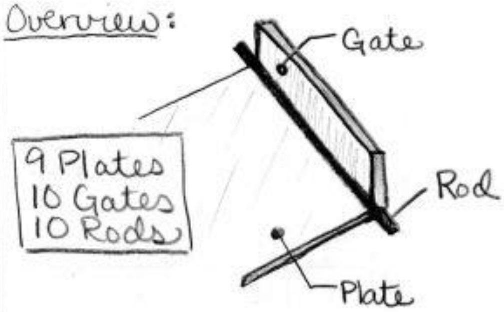

A Rod must be designed to withstand the anticipated bending + torsion due to the pressure force on the attached gate.

Plate thickness = 3/8 in.
Gate thickness = TBD
Rod Length = 10 ft + Sides
Pressure = 1.3 psi (Hydro) + 20 psi (air)

Bending + Torsion

From Shigley's: $\sigma_a = \frac{K_f M_a C}{I}$, $\sigma_m = \frac{K_f M_m C}{I}$, $\tau_{max} = \frac{16T}{\pi d^3}$

For $P_A = 20.0$ psi, width of gate = 10 ft, height of gate = 12 in.

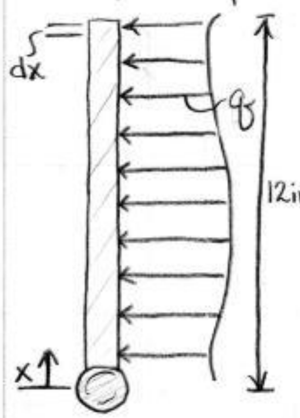

$q = 20.3$ psi, $\omega = 120$ in, $H = 12$ in.

$M_{AIR} = q\omega x\,dx$

$M_{AIR} = \int_0^H q\omega x\,dx$

$M_{AIR} = q\omega\int_0^H x\,dx = \frac{1}{2} q\omega x^2 \Big|_0^H$

$M_{AIR} = \frac{(20\,lb/in^2)(120\,in)x^2}{2}\Big|_0^{12}$

$M_{AIR} = 172{,}800$ lb-in

For $P_{H_2O} = 1.3$ psi, $q = 1.3$ psi, $\omega = 120$ in, $H = 36$ in.

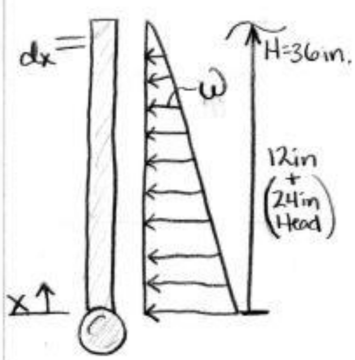

$P = \gamma h$ and $F = PA$,

$P = \gamma(H-x)$
$A = \omega\,dx$
$F = \gamma\omega(H-x)\,dx$

$M_{H_2O} = \gamma\omega x(H-x)\,dx$

$M_{H_2O} = \int_0^H \gamma\omega x(H-x)\,dx$

Continued →

$$M_{H_2O} = \gamma \omega \int_0^H Hx - \int_0^H x^2\,dx$$

$$M_{H_2O} = \gamma \omega \left[\frac{Hx^2}{2}\Big|_0^H - \frac{x^3}{3}\Big|_0^H \right] \quad , \; H = 3\,ft, \; \omega = 10\,ft$$

$$M_{H_2O} = (62.4\,lb/ft^3)(10\,ft)\left[\frac{27\,ft^3}{2} - \frac{27\,ft^3}{3} \right]$$

$$M_{H_2O} = 2808\,lbf\text{-}ft = 33{,}696\,lbf\text{-}in.$$

Total Bending Moment acting on Rod,

$$M_{AIR} + M_{H_2O} = (172{,}800\,lb\text{-}in + 33{,}696\,lb\text{-}in) = 206{,}496\,lb\text{-}in$$

$$\sigma = \frac{32 M_a}{\pi d^3} \rightarrow d = \left(\frac{32 M_a}{\pi \sigma} \right)^{1/3}$$

Yield stress of A36 steel, $\sigma_y = 36{,}000$ psi

$$d = \left(\frac{32(206{,}496\,lb\text{-}in)}{\pi(36{,}000\,lb/in^2)} \right)^{1/3} = 3.88''$$

So, a 3.88" dia. A36 rod will yield under this load

We can't have a 4" dia. rod, so the load must be decreased substantially. If we can wait to apply the 20 psi of pressure at the moment we open the gates, we can decrease the moment to 33,696 lb-in for only the 3' of static head.

$$d = \left(\frac{32(33{,}696\,lb\text{-}in)}{\pi(36{,}000\,lb/in^2)} \right)^{1/3} = 2.12''$$

This is still too large and at yield. This rod would take up 1/6 of our orifice.

If we decrease the static head to only account for the water in the channel (1ft),

$$M = \int_0^1 \gamma \omega x(h-x)\,dx = \gamma \omega \left[\frac{Hx^2}{2}\Big|_0^1 - \frac{x^3}{3}\Big|_0^1 \right]$$

$$M = (62.4\,lb/ft^3)(10\,ft)\left[\frac{1}{2} - \frac{1}{3} \right] ft^3 = 104\,lb\text{-}ft = 1248\,lb\text{-}in$$

$$d = \left(\frac{32(1248\,lb\text{-}in)}{\pi(36{,}000\,lb/in^2)} \right)^{1/3} = 0.7068'' \quad \text{(acceptable)}$$

R.C. L. Nichols 3/4

Now we need to look at the gate thickness.

As a Cantilever, $\ell = 12"$, $b = 120"$, $h = TBD$

$$\sigma_B = \frac{Mc}{I}, \quad c = \frac{h}{2} \text{ and } I = \frac{bh^3}{12}$$

$$\rightarrow \frac{I}{c} = \frac{M}{\sigma} \rightarrow \frac{bh^{\cancel{3}\,2}\,2}{\cancel{h}\,12} = \frac{M}{\sigma}$$

$$\text{Finally, } h = \left(\frac{12M}{2b\sigma}\right)^{1/2}$$

For our $M = 1248$ lb-in,

$$h = \left(\frac{12(1248\,\text{lbin})}{2(120\text{in})(36{,}000\,\text{lb/in}^2)}\right)^{1/2} = 0.0416"$$

Now to check this deflection, $F = \frac{M}{x_c} = \frac{1248\text{ lb-in}}{2} = 624\text{lbf}$

$$y_{max} = \frac{F\ell^3}{3EI} = \frac{(624\text{ lbf})(12\text{in})^3}{3(29E6\text{psi})(1/12(120\text{in})(0.0416\text{in})^3}$$

$y_{max}(h = 0.0416") = 17.22$ in. (Not acceptable)

Working backward,

$y_{max} = \frac{F\ell^3}{3EI}$, set $y_{max} = 0.01$ in.

$$I = \frac{F\ell^3}{3Ey} \rightarrow \frac{bh^3}{12} = \frac{F\ell^3}{3Ey} \rightarrow h = \left(\frac{12F\ell^3}{3bEy}\right)^{1/3}$$

$$h = \left(\frac{12(624\text{ lbf})(12\text{in})^3}{3(120\text{in})(29E6\text{psi})(0.01\text{in})}\right)^{1/3} = 0.499\text{ in.} \checkmark$$

So the gate will have to be 1/2" thick.

From Grainger.com

Keyed Shaft for 1/2 in Key size = 2"

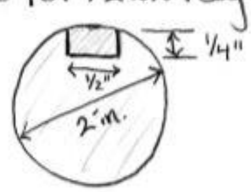

R.C. L.Nichols 4/4

This is larger than we had hoped, but it is the best option so far.

Results and support options will be checked using Solidworks.

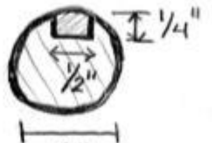

For 2" Shaft, $M = 1248\ lb\text{-}in$

$$\sigma = \frac{32M}{\pi d^3}$$

$$\sigma = \left(\frac{32(1248\ lb\text{-}in)}{\pi (2in)^3}\right) = 1589\ psi$$

FOS = 22.7

Options for hinges, supports need to be explored to see if a smaller shaft might be suitable with a thinner gate.

For Torsion : $\tau_{max} = \frac{16T}{\pi d^3} = \left(\frac{16(2496\ lb\text{-}in)}{\pi (2in)^3}\right) = 1589.0\ psi$ ✓

★ To Discuss, how much deflection can be allowed on gates to avoid overdesign of shaft. (Shaft is limited by gate thickness/bending)

Also, is it feasible to decrease P = 0.433 for only 1-ft static head, no 3ft head, no air pressure?

BOX 232 • MINNEAPOLIS, KS • 67467
SALES@HUYETT.COM • FAX 785-392-2845

KEYED – IMPERIAL

DESCRIPTION

Fully keyed shafts provide a good fit between the key and the key way. Key ways are cut in accordance with ANSI B17.1. Partial key ways and other materials are available including turned and polished and medium carbon steel (suitable to heat treat).

HOW TO IDENTIFY

1. Measure diameter (A).
2. Measure length (C).
3. Build the part number from the chart on the next page.

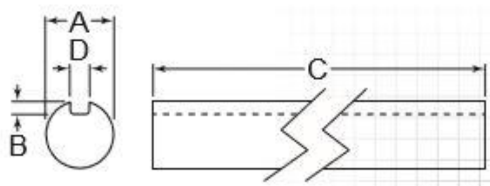

PREFIX MATERIAL/FINISH

KF = COLD FINISHED STEEL, PLAIN* (1018)
KF44 = COLD FINISHED STEEL, PLAIN* (1144)
KF45 = COLD FINISHED STEEL, PLAIN* (1045)
KFS = 303 STAINLESS STEEL, PLAIN
KFS6 = 316 STAINLESS STEEL, PLAIN
KFTP = COLD FINISHED STEEL, PLAIN* (1045) TURNED & POLISHED
KFZ = COLD FINISHED STEEL, ZINC CLEAR (1018)

DIAMETER (A) TOLERANCES

MATERIAL		DIAMETER	
(Prefix)	*(Material/Finish)*	*(Size Range)*	*(Tolerance)*
KF	Cold Finished Steel, Plain* (1018)	All Sizes	+0/-.0020"
KF44	Cold Finished Steel, Plain* (1144)		
KF45	Cold Finished Steel, Plain* (1045)	All Sizes	+0/-.0010"
KFS	303 Stainless Steel, Plain		
KFS6	316 Stainless Steel, Plain	All Sizes	+0/-.0020"
KFTP	Cold Finished Steel, Plain* (1045), Turned & Polished	All Sizes	-.0005/-.0015"
KFZ	Cold Finished Steel, Zinc Clear (1018)	All Sizes	+0/-.0020"

KEYED SHAFTING CAN BE PRODUCED IN MANY DIAMETER AND LENGTH COMBINATIONS

KEY WAY (D X B) SIZE

DIAMETER	KEY WAY
(Shaft Size Range)	*(D) × (B)*
1/2"	1/8" × 1/16"
5/8 – 7/8"	3/16" × 3/32"
15/16 – 1-1/4"	1/4" × 1/8"
1-5/16 – 1-3/8"	5/16" × 5/32"
1-7/16 – 1-3/4"	3/8" × 3/16"
1-7/8 – 2-3/16"	1/2" × 1/4"
2-7/16 – 2-1/2"	5/8" × 5/16"
2-15/16 – 3-1/4"	3/4" × 3/8"
3-3/8 – 3-3/4"	7/8" × 7/16"
3-15/16 – 4-1/2"	1" × 1/2"

LENGTH (C) TOLERANCES

LENGTH		TOLERANCE
(Suffix)	*(Length)*	*(Tolerance)*
-12	12" (1')	±2"
-36	36" (3')	
-72	72" (6')	
-144	144" (12')	

Nonstandard lengths up to 144" are available. Lengths over 3' may be subject to a packaging charge.

PLAIN FINISH PARTS REQUIRE SPECIAL HANDLING TO PREVENT SURFACE CORROSION AND EXTEND SHELF LIFE

*Limited warranty for surface finish: 30 days from date of shipment. See page 12 for details.

APPENDIX E: 650 LB Holding Force Electromagnets

Electromagnetic Locks

DynaLock For Life

2511

2522

2511TJ

2522TJ2

2585

2585-TJ85

2500 Series 650 Lb. "Mini"

Mini electromagnetic locks, surface mounted for single and double outswing or inswing doors.
Size: 1-1/4"D x 1-3/4"H x 10-1/2"L Single or 21"L Double
Multi-voltage field selectable 12/24 VAC/VDC
Current Draw: 500 mA @ 12V Single / 1 Amp Double
250 mA @ 24V Single / 0.50 Amps Double

MODEL	PRODUCT	FINISH	WEIGHT
2511	Single Electromagnetic Lock Outswing	US28	4.5 Lbs.
2522	Double Electromagnetic Lock Pair Outswing	US28	9 Lbs.
2511TJ	Single Electromagnetic Lock Inswing	US28	7.5 Lbs.
2522TJ2	Double Electromagnetic Lock Pair Inswing	US28	15 Lbs.

2585 Series 650 Lb. "Bantam"

"Bantam" electromagnetic lock, surface mounted for single outswing or inswing doors.
Size: 1-1/4"D x 1-3/4"H x 8-1/2"L
Field Selectable 12/24 VDC.
Current Draw: 500 mA @ 12VDC
250 mA @ 24VDC

MODEL	PRODUCT	FINISH	WEIGHT
2585	Single Lock Outswing	US28	4 Lbs.
2585-TJ85	Single Lock Inswing	US28	8 Lbs.

OPTIONS

• ATS	Anti-Tamper Switch - Signals removal of the housing cover.
• CLH	Custom Length Housing - See page 24.
DSM	Door Status Switch - Signals door closed or ajar.
DSM2	Door Status Switch - For the 2522 Series only.
DYN	Dynastat Force Sensor - Indicates efficient magnetic bond.
DYN2	Dynastat Force Sensor - For the 2522 Series only.
LED	Bi-Color LED - For local signaling of lock status. (Requires DYN Option. Not available on TJ models.)
LED2	Bi-Color LED's (2) - For the 2522 Series only. (Requires DYN2 Option. Not available on TJ models.)
SF	Special Finish - Standard finish US28. Special anodized finishes see page 56.

Notes: • ATS and CLH options not available on the 2585 Series.

Note: For AC operation order #7088 Pre-wired Rectifier Bridge. See page 48.

c UL us LISTED

APPENDIX F: Hand Calculations for Angular Velocity of Shaft

SHAFT – ω L. Nichols 1/1

Angular velocity of shaft from 0.433psi

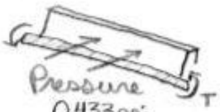

Moment from 0.433psi = 1248 lb-in

$\Theta = 90° = \pi/2$ radians

$T = (1248 \text{ lb-in})(\pi/2) \doteq 1960 \text{ lb-in}$

Since we accelerating from rest, the moment right before we finish rotating = t_2 $(t_1 = 0)$

Using Work-Energy Principle,

$$\cancel{T_1}^{0} + \cancel{V_1}^{0} + (\cancel{U_{1-2}})^{ext}_{nc}{}^{0} + (U_{1-2})^{int}_{nc} = T_2 + \cancel{V_2}^{0}$$

$$(U_{1-2})^{int}_{nc} = T_2 = \frac{1}{2} m v_2^2 + 2 I_G \omega_{w2}^2$$

Mass (m) of rod $\approx$ 60 lbm

$$I_G = \frac{mr^2}{2} = \frac{60 \text{ lbm} \left(\frac{1.75 in}{2}\right)^2}{2} \doteq 23 \text{ lbm-in}^2$$

Need ω_{w_2} and v_2.

$$\text{Since } \omega_{w_2} = \frac{v_2}{r} \rightarrow T_2 = \frac{1}{2} m v_2^2 + 2 I_G \left(\frac{v_2}{r}\right)^2$$

$$T_2 = \tfrac{1}{2} m v_2^2 + 2 I_G (v_2^2/r^2)$$

$$T_2 = v_2^2 (\tfrac{1}{2} m + 2/r^2 I_G)$$

$$v_2 = \left(\frac{T_2}{\tfrac{1}{2} m + 2/r^2 I_G}\right)^{1/2}$$

$$v_2 = \left(\left(\frac{1960 \text{ lbf-in}}{60 \text{ lbm}/2 + 2/0.765625 \text{ in}^2 (23 \text{ lbm-in}^2)}\right)\left(\frac{\text{lbm-}32.2\text{ft}}{\text{lbf-s}^2}\right)\left(\frac{12 \text{ in}}{1 \text{ ft}}\right)\right)^{1/2}$$

v_2 = 79.4 in/second

$$\omega_{w_2} = \frac{v_2}{r} = \frac{79.4 \text{ in/s}}{0.875 \text{in}} = 90.76 \text{ rad/s}$$

$$t = \pi/2 \text{ rad} \left(\frac{s}{90.76 \text{ rad}}\right) = \underline{\underline{0.0173 \text{ seconds}}}$$

APPENDIX G: Pneumatics

Thesis Pressure Calculations　　　Larinda Nichols　　1/8

Dynamics – Rectilinear Motion for Prototype to Verify Method

Per Level,

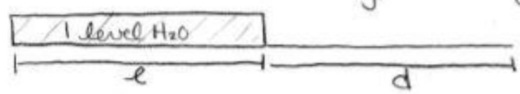

Where ℓ = length of water column, d = wave development length

★ Neglecting Friction in all Calculations

Known Velocity (V) = 25.4 ft/s
Prototype level height (h) = 1 ft/level
Prototype level width (ω) = 10 ft

Dynamics Equations for Acceleration (a), Velocity (V), Displacement (d), Time (t)

$a = \frac{dV}{dt}$, $a = \beta t^2$ (where β is some unknown constant)

so, $\beta t^2 = \frac{dV}{dt} \rightarrow dV = \beta t^2 \rightarrow \int_0^V dV = \int_0^t \beta t^2 dt \rightarrow V = \frac{1}{3}\beta t^3$

$V = \frac{ds}{dt} \rightarrow \frac{1}{3}\beta t^3 = \frac{ds}{dt} \rightarrow ds = \frac{1}{3}\beta t^3 dt \rightarrow \int_{s_0}^{s} ds = \int_0^t \frac{1}{3}\beta t^3$

When $t = t_f$, $V = V_f$, and $S - S_0 = d = \frac{1}{12}\beta t_f^4$

Then $V_f = \frac{1}{3}\beta t_f^3$

So, $\beta = \frac{3V_f^4}{64d^3}$ and $t_f = \frac{4d}{V_f}$　[Ref: Engineering Mechanics Dynamics – Gray, 2nd Ed]

When V_f = 25.4 ft/s and d = 15 ft

$\beta = \frac{3(25.4\,ft/s)^4}{64(15ft)^3} = 5.78\,ft/s^4$　　$t_f = \frac{4(15ft)}{25.4ft/s} = 2.36\,s$

Then, $a = \beta t^2 = (5.78\,ft/s^4)(2.36s)^2 = 32.3\,ft/s^2$

If $\ell = 15\,ft$, $\forall = (1ft)(10ft)(15ft) = 150\,ft^3$ with $A = 10\,ft^2$

$m = \rho\forall = (62.4\,lbm/ft^3)(150ft^3) = 9360\,lbm$

$F = ma = (9360\,lbm)\left(\frac{lbf-s^2}{32.2\,lbm-ft}\right)(32.3ft/s^2) = 9376.9\,lbf$

$P = \frac{F}{A} = \frac{9376.9lbf}{10ft^2(144in^2/ft^2)} = \underline{6.5\,psi}$ Required to accelerate (1×10×15) ft level to 25.4 ft/s in 15 ft, (Per Level), in 2.36s.

P.C. Larinda Nichols 2/8

If d is decreased to only 5 ft develop distance,

$$\beta = \frac{3\,(25.4\ \mathrm{ft/s})^4}{64\,(5\mathrm{ft})^3} = 156\ \mathrm{ft/s^4} \qquad t_f = \frac{4\,(5\mathrm{ft})}{25.4\ \mathrm{ft/s}} = 0.787\ \mathrm{s}$$

$$a = (156\ \mathrm{ft/s^4})(0.787\mathrm{s})^2 = 96.77\ \mathrm{ft/s^2}$$

$$m = (62.4\ \mathrm{lbm/ft^3})(150\ \mathrm{ft^3}) = 9360\ \mathrm{lbm}$$

$$F = (9360\ \mathrm{lbm})(96.77\ \mathrm{ft/s^2})(\mathrm{lbf\text{-}s^2/lbm\cdot 32.2ft}) = 28{,}131\ \mathrm{lbf}$$

$$P = \frac{28{,}131\ \mathrm{lbf}}{10\mathrm{ft}^2(144\mathrm{in}^2/\mathrm{ft}^2)} = \underline{\underline{19.5\ \mathrm{psi}}}$$ Required to accelerate (1x10x15) ft level to 25.4 ft/s in 5 ft, per level, in 0.787 s. (Close agreement with Flow-3D ✓)

For Pipe Model,

Schedule 40 PVC

			Flow Area
4NPS →	O.D. = 4.5 in,	I.D. = 4.026 in,	$A = 12.73\ \mathrm{in^2}$
½NPS →	O.D. = 0.840,	I.D. = 0.622 in,	$A = 0.304\ \mathrm{in^2}$

V_f = (scaled from Prototype) = 11.36 ft/s [RojinT.]

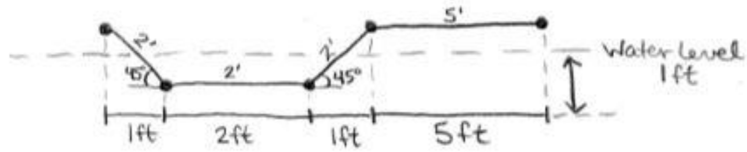

Overall Run Length of (d) = 5 ft + (2ft − 1.41ft) ≈ 5.6 ft

Overall ~~Volume~~ of water in pipe,

$(\ell) = 1.41\ \mathrm{ft} + 2\ \mathrm{ft} + 1.41\ \mathrm{ft} = 4.82\ \mathrm{ft}$

$(r) = 2.013\ \mathrm{in} = 0.16775\ \mathrm{ft}$

$\forall = \ell\pi r^2 = (4.82\mathrm{ft})\pi(0.16775\mathrm{ft})^2 = 0.426\ \mathrm{ft}^3$

Acceleration from V=0 to V=11.36 ft/s in 5.6 ft,

$$\beta = \frac{3(11.36\ \mathrm{ft/s})^4}{64\,(5.6\ \mathrm{ft})^3} = 4.45\ \mathrm{ft/s^4}$$

$$t = \frac{4\,(5.6\mathrm{ft})}{(11.36\mathrm{ft/s})} = 1.97\ \mathrm{s}$$

$$a = (4.45\mathrm{ft/s^4})(1.97\mathrm{s})^2 = 17.3\ \mathrm{ft/s^2}$$ for constant acceleration

P.C. Launda Nichols 3/8

Looking at Force required at t_o

At t_o,

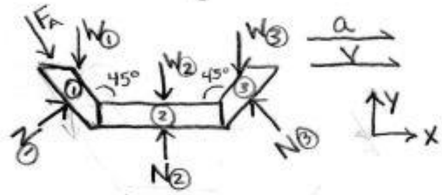

$\Sigma F_x: \; F_A \cos\theta + N_1 \cos\theta - N_3 \cos\theta = ma_x$

$\Sigma F_y: -F_A \sin\theta + N_1 \sin\theta - W_1 + N_2 - W_2 + N_3 \sin\theta = ma_y$

also, $W_1 = W_3$, so $N_1 = N_3$

$N_2 = W_2$, assume N_2 will cancel W_2, so $N_1 = N_3 = N$

So, $F_A \cos\theta + N\cancel{\cos\theta} - N\cancel{\cos\theta} = ma_x$

$F_A \cos\theta = ma_x$

$-F_A \sin\theta + 2N\sin\theta - W_1 - W_3 = ma_y$

$-F_A \sin\theta = 2N\sin\theta - W_1 - W_3 - ma_y$

Since $a = a_x$, $a_y = 0$

$F_A \sin\theta = 2N\sin\theta - W_1 - W_3$

$F_A = \dfrac{ma_x}{\cos\theta} = \dfrac{m(17.3 \text{ ft/s}^2)}{0.707} = 24.47 m$

Mass of all 3 pieces,

$\forall = \{2[(16.92\text{in})\pi(2.013\text{in})^2] + (24\text{in})\pi(2.013\text{in})^2\}$

$\forall = 736.32 \text{ in}^3 = 0.426 \text{ ft}^3$

$m = \rho\forall = (62.4 \text{ lb/ft}^3)(0.426 \text{ ft}^3) = 26.6 \text{ lbm}$

$F_A = \dfrac{(26.6 \text{ lbm})(\text{lbf·s}^2/32.2\text{ft})(17.3 \text{ ft/s}^2)}{0.707} = 20.21 \text{ lbf}$

$P = \dfrac{F}{A} = \dfrac{20.21 \text{ lbf}}{12.73 \text{ in}^2} = 1.59 \text{ psi}$

P.C. Laurinda Nichols 4/8

Now Breaking down into times to find max F required

At t_o,

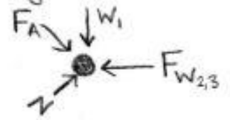

$F_{W_{2,3}} = W_2, N_2, W_3, N_3$

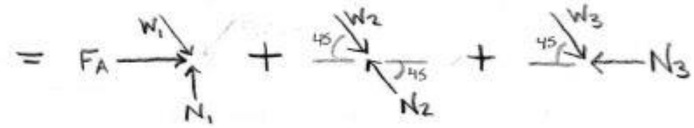

$$\Sigma F_x: \; F_A + W_1 + W_2\cos\theta - N_2\cos\theta + W_3\cos\theta - N_3 = m a_x$$

$$F_A = M_2 g\cos\theta + m_3 g - W_1 - W_2\cos\theta - W_3\cos\theta + m a_x$$

$$F_A = m_2 g\cos\theta + m_3 g - m_1 g - m_2 g\cos\theta - m_3 g\cos\theta + m_T a_x$$

$$F_A = (32.2\,ft/s^2)\left[\cancel{(11\,lbm)(\cos\theta)} + \cancel{(7.78\,lbm)} - \cancel{(7.78\,lbm)} - \cancel{(11\,lbm)(\cos\theta)} - (7.78\,lbm)(\cos\theta)\right] + (26.6\,lbm)(17.3\,ft/s^2)$$

$$F_A = (283.04\,lbm\,ft/s^2)(lbf\text{-}s^2/32.2\,lbm\text{-}ft)$$

$F_A = 8.79\,lbf$ $\quad P = 0.69\,psi$

This pressure would only be valid for a short time until force vector changes, So looking instead at a "Worse Case Scenario" Constant Uphill @ 45°

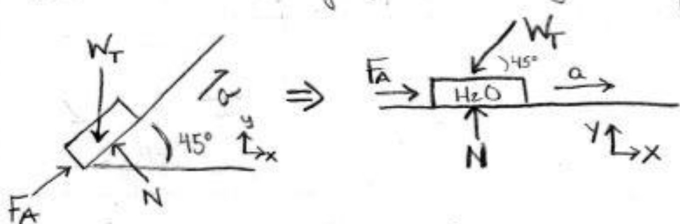

$W_T = m_T(32.2\,ft/s^2)$

$m_T = 26.6\,lbm$

$$\Sigma F_x: \; F_A - W_T\cos\theta = ma$$

$$F_A = W_T\cos\theta + ma$$

$$F_A = (26.6\,lbm)(32.2\,ft/s^2)\cos 45° + (26.6\,lbm)(17.3\,ft/s^2)$$

$$F_A = (1065.83\,lbm\,ft/s^2)(lbf\text{-}s^2/32.2\,lbm\,ft)$$

$$F_A = 33.1\,lbf$$

$P = \underline{2.6\,psi}$ to push all water up the 45° incline

P.C Larinda Nichols 5/8

Using $P_{max} = P = 2.6$ and treating air as ideal gas,

$$\rho = \frac{P}{RT} = \frac{(2.6\ lb/in^2 + 14.7\ lb/in^2)(144 in^2/ft^2)}{(1716\ ft\,lb/Slug\,R)(519\ R)} = \frac{0.0028\ lb/ft^2}{ft\,lb/Slug}$$

$$\rho = \frac{0.0028\ lbf\,slug}{ft^3\ lbf}\left(\frac{lbf\text{-}s^2}{Slug\ ft}\right)\left(\frac{32.2 ft\cdot lbm}{lbf\text{-}s^2}\right) = \frac{0.09\ lbm}{ft^3} = 5.2\times10^{-5}\frac{lbm}{in^3}$$

So, with gauge pressure of $2.6\ lb/in^2$, $\rho_{air}(59°F) = \underline{5.2\times10^{-5}\ lbm/in^3}$

From Table 1.7, Fundamentals of Fluid Mechanics, Munson, 7th

$\rho_{air}(59°) = 2.38\times10^{-3}\ slugs/ft^3$

our case, $\rho = 2.8\times10^{-3}\ slugs/ft^3$

Compression ratio is (1.175 : 1) Not much

Using continuity equation,

$\Sigma \dot{m}_{out} = \Sigma \dot{m}_{in}$, where $\dot{m}$ = mass flowrate $= \rho Q = \rho AV$

Then, $\rho_1 A_1 V_1 = \rho_2 A_2 V_2$

Since we want constant velocity, $V_1 = V_2$, and

$\rho_1 A_1 = \rho_2 A_2$ where ρ_1 = our calculated density
A_1 = flowarea of 4" NPS PVC
A_2 = flow area of 1/2" NPS PVC

$A_1 = 12.73 in^2$
$A_2 = 0.304\ in^2$

$$\text{So, } \rho_2 = \frac{\rho_1 A_1}{A_2} = \frac{(2.8\times10^{-3} slugs/ft^3)(ft^3/1728 in^3)(12.73 in^2)}{(0.304\ in^2)}$$

$$\rho_2 = 6.785\times10^{-5} slugs/in^3 = 0.11725\ slugs/ft^3$$

This is a compression ratio of (49.26 : 1) to Standard air

Back to Ideal Gas Equation, (assume no ΔT)

$$P = \rho RT = (0.11725\ Slugs/ft^3)(1716\ ft\,lb/Slug\,R)(519\,R)$$

$$P = 104{,}423.319\ lb/ft^2 = 725\ psi - 14.7 psi$$

$$P(\tfrac{1}{2}"NPS) = 710.5\ psi$$

Need new equation!
— Need to account for Compression somehow,

P.C. Larinda Nichols 6/8

For ISOTHERMAL Process,

$$\frac{P}{\rho} = \text{constant}$$

For P = 2.6 psi and 2.8×10^{-3} slugs/ft^3

$$\frac{P}{\rho} = \frac{2.6}{2.8\times10^{-3}} = 928.57$$

Then using assumption of isentropic compression

$$\frac{P_i}{\rho_i^{K}} = \frac{P_f}{\rho_f^{K}} \longrightarrow P_f = \left(\frac{\rho_f}{\rho_i}\right)^{K} P_i \qquad (K = C_P/C_v)$$

where K is the ratio of the specific heat at constant pressure, C_P, to the specific heat at constant volume C_v. (assuming K = 1.4, Standard air)

$$P_f = \left(\frac{0.11725}{0.0028}\right)^{1.4}(17.3\,\text{psi}) = 3{,}226.9\ \text{psi} \ldots \text{What?!}$$

★ Note on Pg 22 of Fluid Mechanics, Munson

"As the volume, $\forall$ is reduced by one-half, the density must double since the mass, $m = \rho\forall$ of the gas remains constant.

From figure E1.6b, to keep input pressure under 50 psi, we need a compression ratio of 0.4 or less.

Trying a standard 2" NPS PVC, I.D. = 2.067 in.

Max Op. Pressure = 166 psi (Sch 40)

$$A = \pi r^2 = \pi(1.0335\,in)^2 = 3.356\,in^2$$

Or, Standard 1" NPS PVC, I.D. = 1.049 in., $A = 0.864\,in^2$

Max Op. Pressure = 270 psi (Sch 40)

Or, Standard 1½" NPS PVC, ID = 1.610 in, $A = 2.04\,in^2$

Max Op. Pressure = 198 psi (Sch 40)

P.C. Larinda Nichols 7/8

Starting with 2" NPS PVC

$$\rho_2 = \frac{\rho_1 A_1}{A_2} = \frac{(2.8\times10^{-3}\ slugs/ft^3)(12.73in^2)}{(3.356in^2)} = 0.0106\ \frac{slugs}{ft^3}$$

Now, isentropic compression,

$$P_f = \left(\frac{\rho_f}{\rho_i}\right)^k P_i = \left(\frac{0.0106}{0.0028}\right)^{1.4}(17.3\ psi) = 111.85\ psi$$

$$\text{Gauge Pressure} = (111.85 - 14.7)\ psi = 97.15\ psi$$

For 1½" NPS PVC

$$\rho_2 = \frac{\rho_1 A_1}{A_2} = \frac{(2.8\times10^{-3}\ slugs/ft^3)(12.73in^2)}{(0.864\ in^2)} = 0.04125\ \frac{slugs}{ft^3}$$

$$P_f = \left(\frac{0.04125}{0.0028}\right)^{1.4}(17.3\ psi) = 747.6\ psi$$

$$\text{Gauge Pressure} = (747.6\ psi - 14.7\ psi) = 732.9\ psi$$

Best Choice: 2" NPS Schedule 40 PVC

Summary of Pressure Calculations

1. Pressure required to accelerate water to 11.36 ft/s in 5 ft,
   $P_{req} = 2.6$ (Gauge Pressure)
2. Time required to accelerate water to 11.36 ft/s in 5 ft,
   $t_{req} = 1.97s$
3. Pipe Model = 4" NPS Schedule 40 PVC
4. Air Supply Pipe = 2" NPS Schedule 40 PVC
5. Pressure required to achieve 2.6 PSI in 4" Pipe
   $P_{air} = 97.15\ psi$

★ No friction forces were accounted for in calculations
(Friction Losses estimated on next page.)

P.C. Larinda Nichols 8/8

Friction Loss Estimates for PVC (Wiley)

$Q = AV$, assuming 11.36 ft/s Velocity

2" Pipe : $Q_2 = (3.356\ in^2)(1ft^2/144in^2)(11.36\ ft/s)$

$$Q_2 = 0.265\ ft^3/s\left(\frac{7.481\ gal}{1\ cuft}\right)\left(\frac{60s}{min}\right) = 118.84\ GPM$$

Friction loss @ 100 GPM = 6.5 psi / 100 ft

Estimated pipe length = 10 ft

$$P_{loss} = 10\ ft\left(\frac{6.5\ psi}{100\ ft}\right) = 0.65\ psi$$

So New $\underline{P \cong 98.0\ psi}$ for 2" Pipe (Gauge P)

4" Pipe : $Q_4 = (12.73\ in^2)(1ft/144in^2)(11.36\ ft/s)$

$$Q_4 = 1.00\ ft^3/s\left(\frac{7.481\ gal}{1\ cuft}\right)\left(\frac{60s}{min}\right) = 448.8\ GPM$$

Friction Loss @ 400 GPM = 3.3 psi/100 ft

Estimated pipe length = 10 ft

$$P_{loss} = 10\ ft\left(\frac{3.3\ psi}{100\ ft}\right) = 0.33\ psi$$

So New $\underline{P \cong 3.0\ psi}$ for 4" Pipe (Gauge P)

Parker Pneumatic
Pneumatic Division North America
Richland, Michigan 49083

TEC-15
Pipe Air Flow

ISSUED: January, 1999
Supersedes: June, 1998

Pipe Air Flow

The following pages contain 6 sets of curves for schedule 40 pipe that can be used to help select the appropriate pipe size for pneumatic systems, or given a system, allow system performance to be estimated.

Generally accepted practice for sizing piping for pneumatic systems is to use a pressure drop of 10% of gage for nominal pipe sizes up to and including 1/2", and 5% of gage for nominal pipe sizes of 3/4" and larger. The following curves allow the use of these guidelines for selecting piping sizes and include other pressure drop percentages for evaluating existing systems. Generally, curves of this type are shown only for 100 feet pipe lengths, but theoretic calculations show the curves for 10 feet are also valid.

Below is a listing of the charts involved with their identification:

Pipe Size Range	Pressure Drop (Percentage of Inlet Gage Pressure)					
1/8" - 1/2"	5	10	15	5	10	15
3/4" - 3"	2.5	5	7.5	2.5	5	7.5
Pipe Length (Feet)	100	100	100	10	10	10
Chart	A	B	C	D	E	F

Generally accepted practice.

Perhaps the best way to explain the use of these curves is by example.

Example 1

Given a system with desired airflow of 700 SCFM and a supply pressure of 60 PSIG and a header length of 100 feet, what size pipe should be used? The generally accepted practice of 10% pressure drop for pipes up to 1/2" and 5% for 3/4" and larger should be used.

The above table indicates, Chart B should be used (Step 1). Along the bottom horizontal axis locate the 60 PSIG vertical line (Step 2). On the left vertical axis locate the 700 SCFM horizontal line (Step 3). Follow both of these lines to the point of intersection. This occurs between the sloping lines for the 2" and 2-1/2" pipes. The larger pipe size (2-1/2") should be selected (Step 4). Further evaluation of this chart shows that for the conditions given, the pipe will flow over 800 SCFM at 60 PSIG inlet and 3 PSI (5%) pressure drop. (The intersection of the 60 PSIG primary pressure line and the 2-1/2" pipe size line).

Further uses of the curves would be to compare the size pipe required at the other sets of pressure drops for 100 feet of pipe length. Using Chart A shows that if a more conservative pressure drop were used, the pipe size would increase to 3". Using Chart C shows that if a more aggressive pressure drop were allowed, perhaps a 2" pipe could be used.

Using the curves for 10 feet of pipe length, it can be seen because of the shorter length, much smaller pipe diameters could be used than if the length were at 100 feet.

These curves should only be used as general guidelines for selecting piping systems. Also, these curves are based on using schedule 40 steel pipe. Different types of plumbing with different internal roughness will have different results. If more detailed or precise information is required, the system should be designed by a competent professional.

Flow of Air Through a Pipe

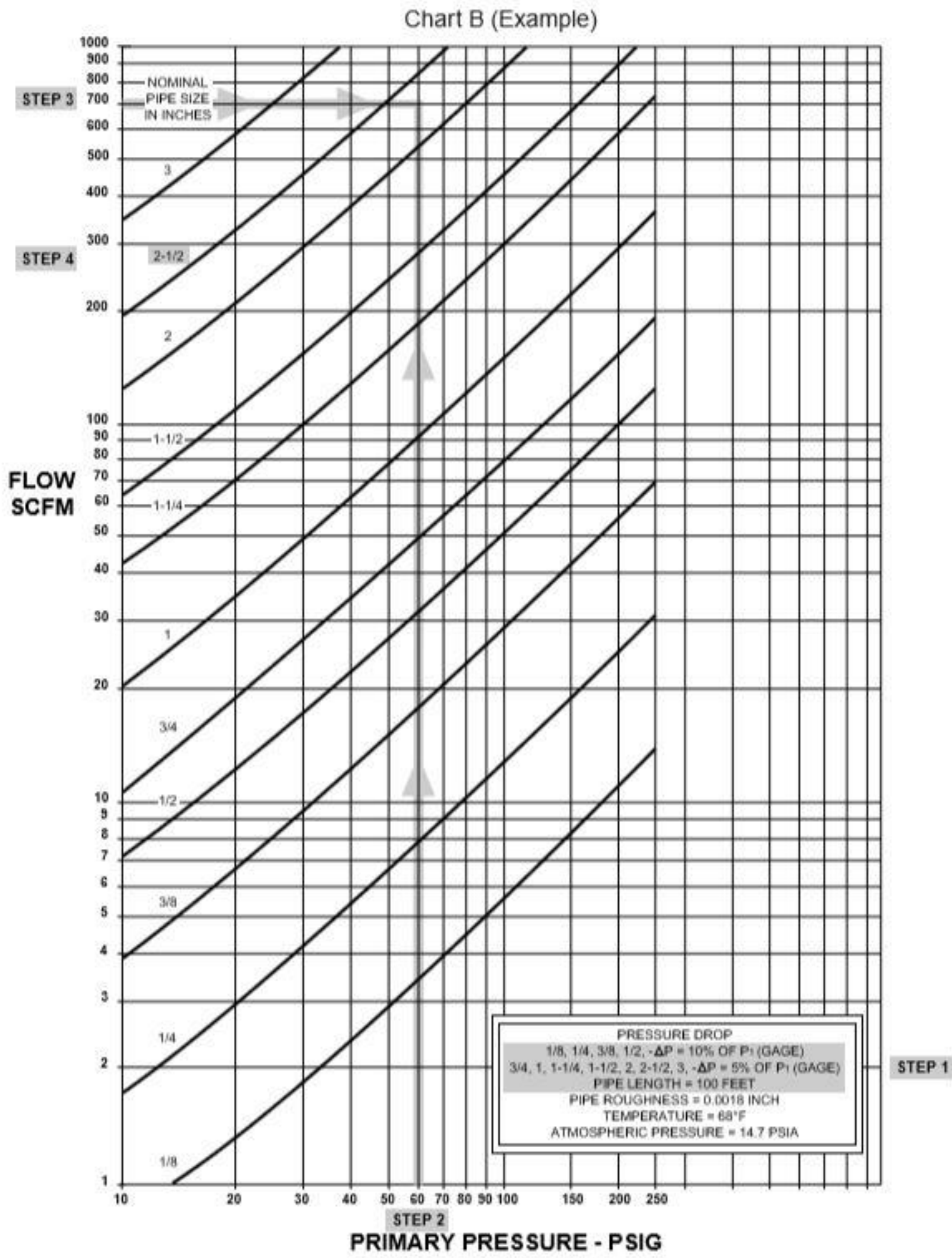

APPENDIX H: Modular Sectional Model Drawings

Sectional Model

S.no.	Description	Quantity	Drawing No.
1	Inclined Inlet 25 ° 35 ° 45 °	 1 1 1	2-10
2	Gate Channel	1	11-13
3	Outlet box	1	14-17
4	Additional Length component 0.2′ 0.4′ 1′	 2 4 2	18-26
5	Flanges	22	27-28

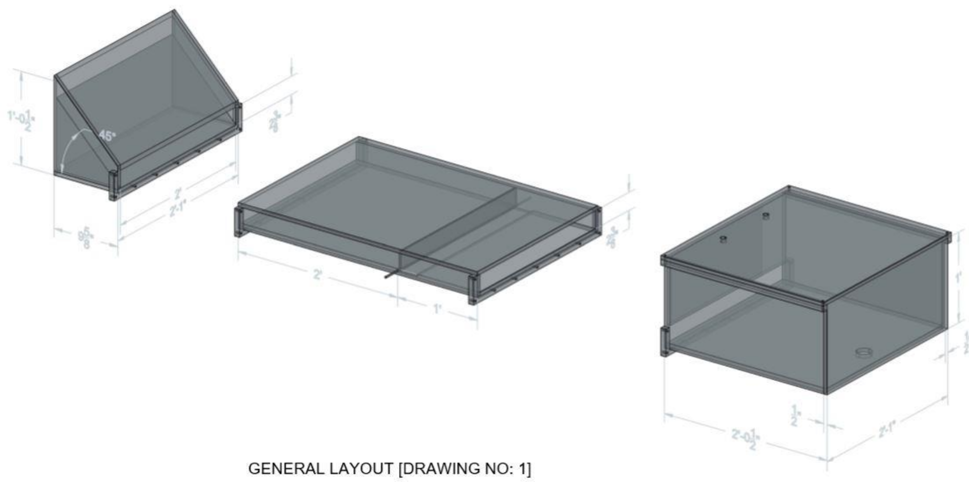

GENERAL LAYOUT [DRAWING NO: 1]

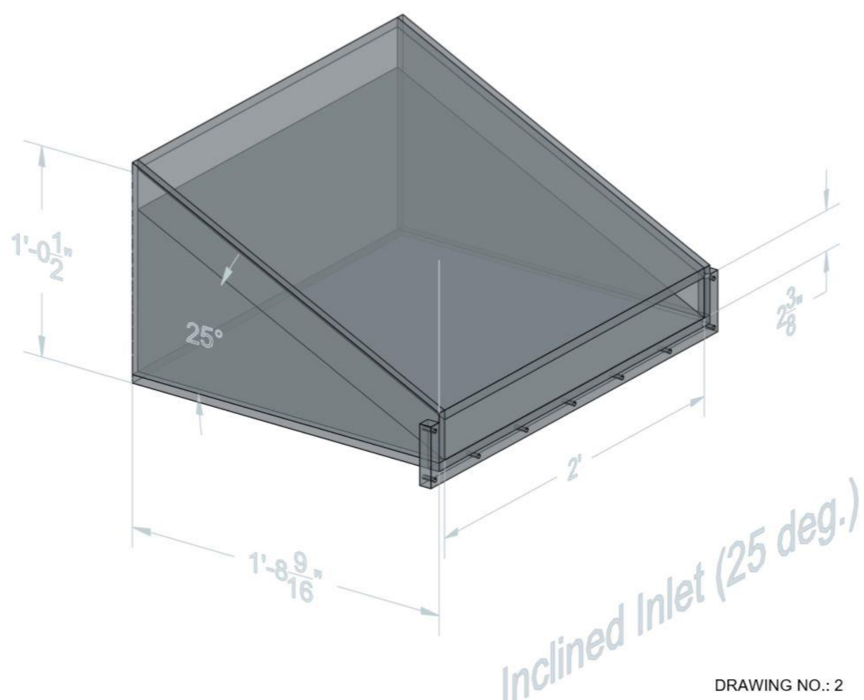

DRAWING NO.: 2

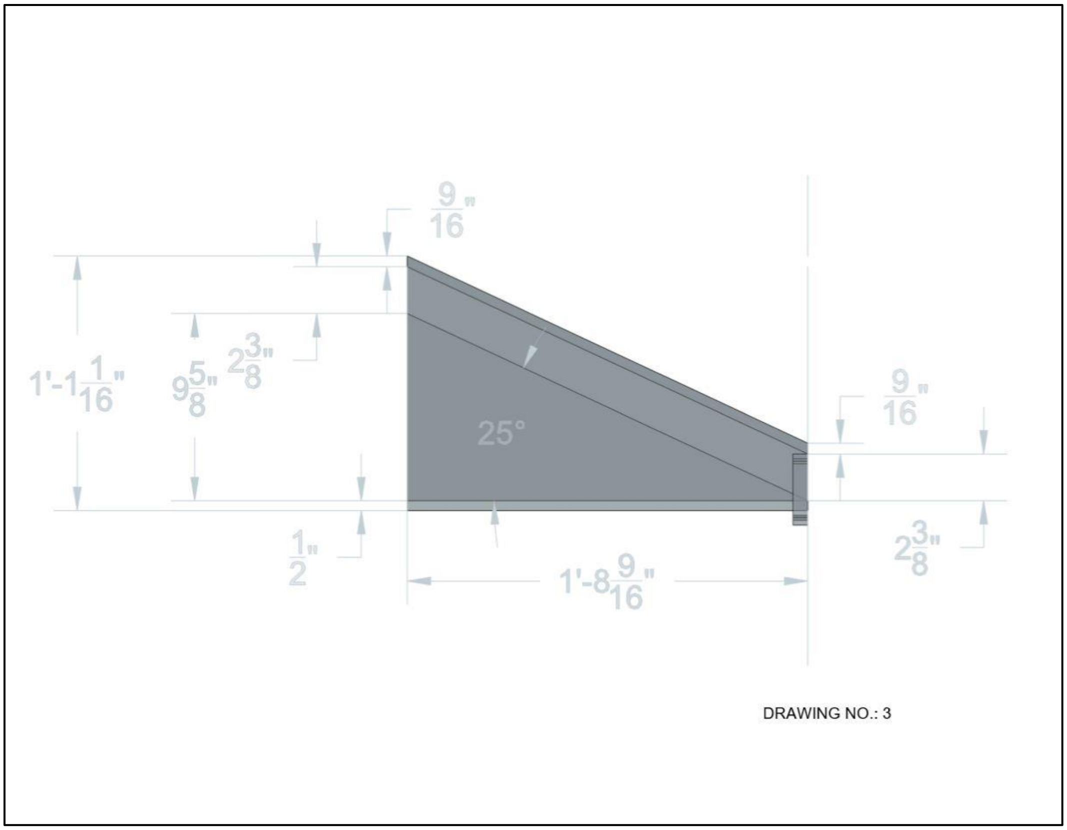

9/16"
1'-1 1/16"
9 5/8"
2 3/8"
25°
9/16"
1/2"
1'-8 9/16"
2 3/8"
DRAWING NO.: 3

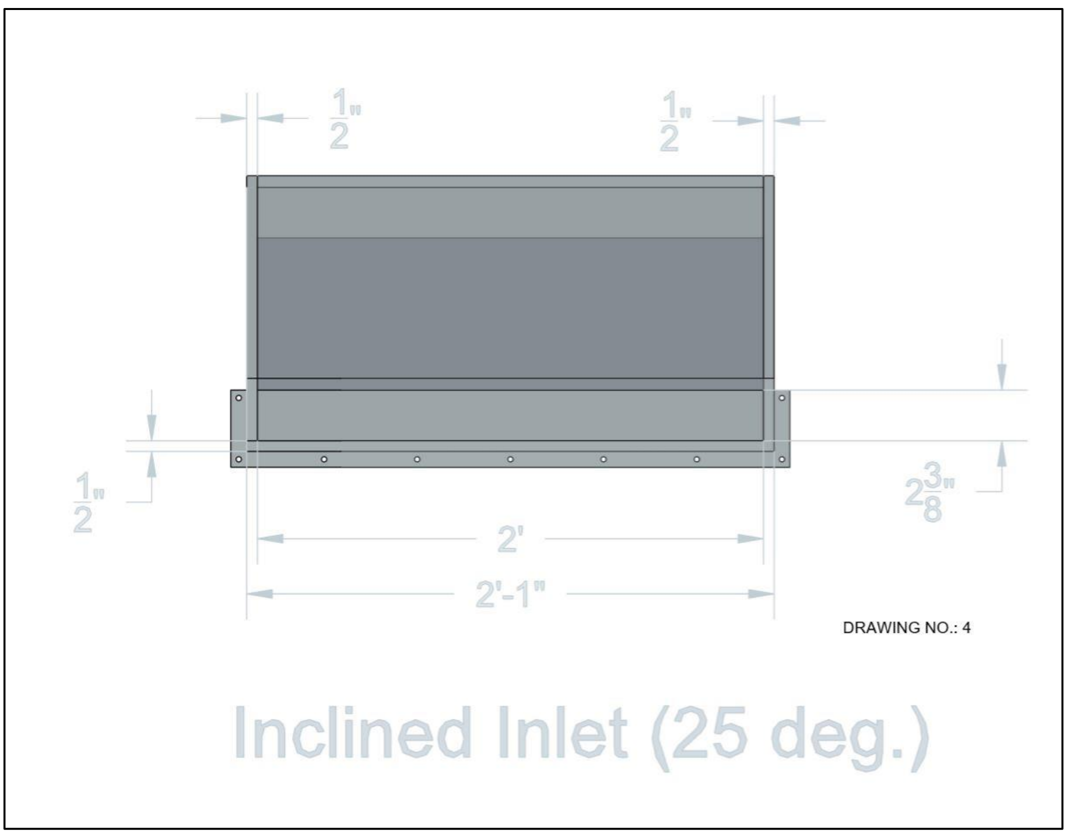

1/2"
1/2"
1/2"
2 3/8"
2'
2'-1"
DRAWING NO.: 4
Inclined Inlet (25 deg.)

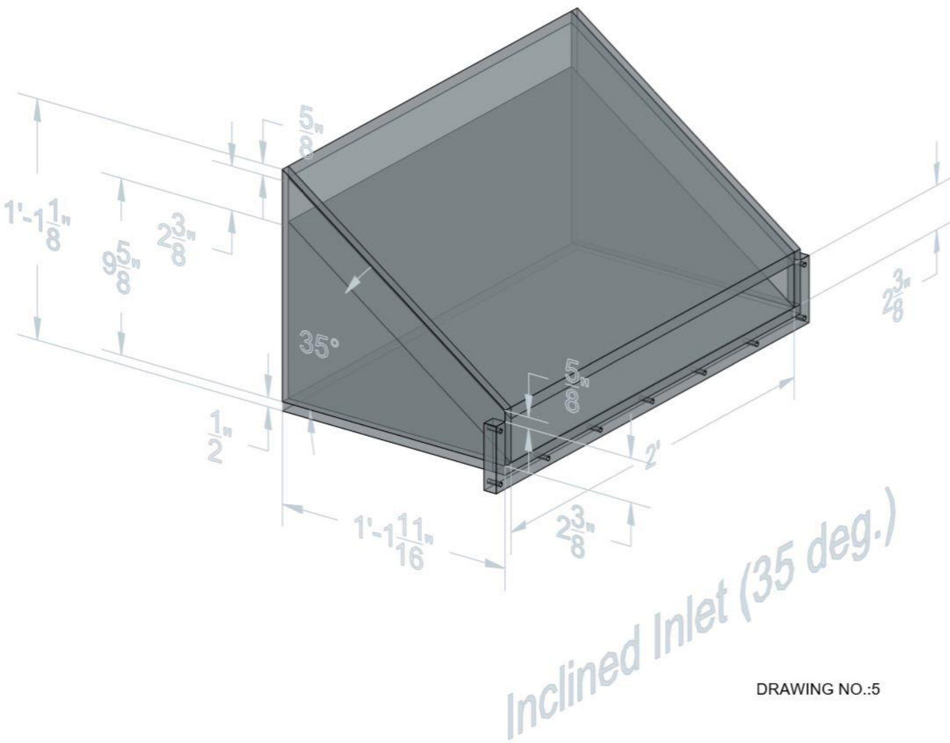

DRAWING NO.:5

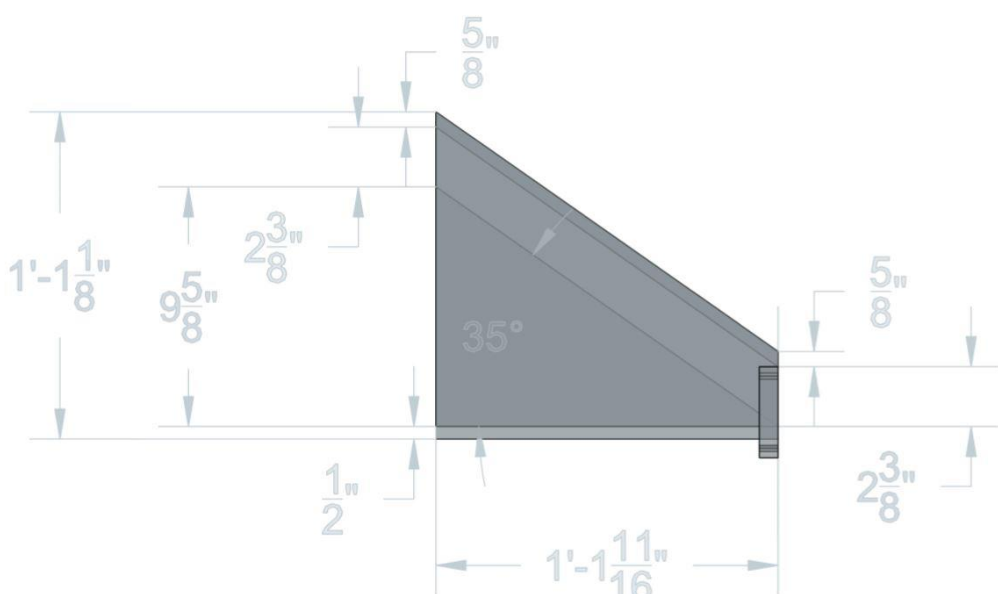

DRAWING NO.: 6

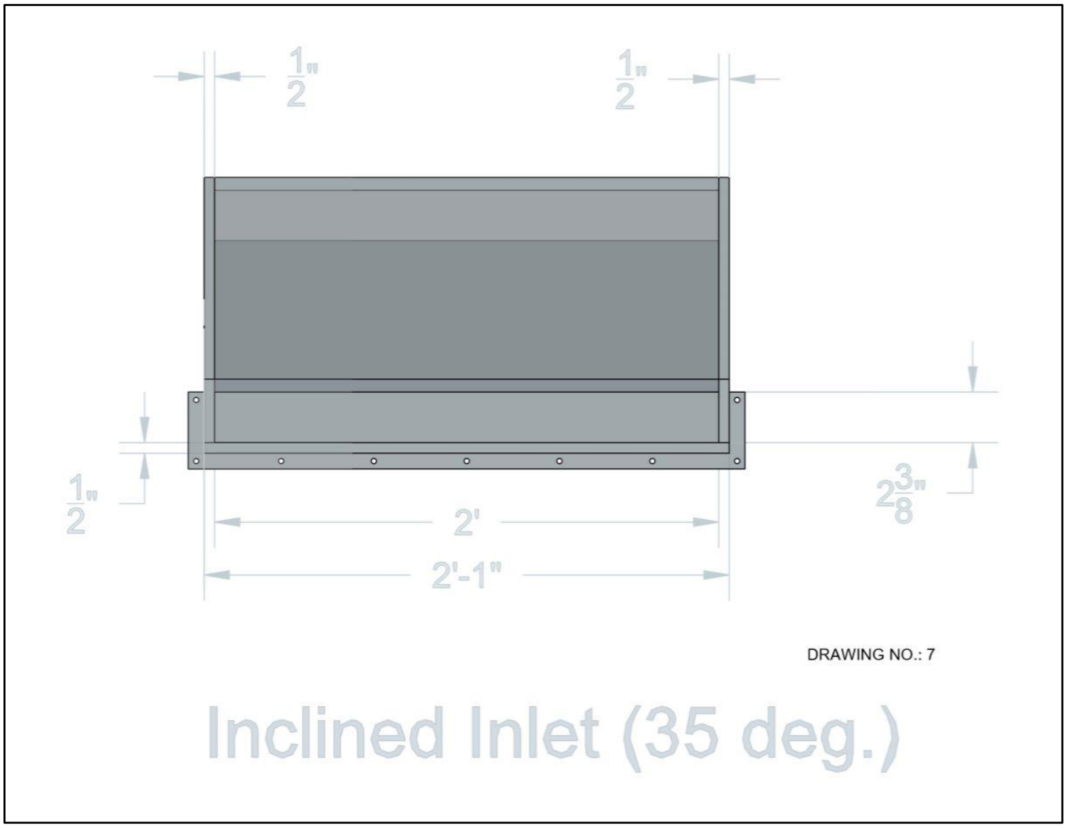
1/2"
1/2"
1/2"
2 3/8"
2'
2'-1"
DRAWING NO.: 7
Inclined Inlet (35 deg.)

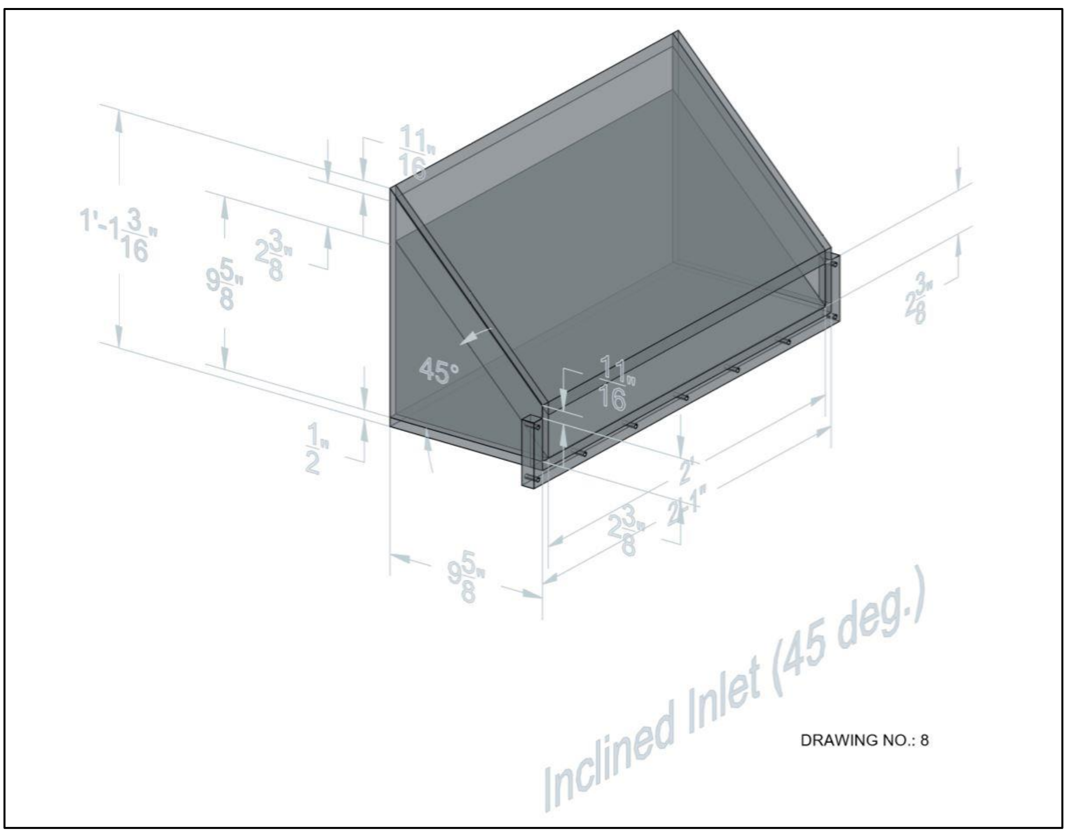
11/16"
1'-1 3/16"
2 3/8"
9 5/8"
45°
11/16"
1/2"
2 3/8"
2'
2'-1"
2 3/8"
9 5/8"
Inclined Inlet (45 deg.)
DRAWING NO.: 8

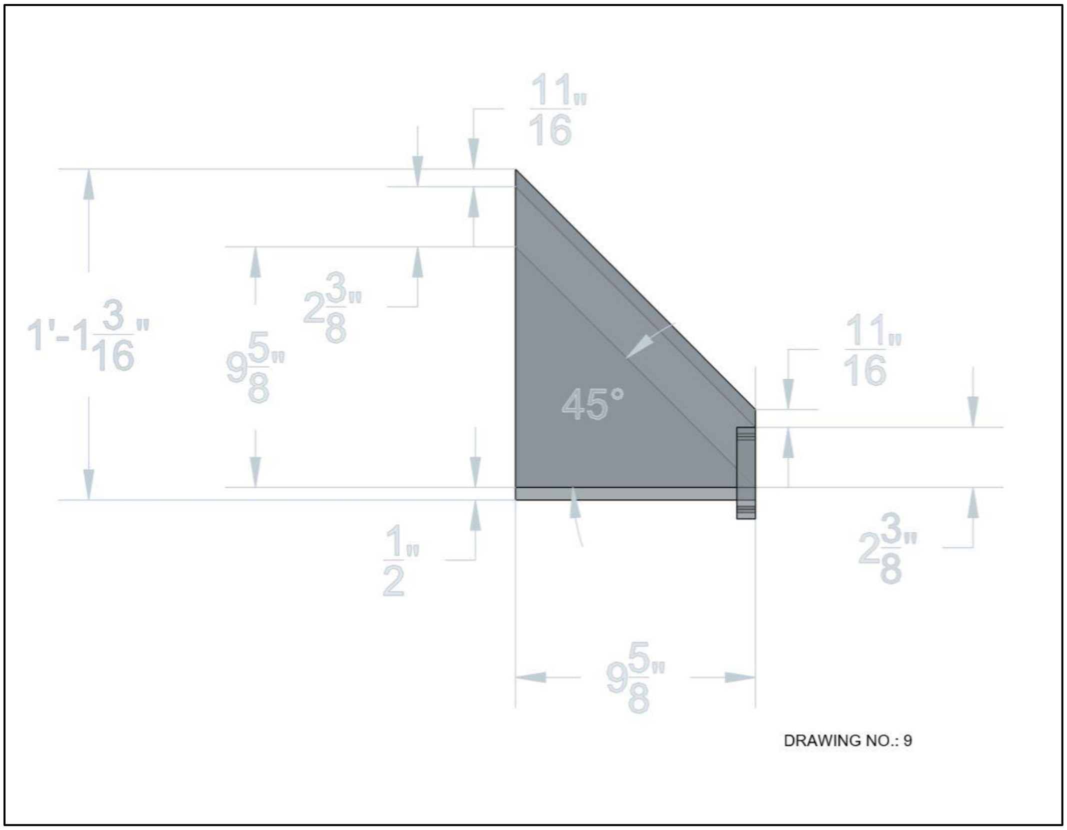
11"/16
1'-1 3/16"
9 5/8"
2 3/8"
45°
11"/16
1"/2
2 3/8"
9 5/8"
DRAWING NO.: 9

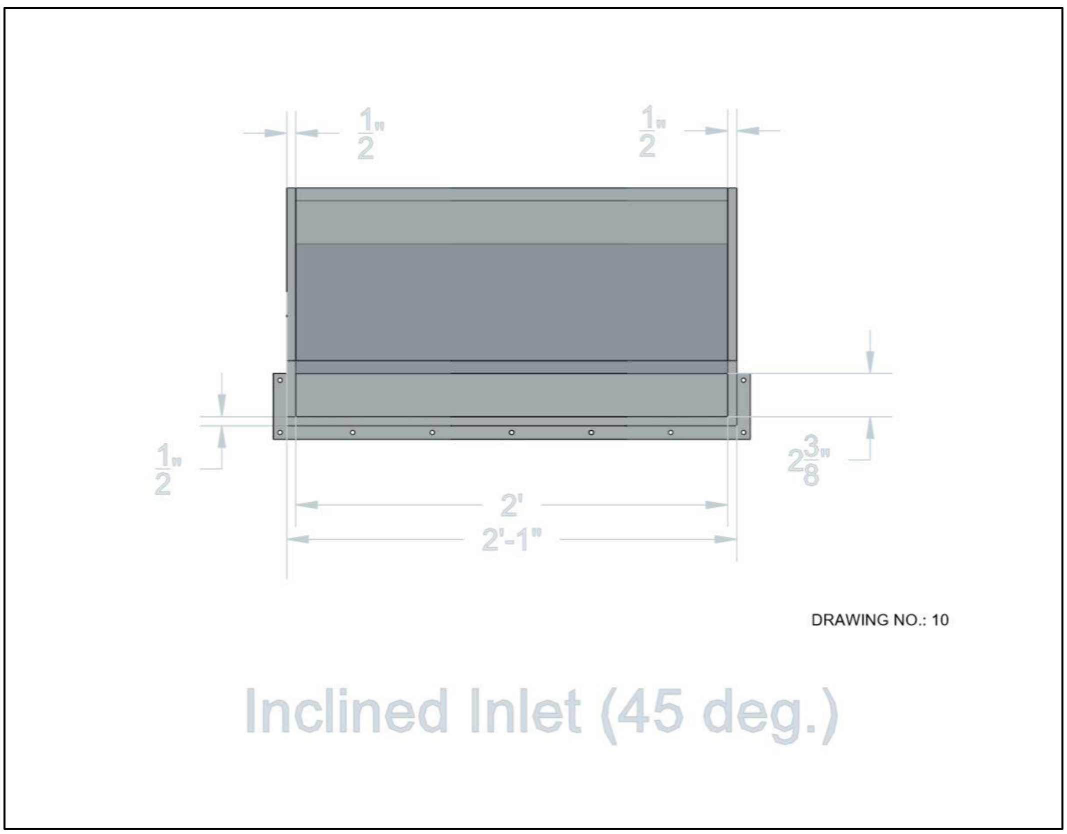
1"/2
1"/2
1"/2
2 3/8"
2'
2'-1"
DRAWING NO.: 10
Inclined Inlet (45 deg.)

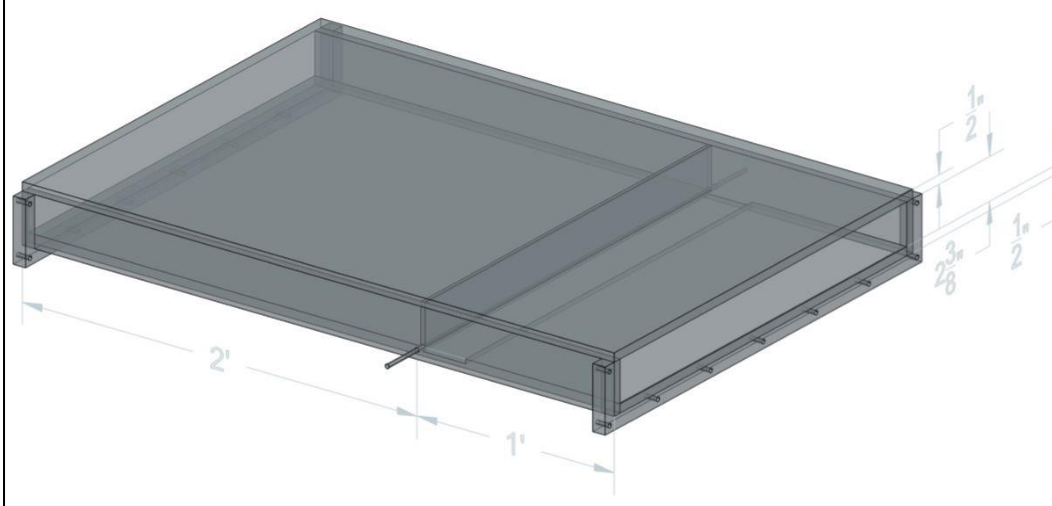

GATE CHANNEL [DRAWING NO.: 11]

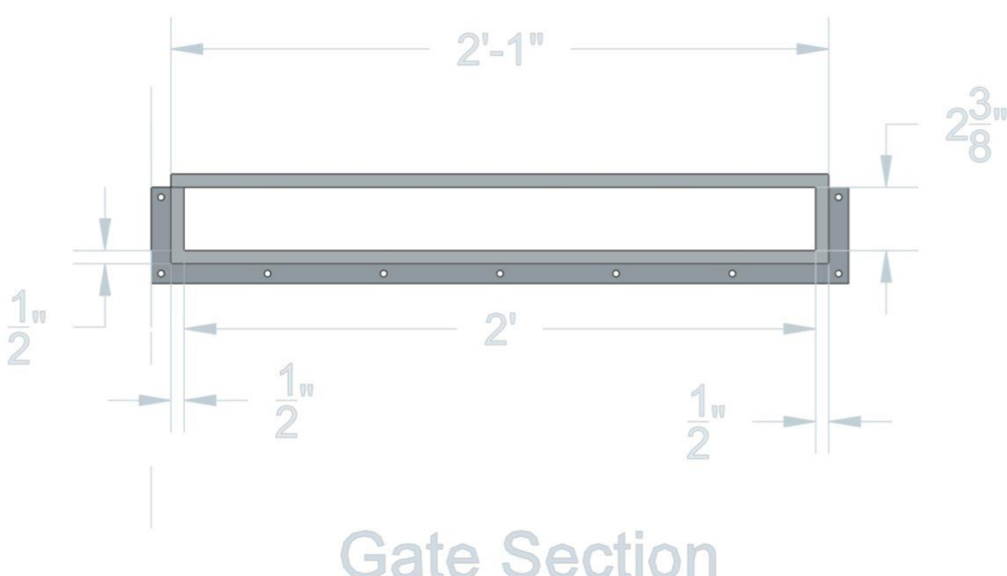

DRAWING NO.: 12

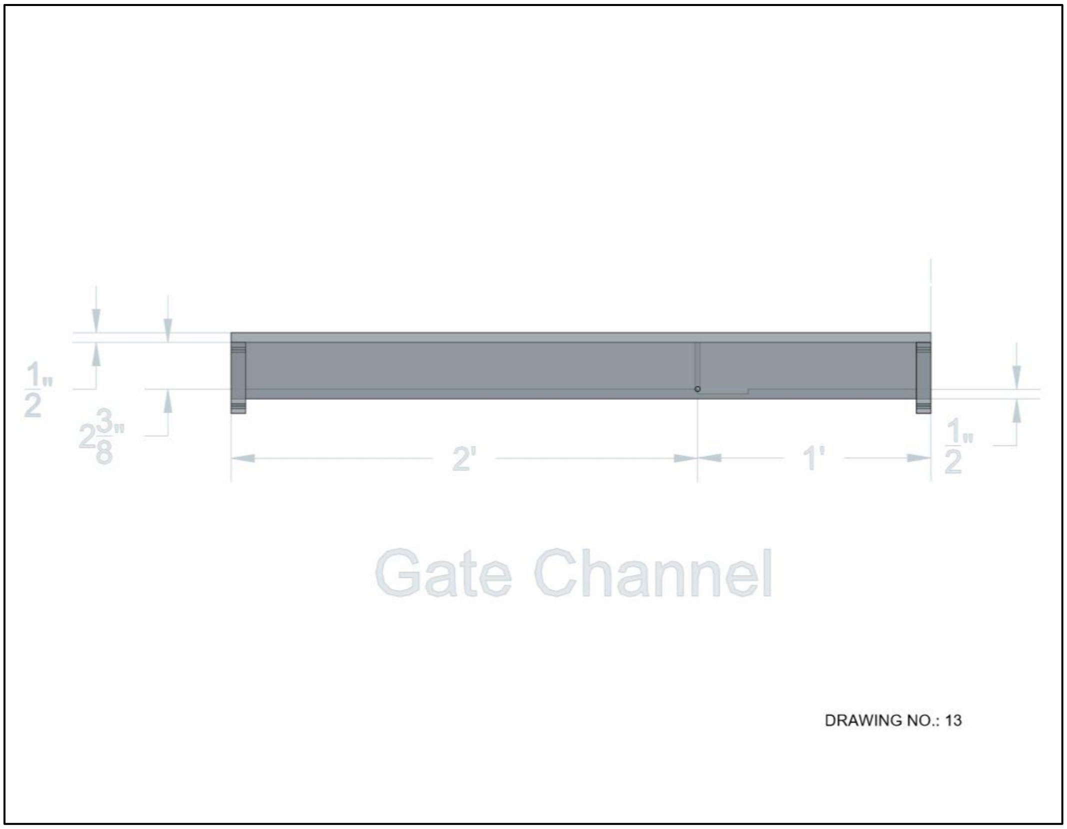
1"
2
2 3/8"
2'
1'
1"
2
Gate Channel
DRAWING NO.: 13

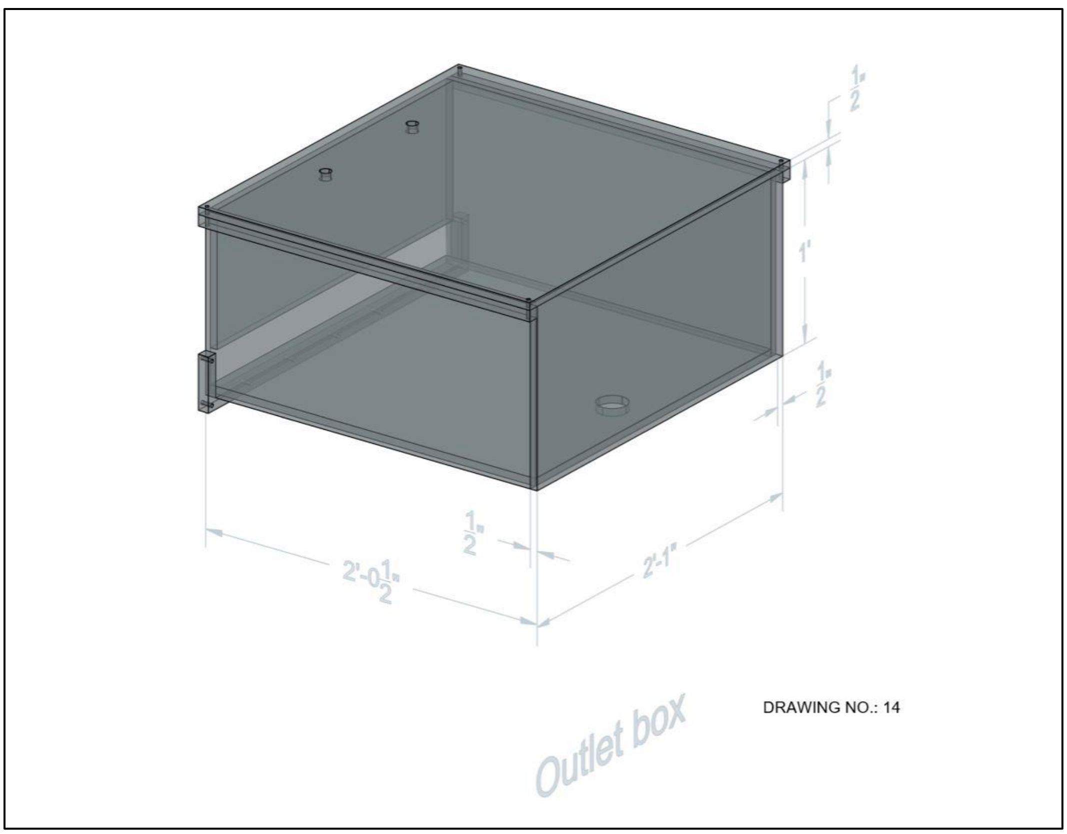
1"
2
1'
1"
2
1"
2
2'-0 1/2"
2'-1"
Outlet box
DRAWING NO.: 14

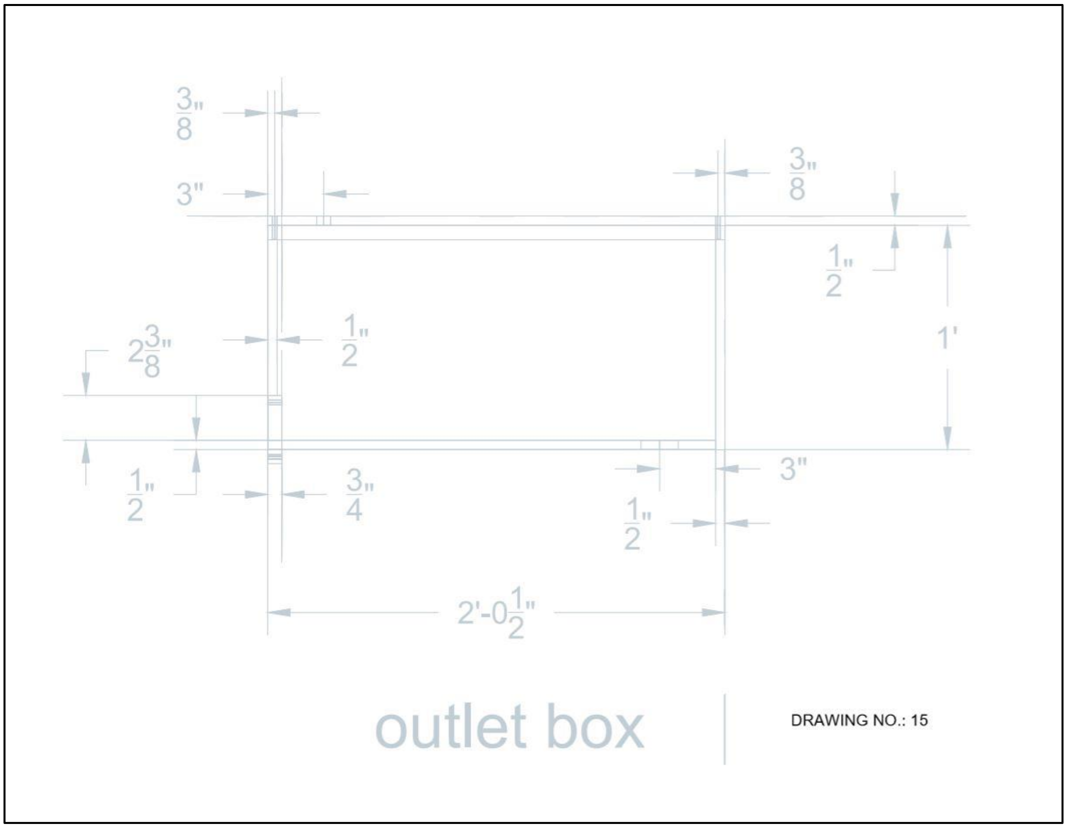
3"/8
3"
3"/8
1"/2
2 3"/8
1"/2
1'
1"/2
3"/4
3"
1"/2
2'-0 1"/2
outlet box
DRAWING NO.: 15

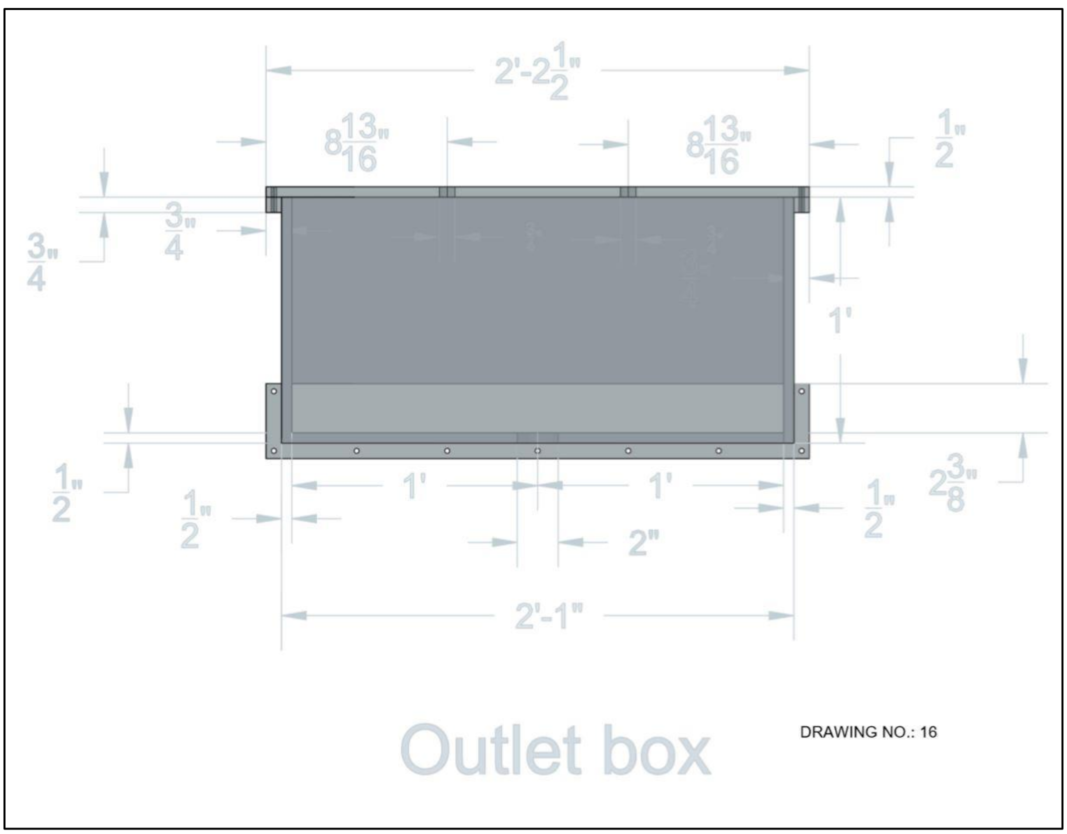
2'-2 1"/2
8 13"/16
8 13"/16
1"/2
3"/4
3"/4
1'
1"/2
1"/2
1'
1'
1"/2
2 3"/8
2"
2'-1"
Outlet box
DRAWING NO.: 16

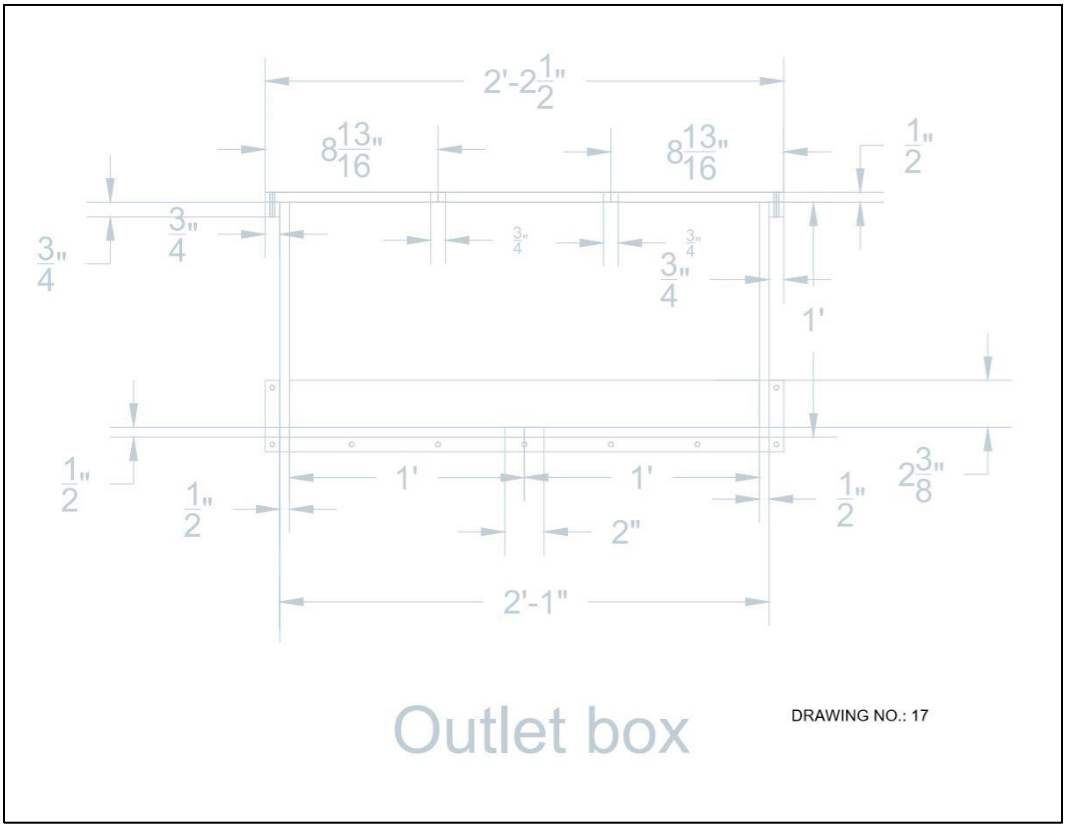
2'-2 1/2"
8 13/16"
8 13/16"
1/2"
3/4"
3/4"
3/4
3/4
3/4"
1'
1/2"
1/2"
1'
1'
1/2"
2 3/8"
2"
2'-1"
Outlet box
DRAWING NO.: 17

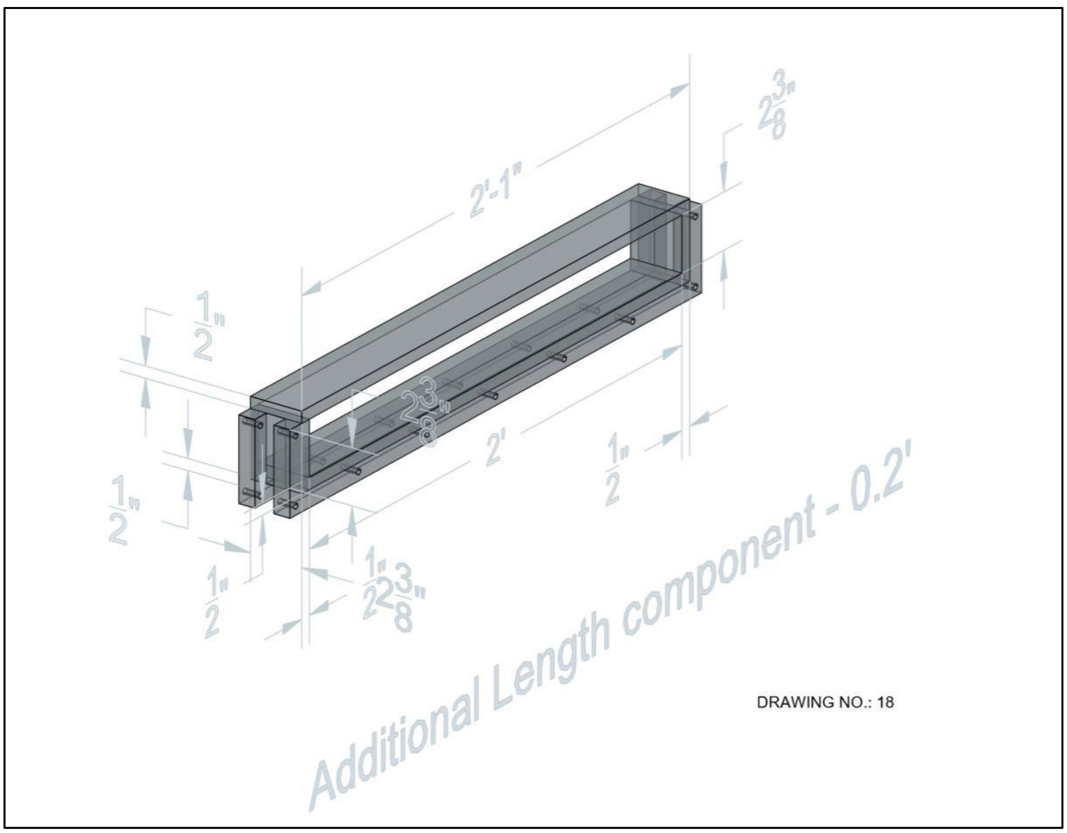
2 3/8"
2'-1"
1/2"
2 3/8"
2'
1/2"
1/2"
1/2"
1/2"
2 3/8"
Additional Length component - 0.2'
DRAWING NO.: 18

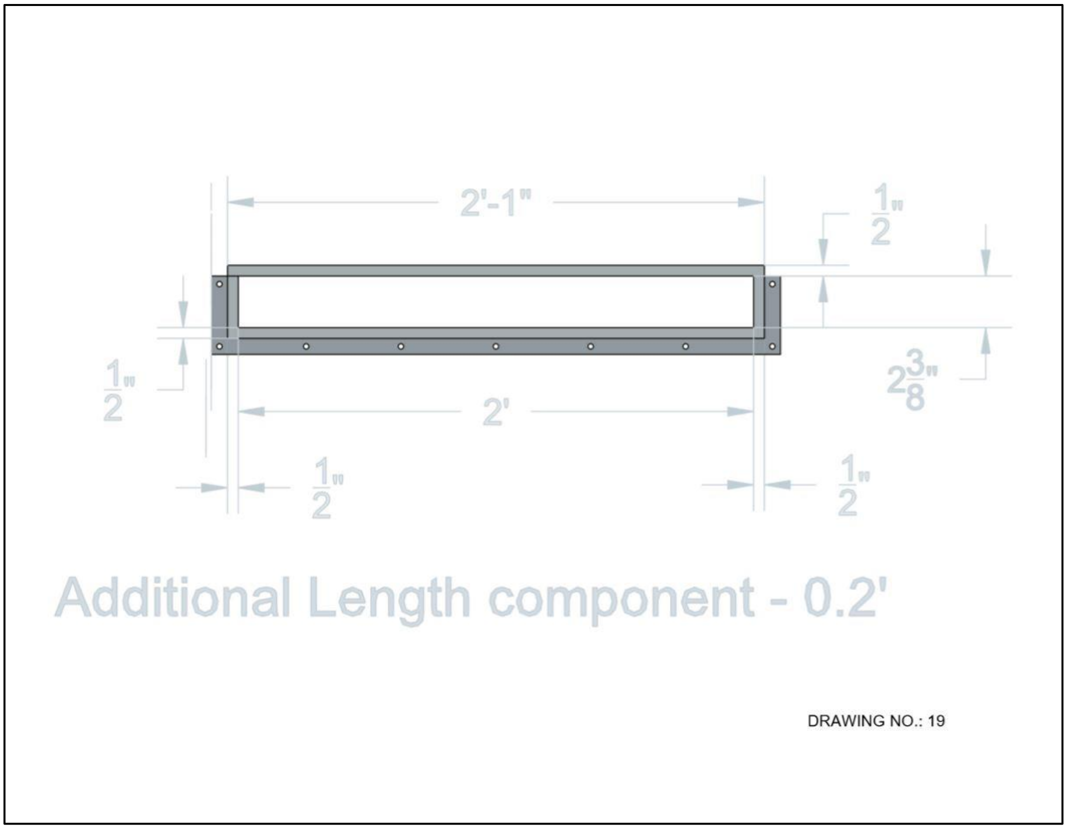

2'-1"
1/2"
1/2"
2 3/8"
2'
1/2"
1/2"
Additional Length component - 0.2'
DRAWING NO.: 19

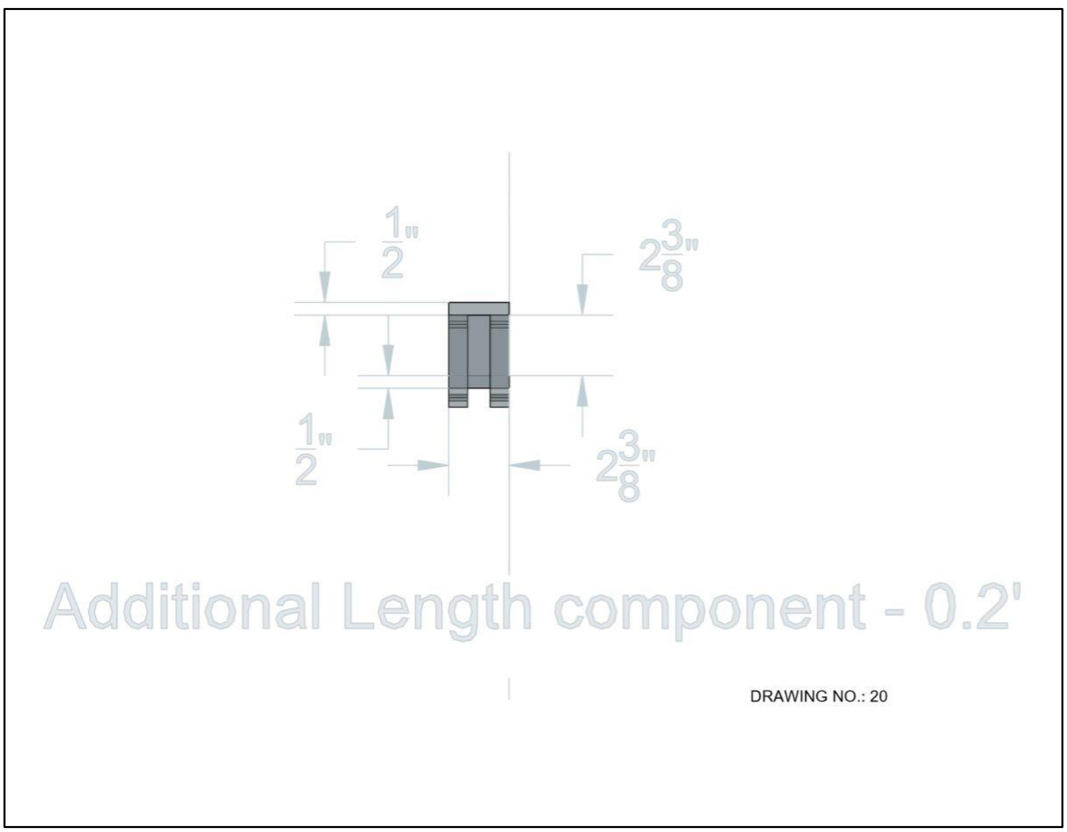

1/2"
2 3/8"
1/2"
2 3/8"
Additional Length component - 0.2'
DRAWING NO.: 20

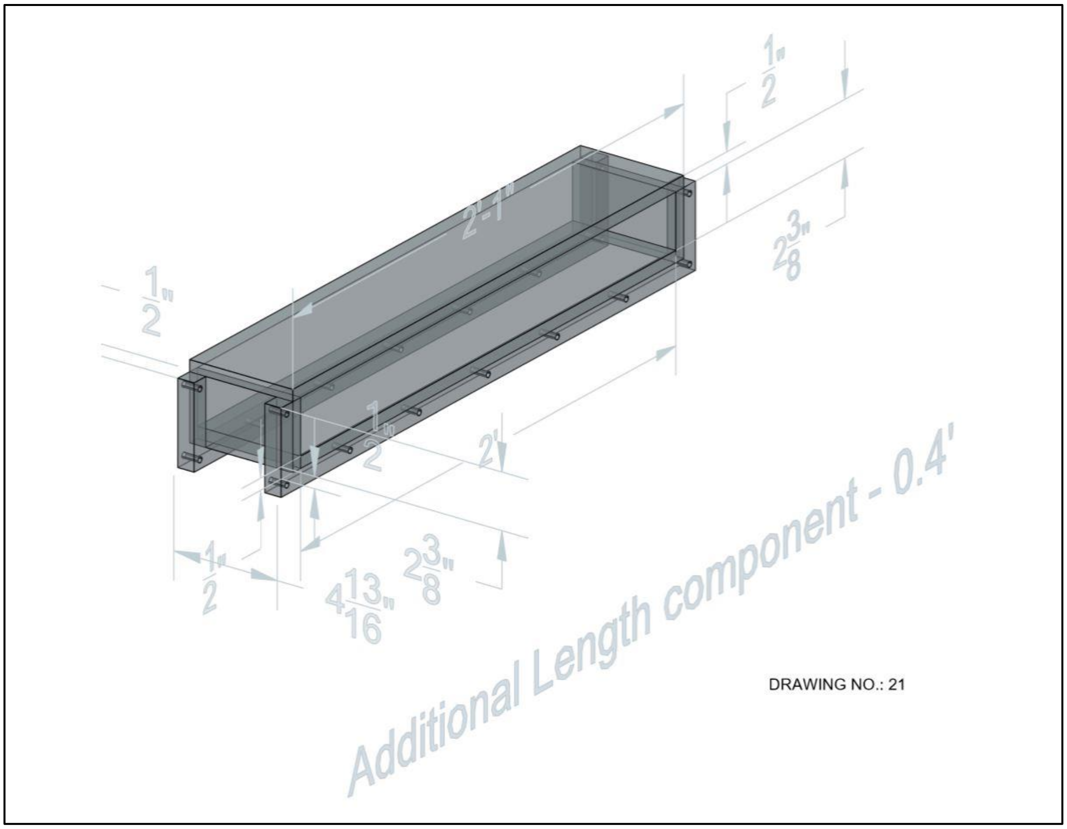
2'-1"
1/2"
2 3/8"
1/2"
1/2"
2'
1/2
4 13/16"
2 3/8"
Additional Length component - 0.4'
DRAWING NO.: 21

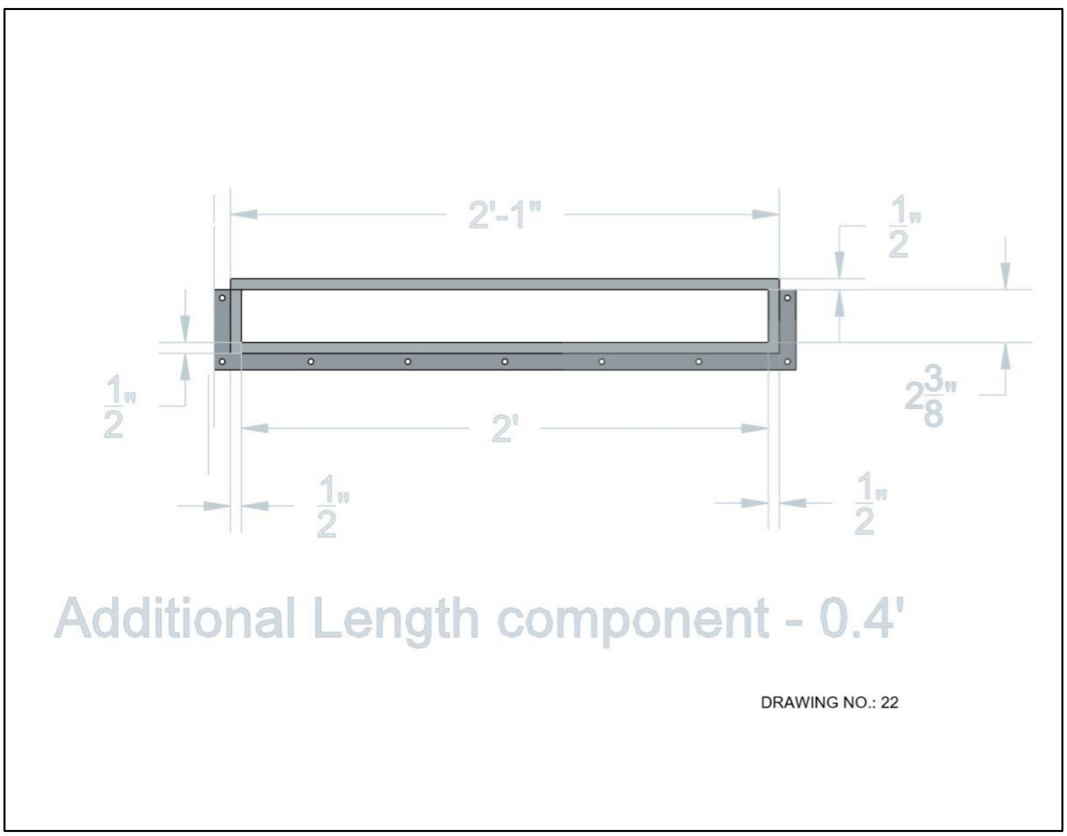
2'-1"
1/2"
1/2"
2 3/8"
2'
1/2"
1/2"
Additional Length component - 0.4'
DRAWING NO.: 22

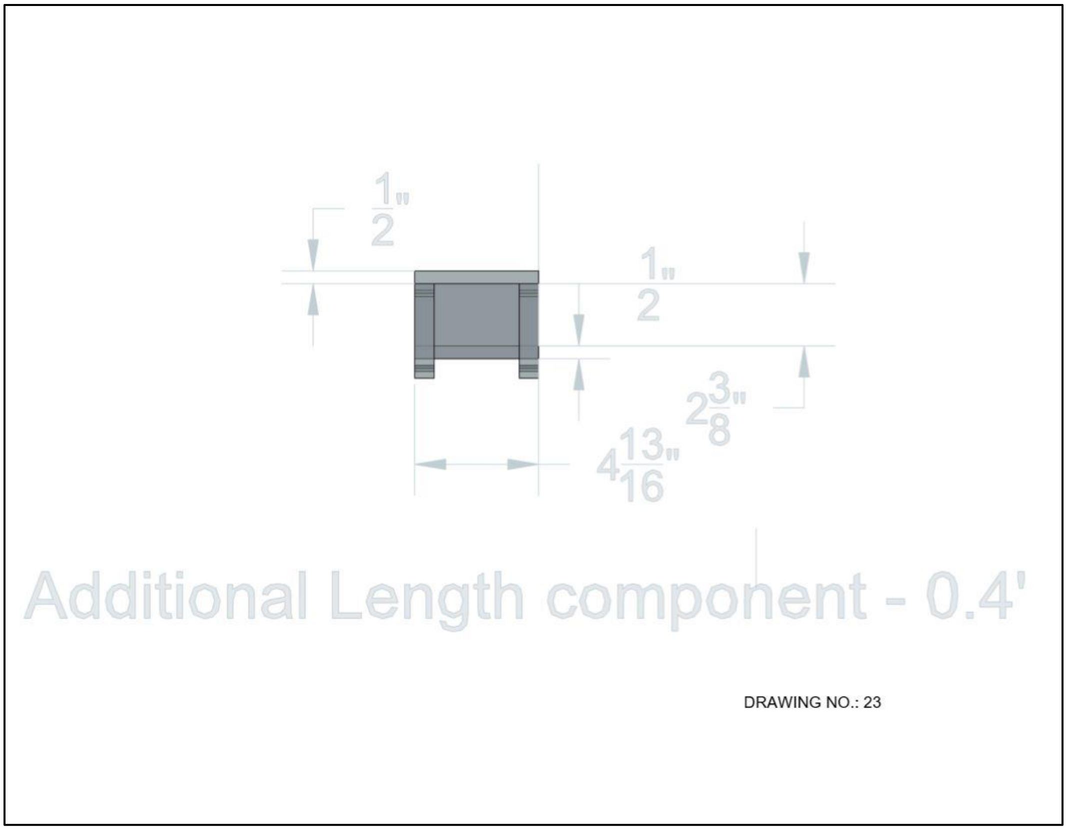
1/2"
1/2"
2 3/8"
4 13/16"
Additional Length component - 0.4'
DRAWING NO.: 23

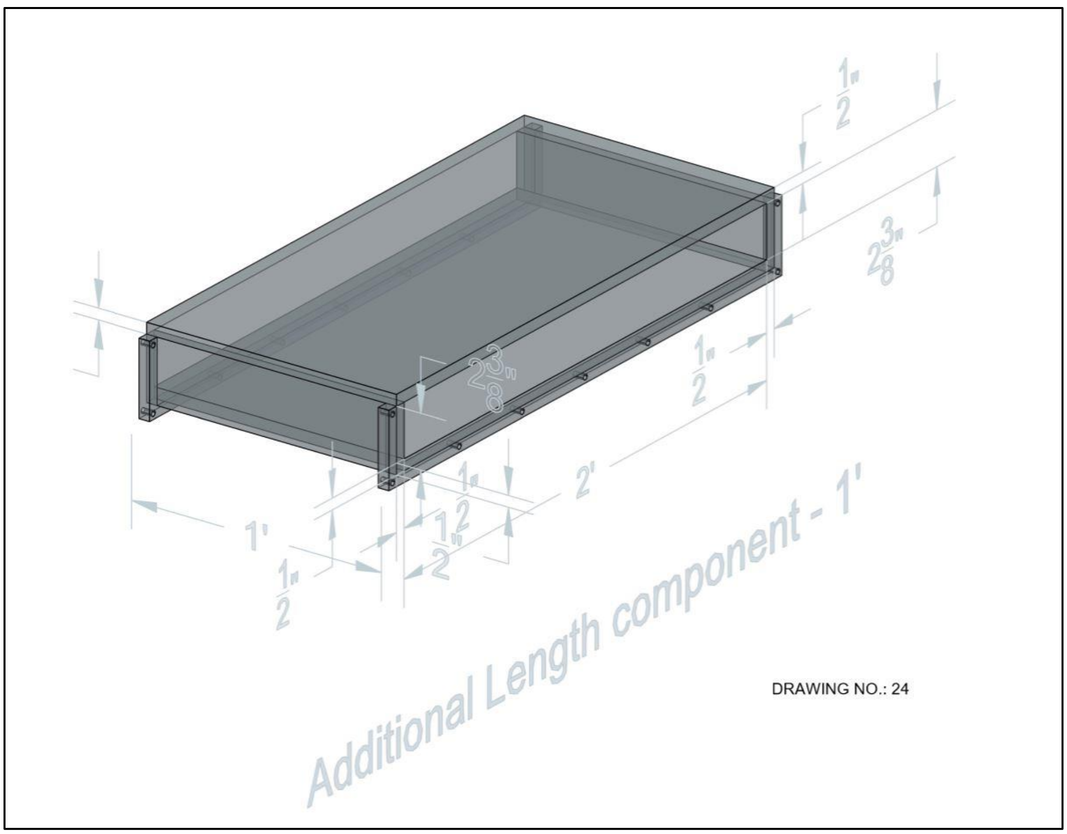
1/2"
2 3/8"
2 3/8"
1/2"
2'
1'
1/2"
1/2"
1/2"
Additional Length component - 1'
DRAWING NO.: 24

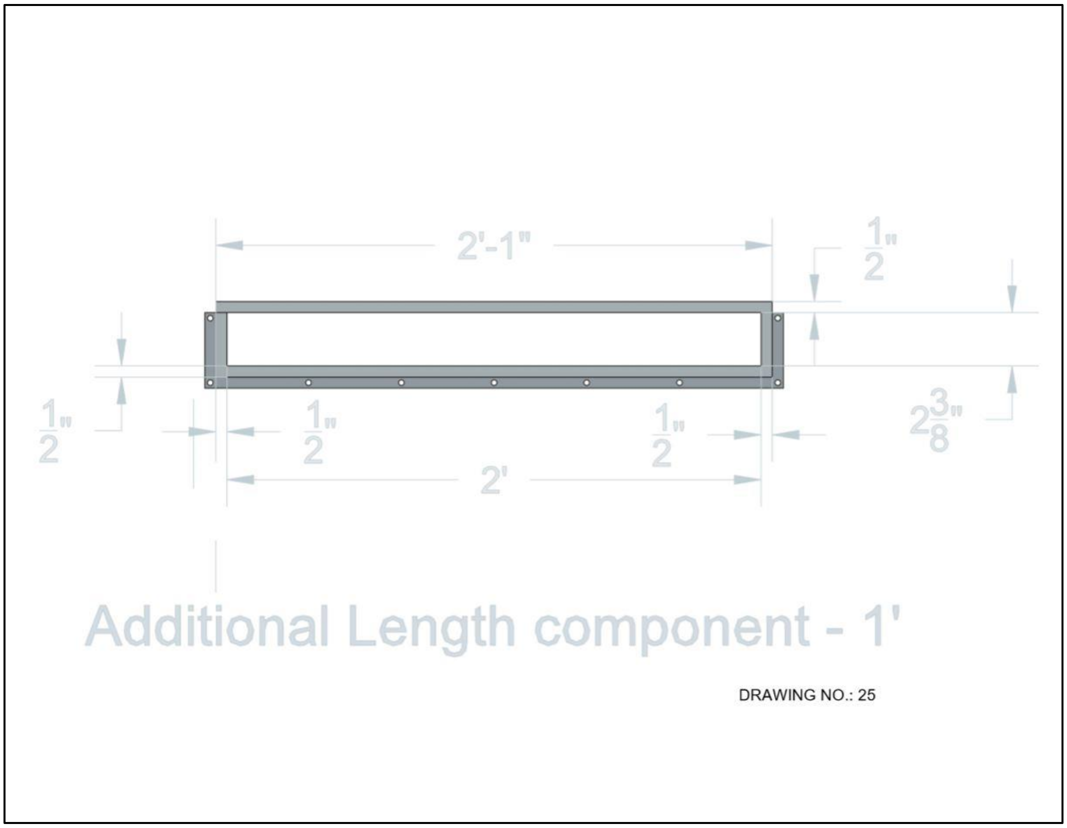
2'-1"
1/2"
1/2"
1/2"
1/2"
2 3/8"
2'
Additional Length component - 1'
DRAWING NO.: 25

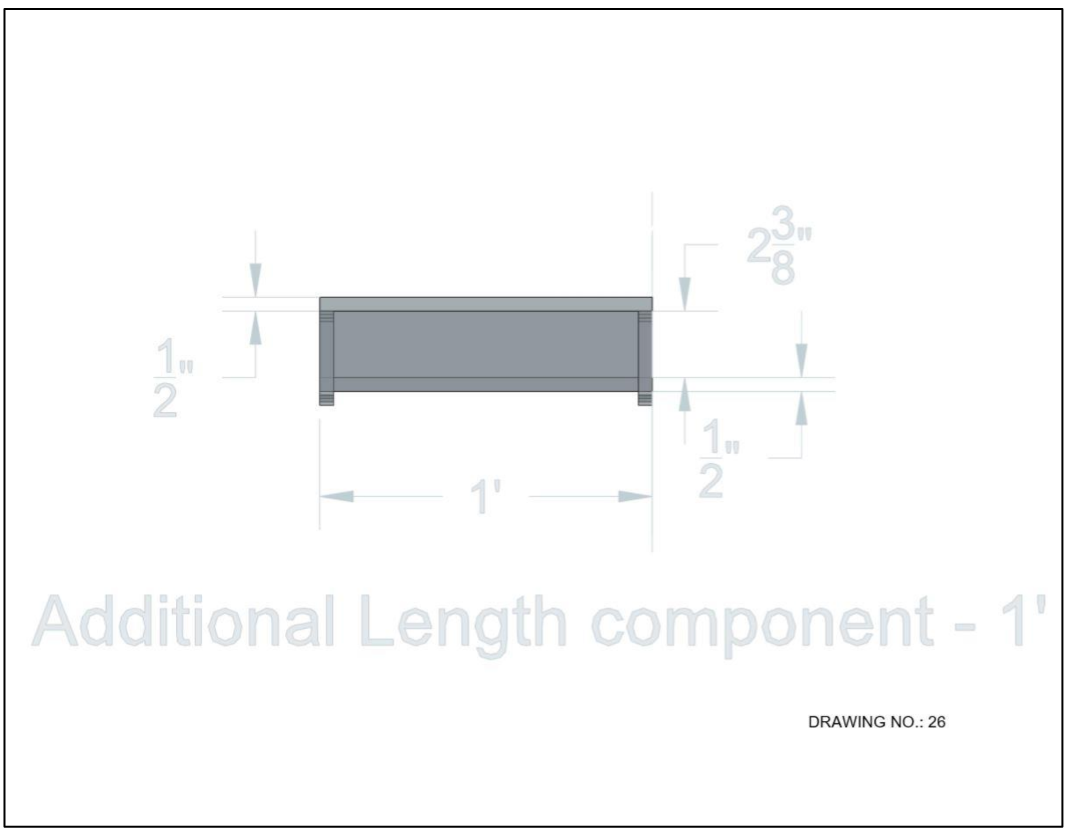
2 3/8"
1/2"
1/2"
1'
Additional Length component - 1'
DRAWING NO.: 26

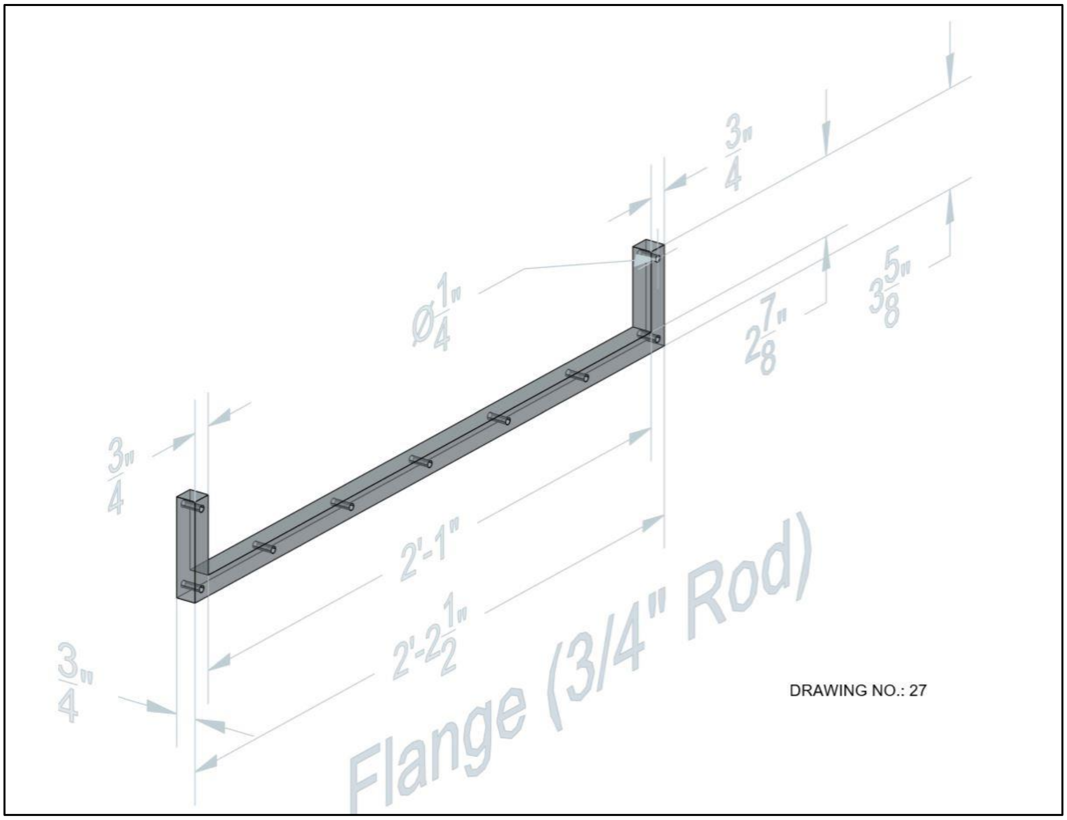

3"/4
Ø1/4"
3"/4
2'-1"
2'-2 1/2"
2 7/8"
3 5/8"
3"/4
Flange (3/4" Rod)
DRAWING NO.: 27

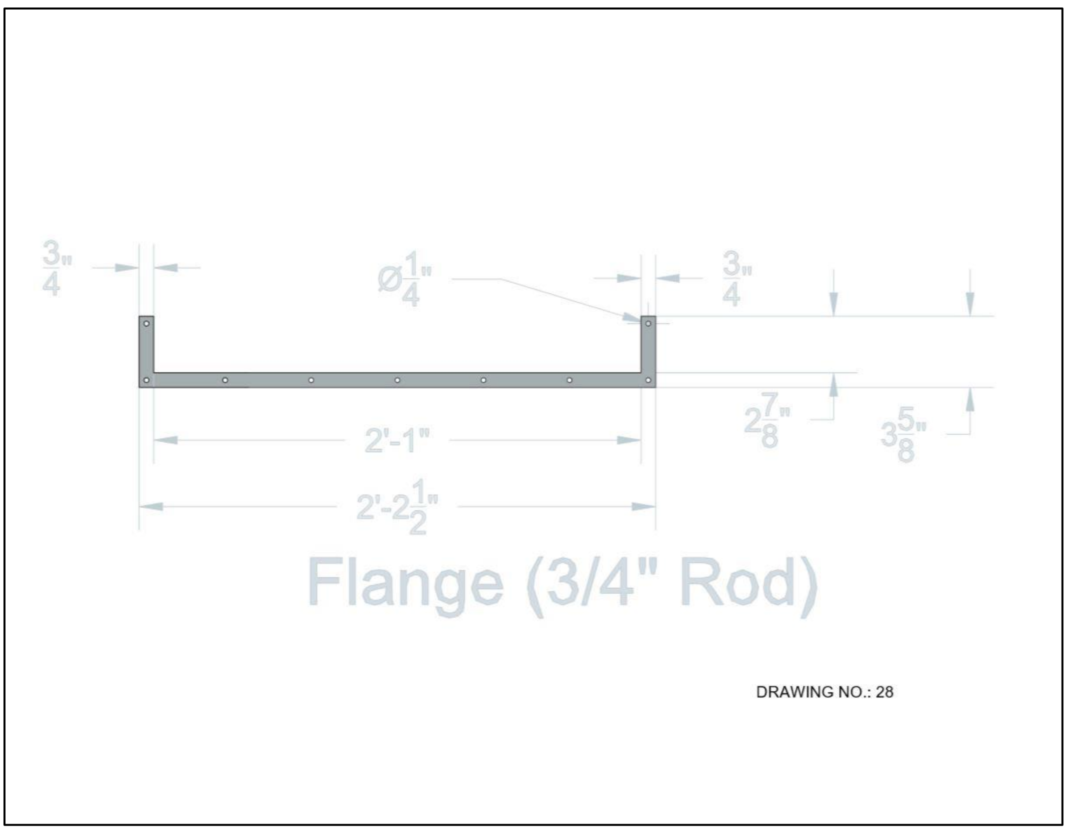

3"/4
Ø1/4"
3"/4
2 7/8"
3 5/8"
2'-1"
2'-2 1/2"
Flange (3/4" Rod)
DRAWING NO.: 28

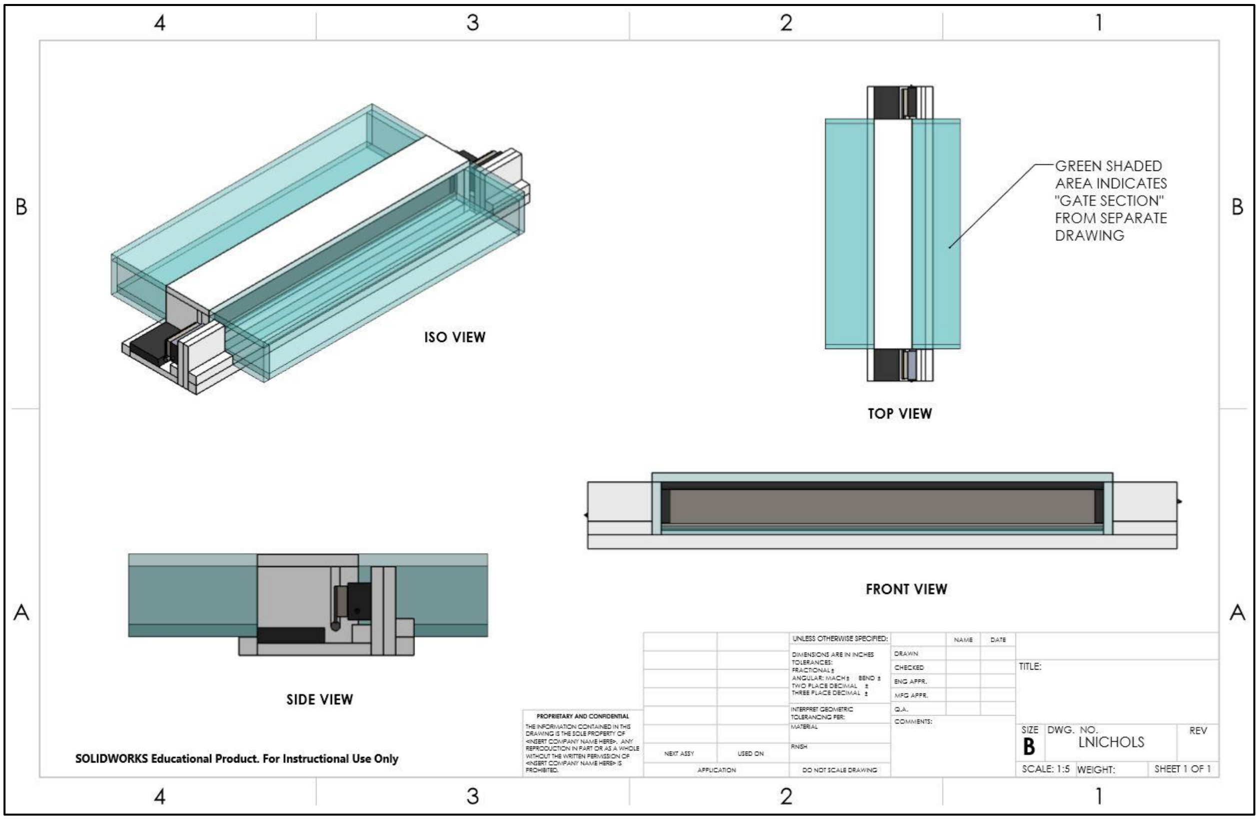
ISO VIEW
TOP VIEW
GREEN SHADED AREA INDICATES "GATE SECTION" FROM SEPARATE DRAWING
FRONT VIEW
SIDE VIEW
SOLIDWORKS Educational Product. For Instructional Use Only
TITLE:
SIZE DWG. NO. REV
B
LNICHOLS
SCALE: 1:5 WEIGHT: SHEET 1 OF 1

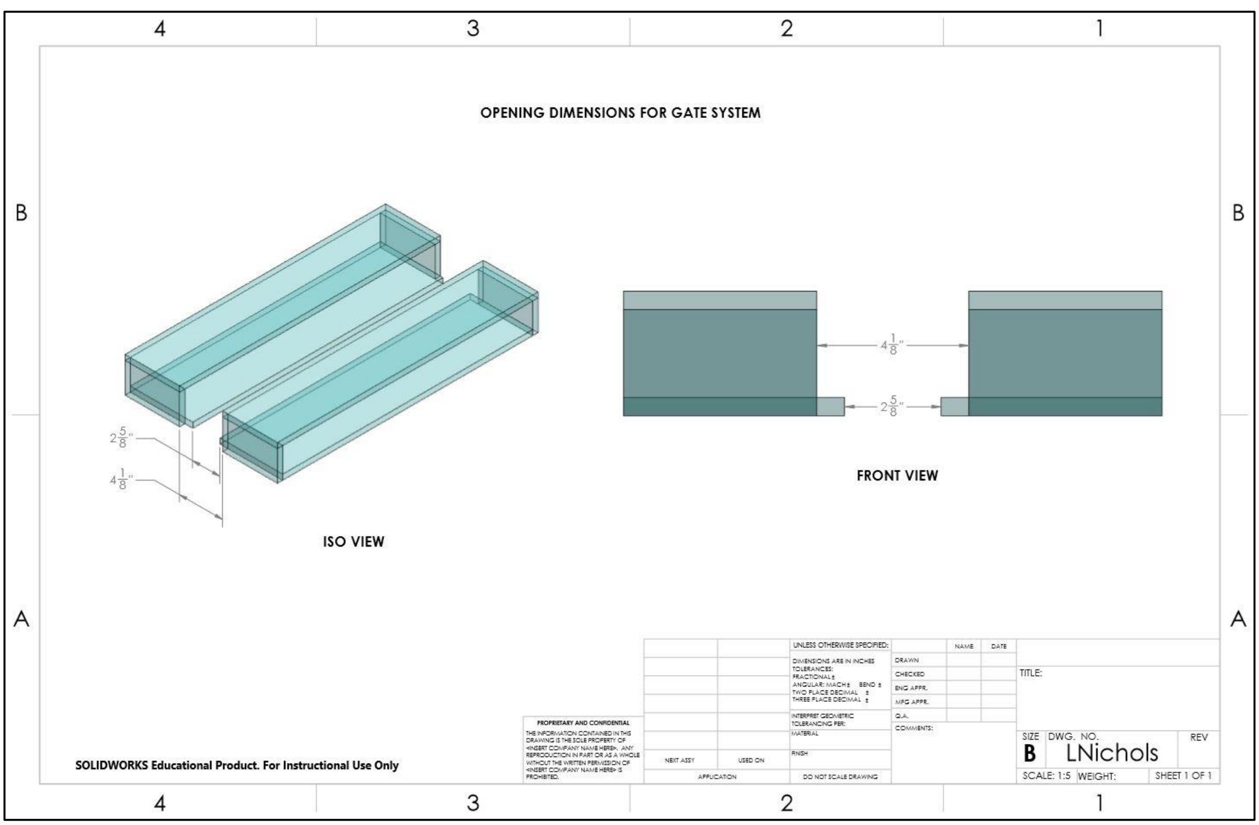
OPENING DIMENSIONS FOR GATE SYSTEM
$2\frac{5}{8}$"
$4\frac{1}{8}$"
ISO VIEW
$4\frac{1}{8}$"
$2\frac{5}{8}$"
FRONT VIEW
SOLIDWORKS Educational Product. For Instructional Use Only
TITLE:
SIZE DWG. NO. REV
B
LNichols
SCALE: 1:5 WEIGHT: SHEET 1 OF 1

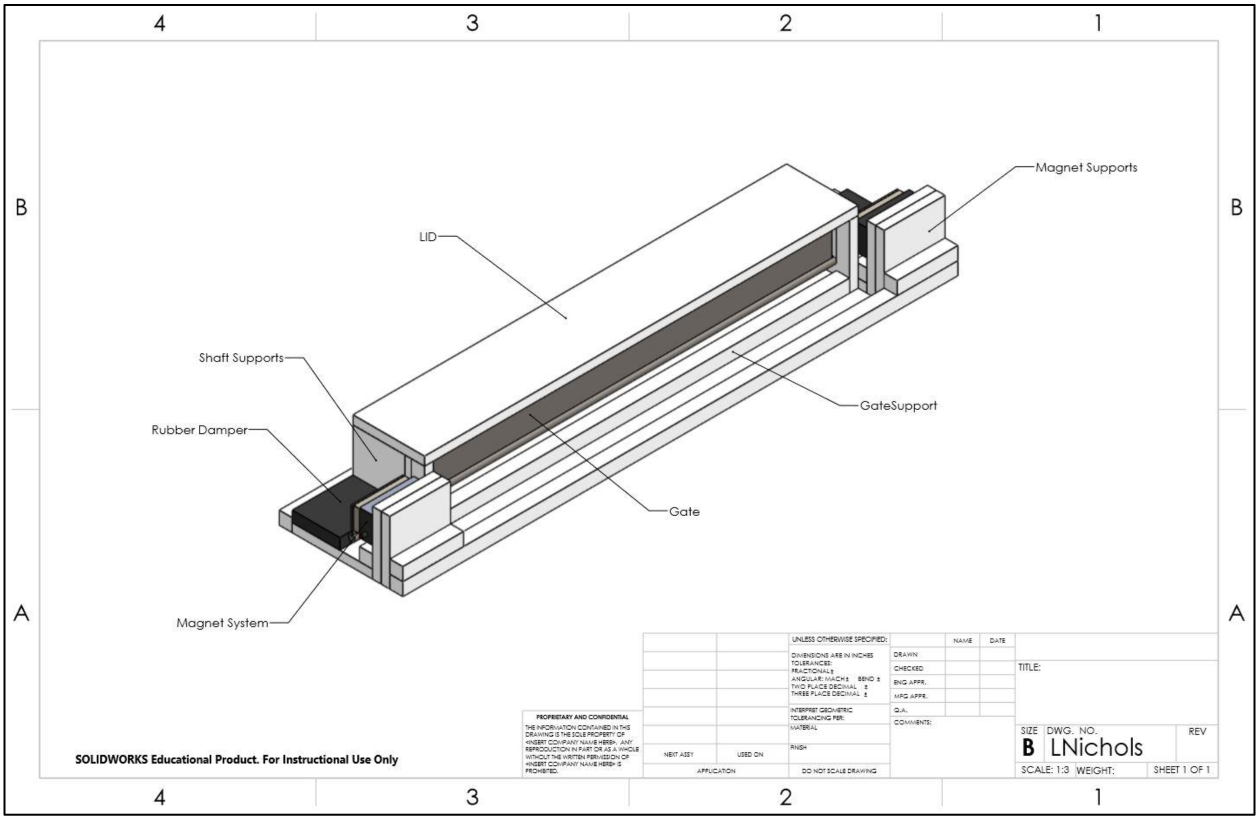
Magnet Supports
LID
Shaft Supports
GateSupport
Rubber Damper
Gate
Magnet System
SOLIDWORKS Educational Product. For Instructional Use Only
SIZE B DWG. NO. LNichols
SCALE: 1:3 SHEET 1 OF 1

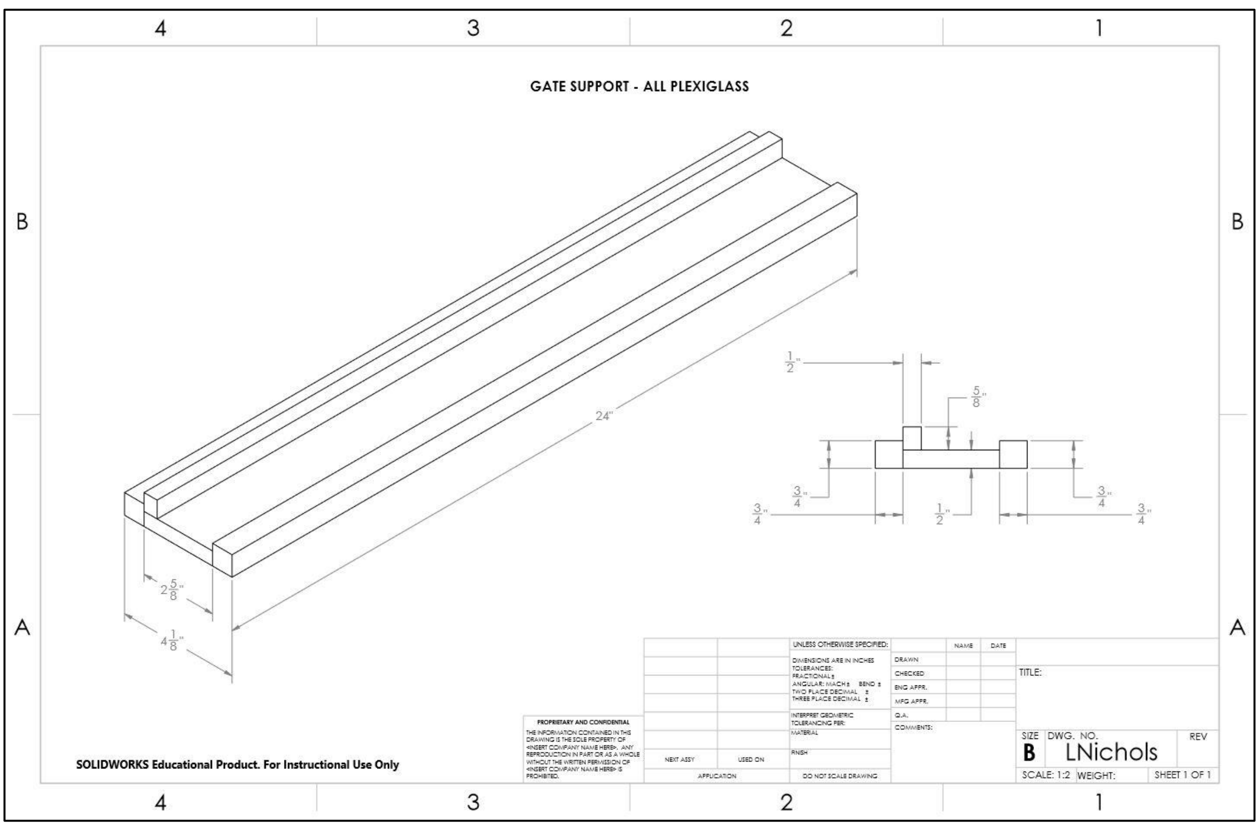
GATE SUPPORT - ALL PLEXIGLASS
24"
$2\frac{5}{8}$"
$4\frac{1}{8}$"
$\frac{1}{2}$"
$\frac{5}{8}$"
$\frac{3}{4}$"
SOLIDWORKS Educational Product. For Instructional Use Only
SIZE B DWG. NO. LNichols
SCALE: 1:2 SHEET 1 OF 1

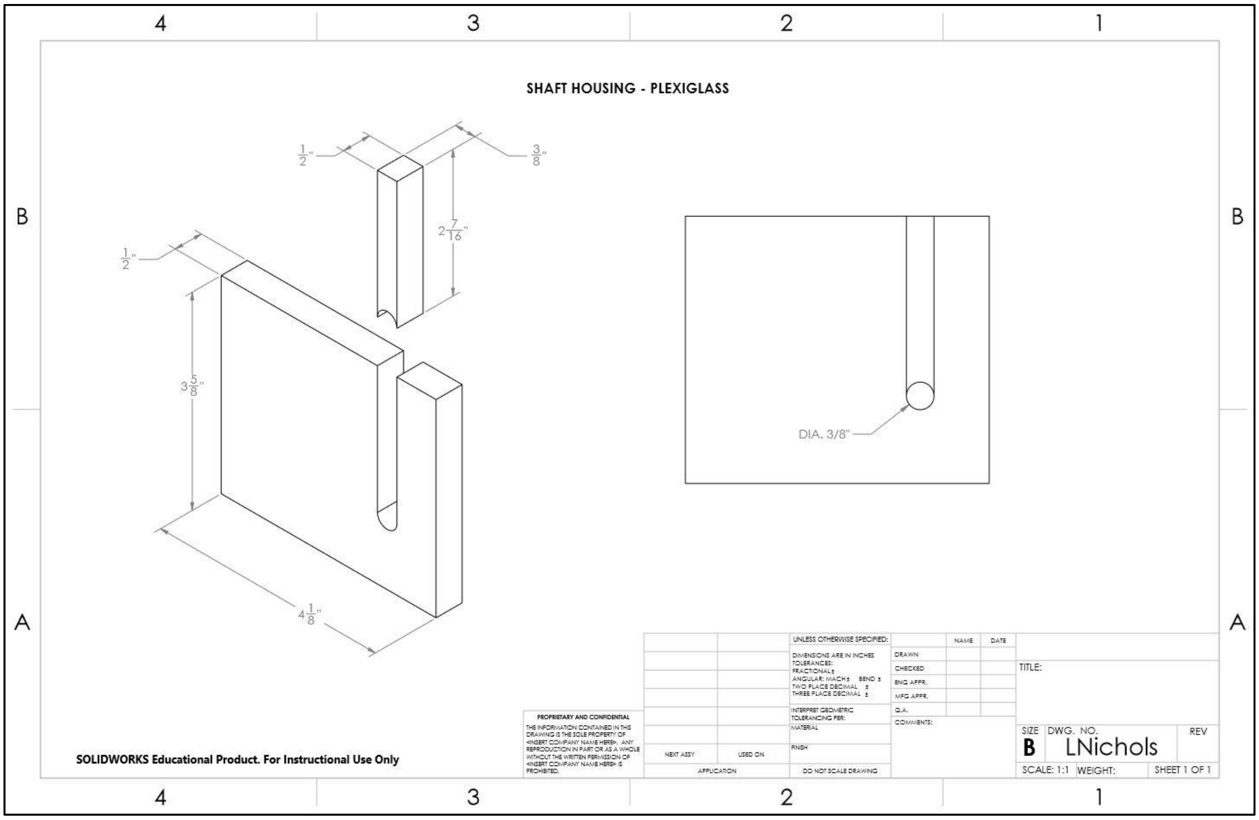
SHAFT HOUSING - PLEXIGLASS
1/2"
3/8"
2 7/16"
1/2"
3 5/8"
4 1/8"
DIA. 3/8"
SOLIDWORKS Educational Product. For Instructional Use Only
SIZE B DWG. NO. LNichols REV
SCALE: 1:1 WEIGHT: SHEET 1 OF 1

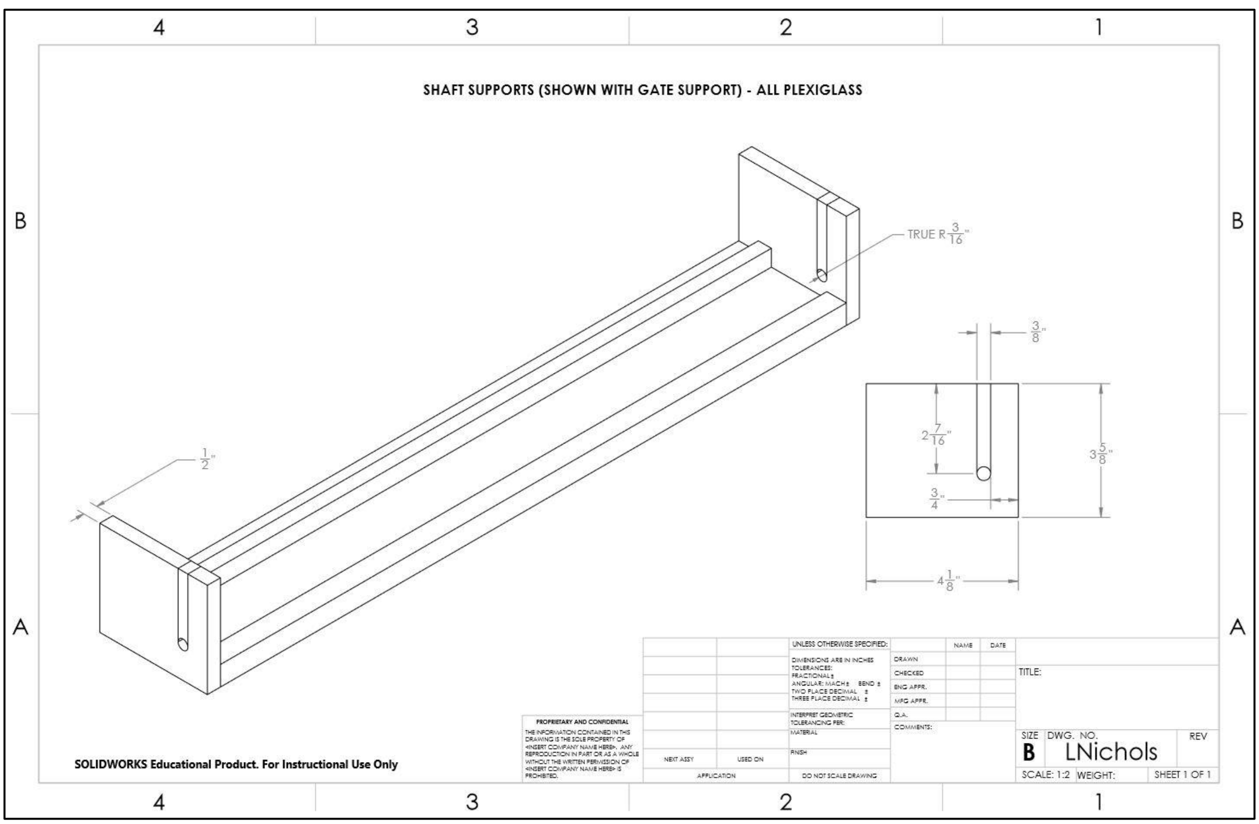
SHAFT SUPPORTS (SHOWN WITH GATE SUPPORT) - ALL PLEXIGLASS
TRUE R 3/16"
3/8"
2 7/16"
3 5/8"
3/4"
4 1/8"
1/2"
SOLIDWORKS Educational Product. For Instructional Use Only
SIZE B DWG. NO. LNichols REV
SCALE: 1:2 WEIGHT: SHEET 1 OF 1

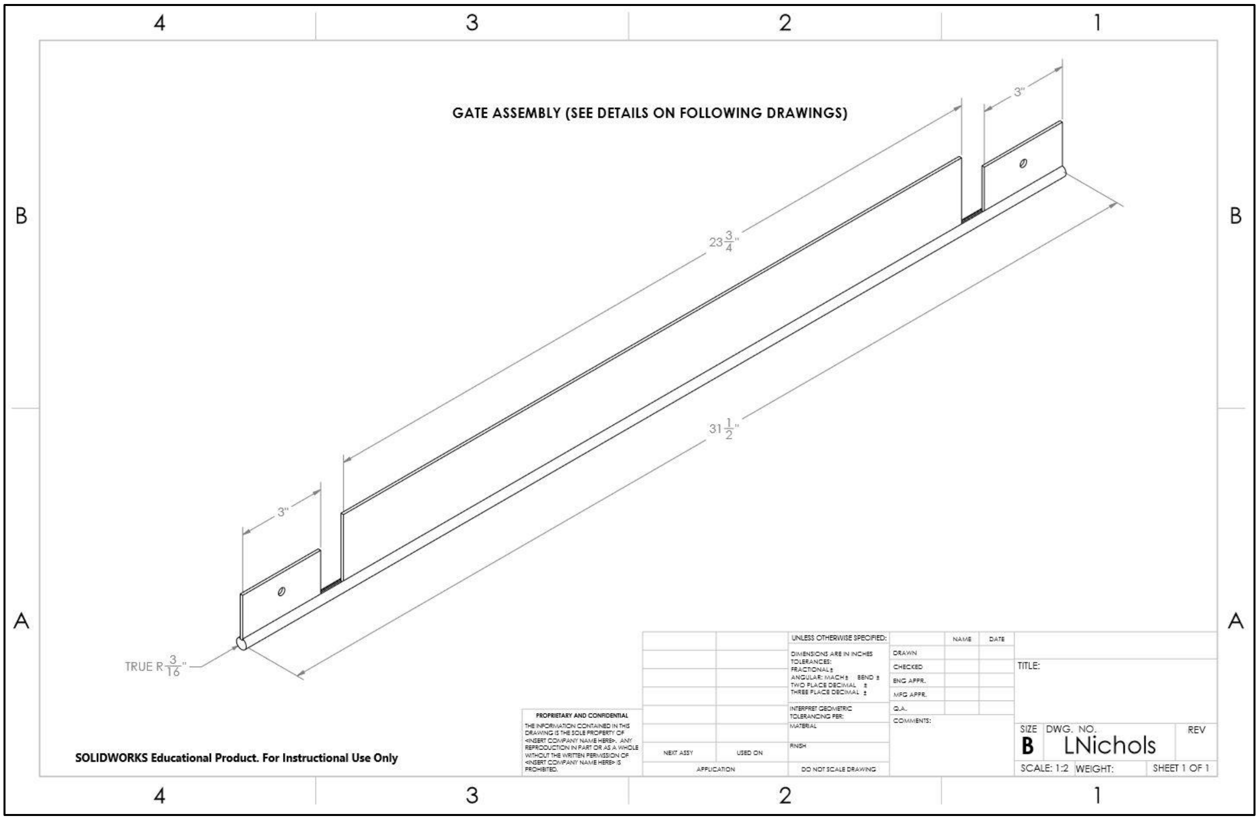
GATE ASSEMBLY (SEE DETAILS ON FOLLOWING DRAWINGS)
3"
23 3/4"
31 1/2"
3"
TRUE R 3/16"
SOLIDWORKS Educational Product. For Instructional Use Only
PROPRIETARY AND CONFIDENTIAL
UNLESS OTHERWISE SPECIFIED:
DIMENSIONS ARE IN INCHES
TITLE:
SIZE DWG. NO. REV
B LNichols
SCALE: 1:2 WEIGHT: SHEET 1 OF 1
DO NOT SCALE DRAWING

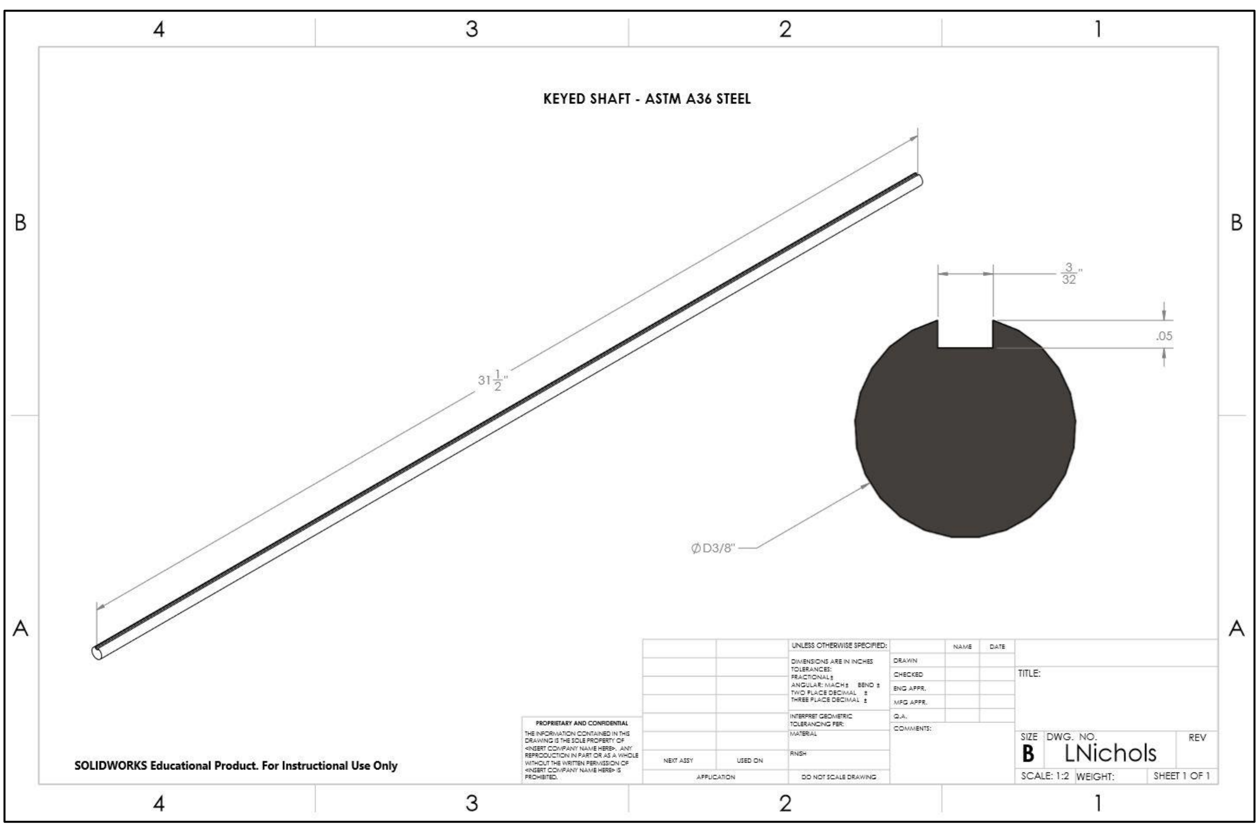
KEYED SHAFT - ASTM A36 STEEL
31 1/2"
3/32"
.05
⌀D3/8"
SOLIDWORKS Educational Product. For Instructional Use Only
PROPRIETARY AND CONFIDENTIAL
UNLESS OTHERWISE SPECIFIED:
DIMENSIONS ARE IN INCHES
TITLE:
SIZE DWG. NO. REV
B LNichols
SCALE: 1:2 WEIGHT: SHEET 1 OF 1
DO NOT SCALE DRAWING

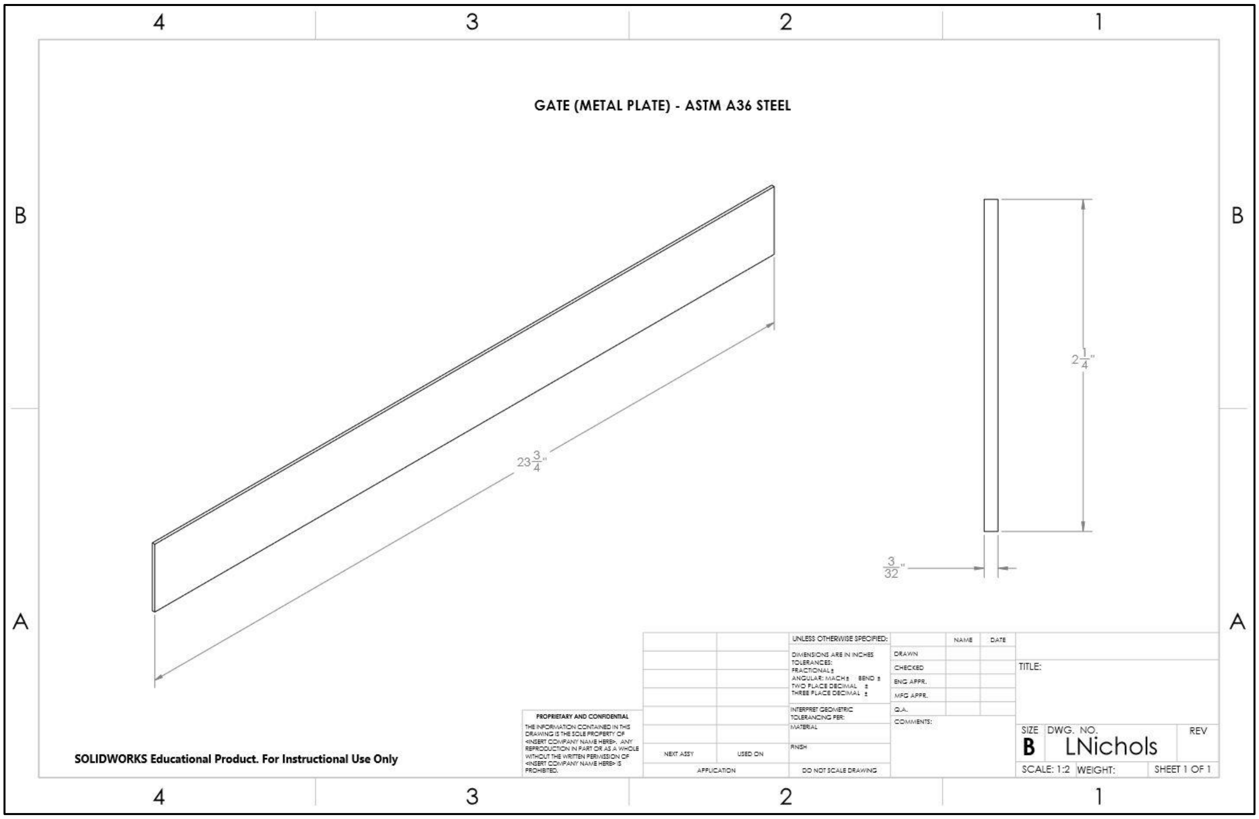
GATE (METAL PLATE) - ASTM A36 STEEL
23 3/4"
2 1/4"
3/32"
SOLIDWORKS Educational Product. For Instructional Use Only
UNLESS OTHERWISE SPECIFIED:
DIMENSIONS ARE IN INCHES
TOLERANCES:
FRACTIONAL ±
ANGULAR: MACH ± BEND ±
TWO PLACE DECIMAL ±
THREE PLACE DECIMAL ±
INTERPRET GEOMETRIC TOLERANCING PER:
MATERIAL
FINISH
DO NOT SCALE DRAWING
NAME
DATE
DRAWN
CHECKED
ENG APPR.
MFG APPR.
Q.A.
COMMENTS:
TITLE:
SIZE
B
DWG. NO.
LNichols
REV
SCALE: 1:2
WEIGHT:
SHEET 1 OF 1
NEXT ASSY
USED ON
APPLICATION

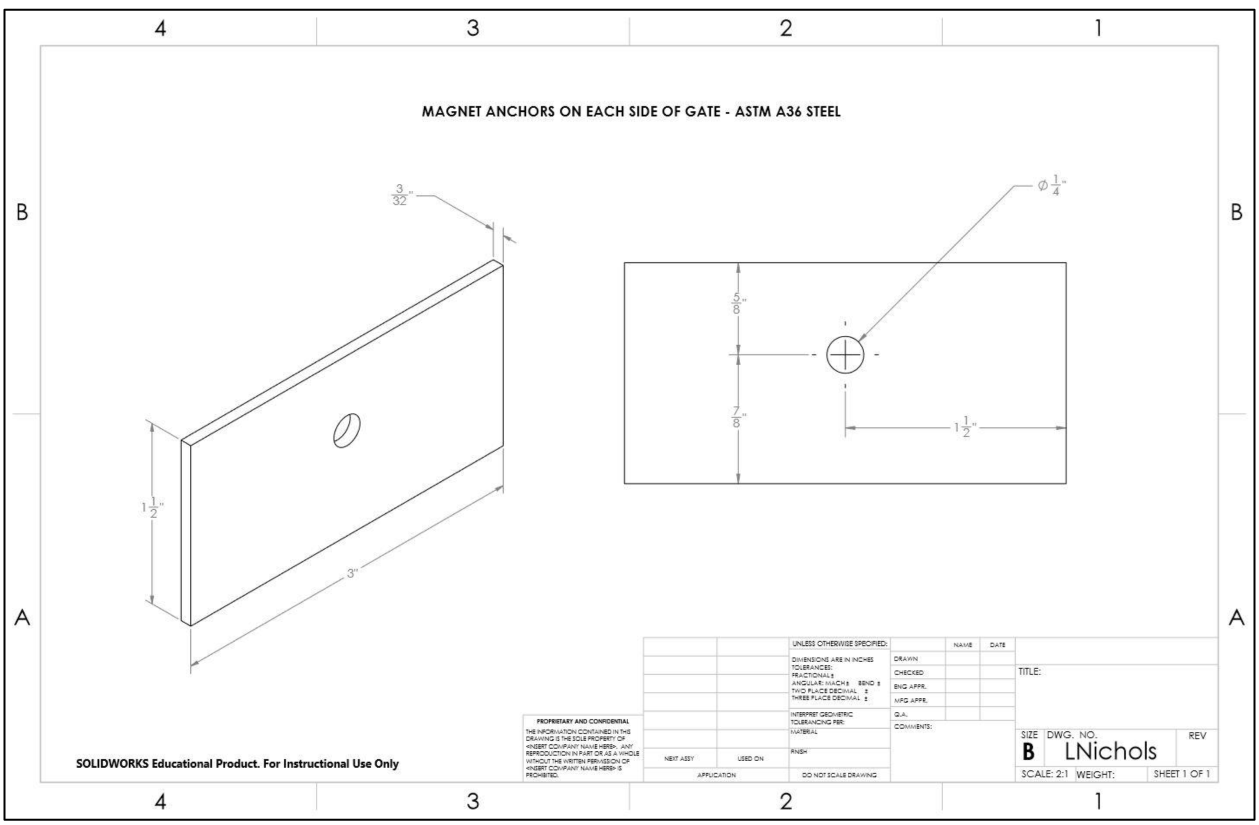
MAGNET ANCHORS ON EACH SIDE OF GATE - ASTM A36 STEEL
3/32"
⌀ 1/4"
5/8"
7/8"
1 1/2"
1 1/2"
3"
SOLIDWORKS Educational Product. For Instructional Use Only
UNLESS OTHERWISE SPECIFIED:
DIMENSIONS ARE IN INCHES
TOLERANCES:
FRACTIONAL ±
ANGULAR: MACH ± BEND ±
TWO PLACE DECIMAL ±
THREE PLACE DECIMAL ±
INTERPRET GEOMETRIC TOLERANCING PER:
MATERIAL
FINISH
DO NOT SCALE DRAWING
NAME
DATE
DRAWN
CHECKED
ENG APPR.
MFG APPR.
Q.A.
COMMENTS:
TITLE:
SIZE
B
DWG. NO.
LNichols
REV
SCALE: 2:1
WEIGHT:
SHEET 1 OF 1
NEXT ASSY
USED ON
APPLICATION

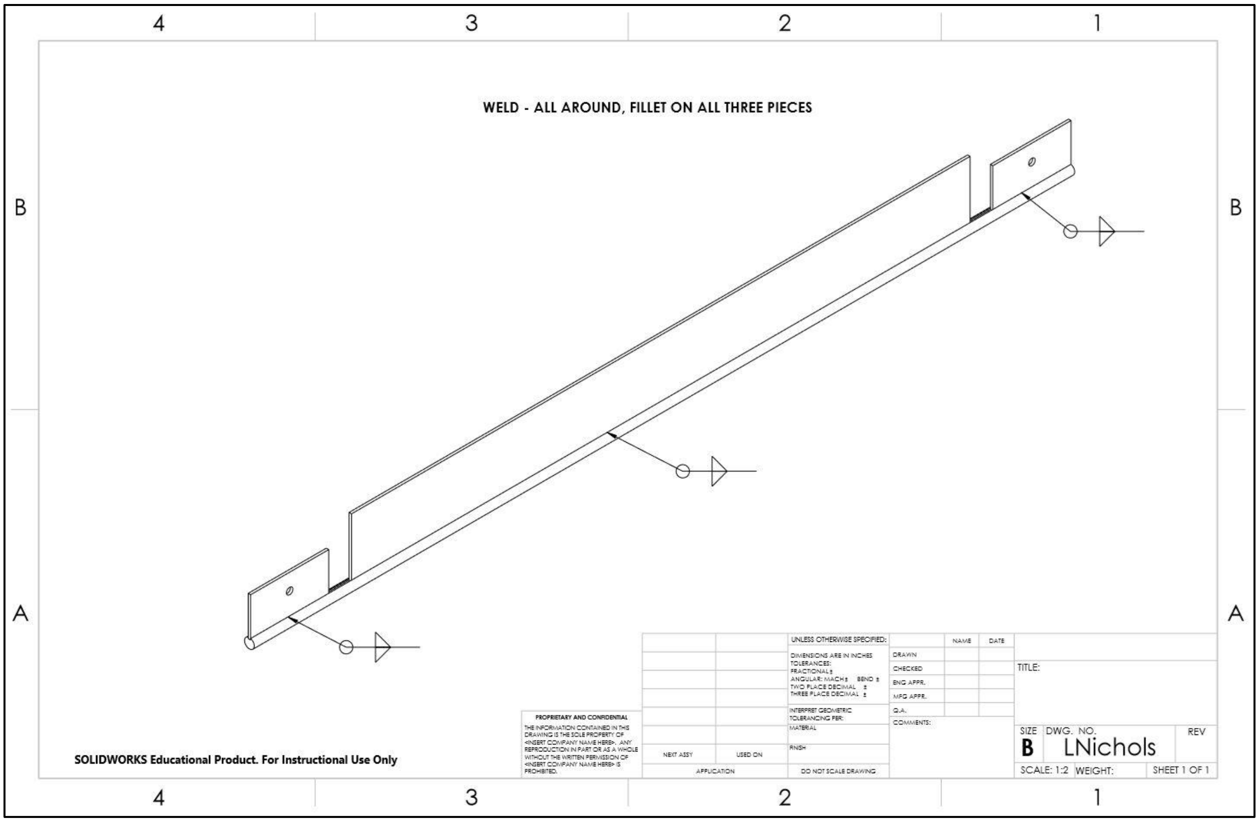
WELD - ALL AROUND, FILLET ON ALL THREE PIECES
SOLIDWORKS Educational Product. For Instructional Use Only
UNLESS OTHERWISE SPECIFIED:
DIMENSIONS ARE IN INCHES
NAME
DATE
DRAWN
CHECKED
ENG APPR.
MFG APPR.
Q.A.
COMMENTS:
TITLE:
PROPRIETARY AND CONFIDENTIAL
NEXT ASSY
USED ON
APPLICATION
DO NOT SCALE DRAWING
SIZE DWG. NO. REV
B LNichols
SCALE: 1:2 WEIGHT: SHEET 1 OF 1

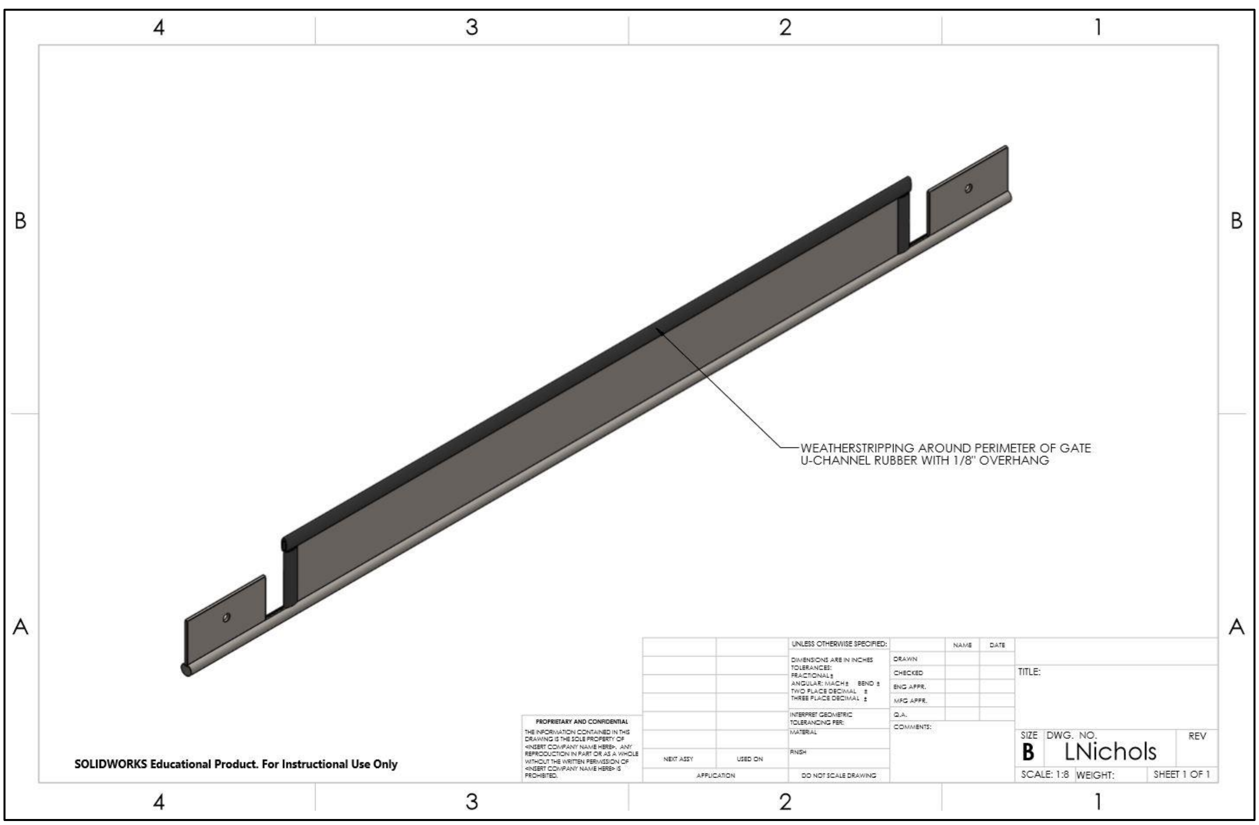
WEATHERSTRIPPING AROUND PERIMETER OF GATE
U-CHANNEL RUBBER WITH 1/8" OVERHANG
SOLIDWORKS Educational Product. For Instructional Use Only
UNLESS OTHERWISE SPECIFIED:
DIMENSIONS ARE IN INCHES
NAME
DATE
DRAWN
CHECKED
ENG APPR.
MFG APPR.
Q.A.
COMMENTS:
TITLE:
PROPRIETARY AND CONFIDENTIAL
NEXT ASSY
USED ON
APPLICATION
DO NOT SCALE DRAWING
SIZE DWG. NO. REV
B LNichols
SCALE: 1:8 WEIGHT: SHEET 1 OF 1

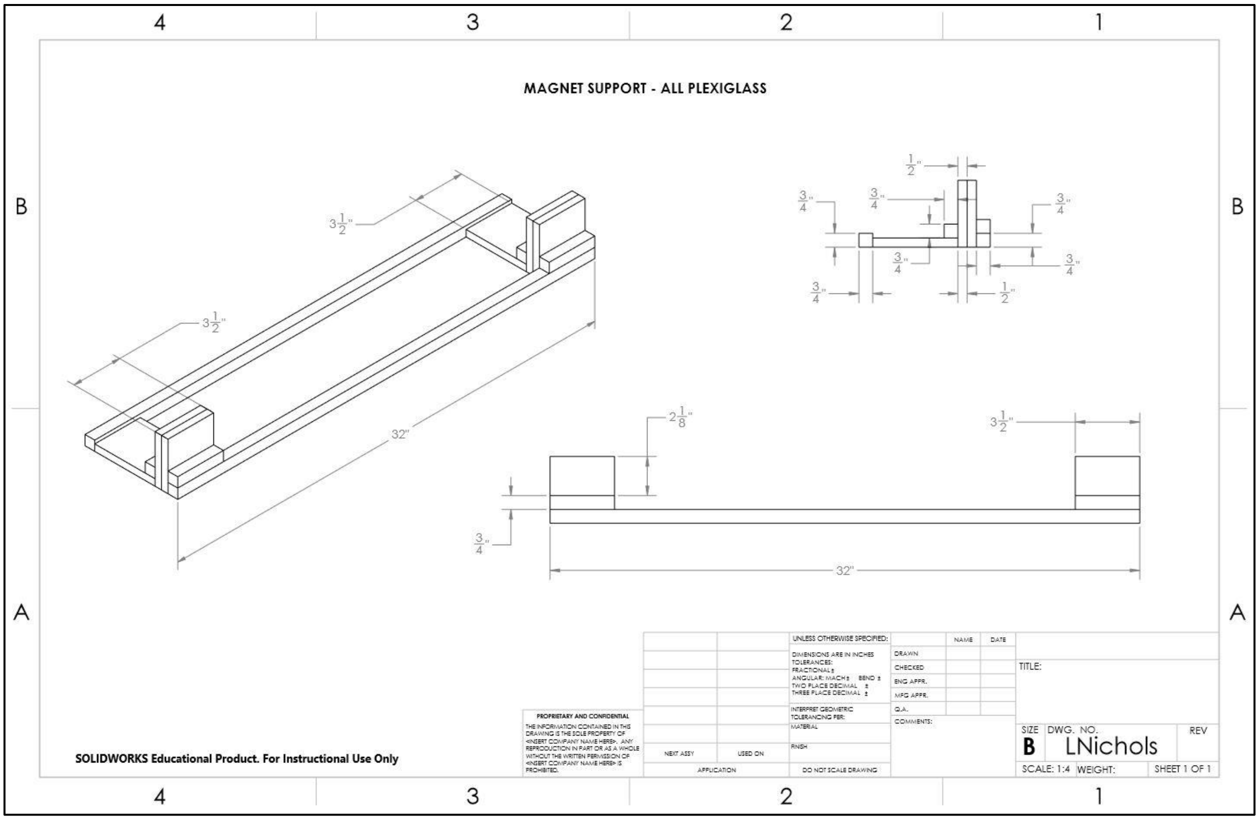

MAGNET SUPPORT - ALL PLEXIGLASS
32"
3 1/2"
2 1/8"
3/4"
1/2"
UNLESS OTHERWISE SPECIFIED:
PROPRIETARY AND CONFIDENTIAL
SOLIDWORKS Educational Product. For Instructional Use Only
SIZE B DWG. NO. LNichols
SCALE: 1:4 WEIGHT: SHEET 1 OF 1

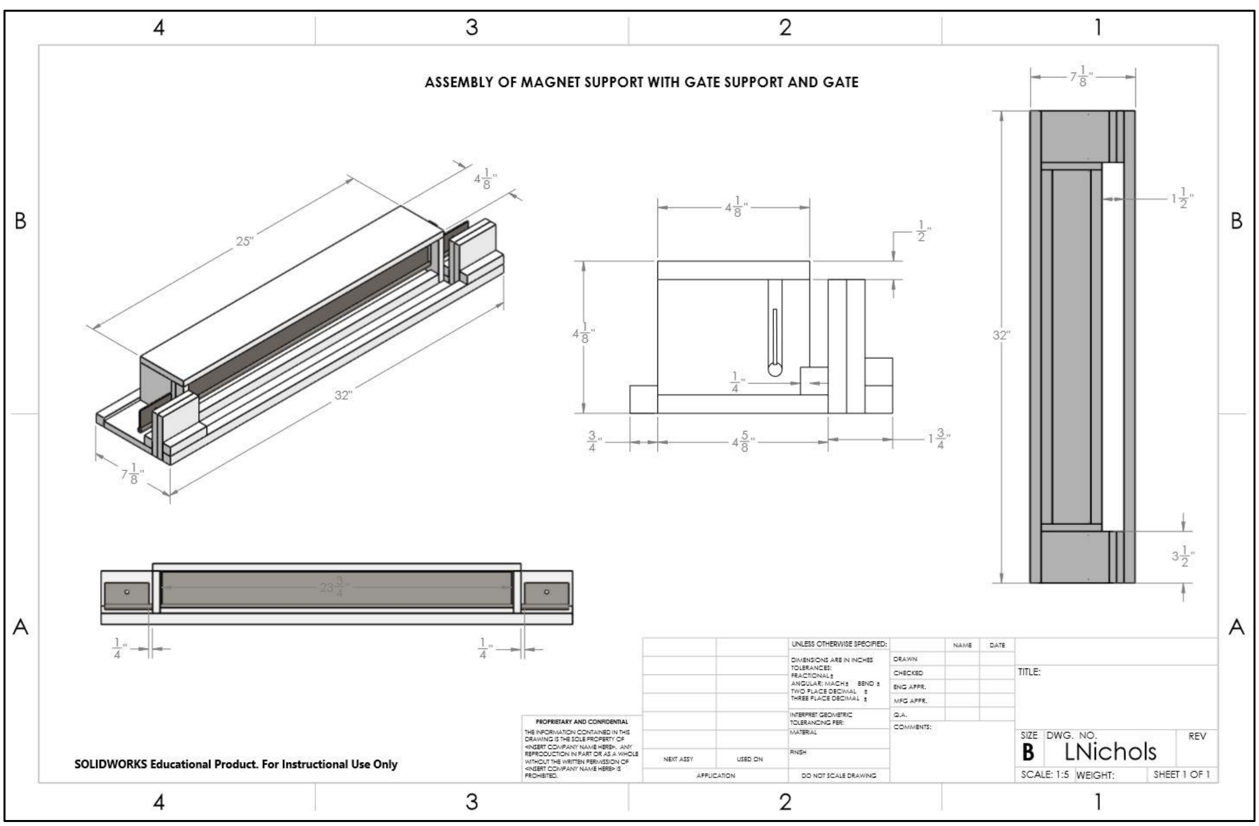

ASSEMBLY OF MAGNET SUPPORT WITH GATE SUPPORT AND GATE
25"
32"
4 1/8"
7 1/8"
1/2"
1/4"
3/4"
4 5/8"
1 3/4"
1 1/2"
3 1/2"
23 3/4
UNLESS OTHERWISE SPECIFIED:
PROPRIETARY AND CONFIDENTIAL
SOLIDWORKS Educational Product. For Instructional Use Only
SIZE B DWG. NO. LNichols
SCALE: 1:5 WEIGHT: SHEET 1 OF 1

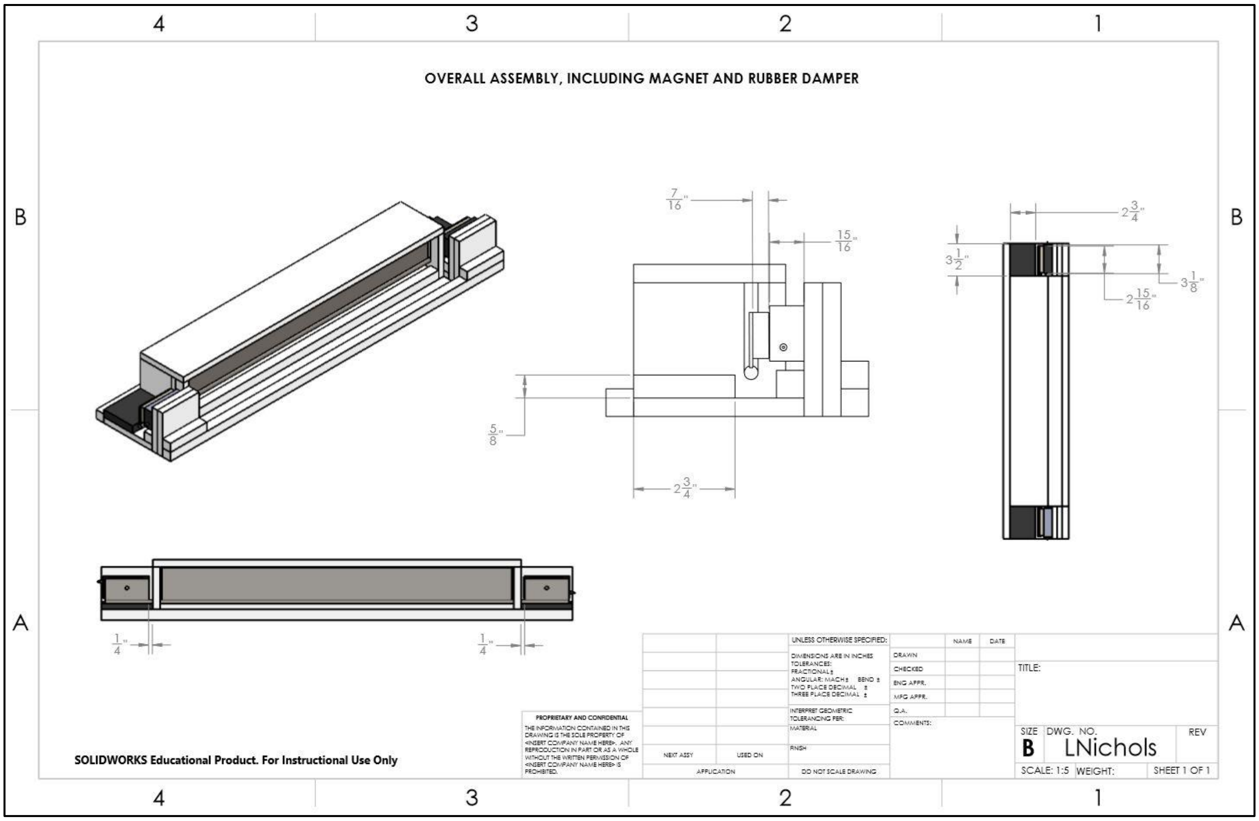
OVERALL ASSEMBLY, INCLUDING MAGNET AND RUBBER DAMPER
SOLIDWORKS Educational Product. For Instructional Use Only
PROPRIETARY AND CONFIDENTIAL
UNLESS OTHERWISE SPECIFIED:
DIMENSIONS ARE IN INCHES
TITLE:
SIZE DWG. NO. REV
B LNichols
SCALE: 1:5 WEIGHT: SHEET 1 OF 1

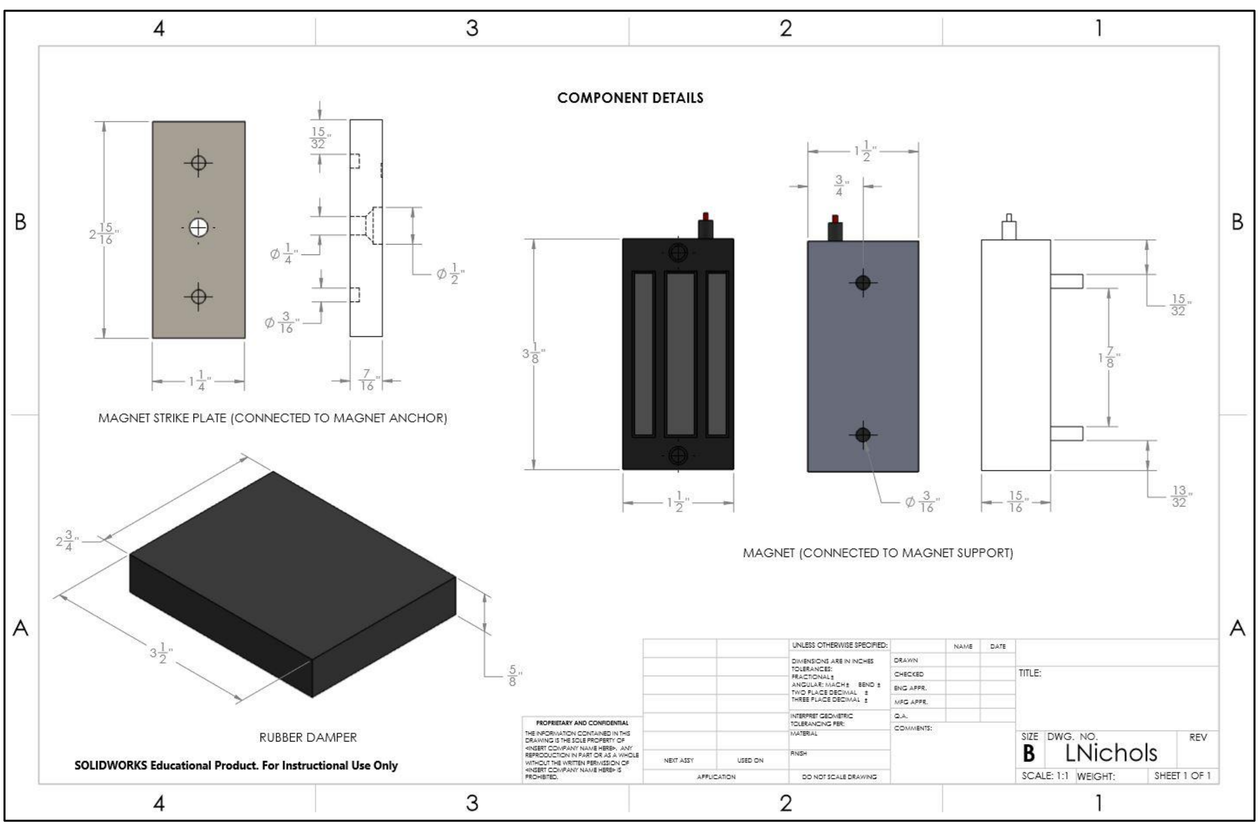
COMPONENT DETAILS
MAGNET STRIKE PLATE (CONNECTED TO MAGNET ANCHOR)
RUBBER DAMPER
MAGNET (CONNECTED TO MAGNET SUPPORT)
SOLIDWORKS Educational Product. For Instructional Use Only
PROPRIETARY AND CONFIDENTIAL
UNLESS OTHERWISE SPECIFIED:
DIMENSIONS ARE IN INCHES
TITLE:
SIZE DWG. NO. REV
B LNichols
SCALE: 1:1 WEIGHT: SHEET 1 OF 1

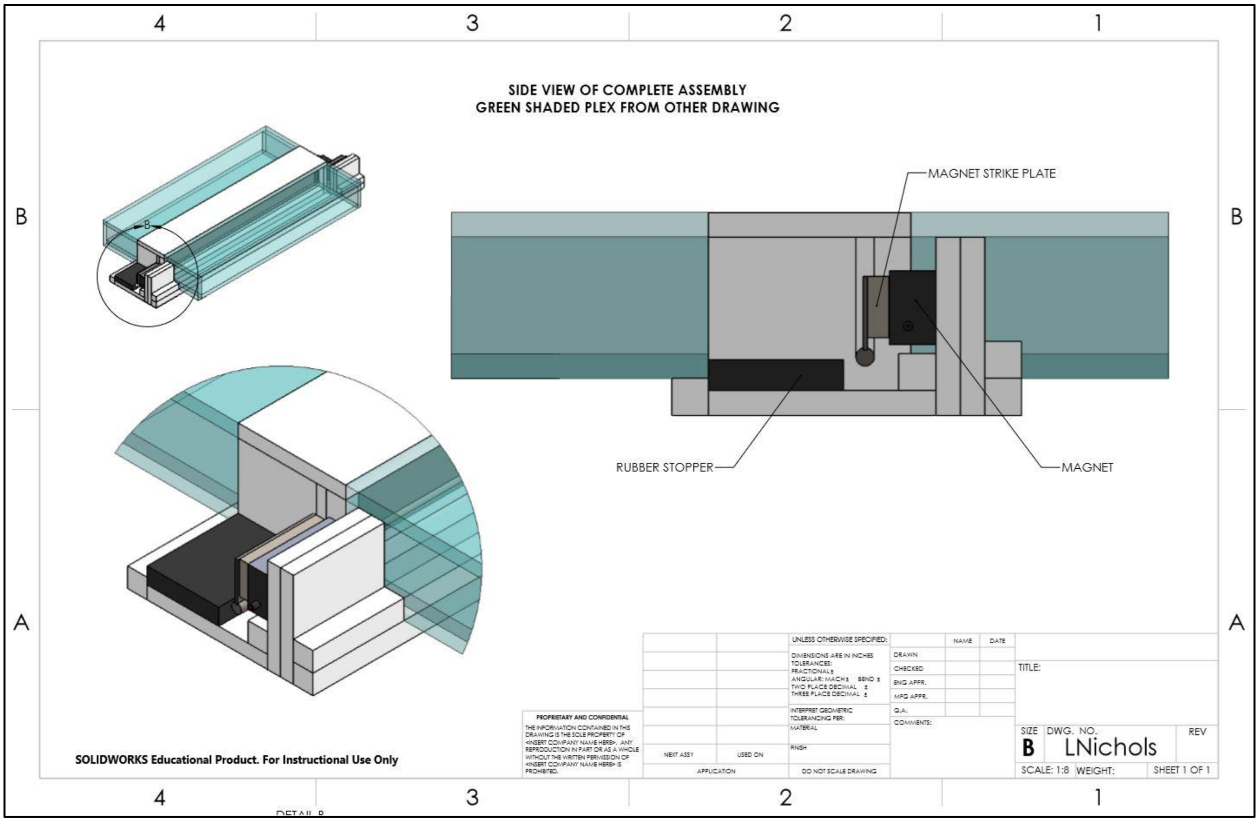
SIDE VIEW OF COMPLETE ASSEMBLY
GREEN SHADED PLEX FROM OTHER DRAWING
MAGNET STRIKE PLATE
RUBBER STOPPER
MAGNET
B
SOLIDWORKS Educational Product. For Instructional Use Only
UNLESS OTHERWISE SPECIFIED:
DIMENSIONS ARE IN INCHES
PROPRIETARY AND CONFIDENTIAL
DO NOT SCALE DRAWING
TITLE:
SIZE DWG. NO. REV
B LNichols
SCALE: 1:8 WEIGHT: SHEET 1 OF 1
DETAIL B

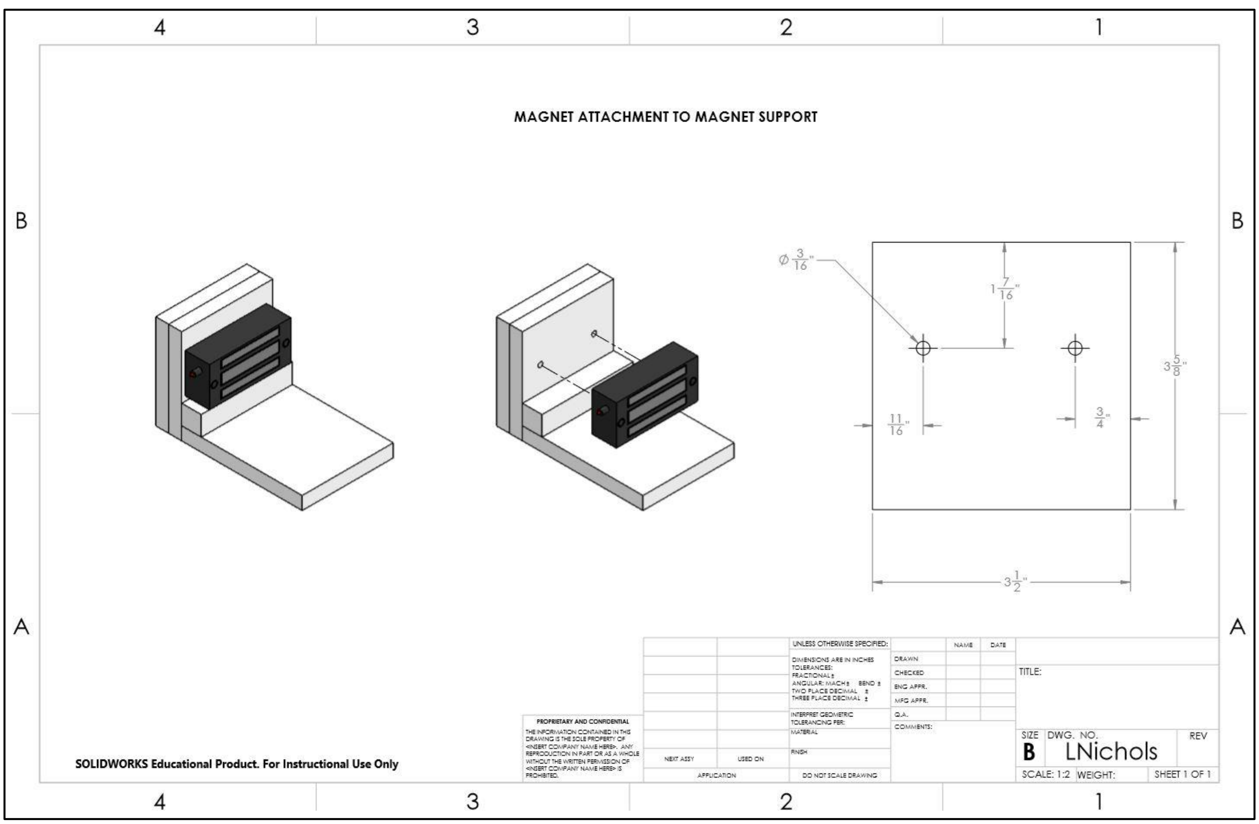
MAGNET ATTACHMENT TO MAGNET SUPPORT
Ø 3/16"
1 7/16"
11/16"
3/4"
3 5/8"
3 1/2"
SOLIDWORKS Educational Product. For Instructional Use Only
UNLESS OTHERWISE SPECIFIED:
DIMENSIONS ARE IN INCHES
PROPRIETARY AND CONFIDENTIAL
DO NOT SCALE DRAWING
TITLE:
SIZE DWG. NO. REV
B LNichols
SCALE: 1:2 WEIGHT: SHEET 1 OF 1

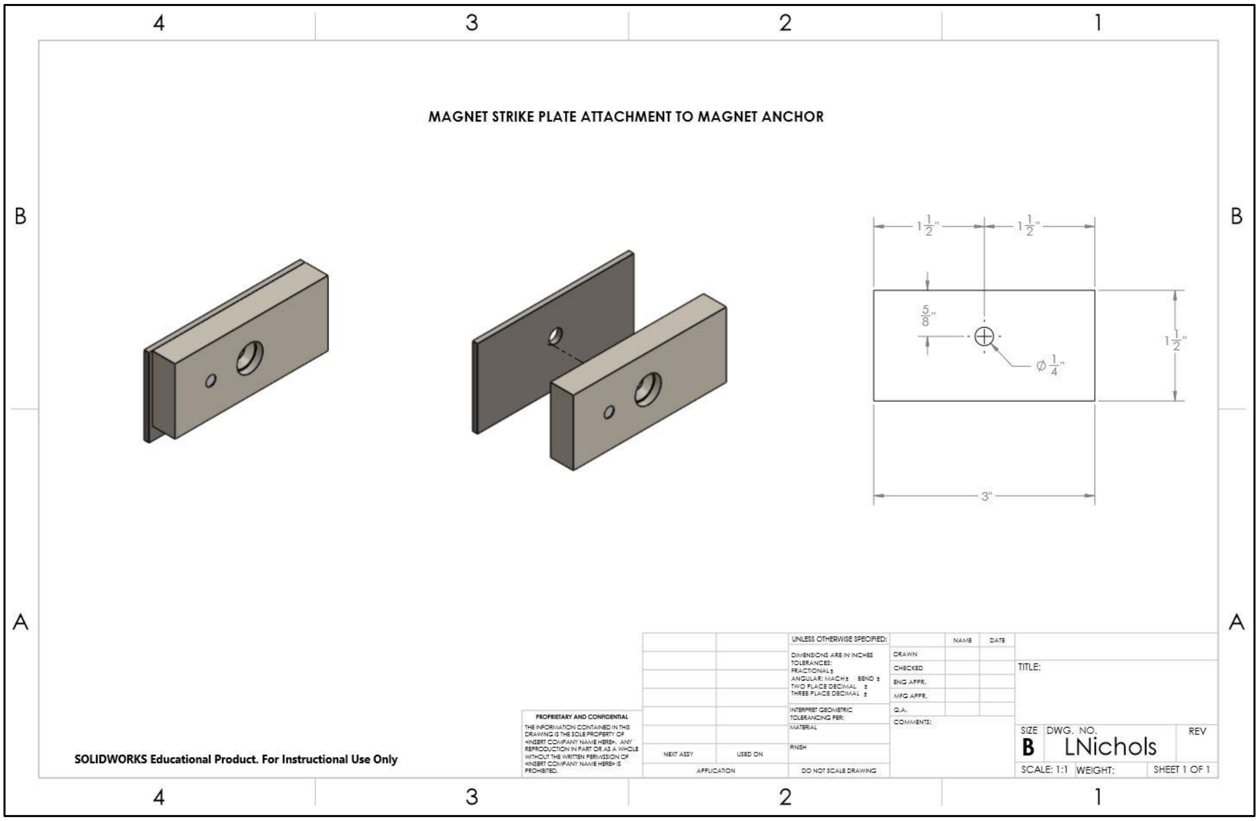
MAGNET STRIKE PLATE ATTACHMENT TO MAGNET ANCHOR
1 1/2"
1 1/2"
5/8"
1 1/2"
Ø 1/4"
3"
UNLESS OTHERWISE SPECIFIED:
DIMENSIONS ARE IN INCHES
NAME
DATE
DRAWN
CHECKED
ENG APPR.
MFG APPR.
Q.A.
COMMENTS:
TITLE:
PROPRIETARY AND CONFIDENTIAL
NEXT ASSY
USED ON
APPLICATION
MATERIAL
FINISH
DO NOT SCALE DRAWING
SIZE
DWG. NO.
REV
B
LNichols
SCALE: 1:1
WEIGHT:
SHEET 1 OF 1
SOLIDWORKS Educational Product. For Instructional Use Only

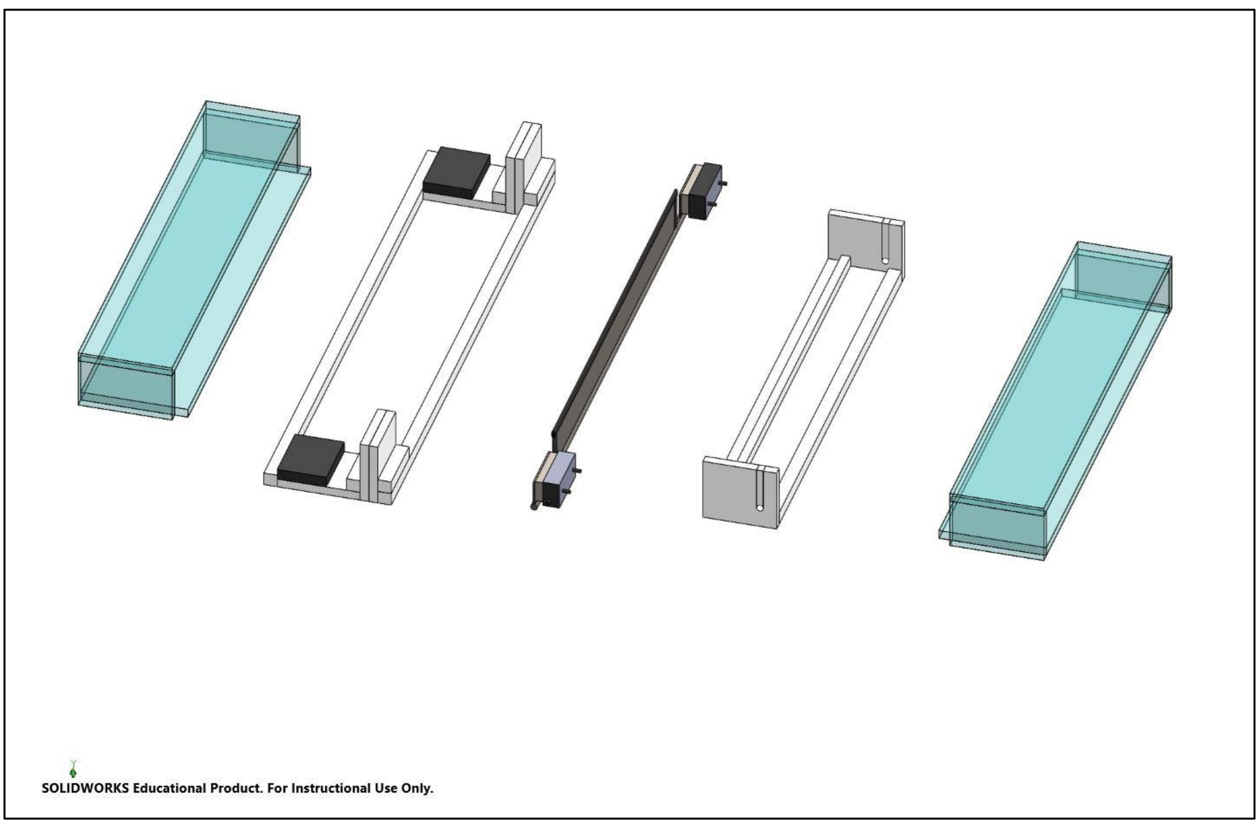
SOLIDWORKS Educational Product. For Instructional Use Only.

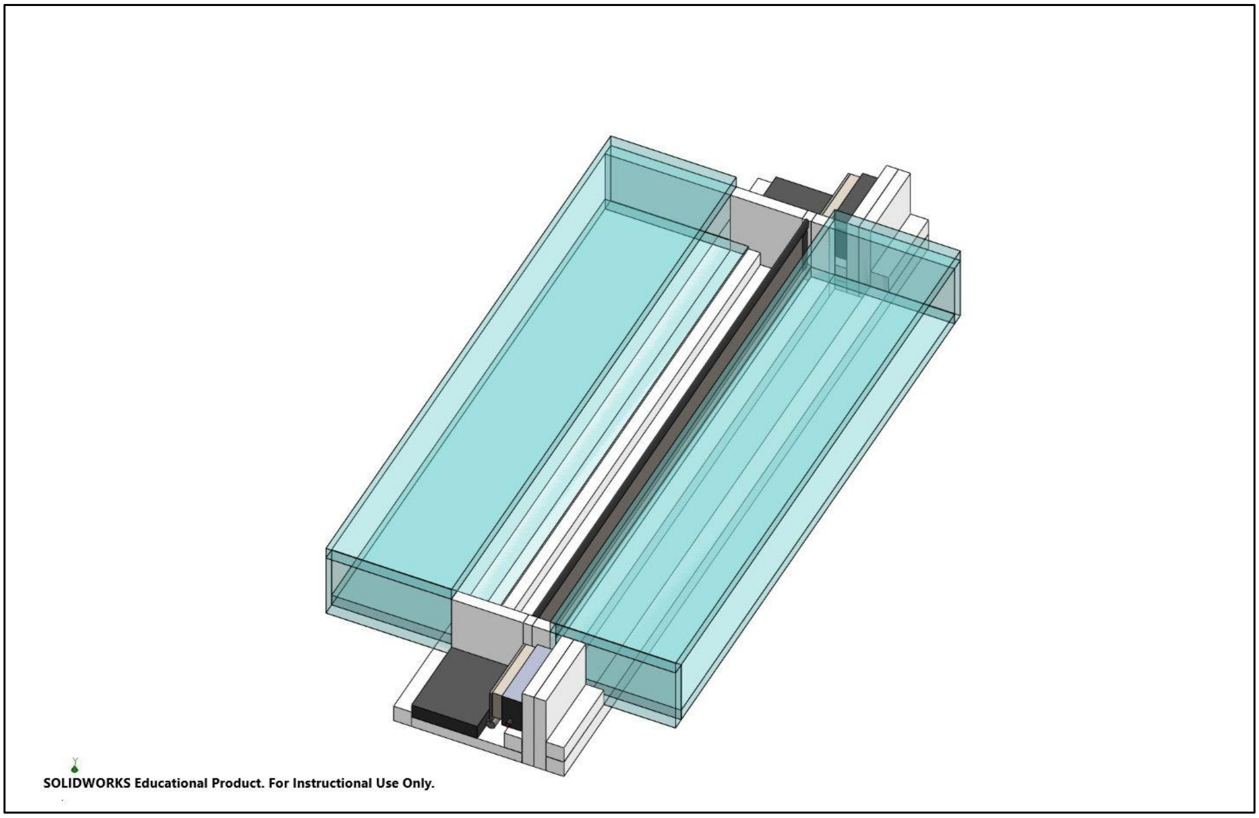
SOLIDWORKS Educational Product. For Instructional Use Only.